Oxidative Medicine and Cellular Longevity

Oxidative Stress and Mitochondrial Damage in Neurodegenerative Diseases: From Molecular Mechanisms to Targeted Therapies

Lead Guest Editor: Roberta Cascella
Guest Editors: Giovanna Cenini and Ana Lloret

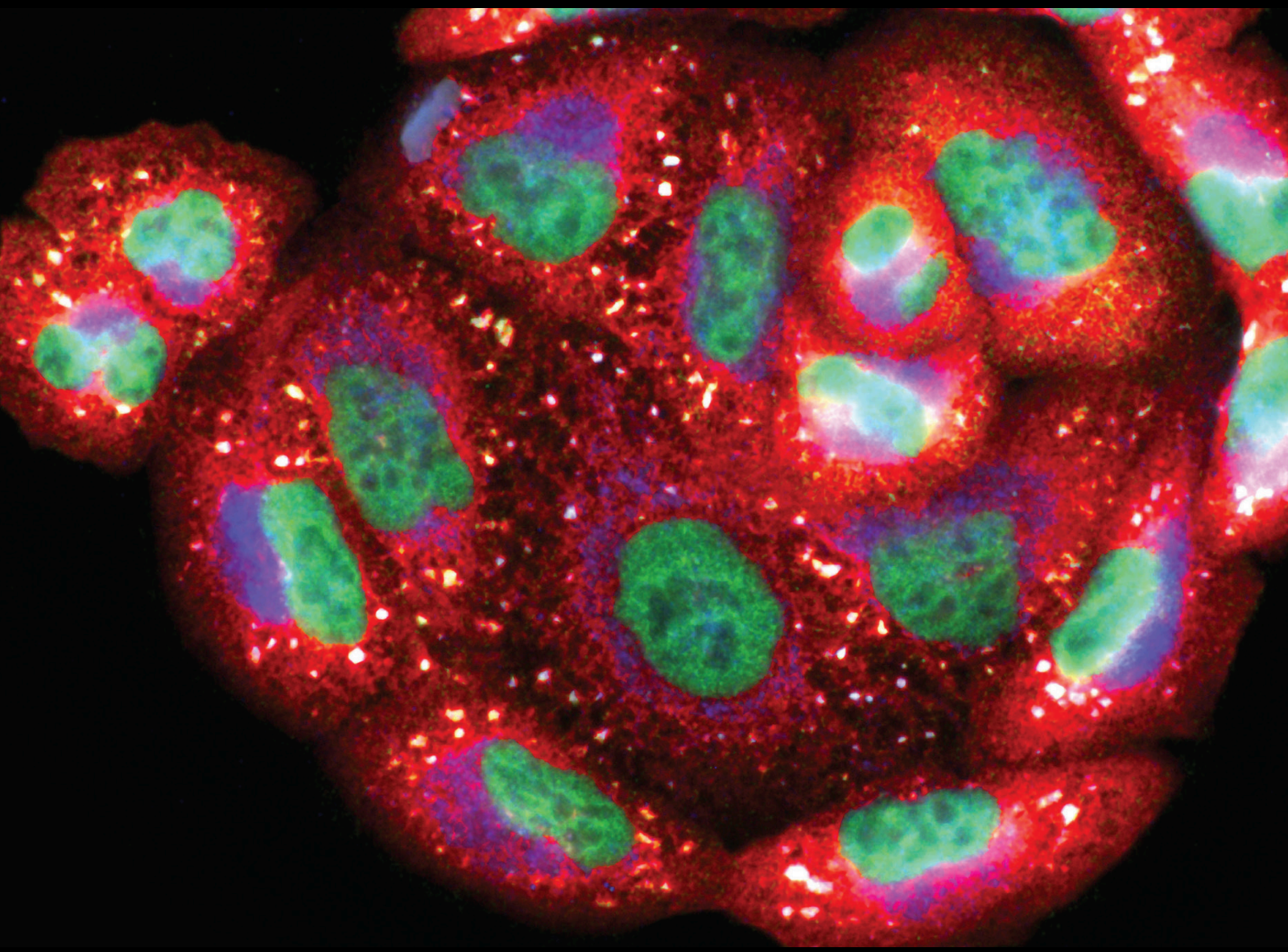

Oxidative Stress and Mitochondrial Damage in Neurodegenerative Diseases: From Molecular Mechanisms to Targeted Therapies

Oxidative Medicine and Cellular Longevity

Oxidative Stress and Mitochondrial Damage in Neurodegenerative Diseases: From Molecular Mechanisms to Targeted Therapies

Lead Guest Editor: Roberta Cascella
Guest Editors: Giovanna Cenini and Ana Lloret

Contents

Hindawi
Oxidative Medicine and Cellular Longevity
Volume 2020, Article ID 1270256, 2 pages
https://doi.org/10.1155/2020/1270256

Editorial

Oxidative Stress and Mitochondrial Damage in Neurodegenerative Diseases: From Molecular Mechanisms to Targeted Therapies

Giovanna Cenini,[1] **Ana Lloret**,[2] **and Roberta Cascella**[3]

[1]*Institut für Biochemie und Molekularbiologie, University of Bonn, 53115 Bonn, Germany*
[2]*Department of Physiology, Faculty of Medicine, University of Valencia, Avda, Blasco Ibañez17, 46010 Valencia, Spain*
[3]*Department of Experimental and Clinical Biomedical Sciences, Section of Biochemistry, University of Florence, 50134 Florence, Italy*

Correspondence should be addressed to Roberta Cascella; roberta.cascella@unifi.it

Received 24 April 2020; Accepted 25 April 2020; Published 5 May 2020

A growing body of evidence suggests the alteration of the reduction-oxidation (redox) homeostasis in the brain grown with the increasing of the age. The brain is composed of highly differentiated cells that populate different anatomical regions and requires about 20% of body basal oxygen for its functions [1]. Thus, it is not surprising that oxidative stress, as well as alterations in brain energy metabolisms, have been implicated in the pathogenesis of several neurodegenerative diseases, including Alzheimer's disease (AD), Parkinson's disease (PD), and amyotrophic lateral sclerosis (ALS). These neurodegenerative disorders are typically characterized by the progressive loss of neuronal cells and compromised motor or cognitive functions. It has been shown that neuronal cells are particularly vulnerable to oxidative damage due to their high polyunsaturated fatty acid content in membranes, high oxygen consumption, and weak antioxidant defence. Cellular energy is mainly produced via oxidative phosphorylation taking place within mitochondria, which are crucial organelles for numerous cellular processes, such as energy metabolism, calcium homeostasis, lipid biosynthesis, and apoptosis [2, 3]. Glucose oxidation is the most relevant source of energy in the brain because of its high rate of ATP generation needed to maintain neuronal energy demands [1]. Thus, neurons rely almost exclusively on the mitochondria, which produce the energy required for most of the cellular processes, including synaptic plasticity and neurotransmitter synthesis [4].

This special issue contributes to original articles that highlight and unravel mechanisms by which oxidative stress and mitochondrial damage are implicated in neurodegenerative diseases and provide new strategies that may counteract these pathological processes.

The manuscript by A.A. Abubaker et al. highlights the importance of NADPH oxidase activation and platelet oxidative responses in the prothrombotic responses induced by Aβ1-42, which is the β-amyloid peptide accumulating in the brain of Alzheimer's and Cerebral Amyloid Angiopathy (CAA) patients. In addition to giving us some direction in the elucidation of the molecular mechanisms underlying platelet activation by β-amyloid peptides, this study suggests a potential therapeutic opportunity aiming at limiting the vascular component of Alzheimer's disease by targeting NADPH oxidase activity.

C.C. Cai et al. provides the first evidence that glycine, a common substance present in numerous biomolecules, attenuated hypoxic-ischemic injury in neurons or nervous systems by decreasing mitochondria–mediated autophagy through regulating the AMPK pathway.

J. Budziosz et al. investigated the effects of low-frequency electromagnetic field (LFEMF) on the human body as electromagnetic sensitivity syndrome is commonly associated with the rapid development of wireless technologies. Several researchers have emphasised that exposure to EMF might also cause increased ROS production and lead to oxidative stress, which has been implicated in the pathogenesis of neurodegenerative diseases. Regardless, the researchers did not find any differences in lipid peroxidation, total oxidant status, and antioxidant systems between the experimental and

control groups, suggesting that LFEMF did not affect oxidative stress in the investigated brain structures.

K-I Tanaka et al. examined the effect of Ni^{2+} on Zn^{2+}-induced neurotoxicity, focusing on the endoplasmic reticulum (ER) stress response, and found that carnosine (an endogenous peptide) attenuated Ni^{2+}/Zn^{2+}-induced neuronal cell death and ER stress occurring before cell death. Based on their results, Ni^{2+} treatment significantly enhances Zn^{2+}-induced neuronal cell death by priming the ER stress response. Thus, compounds that decrease the ER stress response, such as carnosine, may be beneficial for neurological diseases.

The role of mitochondrial quality control (MQC) was investigated by X. Jiang et al. This review focused on three main aspects, that is, mitochondrial biogenesis, mitochondrial dynamics, and mitochondrial autophagy showing how genetic and environmental factors result in PD pathogenesis by interfering with MQC pathways, thereby hopefully contributing to the discovery of novel potential therapeutic targets for PD.

J. Han et al. examined the effects of paraquat (PQ), an herbicide considered an environmental contributor to the development of PD, inducing dopaminergic neuronal loss through reactive oxygen species (ROS) production and oxidative stress by mitochondrial complex I. Their findings indicate that the inhibition of mitochondrial complex I with chloramphenicol (CP) protects dopaminergic neurons and may provide a strategy for preventing neurotoxin-induced PD.

Z. Wang et al. quantitatively pooled data on levels of blood oxidative stress markers in ALS patients from the literature using a meta-analytic technique. They showed significantly increased blood levels of 8-hydroxyguanosine, malondialdehyde, and advanced oxidation protein product as well as decreased glutathione and uric acid levels in the peripheral blood of ALS patients. Thus, this meta-analysis clarifies the oxidative stress marker profile in the blood of ALS patients and strengthens the clinical evidence that prooxidative imbalances contribute to ALS pathophysiology.

H-S. Lim et al. investigated the protective effects of Cicadidae Periostracum (CP), the cast-off skin of Cryptotympana pustulata Fabricius, on 1-8 methyl-4-phenyl-1,2,3,6-tetrahydropyridine- (MPTP-) induced PD in mice and investigated the underlying mechanisms of action, focusing on Nuclear receptor-related 1 protein (Nurr1), a nuclear hormone receptor implicated in limiting mitochondria dysfunction, apoptosis, and inflammation in the central nervous system and protecting dopaminergic neurons. They showed that CP might contribute to neuroprotective signalling by regulating neurotrophic factors primarily via Nurr1 signalling, neuroinflammation, and mitochondria-mediated apoptosis.

J.H. Cater et al. reviewed the ability of hypochlorite, an oxidant that is generated during inflammation, to regulate alpha-2-macroglobulin (α2M). This tetrameric protein is constitutively abundant in biological fluids and is involved in several biological processes, including the clearance of the Aβ peptide.

In the end, the role of mitochondrial oxidative stress in the aging process and neurodegenerative diseases has been further explored by G. Cenini et al. The review tried to summarize the molecular mechanisms involving mitochondria and oxidative stress in the aging process with the aim at identifying new strategies for improving a healthy and extending lifespan.

Conflicts of Interest

The editors declare that they have no conflicts of interest regarding the publication of the special issue.

Acknowledgments

The guest editors thank all the authors for having submitted their research to this special issue and all the reviewers for having provided their valuable contribution to improve the quality of this work. Finally, they thank the editorial board and all the staff for the opportunity and support that made this special issue publication possible.

Giovanna Cenini
Ana Lloret
Roberta Cascella

References

[1] P. Schonfeld and G. Reiser, "Why does brain metabolism not favor burning of fatty acids to provide energy? Reflections on disadvantages of the use of free fatty acids as fuel for brain," *Journal of Cerebral Blood Flow & Metabolism*, vol. 33, no. 10, pp. 1493–1499, 2013.

[2] E. F. Smith, P. J. Shaw, and K. J. De Vos, "The role of mitochondria in amyotrophic lateral sclerosis," *Neuroscience Letters*, vol. 710, article 132933, 2019.

[3] B. G. Hill, G. A. Benavides, J. R. Lancaster Jr. et al., "Integration of cellular bioenergetics with mitochondrial quality control and autophagy," *Biological Chemistry*, vol. 393, no. 12, pp. 1485–1512, 2012.

[4] M. P. Mattson, M. Gleichmann, and A. Cheng, "Mitochondria in neuroplasticity and neurological disorders," *Neuron*, vol. 60, no. 5, pp. 748–766, 2008.

Hindawi
Oxidative Medicine and Cellular Longevity
Volume 2019, Article ID 5797512, 17 pages
https://doi.org/10.1155/2019/5797512

Research Article

Cicadidae Periostracum, the Cast-Off Skin of Cicada, Protects Dopaminergic Neurons in a Model of Parkinson's Disease

Hye-Sun Lim,[1] **Joong-Sun Kim**,[1] **Byeong Cheol Moon**,[1] **Goya Choi**,[1] **Seung Mok Ryu**,[1] **Jun Lee**,[1] **Mary Jasmin Ang**,[2] **Mijin Jeon**,[2] **Changjong Moon**,[2] **and Gunhyuk Park**[1]

[1]*Herbal Medicine Resources Research Center, Korea Institute of Oriental Medicine, 111 Geonjae-ro, Naju-si, Jeollanam-do 58245, Republic of Korea*
[2]*College of Veterinary Medicine and BK21 Plus Project Team, Chonnam National University, Gwangju 61186, Republic of Korea*

Correspondence should be addressed to Gunhyuk Park; gpark@kiom.re.kr

Received 18 April 2019; Revised 30 July 2019; Accepted 10 August 2019; Published 24 October 2019

Guest Editor: Giovanna Cenini

Parkinson's disease (PD) is characterized by dopaminergic neuronal loss in the substantia nigra pars compacta (SNPC) and the striatum. Nuclear receptor-related 1 protein (Nurr1) is a nuclear hormone receptor implicated in limiting mitochondrial dysfunction, apoptosis, and inflammation in the central nervous system and protecting dopaminergic neurons and a promising therapeutic target for PD. Cicadidae Periostracum (CP), the cast-off skin of *Cryptotympana pustulata* Fabricius, has been used in traditional medicine for its many clinical pharmacological effects, including the treatment of psychological symptoms in PD. However, scientific evidence for the use of CP in neurodegenerative diseases, including PD, is lacking. Here, we investigated the protective effects of CP on 1-methyl-4-phenyl-1,2,3,6-tetrahydropyridine- (MPTP-) induced PD in mice and explored the underlying mechanisms of action, focusing on Nurr1. CP increased the expression levels of Nurr1, tyrosine hydroxylase, DOPA decarboxylase, dopamine transporter, and vesicular monoamine transporter 2 via extracellular signal-regulated kinase phosphorylation in differentiated PC12 cells and the mouse SNPC. In MPTP-induced PD, CP promoted recovery from movement impairments. CP prevented dopamine depletion and protected against dopaminergic neuronal degradation via mitochondria-mediated apoptotic proteins such as B-cell lymphoma 2 (Bcl-2), Bcl-2-associated X, cytochrome c, and cleaved caspase-9 and caspase-3 by inhibiting MPTP-induced neuroinflammatory cytokines, inducible nitric oxide synthase, cyclooxygenase 2, and glial/microglial activation. Moreover, CP inhibited lipopolysaccharide-induced neuroinflammatory cytokines and response levels and glial/microglial activation in BV2 microglia and the mouse brain. Our findings suggest that CP might contribute to neuroprotective signaling by regulating neurotrophic factors primarily via Nurr1 signaling, neuroinflammation, and mitochondria-mediated apoptosis.

1. Introduction

Parkinson's disease (PD) is a progressive neurodegenerative disease characterized by bradykinesia, resting tremor, postural instability, and rigidity [1]. The disease affects 1–2% of the global population over the age of 65. In the brain of patients with PD, loss of dopamine-producing neurons in the substantia nigra pars compacta (SNPC) and the striatum (ST) may occur even prior to the onset of the symptoms of neurodegeneration [1, 2]. Available treatments work by relieving the symptoms of PD by increasing dopaminergic signaling through one of the three mechanisms: (1) increasing the dopamine levels by increasing the levels of its biosynthetic precursor (L-3,4-dihydroxyphenylalanine (L-DOPA)), (2) blocking the breakdown of dopamine by inhibiting its metabolic enzymes (monoamine oxidase, catechol-O-methyltransferase), and (3) mimicking the activity of dopamine by directly agonizing dopamine receptors [1, 3]. However, there is still an unmet clinical need to develop mechanism-based and/or disease-modifying medications to treat both the symptoms and progression of PD.

Nuclear receptor-related 1 protein (Nurr1) is a transcription factor that regulates the expression of genes that are critical for the development, maintenance, and survival of

dopaminergic neurons [4, 5]. In particular, Nurr1 plays a fundamental role in maintaining dopamine homeostasis by regulating the transcription of genes governing dopamine synthesis, packaging, and reuptake [4]. Nurr1 also regulates the survival of dopaminergic neurons by stimulating the transcription of genes coding for neurotrophic factors, anti-inflammatory responses, and oxidative stress and mitochondrial dysfunction management, as well as repressing the transcription and expression of proinflammatory genes [4, 6, 7]. A lack of Nurr1 in embryonic ventral midbrain cells hinders their migration into striatal areas [8]. In microglia and astrocytes, Nurr1 represses proinflammatory responses and protects dopaminergic neurons from inflammation-induced neuronal toxicity or death in the midbrain [5, 9]. In patients with PD, the expression of Nurr1 is reduced compared to age-matched controls, and a few, yet rare, Nurr1 polymorphisms appear to be associated with the disease [10, 11]. Stimulation of Nurr1 activity may combat both the reduced dopamine levels and the increased oxidative stress and inflammation associated with PD [12–14]. Together, these findings strongly suggest that disrupted function/expression of Nurr1 is related to neurodegeneration of dopaminergic neurons and alleviates inflammation and mitochondrial dysfunctions; thereby, it may improve the pathogenesis of PD.

Cicadidae Periostracum (CP), the cast-off skin of *Cryptotympana pustulata* Fabricius (also known as cicada or Sun-Tae), was originally described in the Chung-bu category of *Dongui Bogam*, an ancient Korean medical book [15, 16]. In Korean traditional medicine, CP has been used to treat epilepsy, shock, smallpox, sedation, edema, and night terror symptoms. In traditional Chinese medicine, CP is known as chantui and has long been used to treat soreness of the throat, hoarseness, itching, spasms, and other symptoms [17]. Since then, it has been used in traditional medicine for its many pharmacological effects. In 2003, a World Health Organization (WHO) international expert meeting to review and analyze the clinical reports on severe acute respiratory syndrome (SARS) treatment noted that the Chinese were using a combination of cicada and silkworm droppings to treat SARS-associated fever [18, 19]. Recently, several studies have confirmed the pharmacological effects of CP, including its anti-skin aging, anti-kidney injury, anticonvulsive, sedative, antiallergy, and antianaphylactic shock actions [20–23]. However, scientific evidence for the use of CP in neurodegenerative diseases, including PD, is lacking. Therefore, in this study, we investigated the protective effects of CP on 1-methyl-4-phenyl-1,2,3,6-tetrahydropyridine- (MPTP-) induced neurotoxicity in mice and explored the underlying mechanisms of action, focusing on Nurr1.

2. Materials and Methods

2.1. Preparation of the CP Extract. CP was purchased from Kwong-Mung-dang Company (Ulsan, Korea) and authenticated by Dr. Goya Choi (Herbal Medicine Resources Research Center, Korea Institute of Oriental Medicine, Naju, Korea), and a voucher specimen (3-18-0038) was deposited at the Herbal Medicine Resources Research Center, Korea Institute of Oriental Medicine. Briefly, CP was extracted in distilled water for 3 h under reflux (100 ± 2°C). Then, the extract was filtered, evaporated on a rotary vacuum evaporator, and lyophilized (yield, 6.30%). The powder was kept at 4°C until use.

2.2. Animals. Male C57BL/6 mice (8 weeks, 23–24 g) were purchased from Doo Yeol Biotech (Seoul, Korea) and maintained under temperature- and light-controlled conditions (20–23°C, 12 h light/12 h dark cycle) with food and water provided ad libitum. All animals were acclimatized for 7 days prior to drug administration. The experimental protocol was approved by the institutional animal care committee of KIOM (KIOM-18-056) and performed according to the guidelines of the Animal Care and Use Committee at KIOM.

2.3. Drug Administration. Mice were assigned to 1 of 11 groups: (1) control ($n = 11$), (2) MPTP ($n = 11$), (3) MPTP+CP 1 mg/kg/day ($n = 11$), (4) MPTP+CP 10 mg/kg/day ($n = 11$), (5) MPTP+CP 25 mg/kg/day ($n = 11$), (6) MPTP+ropinirole 1 mg/kg/day ($n = 11$), (7) CP 5 mg/kg/day ($n = 5$), (8) CP 25 mg/kg/day ($n = 5$), (9) control ($n = 7$), (10) lipopolysaccharide (LPS, $n = 7$), and (11) LPS+CP 25 mg/kg/day ($n = 7$). CP, dissolved in normal saline, was administered for 5 days consecutively. The control group received an equal volume of normal saline for the same duration. MPTP (Sigma-Aldrich, St. Louis, MO, USA) or LPS (Sigma-Aldrich) were administered acutely as described previously [24–29]. On day 3 of CP treatment, MPTP (20 mg/kg, dissolved in saline) was injected intraperitoneally four times at 2 h intervals. Vehicles of equal volume (0.25 mL) were given to the control group (Figure 1(a)). In the LPS group, 3 h after the last administration of CP, LPS was dissolved in saline and injected intraperitoneally at a dose of 5 mg/kg (Figure 1(b)). Since MPTP is a very dangerous chemical, we conducted the experiment in compliance with previously described procedures [30]: (1) we used laboratory clothing and boots made of nonabsorbable material, (2) we wore a mask with a HEPA filter, (3) 1% bleach was used to clean all equipment used in the experiments, and (4) all waste was disposed in a biohazard safety bin.

2.4. Rotarod Test and Pole Test. The rotarod test and pole test were assessed according to previously published methods [25, 29, 31]. The rotarod test is a useful method for measuring hypokinesia in a mouse model of PD [32]. Mice were evaluated on the rotarod 1 day after the last MPTP injection to assess sensorimotor coordination. The rotarod unit (Ugo Basile, Comerio, Varese, Italy) consisted of a rotating spindle (diameter 3 cm) and five individual compartments, which allowed five mice to be tested simultaneously. After two successive days of twice-daily training (4 rpm rotation speed on the first day and 20 rpm on the second day), the test rotation speed was increased to 25 rpm on the third day in a test session. The time each mouse remained on the rotating bar was recorded over three trials per mouse, at 5 min intervals and a maximum trial length of 300 s per trial. Data are presented as mean time on the rotating bar over the three test trials.

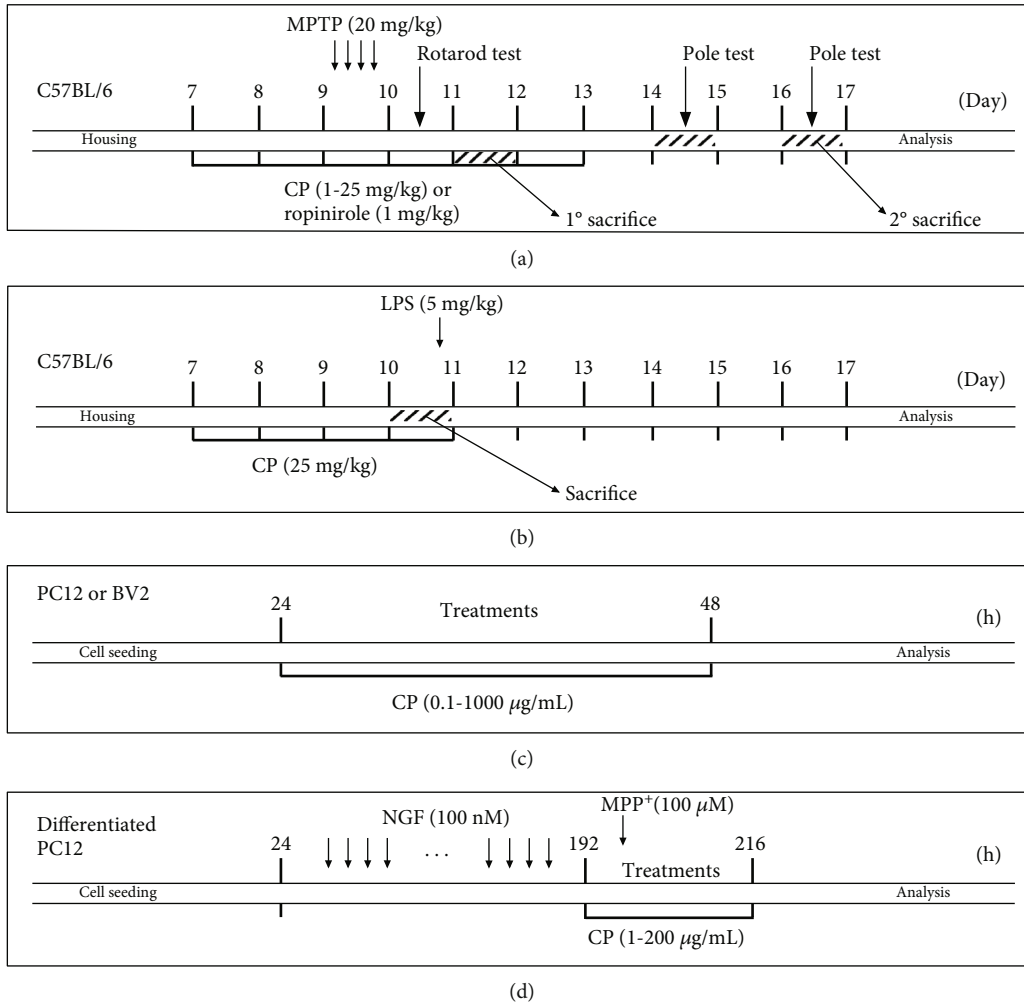

Figure 1: Summary of the experimental design.

The pole test is a useful method to measure bradykinesia in a mouse model of PD [32]. We performed the pole test on days 5 and 7 after the last MPTP injection. The mice were held on the top of the pole (diameter 8 mm, height 55 cm, with a rough surface). The time that mice needed to turn down completely was recorded as the time to turn (T-turn). The time needed for the mice to climb down and place four feet on the floor was recorded as the time for locomotion activity (T-LA). Each trial had a cut-off limit of 50 s.

2.5. Brain Tissue Preparation. On days one and seven after MPTP treatment or at 3 h after LPS treatment, mice were anesthetized immediately and perfused transcardially with 0.05 M phosphate-buffered saline (PBS, Sigma-Aldrich), followed by cold 4% paraformaldehyde (PFA, Sigma-Aldrich) in 0.1 M phosphate buffer. Brains were removed and postfixed in 0.1 M phosphate buffer (Sigma-Aldrich) containing 4% PFA overnight at 4°C and then immersed in a solution containing 30% sucrose in 0.05 M PBS for cryoprotection. Serial 15 or 30 μm thick coronal sections were cut on a freezing microtome (Leica Instruments GmbH, Nussloch, Germany) and stored in a cryoprotectant (25% ethylene glycol, Sigma-Aldrich), 25% glycerol (Sigma-Aldrich), and 0.05 M phosphate buffer at 4°C until use for immunohistochemistry (IHC) study. For western blotting mRNA analysis, and kit-based analyses, in brief, the SNPC and ST were rapidly dissected, homogenized, and centrifuged using standard laboratory techniques. The final supernatant was stored at 70°C until use [33].

2.6. Immunohistochemistry (IHC) and Immunofluorescence Analysis. For IHC analysis, the assessment of dopaminergic neurons in the SNPC was made by analyzing coronal sections at approximately 3.28 mm behind the bregma [34]. Brain sections were rinsed briefly in PBS and treated with 1% hydrogen peroxide (Sigma-Aldrich) for 15 min. The sections were incubated with rabbit anti-tyrosine hydroxylase (TH) (1 : 1000) overnight at 4°C in the presence of 0.3% Triton X-100 (Vector Laboratories, Burlingame, CA, USA) and normal goat serum (Vector Laboratories) or normal horse serum (Vector Laboratories). After rinsing in PBS, the sections were incubated with biotinylated anti-rabbit IgG (Vector Laboratories) (1 : 200) for 90 min, rinsed, and incubated with ABC (Vector Laboratories) (1 : 100) for 1 h at room

temperature. Peroxidase activity was visualized by incubating sections with DAB (Sigma-Aldrich) in 0.05 M Tris-buffered saline (Sigma-Aldrich). After several rinses with PBS, sections were mounted on gelatin-coated slides, dehydrated, and cover-slipped using histomount medium. For immunofluorescence analysis, brain sections were rinsed briefly in PBS and treated with 0.5% BSA (Sigma-Aldrich) for 30 min. The sections were incubated with mouse anti-TH (1 : 100) or rabbit anti-glial fibrillary acidic protein (GFAP), ionized calcium-binding adaptor molecule 1 (Iba-1), Nurr1, or cyclooxygenase (Cox)-2 (1 : 200) overnight at 4°C in the presence of 0.3% Triton X-100 and normal serum. Next, they were incubated for 1 h with Alexa Fluor-conjugated secondary antibodies (1 : 500). The sections were finally washed in PBS and mounted using Vectashield mounting medium containing DAPI (Vector Laboratories). Images were photographed at 40x and 100x magnification using an optical light microscope (Olympus Microscope System BX53; Olympus, Tokyo, Japan) equipped with a 20x objective lens. Further, to analyze the intensity of striatal TH-positive nerve fibers, brain sections were sampled at approximately 0.62 mm ahead of the bregma. Primary antibodies are listed in Supplementary Table 1.

2.7. RNA Extraction and Real-Time Reverse Transcription Polymerase Chain Reaction. Homogenization of SNPC tissue was conducted using TRIzol reagent (Invitrogen, Carlsbad, CA, USA). After homogenization, 0.2 mL of chloroform was added to each sample. The tubes were shaken vigorously by hand for 15 s and then incubated at room temperature for 3 min. Next, the mixture was centrifuged at 14,000 rpm for 15 min at 4°C, after which the resulting upper aqueous phase (400 μL) was transferred to a fresh tube into which 0.5 mL of 2-propanol was also added. After incubation for 10 min at 4°C, the mixture was centrifuged again at 14,000 rpm for 10 min at 4°C. After separation, the supernatant was removed, washed with 1 mL of 75% ethanol, and centrifuged again at 10,000 rpm for 5 min at 4°C. The resulting RNA pellet was then dried, and the purified RNA was dissolved in diethyl pyrocarbonate- (DEPC-) distilled water. Equal amounts of RNA (200 ng) were reverse transcribed (RT) into cDNA using an iScript cDNA synthesis kit (Bio-Rad, Hercules, CA, United States) according to the manufacturer's protocol. Real-time RT polymerase chain reaction (PCR) analysis was performed for selected genes using the CFX96 real-time PCR system (Bio-Rad) and the SYBR green fluorescence quantification system (Bio-Rad) to quantify the amplicons. The PCR conditions were 50 cycles of 95°C (30 s) and 58°C (30 s) and a standard denaturation curve. The primer sequences are listed in the 5′ to 3′ orientation in Supplementary Table 2. The PCR conditions for each target were optimized according to the primer concentration, the absence of primer dimer formation, and the efficiency of amplification of both the target genes and the housekeeping control gene. PCR reaction mixture comprised 1 μL of cDNA and 9.5 μL of PCR master mix, which contained 2× SYBR Green, 10 pmol each of the forward and reverse primers, and 4.5 μL of DEPC-distilled water in a final volume of 15 μL. To normalize the cDNA content of the samples, we used the comparative threshold (CT) cycle method, which includes normalization of the number of target gene copies vs. the endogenous reference gene glyceraldehyde 3-phosphate dehydrogenase. The CT is defined as the fractional cycle number at which the fluorescence generated by cleavage of the probe passes a fixed threshold baseline when amplification of the PCR products is first detected.

2.8. Differentiated PC12 Cell and Microglial BV2 Cell Culture. The pheochromocytoma PC12 cell line, derived from the rat adrenal medulla, was obtained from the Korean Cell Line Bank (#21721). PC12 cells were maintained in Roswell Park Memorial Institute medium (Gibco, MD, USA) supplemented with 10% heat-inactivated fetal bovine serum (Gibco) and 1% penicillin/streptomycin (Gibco) in an atmosphere of 95% air and 5% CO_2 at 37°C. The PC12 cells were seeded on 96-well plates or 6-well plates at a density of 1 or 2×10^5 cells/mL and treated with CP (0–1000 μg/mL) for 24 h (Figure 1(c)). For differentiated PC12, culturing media were renewed every 2 to 3 days. Cultured PC12 cells were treated with nerve growth factor (Sigma-Aldrich) for 7 days, with fresh medium and reagents supplied every 24 h. The differentiated PC12 cells were treated with CP (1–200 μg/mL) for 1 h. Then, they were stimulated with MPP^+ (100 μM) for an additional 23 h (Figure 1(d)).

The mouse microglial BV2 cell line was kindly donated by Prof. Jung at Seoul National University Hospital in Korea. The cells were kept in Dulbecco's modified Eagle's medium (Gibco) supplemented with 10% heat-inactivated fetal bovine serum and 1% penicillin/streptomycin in an atmosphere of 95% air and 5% CO_2 at 37°C. The BV2 cells were seeded on 24-well plates at a density of 1.5×10^5 cells/mL and treated with CP (0–1000 μg/mL) for 24 h (Figure 1(c)).

2.9. Measurement of Living Cells. Living cells were evaluated using the Cell Counting Kit (CCK-8; Dojindo, Kumamoto, Japan) according to the manufacturer's protocol. In brief, cells were seeded on 96-well plates and treated with CP. The CCK-8 reagent was added to each well, and the mixture was incubated for 4 h. The absorbance was read at 450 nm using the SpectraMax i3 Multi-Mode Detection Platform (Molecular Devices, Sunnyvale, CA, USA). Cell viability was calculated using the following equation: %of living cells left after CP treatment = (mean absorbance in CP – treated cells/mean absorbance in untreated controls) × 100.

2.10. Western Blotting Analysis and Measurement of Mitochondrial Membrane Potential. Western blotting was performed according to previously published methods [28, 35, 36]. Moreover, $\Delta\psi$m was monitored with the lipophilic cationic probe tetraethylbenzimidazolylcarbocyanine iodide (JC-1) reagent, supplied with the $\Delta\psi$m detection kit, according to the manufacturer's instructions. Differentiated PC12 cells were seeded on coverslips in 96-well plates and treated simultaneously with CP at concentrations of 1, 10, or 50 μg/mL and 100 μM MPP^+ for 24 h. Then, the cells were rinsed with PBS and incubated with the diluted lipophilic cationic probe 5,5′,6,6′-tetrachloro-1,1′,3,3′-tetraethylbenzimidazol-carbocyanine iodide (JC-1)

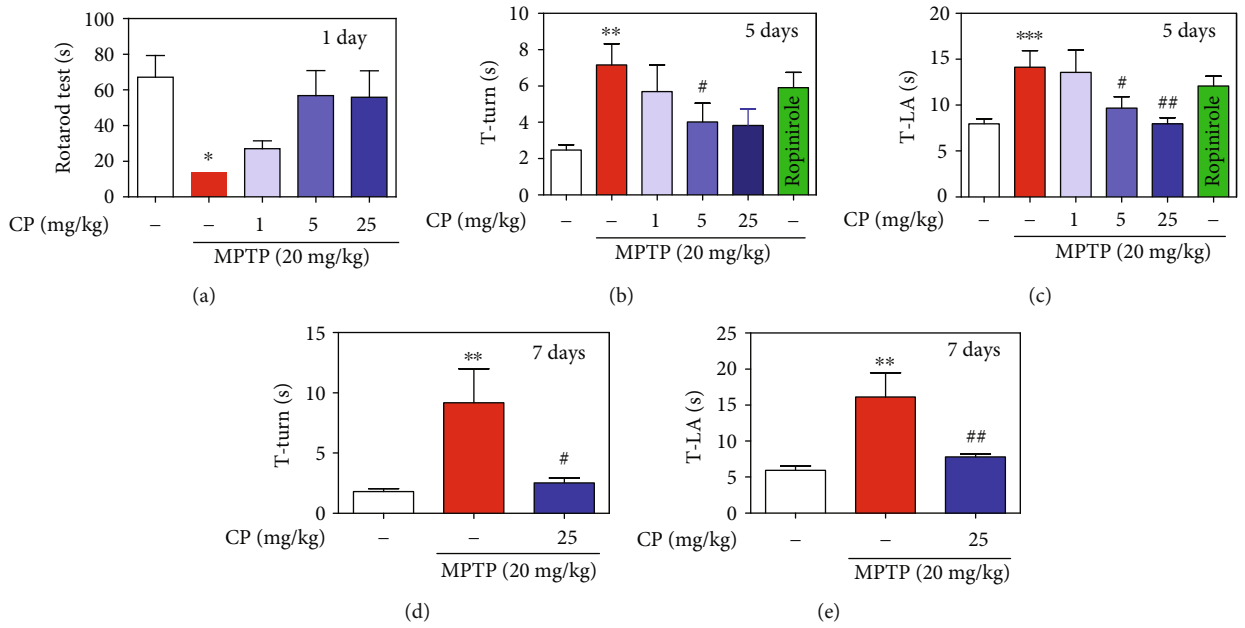

Figure 2: Effects of CP on MPTP-induced movement impairment in mice. CP was administered for 5 days. On day 3, at 2 h after CP administration, MPTP was injected four times. One day after MPTP injection, latency time on the rotating rod was recorded with a 300 s cut-off limit (a). At days 5 and 7 after MPTP injection, time to turn completely downward (b, d) and time to fall off the rod onto the floor (c, e) were recorded with a 60 s cut-off limit. Values shown represent means ± S.E.M. $^{*}p < 0.05$, $^{**}p < 0.01$, and $^{***}p < 0.001$ compared with the control group and $^{\#}p < 0.05$ and $^{\#\#}p < 0.01$ compared with the MPTP-treated group.

at 37°C for 30 min, after which the cells were washed and transferred to 96-well plates. The ratio of red (585/590 nm) and green (510/527 nm) fluorescence was determined using a fluorescence plate reader.

2.11. Small Interfering RNA Transfection. Differentiated PC12 cells were used at a confluence of 80–85% in 100 mm dishes. Cells were transfected with stealth small interfering RNA (siRNA) using Lipofectamine 2000 (Invitrogen). Lipofectamine 2000 (10 μL) was mixed with 40 μM siRNA solution (an equimolar mix of both Nurr1 siRNA and scrambled siRNA) and 2.5 mL of Opti-MEM (Gibco). After 30 min at room temperature, 300 μL of the mix was added to 300 μL of serum-free RPMI in each dish and incubated for 24 h.

2.12. Dopamine and Cytokine Array Levels. The dopamine contents in the ST of the mouse brain were assessed using a commercially available fluorometric assay kit, following the protocol supplied by the manufacturer (Rocky Mountain Diagnostics). Moreover, cytokine proteins were determined using a cytokine membrane array kit following the manufacturer's instructions (R&D Systems, Minneapolis, MN, USA).

2.13. Statistical Analyses. All statistical parameters were calculated using the GraphPad Prism 7.0 software (GraphPad Software, San Diego, CA, USA). Values are expressed as means ± standard error of the mean (S.E.M.). Statistical comparisons between the different treatments were performed using one-way analysis of variance (ANOVA) with Tukey's multiple comparison posttest. A p value < 0.05 was considered to be statistically significant.

3. Results

3.1. Effect of CP on MPTP-Induced Movement Impairment. To examine the effect of CP on MPTP-induced poor motor coordination and postural balance, a rotarod test was performed. We found that MPTP significantly decreased the retention time to 13.71 ± 2.06 s on day 1, compared with the control. However, retention times were significantly increased in the MPTP+1–25 mg/kg/day CP and ropinirole groups from 27.14 ± 4.31 to 56.86 ± 13.99 s and 55.86 ± 14.81 s, respectively, on day 1 (Figure 2(a)). In addition, to evaluate the effects of CP on MPTP-induced bradykinesia, a pole test was performed. T-turn and T-LA were significantly prolonged to 7.17 ± 1.10s and 14.13 ± 1.72 s, respectively, on day 5, compared with the control. However, T-turn was significantly shortened in the MPTP+1–25 mg/kg/day CP and ropinirole groups from 5.70 ± 1.41 to 3.83 ± 0.76 s and 5.91 ± 0.81 s, respectively, on day 5. However, T-LA was significantly shortened in the MPTP+1–25 mg/kg/day CP and ropinirole groups from 13.58 ± 2.34 to 7.97 ± 0.63 s and 12.09 ± 1.02 s, respectively, on day 5 (Figures 2(b) and 2(c)). T-turn and T-LA were significantly prolonged to 9.18 ± 2.23 s and 16.12 ± 2.66 s, respectively, on day 7, compared with the control. However, T-turn and T-LA were significantly shortened in the MPTP 25 mg/kg/day CP groups to 2.52 ± 0.40 s and 7.79 ± 0.40 s, respectively, on day 7 (Figures 2(d) and 2(e)).

3.2. Effects of CP on MPTP-Induced Dopaminergic Neuronal Loss and Dopamine Depletion. To confirm the effects of CP on dopaminergic neuronal death, we performed TH-specific immunohistochemistry in the SNPC and ST

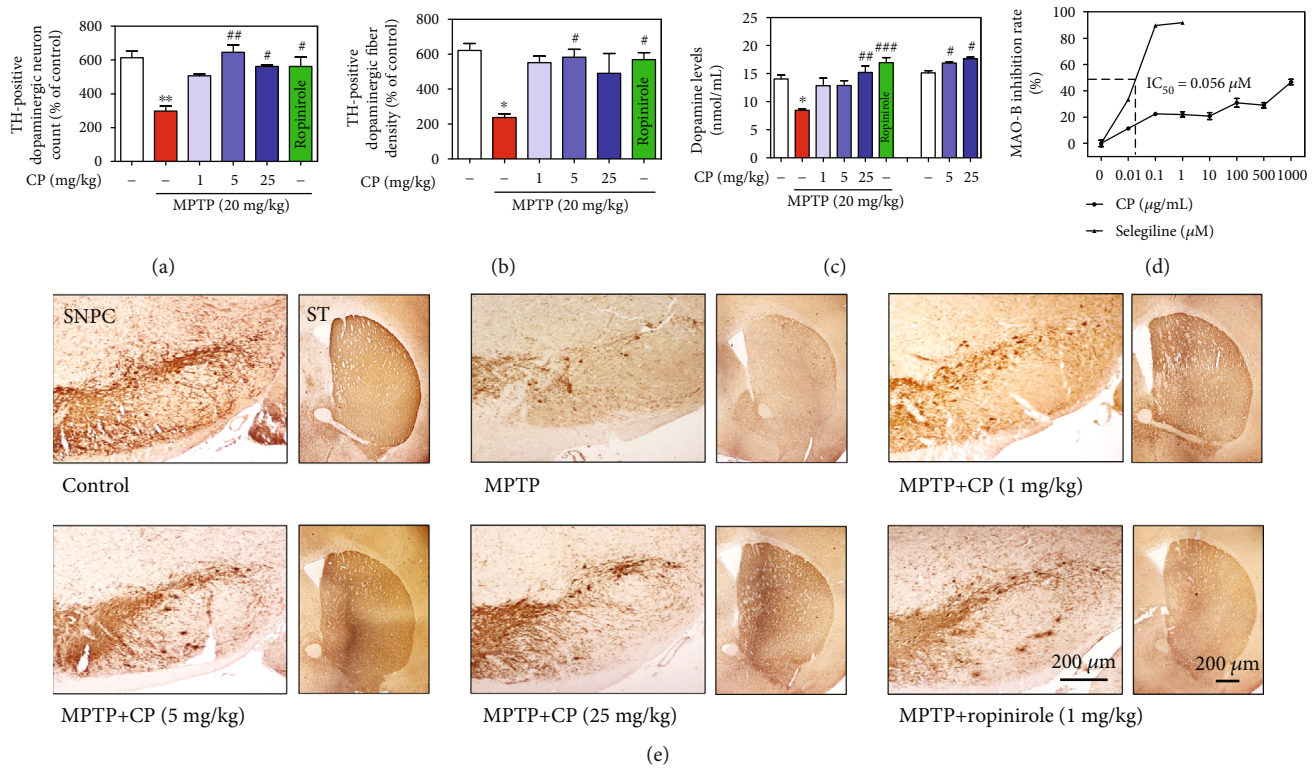

Figure 3: Effects of CP on MPTP-induced dopaminergic neuronal death. Dopaminergic neurons were visualized by TH-specific immunostaining. The number of TH-immunopositive neurons in the SNPC (a) was counted, and the optical density in the ST (b) was measured. Dopamine levels in the ST were measured using ELISA (c). MAO-B inhibition rate in a cell-free system was measured using ELISA (d). Representative photomicrographs of the SNPC and ST were taken (e). Values are presented as means ± S.E.M. $^{*}p < 0.05$, $^{**}p < 0.01$, and $^{***}p < 0.001$ compared with the control group and $^{\#}p < 0.05$, $^{\#\#}p < 0.01$, and $^{\#\#\#}p < 0.001$ compared with the MPTP-treated group (a, b, or c) or control group (c in the cell-free system).

of mouse brains. In MPTP-treated mice, the number of TH-positive cells in the SNPC and the optical intensity in the ST were decreased by 48.51 ± 3.85% and 38.20 ± 3.37%, respectively, compared with the control group. However, these values were significantly increased by 1–25 mg/kg CP or ropinirole treatment (82.64 ± 1.31% to 91.50 ± 1.31% and 91.61 ± 7.30% and 88.88 ± 4.75% to 79.01 ± 18.21% and 91.64 ± 6.30%, respectively, compared with the control group) (Figures 3(a), 3(b), and 3(e)). Moreover, to measure the effects of CP on dopamine levels, we determined striatal dopamine levels in the ST of mouse brains (Figure 3(c)). Treatment with MPTP significantly decreased striatal dopamine (by 8.47 ± 0.25 nmol/mL) compared with the control group, while treatment with 1–25 mg/kg CP or ropinirole reduced MPTP-induced striatal dopamine (by 12.84 ± 1.36 to 15.20 ± 1.18 nmol/mL and 16.94 ± 0.93 nmol/mL). Moreover, only the treatment with 5–25 mg/kg CP increased striatal dopamine (by 16.86 ± 0.21 to 17.65 ± 0.29 nmol/mL) compared with the control group (Figure 3(c)). We also investigated the effect of CP on MAO-B activity. Selegiline (positive control, 0–1 μM) inhibited MAO-B activity in a dose-dependent manner; in contrast, CP had no effect on MAO-B activity (Figure 3(d)).

3.3. Effects of CP on the Induction of Nurr1 and Its Regulating Proteins and Dopamine Depletion. Treatment with CP at 100 μg/mL, but not at 1–50 μg/mL, increased neuronal shrinkage and damage and decreased dendritic length of PC12 and differentiated PC12 cells 24 h after treatment (Figures 4(a) and 4(b)). Thus, all further experiments were performed with CP at 1–50 μg/mL. To investigate the effects of CP on Nurr1 and its regulating proteins, we determined the levels of Nurr1, TH, DDC, DAT, and VMAT2 in differentiated PC12 cells. The protein expression levels of Nurr1, TH, DDC, DAT, and VMAT2 were increased 20 h after CP treatment (Nurr1: 95.42 ± 8.31% to 226.96 ± 22.30%, TH: 152.26 ± 14.77% to 272.45 ± 29.81%, DDC: 128.03 ± 2.89% to 173.43 ± 22.66%, DAT: 118.17 ± 6.47% to 278.32 ± 29.55%, and VMAT2: 147.26 ± 3.32% to 203.69 ± 31.21% compared with the control group) (Figures 4(c) and 4(f)–4(j)). We confirmed the effects of CP on Nurr1 and its regulating proteins in the mouse SNPC (Nurr1: 201.02 ± 32.55%, TH: 197.50 ± 33.64%, DDC: 161.74 ± 27.33%, DAT: 140.97 ± 14.67%, and VMAT2: 142.77 ± 22.56% compared with the control group) (Figures 4(d) and 4(f)–4(j)).

To investigate whether ERK activation contributed to CP-induced increased Nurr1 expression, we used SCH772984, a selective inhibitor of ERK. SCH772984 inhibited a CP-induced increase in Nurr1, TH, DDC, DAT, and VMAT2 in differentiated PC12 cells (Nurr1: 196.24 ± 30.19% and 94.31 ± 11.10%, TH: 258.87 ± 33.33% and 111.47 ± 19.10%, DDC: 166.88 ± 23.84% and 68.21 ± 7.94%,

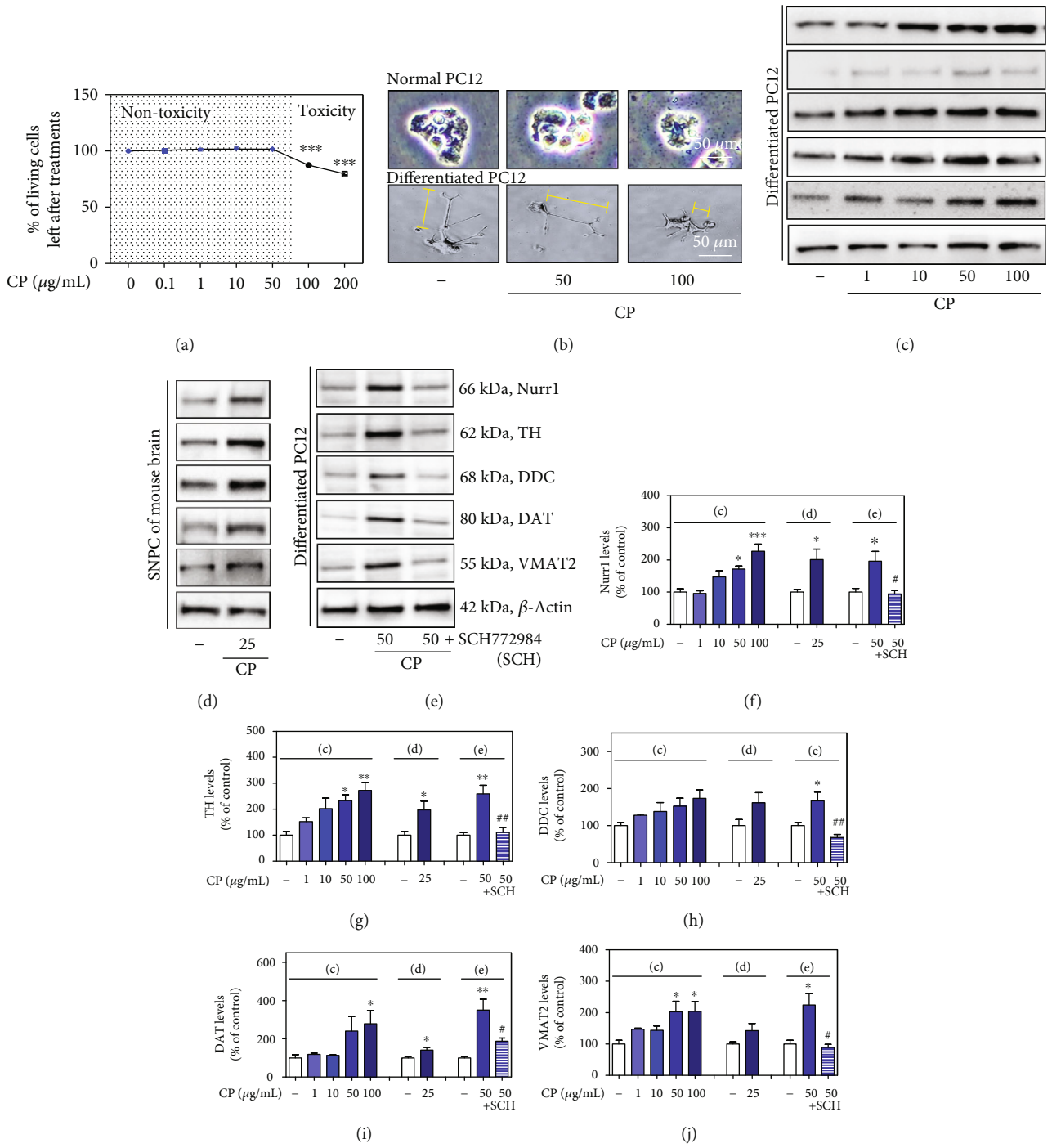

FIGURE 4: Effects of CP on cell viability and Nurr1 and its regulating neurotrophic factors. Effects of CP on PC12 and differentiated PC12 cell neuronal damage (a, b). The protein levels of Nurr1 and its regulating neurotrophic factors were measured by western blotting in differentiated PC12 cells (c) and the mouse SNPC (d). Differentiated PC12 cells were pretreated with CP and an ERK inhibitor (SCH) for 10 h, and the protein levels of Nurr1 and its regulating neurotrophic factors were measured by western blotting (e). β-Actin protein was used as an internal control. Bar graphs represent the relative expression of Nurr1 (f), TH (g), DDC (h), DAT (i), and VMAT2 (j) for (c)–(e). Values are presented as means ± S.E.M. $^{*}p < 0.05$, $^{**}p < 0.01$, and $^{***}p < 0.001$ compared with the control group and $^{\#}p < 0.05$ and $^{\#\#}p < 0.01$ compared with the CP-treated group.

DAT: 350.47 ± 56.53% and 187.24 ± 16.89%, and VMAT2: 224.09 ± 36.33% and 89.09 ± 10.16% compared with the control group) (Figures 4(e) and 4(f)–4(j)).

3.4. Effects of CP on MPTP-Induced Nurr1 Expression in Dopaminergic Neurons. To evaluate the effects of CP on Nurr1 expression, we performed Nurr1-specific

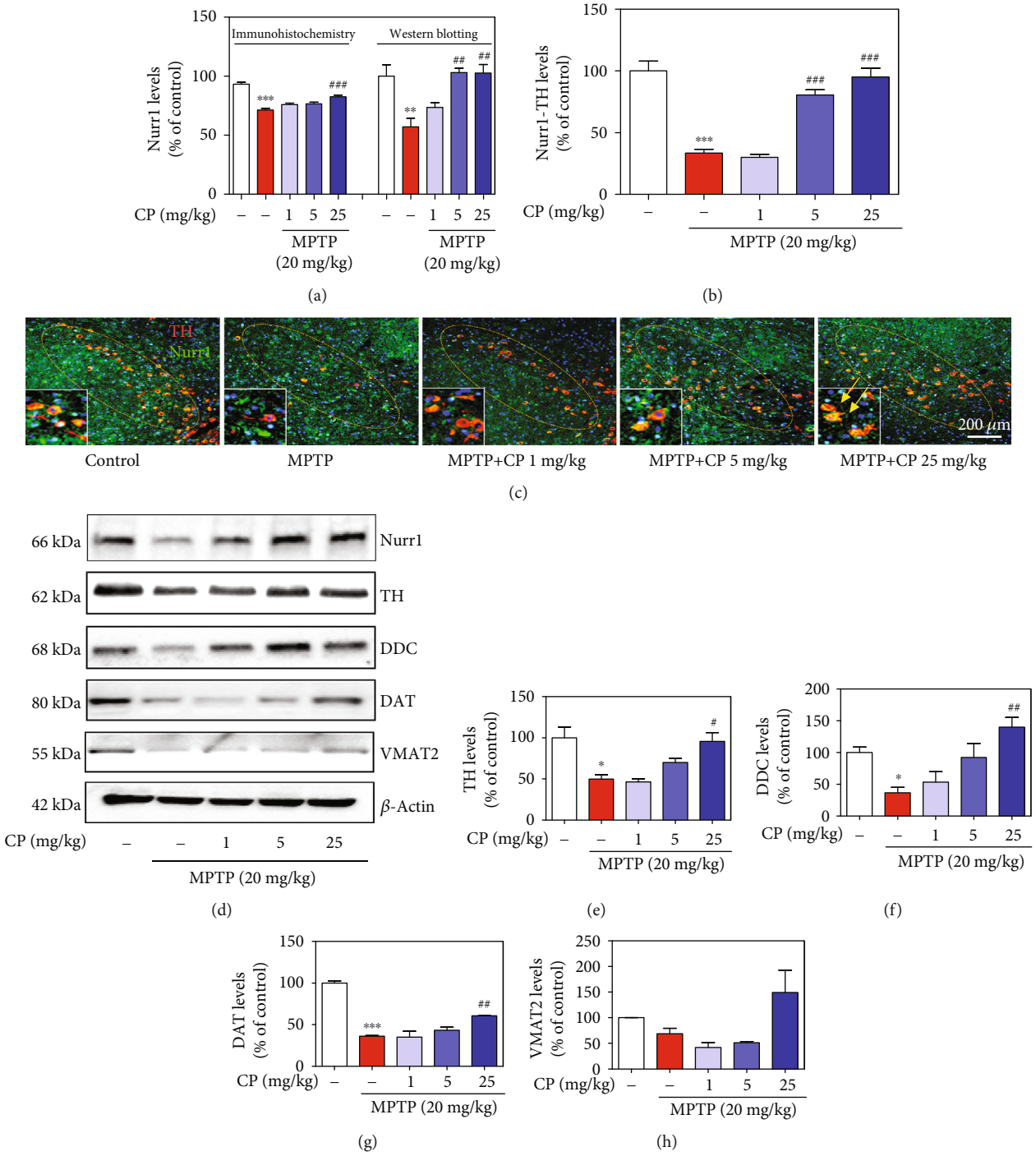

Figure 5: Effects of CP on MPTP-induced Nurr1 and neurotrophic proteins. Seven days after the last MPTP treatment, Nurr1 levels were measured by IHC in dopaminergic neurons (a, b) and western blotting in the SNPC (a). Representative photomicrographs of the SNPC were taken (c). The expressions of Nurr1, TH, DDC, DAT, and VMAT2 were detected by western blotting using specific antibodies in the SNPC (d). β-Actin protein was used as an internal control. Bar graphs represent the relative expression of Nurr1 (a), TH (e), DDC (f), DAT (g), and VMAT2 (h) for (d). Values shown represent means ± S.E.M. $^{*}p < 0.05$ and $^{***}p < 0.001$ compared with the control group and $^{\#}p < 0.05$ and $^{\#\#}p < 0.01$ compared with the MPTP-treated group.

immunofluorescence staining and western blotting. MPTP significantly decreased Nurr1 (by 71.49 ± 1.27%) in shrunken dopaminergic neurons (by 33.40 ± 3.17%) compared with the control, and treatment with 5–25 mg/kg CP reduced MPTP-induced Nurr1 (by 76.08 ± 1.15% to 82.67 ± 1.30%) and Nurr1 in dopaminergic neurons further (by 30.06 ± 2.40% to 95.06 ± 7.22%) (Figures 5(a)–5(c)). Moreover, we confirmed Nurr1 expression levels by western blotting, and MPTP significantly decreased Nurr1 (by 33.40 ± 3.13%) in the SNPC, compared with the control,

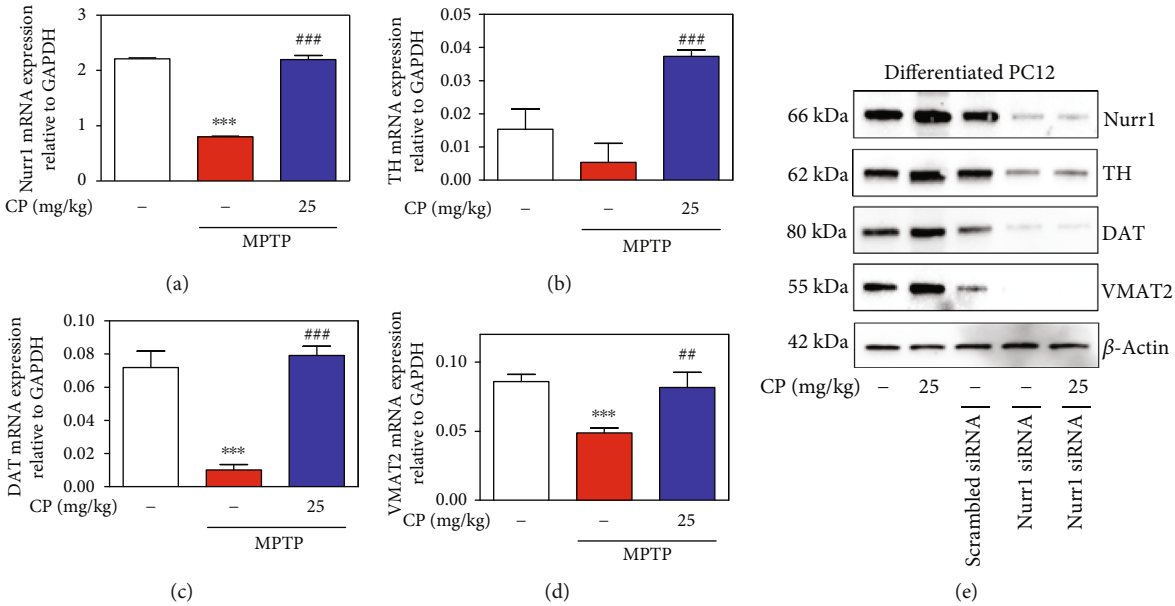

Figure 6: Effects of CP on MPTP-induced mRNA levels of Nurr1 and its regulating neurotrophic factors. Real-time RT-PCR was performed to see the effects of CP on mRNA expression of Nurr1 (a), TH (b), DAT (c), and VMAT2 (d). Then, effects of Nurr1 on upregulating neurotrophic factors (TH, DAT, and VMAT2) in Nurr1 siRNA-transfected differentiated PC12 cells (e). Values shown represent means ± S.E.M. $^{***}p < 0.001$ compared with the control group and $^{\#\#}p < 0.01$ and $^{\#\#\#}p < 0.001$ compared with the MPTP-treated group.

and treatment with 5–25 mg/kg CP reduced MPTP-induced Nurr1 (by 30.06 ± 2.34% to 95.06 ± 7.07%) (Figures 5(a)–5(d)). Representative photomicrographs were taken of double-labeled immunofluorescence staining with anti-Nurr1 and anti-TH antibodies in the SNPC (Figure 5(c) and Supplementary Fig. 1).

3.5. Effects of CP on MPTP-Induced Expression of Nurr1 Regulating Proteins. To evaluate the effects of CP on MPTP-induced expression of Nurr1 and its regulating proteins, we assessed the levels of TH, DDC, DAT, and VMAT2 in the mouse SNPC by western blotting. MPTP significantly decreased TH (by 49.87 ± 5.21%), DDC (by 36.73 ± 8.28%), DAT (by 36.17 ± 0.97%), and VMAT2 (by 69.12 ± 10.67%) levels, compared with the control, while treatment with 1–25 mg/kg CP reduced MPTP-induced expression of TH (by 46.31 ± 3.94% to 95.71 ± 10.59%), DDC (by 53.45 ± 16.29% to 140.27 ± 15.04%), DAT (by 34.98 ± 7.3% to 60.85 ± 1.08%), and VMAT2 (by 42.14 ± 9.55% to 149.34 ± 43.42%), compared with the control group (Figures 5(d)–5(h)). In addition, we measured the mRNA expression levels of Nurr1 and its regulating proteins using real-time RT-PCR analysis. MPTP significantly decreased Nurr1 (by 0.82 ± 0.01), TH (by 0.01 ± 0.01), DAT (by 0.01 ± 0.003), and VMAT2 (by 0.05 ± 0.003) levels, while treatment with 25 mg/kg CP reduced MPTP-induced expression of Nurr1 (by 2.20 ± 0.08), TH (by 0.04 ± 0.001), DAT (by 0.08 ± 0.01), and VMAT2 (by 0.08 ± 0.01) (Figures 6(a)–6(d)). Moreover, to further verify whether CP-induced TH, DAT, and VMAT2 were mediated through Nurr1 activation, we transfected differentiated PC12 cells with siRNA targeting Nurr1. Results showed that TH, DAT, and VMAT2 levels were not affected by CP in Nurr1 siRNA-transfected cells (Figure 6(e)).

3.6. Effects of CP on MPTP-Induced Mitochondrial Dysfunction and Mitochondria-Mediated Apoptosis. To investigate whether CP affects mitochondrial dysfunction and mitochondria-mediated apoptosis, we assessed the mitochondrial membrane potential in differentiated PC12 cells and the levels of Bcl-2, Bax, Cyt-c, poly (ADP-ribose) polymerase (PARP), cleaved caspase-9, and cleaved caspase-3 in the mouse SNPC. MPTP caused a significant decrease in Bcl-2 and an increase in Bax, Cyt-c, PARP, cleaved caspase-9, and cleaved caspase-3, while 1, 5, or 25 mg/kg CP increased Bcl-2 and decreased Bax, Cyt-c, PARP, cleaved caspase-9, and cleaved caspase-3 (Figure 7(a)). Green fluorescence (monomeric form, low $\Delta\psi$m) and red fluorescence (aggregate form, high $\Delta\psi$m) indicate $\Delta\psi$m depolarization. MPP^+-induced toxicity decreased $\Delta\psi$m (by 4.64 ± 0.08 ratio), whereas CP pretreatment prevented depolarization of the mitochondrial membrane (by 1.99 ± 0.05 to 1.42 ± 0.07 ratio) (Figures 7(b) and 7(c)).

3.7. Effects of CP on MPTP-Induced Expression of Glial Cell Line-Derived Neurotrophic Factor (GDNF) and Ret in the SNPC. To investigate whether CP affects dopaminergic production, we assessed the levels of GDNF and Ret in the mouse SNPC. MPTP significantly decreased the expression of GDNF and Ret, while 5 or 25 mg/kg CP treatment increased the levels of GDNF and Ret (Figure 7(d)). Using an enzyme-linked immunosorbent assay (ELISA) kit, we found that MPTP decreased GDNF in the SNPC (by 1.80 ± 0.54 pg/mL) and ST (by 2.45 ± 1.30 pg/mL), while treatment with 1–25 mg/kg CP reduced the MPTP-induced expression

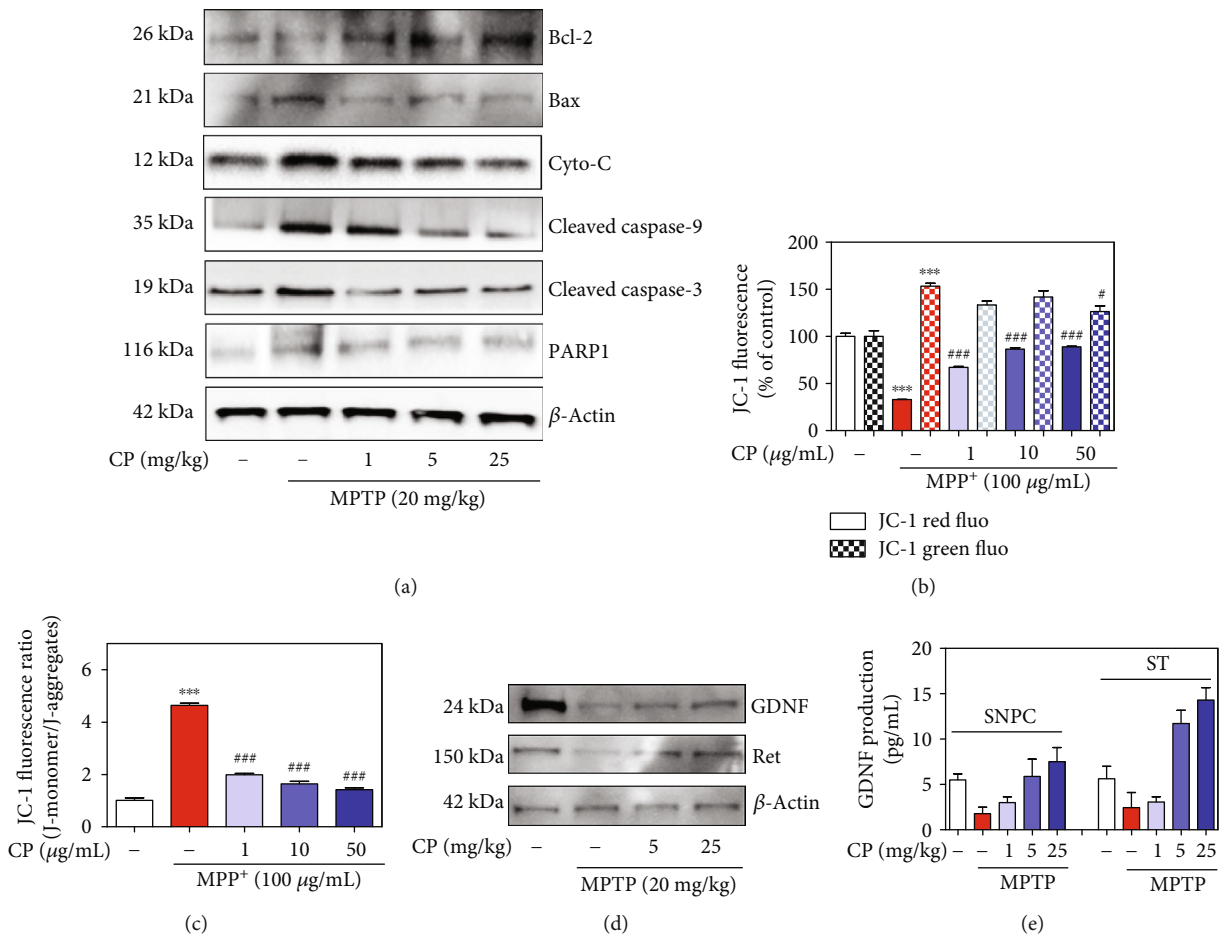

FIGURE 7: Effects of CP on MPTP-induced mitochondria-mediated apoptosis. Seven days after the last MPTP treatment, mitochondria-induced apoptotic factors (Bcl-2, Bax, Cyt-c, cleaved caspase-9, cleaved caspase-3, and PARP1) were measured by western blotting (a). Differentiated PC12 cells were treated with CP and exposed to MPP^+ for 48 h. Moreover, red and green (b) and the ratio (c) of these fluoresces of mitochondrial membrane potential were expressed as a percentage of control. Effects of CP on MPTP-induced survival-related GDNF signaling. Its factors (GDNF and Ret) were measured by western blotting (d) and ELISA kit (e). Values are presented as means ± S.E.M. $^{***}p < 0.001$ compared with the control group and $^{\#}p < 0.05$ or $^{\#\#\#}p < 0.001$ compared with the MPP^+- or MPTP-treated group.

of GDNF in the SNPC (by 3.01 ± 0.63 to 7.51 ± 1.55 pg/mL) and ST (by 3.08 ± 0.56 to 14.30 ± 1.35 pg/mL) (Figure 7(e)).

3.8. Effects of CP on MPTP- or LPS-Induced Glial/Microglial Activation and Neuroinflammatory Factor Production. To investigate whether CP affects the neuroinflammatory response, we assessed glial/microglial activation and the levels of neuroinflammatory factors in microglial BV2 cells and the mouse SNPC. We measured the expression levels of GFAP, Iba-1, iNOS, and Cox-2, which are released following inflammatory stimuli, by western blotting. Western blotting analysis revealed that the levels of GFAP, Iba-1, iNOS, and Cox-2 were significantly increased (by 482.97 ± 28.90%, 384.06 ± 65.22%, 264.07 ± 77.82%, and 179.78 ± 11.50%, respectively) in the SNPC of the MPTP-treated group. In contrast, CP suppressed this decrease in GFAP, Iba-1, iNOS, and Cox-2 (by 381.29 ± 19.15% to 52.02 ± 24.48%, 407.13 ± 85.73% to 124.79 ± 19.71%, 164.17 ± 23.04% to 63.20 ± 24.39%, and 109.09 ± 23.71% to 92.02 ± 2.36%, respectively) (Figures 8(a)–8(f)). Representative photomicrographs were taken of immunofluorescence staining with anti-Cox-2, GFAP, and Iba-1 antibodies in the SNPC (Figures 8(b) and 8(g)). Microglial BV2 cell cytotoxicity was not affected by 1–62.5 μg/mL CP, as assessed by the MTT assay at 24 h after treatment. However, 125–1000 μg/mL CP increased cytotoxicity (data not shown). Thus, all further experiments were performed with CP at 1–62.5 μg/mL. Cytokine array kits revealed that the levels of intercellular adhesion molecule 1 (ICAM-1), interleukin-6 (IL-6), KC, MCP-5, and RANTES were significantly increased (by 205.03 ± 4.24%, 3468.59 ± 51.63%, 687.96 ± 6.04%, 336.64 ± 0.07%, and 192.58 ± 1.65%, respectively) in LPS-treated microglial BV2 cells. In contrast, CP suppressed the increase in ICAM-1, IL-6, KC, monocyte chemotactic protein 5 (MCP-5), and RANTES (by 62.45 ± 12.28%, 2185.72 ± 11.60%, 102.53 ± 2.19%, 168.26 ± 3.22%, and 104.78 ± 0.46%, respectively) (Figures 9(a)–9(f)). The levels of iNOS and Cox-2 were also significantly increased (by 235.75 ±

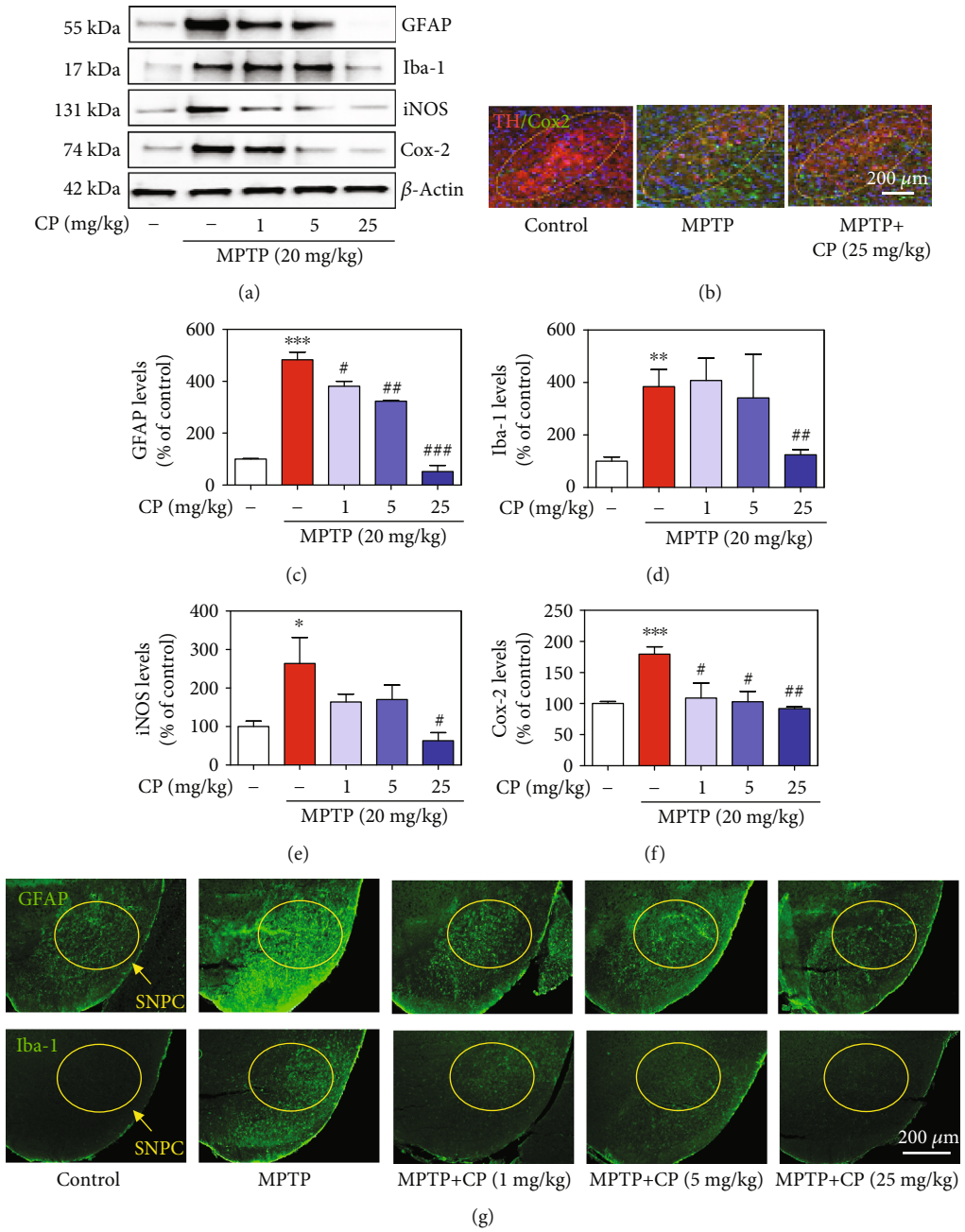

Figure 8: Effects of CP on MPTP-induced neuroinflammatory signaling factors. One day after the last MPTP treatment, glial activation proteins (GFAP and Iba-1) and neuroinflammatory signaling factors (iNOS and Cox-2) were measured by western blotting or IHC (a, b). Levels of neuroinflammatory signaling factors were normalized to β-actin (c–f). Moreover, representative photomicrographs of the SNPC were taken (g). Values shown represent means ± S.E.M. $^{*}p < 0.05$, $^{**}p < 0.01$, and $^{***}p < 0.001$ compared with the control group and $^{\#}p < 0.05$, $^{\#\#}p < 0.01$, and $^{\#\#\#}p < 0.001$ compared with the MPTP-treated group.

18.69% and 555.89 ± 55.49%, respectively) in the SNPC of the LPS-treated group. Moreover, CP treatment suppressed this increase in iNOS and Cox-2 (by 118.92 ± 10.06% and 301.61 ± 58.46%) (Figures 9(g) and 9(h)).

4. Discussion

Many intrinsic signals and extrinsic transcription factors have been identified to play critical roles in dopaminergic neuronal development in the midbrain in PD. This process depends on two major signaling pathways: (i) Sonic hedgehog/FoxA2 and (ii) wingless-type MMTV integration site family, member 1/Lmx1a, and their downstream signaling molecules [37, 38]. These two signaling pathways merge to control the expression levels of Nurr1, suggesting Nurr1 as a key regulator of dopaminergic neurons [39, 40]. Indeed, dopaminergic neurons fail to develop in mice lacking the Nurr1 receptor [12]. We used the VOSviewer software to

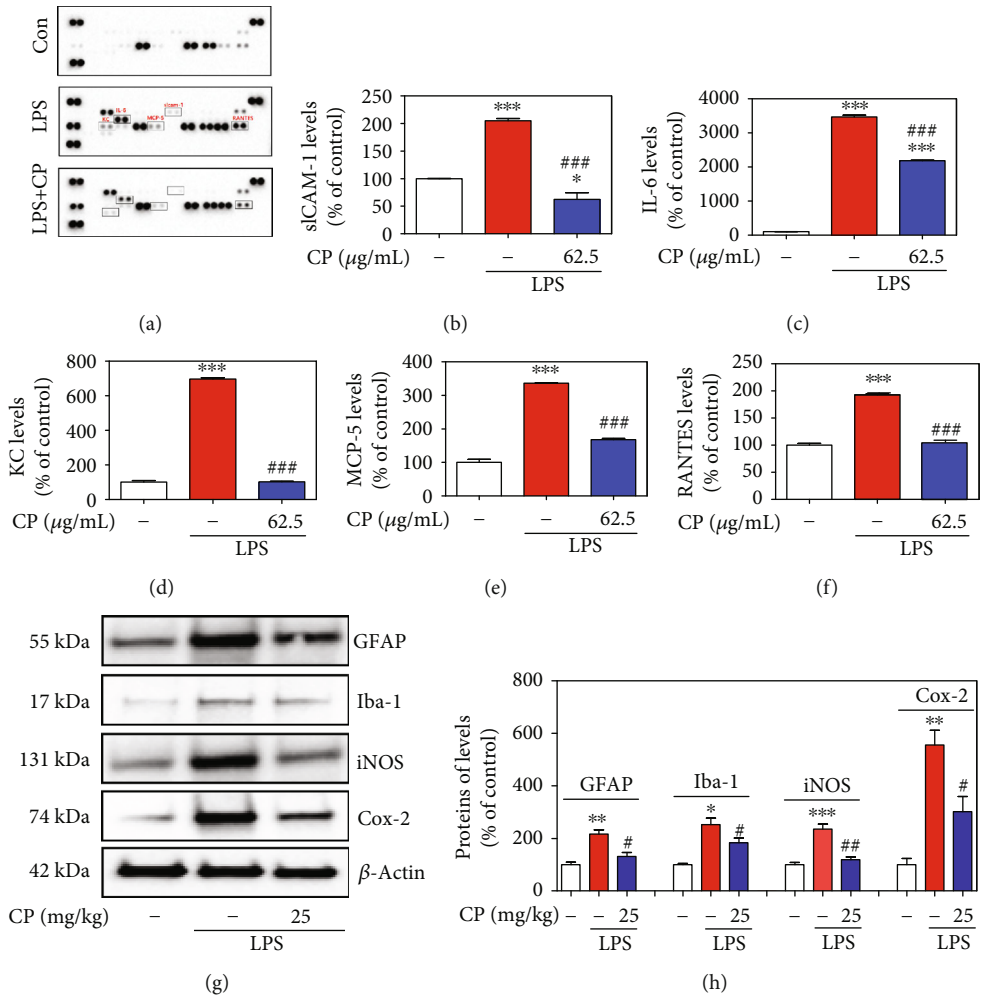

Figure 9: Effects of CP on LPS-induced neuroinflammatory signaling factors. Microglial BV2 cells were treated with CP for 2 h and with LPS for an additional 22 h. After 24 h incubation, the cultures were subjected to a cytokine antibody array assay (h). Densitometric ratios of the arrays showed differences in the cytokine markers (ICAM-1, KC, IL-6, MCP-5, and RANTES) (i–m). The glial activation markers (GFAP and Iba-1) and neuroinflammatory signaling factors (iNOS and Cox-2) were measured using western blotting (n). Bar graphs represent the relative expression of GFAP, Iba-1, iNOS, and Cox-2 (o) for (n). Values shown represent means ± S.E.M. $^{*}p < 0.05$, $^{**}p < 0.01$, and $^{***}p < 0.001$ compared with the control group and $^{\#}p < 0.05$, $^{\#\#}p < 0.01$, and $^{\#\#\#}p < 0.001$ compared with the LPS-treated group.

visualize network similarities [41, 42]. We found a cluster of keywords across publications related to Nurr1, Alzheimer's disease pathology, PD, dopaminergic neurons, GDNF, alpha-synuclein, canonical ligand-binding pocket, and cilostazol (Supplementary Fig. 2). These results led us to think that Nurr1 may be a promising target in the treatment of PD.

According to the WHO, as much as 80% of the world's population relies primarily on animal- and plant-based medicines [43–45]. Animal-assisted therapy is known as zootherapy (ZT) [45]. The phenomenon of ZT is marked both by a broad geographical distribution and very deep historical origins [45]. Despite its importance, studies on ZT have been neglected, when compared to those on plant-based therapies. However, in modern societies, ZT constitutes an important alternative to other therapies practiced worldwide [45]. Wild and domestic animals and their by-products (e.g., hooves, skins, bones, feathers, and tusks) provide important ingredients to curative, protective, and preventive medicine [46–48]. Recently, there has been increased interest in animal-based medicines, and several animals have been tested by pharmaceutical companies as potential sources of modern drugs [49]. Based on the previous study on Nurr1, we screened a Korean traditional medicine library composed of clinically used drugs (Chung-bu category in *Dongui Bogam*) and identified one hit drug. A previous report showed that Nurr1 promotes dopaminergic neuronal development by inducing the expression of neurotrophic factors, such as TH, DDC, DAT, and VMAT2 [4, 27]. Dopamine is transported into synaptic vesicles by VMAT2, a major factor in maintaining dopamine homeostasis in dopaminergic presynaptic terminals [50, 51]. It has also been demonstrated that Nurr1 gene expression in peripheral blood lymphocytes of patients with PD is decreased compared to that of healthy people [10]. In the present study, CP increased the levels of Nurr1 and its

regulating proteins, TH, DDC, DAT, and VMAT2, in differentiated PC12 cells and the mouse SNPC. Moreover, Nurr1 knockdown using siRNA blocked a CP-mediated increase in TH, DAT, and VMAT2 protein expression, suggesting that Nurr1 activation is crucial for CP-induced TH, DAT, and VMAT2 upregulation. Recently, studies have shown that two regions in Nurr1, the N-terminal and C-terminal regions, are important for its transcriptional activation [52]. The Nurr1 N-terminus is important for regulating transcription in a mitogen-activated protein kinase- (MAPK-) dependent manner [52]. It has been reported that Nurr1 can be phosphorylated by ERK1/2 and translocate to the nucleus, where it upregulates TH expression [52–54]. In the present study, an ERK inhibitor inhibited a CP-induced increase in Nurr1, TH, DDC, DAT, and VMAT2 in differentiated PC12 cells. We also found that CP can regulate striatal dopamine levels in the mouse ST. MAO-B is mainly involved in dopamine metabolism [55]. To confirm that the disease-modifying actions of CP could not be ascribed to the prevention of conversion of MPTP to MPP+, we also measured the activity of MAO-B [25, 55]. However, CP had no effect on MAO-B activity. These results suggest that CP increases neurotrophic factors by upregulating Nurr1 expression via ERK phosphorylation. It has been recently suggested that Nurr1 inducers exert neuroprotective effects in experimental models of PD; thus, possible future therapeutic strategies for PD may include inducing Nurr1 signaling by CP.

The above-described findings prompted us to test whether CP can ameliorate motor behavior deficits in a mouse model of MPTP-induced PD. This animal model is used widely because dopaminergic neuronal loss in the SNPC and ST is associated with the onset of motor symptoms, and there is a direct relationship between the extent of dopamine loss and motor dysfunction [28, 56]. The pole test assesses animal agility and includes measures of muscle rigidity and bradykinesia [57]. The rotarod test can be used to assess motor coordination and postural balance [57]. In the pole test, CP-treated mice showed a significant improvement in T-turn and T-LA, with measurements similar to those in the control group. In addition, in the rotarod test, CP prolonged the duration spent by the mice on the rotarod. Similar to our study, Hsieh et al. reported that CP increases hypomotility induced by a TH inhibitor or 5-hydroxytryptophan (a precursor of serotonin) [21]. Moreover, our results showed that CP significantly increased MPTP-induced dopamine levels. CP can stabilize central catecholaminergic and serotonergic activity and is expected to be effective in various disorders, such as convulsion and insomnia [21]. Therefore, we think there is a need to focus on further studies on catecholamine and behavioral changes. Furthermore, we confirmed these effects by TH-specific IHC, which demonstrated that CP protected both dopaminergic neurons in the SNPC and their fibers in the ST, compared with mice treated with MPTP only. In the present study, the number of TH/Nurr1 double-positive neurons and Nurr1 and its regulating proteins in the SNPC declined in the MPTP group compared with the control group, while colocalization and expression levels were increased in the CP-treated groups. GDNF and its canonical receptor Ret can signal together or independently to fulfill many important functions in the midbrain's dopaminergic system [58, 59]. Nurr1 and Ret, its downstream target, were found to be transcriptionally downregulated by α-synuclein accumulation [60]. Reduced Ret protein levels might prevent GDNF-induced survival response in midbrain dopaminergic neurons [61]. Thus, this rationale linked GDNF/Ret signaling to Nurr1, another protein found to be mutated in a rare familial form of PD (autosomal recessive loss-of-function mutation). In this study, CP significantly protected MPTP-induced GDNF/Ret signaling in mice. Taken together, the present study showed that CP significantly improved MPTP-induced PD-like movement problems and protected against dopaminergic neuronal damage and neurotrophic response activity in mouse dopaminergic neurons.

Finally, because Nurr1 has proapoptotic as well as antiapoptotic effects, we also analyzed the effects of CP on mitochondrial dysfunction and mitochondria-mediated apoptosis. The Bcl-2 protein family contains key apoptosis-regulating proteins that can promote cell survival or induce cell death [62]. Bcl-2 appears to directly or indirectly preserve the integrity of the outer mitochondrial membrane, thus preventing Cyt-c release and mitochondria-mediated cell death initiation [62, 63]. On the other hand, the proapoptotic protein Bax promotes Cyt-c release from the mitochondria, with subsequent cleaved caspase-9/caspase-3 and PARP [63]. Recently, Nurr1 has been shown to downregulate the expression of the proapoptotic protein Bax, which is directly transactivated by the tumor suppressor p53 [64]. Microarray analysis revealed that overexpression of Nurr1 downregulates cleaved caspase-3 and other apoptotic factors in neural stem cells [65]. In this study, MPTP induced a slight decrease in Bcl-2 expression and an increase in Bax expression; CP protected against these changes. Moreover, MPTP-induced toxicity increased Cyt-c, whereas CP inhibited Cyt-c release. The induction of Cyt-c-mediated cleaved caspase-9/caspase-3 and PARP levels by proapoptotic agents, including MPTP, appears to be essential for apoptosis, and treatment with CP prevented the MPTP-induced increase in cleaved caspase-9/caspase-3 and PARP levels. Because Nurr1-induced antiapoptotic effects are associated with pro- as well as anti-inflammatory responses, we also checked the effects of CP on proinflammatory cytokines and signaling molecules. Moreover, Xu et al. demonstrated that CP can decrease inflammatory-related proteins such as IL-6, iNOS, and Cox-2 in LPS-induced Raw 264.7 macrophage cells [20]. Moreover, according to Chang et al., CP inhibits inflammation-related proteins such as IL-6 and NF-κB via modulating reactive oxygen species induced by ultraviolet B irradiation on keratinocyte HaCaT cells [23]. Therefore, it was possible to have an anti-inflammatory effect. In our study, CP repressed neuroinflammatory signaling molecules, such as iNOS and Cox-2, and glial/microglial activation in MPTP- or LPS-treated mice. Moreover, when microglial cells were treated with inflammation-inducing LPS for 24 h, the expression of proinflammatory genes (cytokine array: G-CSF, GM-CSF, sICAM-1, IL-1ra, IL-2, IL-3, IL-5, IL-6, IL-7, IL-12 p70, IL-16, IL-17, IL-23, IP-10, I-TAC, KC,

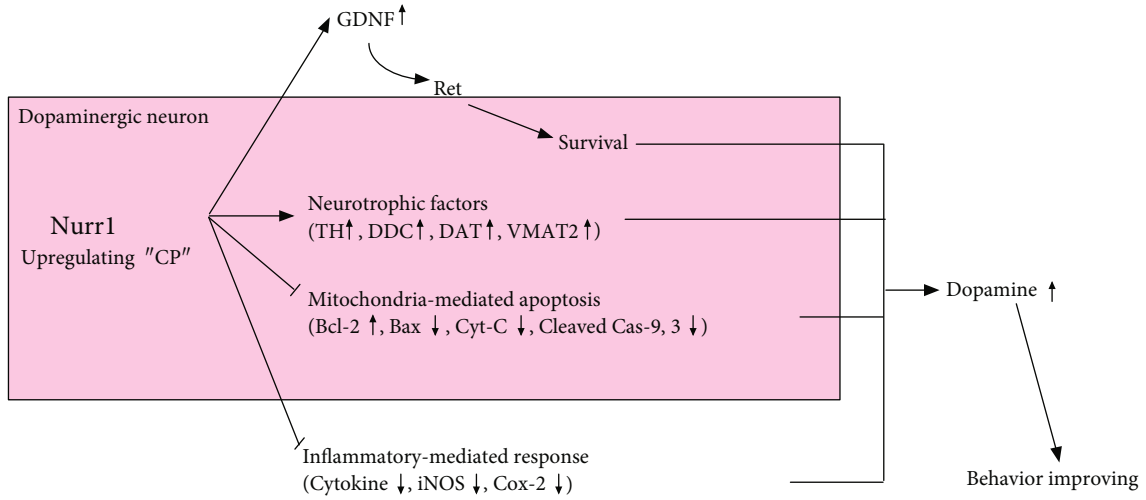

Figure 10: Schematic of the mechanism proposed for the effects of CP on Nurr1 activation and Parkinson's disease pathogenesis.

M-CSF, MCP-5, MIP-2, RANTES, SDF-1, TARC, and TNF-α) was increased more than 2-fold. Remarkably, CP reduced the expression of ICAM-1, KC, IL-6, MCP-5, and RANTES (>30%). However, further studies using Nurr1 transgenic mice will be required to confirm our findings. Next, we analyzed protein-protein interactions using the STRING database and potential molecular mechanisms using the KEGG database (Supplementary Fig. 3). We found functional relationships among the proteins primarily related to inflammatory and neuronal death mechanisms, including small-cell lung cancer, tuberculosis, AGE-RAGE signaling pathway in diabetic complications, apoptosis, amyotrophic lateral sclerosis, hepatitis B, influenza A, platinum drug resistance, pathways in cancer, colorectal cancer, Kaposi's sarcoma-associated herpesvirus infection, toxoplasmosis, TNF signaling pathway, PD, legionellosis, and p53 signaling pathway. Taken together, our data showed that CP enhanced the dual role of Nurr1: CP (i) increased the expression of Nurr1 and its regulating proteins in dopaminergic neurons and (ii) inhibited mitochondria-mediated apoptosis and pro-inflammatory cytokine gene expression.

This study has some limitations. First, we did not investigate the effects of CP on MPTP-induced PD in mice lacking Nurr1. Studies using Nurr1-lacking mice are being carried out; however, more research is still needed because these studies are in their screening stages. Therefore, we confirmed it using siRNA as a pilot study, and we believe that more detailed research is needed through knockout animal models. Second, doses of CP in human were 3-6 g daily [15, 16]. According to human equivalent dose calculation, for body weight of 60 kg, the corresponding human dose of the extract of CP was 121.8 mg/day. Among our unpublished studies, we evaluated the safety of the CP extract using a standard toxicological study design to assess the potential oral dose toxicity. During the study period of 2 weeks, C57BL/6 mice were orally administered once daily with doses of 50, 150, or 450 mg/kg/day of the CP extract after which several study parameters of mortality, clinical signs, changes in body weight, gross findings, organ weight, histopathological examinations, and hematology were assessed. We demonstrated that the CP extract did not have any adverse effects in mice up to a dose of 450 mg/kg/day for a 2-week administration period (data not shown). The human equivalent dose calculated as 121.8 mg/day is 18-fold lower than the 450 mg/kg/day (2189.1 mg/day in human) of the CP extract used in our unpublished study. Therefore, this study provides an important reference for the safety of the CP extract for humans. However, more detailed research on clinicians will not be available until further studies are conducted. Lastly, we did not identify the active compounds of CP that are responsible for its anti-PD effects. In this study, we mainly analyzed and separate catecholamine compounds, focusing on the various neurohormonal changes in insect metamorphosis (Supplementary Fig. 4) [66–68]. This is because we expected a large amount of neurohormones to be released and left in the skin when the insect was exterminated. However, since this study was only a pilot, screening study, we think that more research is needed to reveal more accurate mechanisms. Future studies are needed to analyze the specific contribution of the various active compounds of CP.

In conclusion, we demonstrated that CP increased the expression of Nurr1 and its regulating proteins (TH, DDC, DAT, and VMAT2) in vitro and in vivo (Figure 10). Further, CP protected dopaminergic neurons against MPTP-induced neurotoxicity via regulating mitochondria-mediated apoptotic molecules, such as Bcl-2, Bax, Cyt-c, cleaved caspase-9, caspase-3, and PARP; neuroinflammatory signaling molecules, such as cytokines, iNOS, and Cox-2; and glial/-microglial activation. Our findings suggest that CP might contribute to neuroprotective signaling by regulating neurotrophic factors via Nurr1, mitochondria-mediated apoptosis, and neuroinflammation.

Data Availability

The data used to support the findings of this study are available from the corresponding author upon request.

Ethical Approval

All animals were handled in accordance with the animal care guidelines of the Korea Institute of Oriental Medicine.

Conflicts of Interest

The authors declare no competing financial interests.

Authors' Contributions

Dr. Park and Dr. Lim conceived the idea and designed the experiments. Dr. Lim, Dr. Kim, Dr. Moon, Dr. Choi, Dr. Ryu, Dr. Lee, Ms. Ang, Ms. Jeon, Prof. Moon, and Dr. Park performed the experiments and performed data analysis. Dr. Park and Dr. Lim assisted in data interpretation and manuscript preparation and wrote the entire manuscript. All authors commented on and approved the manuscript.

Acknowledgments

We thank Prof. Dr. H. Yoo (Clinical Trial Center, Dunsan Korean Medicine Hospital) for correcting the clinical part of the manuscript. This work was supported by a grant on the Establishment of Application Base for Chung-bu Medicinal Materials Described in the Dong Ui Bo Gam (KSN1812410) from the Korea Institute of Oriental Medicine, Republic of Korea.

Supplementary Materials

Supplementary Fig. 1: effects of PC on MPTP-induced Nurr1 levels. Seven days after the last MPTP treatment, Nurr1 levels were measured by immunofluorescence in dopaminergic neurons of SNPC. Supplementary Fig. 2: keyword cluster network (A) and density visualization (B) of articles published in 2002–2019. Supplementary Fig. 3: a network of clusters and functional relationships from proteins, generated using the STRING software. Supplementary Fig. 4: LC-MS analysis of PC. UPLC chromatogram monitored at 280 nm. Supplementary Table 1: list of antibodies. Supplementary Table 2: list of primer sequences for real-time RT-PCR. *(Supplementary Materials)*

References

[1] W. Poewe, K. Seppi, C. M. Tanner et al., "Parkinson disease," *Nature Reviews Disease Primers*, vol. 3, no. 1, article 17013, 2017.

[2] S. Sveinbjornsdottir, "The clinical symptoms of Parkinson's disease," *Journal of Neurochemistry*, vol. 139, pp. 318–324, 2017.

[3] V. Ruonala, E. Pekkonen, O. Airaksinen, M. Kankaanpää, P. A. Karjalainen, and S. M. Rissanen, "Levodopa-induced changes in electromyographic patterns in patients with advanced Parkinson's disease," *Frontiers in Neurology*, vol. 9, no. 35, 2018.

[4] C.-H. Kim, B.-S. Han, J. Moon et al., "Nuclear receptor Nurr1 agonists enhance its dual functions and improve behavioral deficits in an animal model of Parkinson's disease," *Proceedings of the National Academy of Sciences of the United States of America*, vol. 112, no. 28, pp. 8756–8761, 2015.

[5] J. Dong, Y. Wang, X. Liu, and W. Le, "Nurr1 deficiency-mediated inflammatory injury to nigral dopamine neurons in Parkinson's disease," *Parkinsonism & Related Disorders*, vol. 46, article e66, 2018.

[6] K. Saijo, B. Winner, C. T. Carson et al., "A Nurr1/CoREST pathway in microglia and astrocytes protects dopaminergic neurons from inflammation-induced death," *Cell*, vol. 137, no. 1, pp. 47–59, 2009.

[7] J. Xu, X. Fu, M. Pan et al., "Mitochondrial creatine kinase is decreased in the serum of idiopathic Parkinson's disease patients," *Aging and Disease*, vol. 10, no. 3, pp. 601–610, 2019.

[8] E. Rodríguez-Traver, O. Solís, E. Díaz-Guerra et al., "Role of Nurr1 in the generation and differentiation of dopaminergic neurons from stem cells," *Neurotoxicity Research*, vol. 30, no. 1, pp. 14–31, 2016.

[9] X. Wei, H. Gao, J. Zou et al., "Contra-directional coupling of Nur77 and Nurr1 in neurodegeneration: a novel mechanism for memantine-induced anti-inflammation and anti-mitochondrial impairment," *Molecular Neurobiology*, vol. 53, no. 9, pp. 5876–5892, 2016.

[10] W. Le, T. Pan, M. Huang et al., "Decreased NURR1 gene expression in patients with Parkinson's disease," *Journal of the Neurological Sciences*, vol. 273, no. 1-2, pp. 29–33, 2008.

[11] J. Dong, S. Li, J. L. Mo, H. B. Cai, and W. D. Le, "Nurr1-based therapies for Parkinson's disease," *CNS Neuroscience & Therapeutics*, vol. 22, no. 5, pp. 351–359, 2016.

[12] B. Kadkhodaei, T. Ito, E. Joodmardi et al., "Nurr1 is required for maintenance of maturing and adult midbrain dopamine neurons," *Journal of Neuroscience*, vol. 29, no. 50, pp. 15923–15932, 2009.

[13] P. Sacchetti, T. R. Mitchell, J. G. Granneman, and M. J. Bannon, "Nurr1 enhances transcription of the human dopamine transporter gene through a novel mechanism," *Journal of Neurochemistry*, vol. 76, no. 5, pp. 1565–1572, 2001.

[14] J. Jankovic, S. Chen, and W. Le, "The role of Nurr1 in the development of dopaminergic neurons and Parkinson's disease," *Progress in Neurobiology*, vol. 77, no. 1-2, pp. 128–138, 2005.

[15] J. Heo, *Dongui-Bogam: Treasured Mirror of Eastern Medicine*, Namsandang Publishers Co, Seoul, 2009.

[16] B. K. Song, J. H. Won, and S. Kim, "Historical medical value of Donguibogam," *Journal of Pharmacopuncture*, vol. 19, no. 1, pp. 16–20, 2016.

[17] C. Hson-Mou and B. Paul Pui-Hay, *Pharmacology and Applications of Chinese Materia Medica*, World Scientific, 1987.

[18] L. Lin, Y.-j. Xu, D.-p. He et al., "A retrospective study on clinical features of and treatment methods for 77 severe cases of SARS," *The American Journal of Chinese Medicine*, vol. 31, no. 6, pp. 821–839, 2003.

[19] N. Lee, D. Hui, A. Wu et al., "A major outbreak of severe acute respiratory syndrome in Hong Kong," *New England Journal of Medicine*, vol. 348, no. 20, pp. 1986–1994, 2003.

[20] M.-Z. Xu, W. S. Lee, J.-M. Han et al., "Antioxidant and anti-inflammatory activities of *N*-acetyldopamine dimers from Periostracum cicadae," *Bioorganic & Medicinal Chemistry*, vol. 14, no. 23, pp. 7826–7834, 2006.

[21] M.-T. Hsieh, W.-H. Peng, F.-T. Yeh, H.-Y. Tsai, and Y.-S. Chang, "Studies on the anticonvulsive, sedative and

hypothermic effects of Periostracum cicadae extracts," *Journal of Ethnopharmacology*, vol. 35, no. 1, pp. 83–90, 1991.

[22] S. Xu, M. Zhang, Y. Wang, Y. Jin, and Z. Liu, "Antitussive, expectorant and antiasthmatic effects of Periostracum cicadae," *Chinese Pharmacological Bulletin*, vol. 23, no. 12, article 1678, 2007.

[23] T.-M. Chang, J.-H. Tsen, H. Yen, T.-Y. Yang, and H.-C. Huang, "Extract from *Periostracum cicadae* inhibits oxidative stress and inflammation induced by ultraviolet B irradiation on HaCaT keratinocytes," *Evidence-based Complementary and Alternative Medicine*, vol. 2017, Article ID 8325049, 12 pages, 2017.

[24] K. N. Nam, Y.-S. Choi, H.-J. Jung et al., "Genipin inhibits the inflammatory response of rat brain microglial cells," *International Immunopharmacology*, vol. 10, no. 4, pp. 493–499, 2010.

[25] G. Park, Y.-J. Park, H. O. Yang, and M. S. Oh, "Ropinirole protects against 1-methyl-4-phenyl-1, 2, 3, 6-tetrahydropyridine (MPTP)-induced neurotoxicity in mice via anti-apoptotic mechanism," *Pharmacology Biochemistry and Behavior*, vol. 104, pp. 163–168, 2013.

[26] H. G. Kim, G. Park, Y. Piao et al., "Effects of the root bark of *Paeonia suffruticosa* on mitochondria-mediated neuroprotection in an MPTP-induced model of Parkinson's disease," *Food and Chemical Toxicology*, vol. 65, pp. 293–300, 2014.

[27] Y. Sim, G. Park, H. Eo et al., "Protective effects of a herbal extract combination of *Bupleurum falcatum*, *Paeonia suffruticosa*, and *Angelica dahurica* against MPTP-induced neurotoxicity via regulation of nuclear receptor-related 1 protein," *Neuroscience*, vol. 340, pp. 166–175, 2017.

[28] G. Park, H. G. Kim, M. S. Ju et al., "6-Shogaol, an active compound of ginger, protects dopaminergic neurons in Parkinson's disease models via anti-neuroinflammation," *Acta Pharmacologica Sinica*, vol. 34, no. 9, p. 1131, 2013.

[29] J. Choi, G. Park, H. Kim, D.-S. Oh, H. Kim, and M. Oh, "*In vitro* and *in vivo* neuroprotective effects of walnut (juglandis semen) in models of Parkinson's disease," *International Journal of Molecular Sciences*, vol. 17, no. 1, p. 108, 2016.

[30] S. Przedborski, V. Jackson-Lewis, A. B. Naini et al., "The parkinsonian toxin 1-methyl-4-phenyl-1,2,3,6-tetrahydropyridine (MPTP): a technical review of its utility and safety," *Journal of Neurochemistry*, vol. 76, no. 5, pp. 1265–1274, 2001.

[31] N. Bae, T. Ahn, S. Chung et al., "The neuroprotective effect of modified Yeoldahanso-tang via autophagy enhancement in models of Parkinson's disease," *Journal of Ethnopharmacology*, vol. 134, no. 2, pp. 313–322, 2011.

[32] R. M. Deacon, "Measuring motor coordination in mice," *Journal of Visualized Experiments*, vol. 29, no. 75, article e2609, 2013.

[33] V. Jackson-Lewis and S. Przedborski, "Protocol for the MPTP mouse model of Parkinson's disease," *Nature Protocols*, vol. 2, no. 1, pp. 141–151, 2007.

[34] B. J. Franklin and G. Paxinos, *The Mouse Brain in Stereotaxic Coordinates*, Academic Press, Cambridge, MA, USA, 2007.

[35] G. Park, Y.-S. Jung, M.-K. Park, C. H. Yang, and Y. Kim, "Melatonin inhibits attention-deficit/hyperactivity disorder caused by atopic dermatitis-induced psychological stress in an NC/Nga atopic-like mouse model," *Scientific Reports*, vol. 8, no. 1, p. 14981, 2018.

[36] G. Park, S. H. Lee, D. S. Oh, and K. Yu, "Melatonin inhibits neuronal dysfunction-associated with neuroinflammation by atopic psychological stress in NC/Nga atopic-like mouse models," *Journal of Pineal Research*, vol. 63, no. 2, article e12420, 2017.

[37] S. Chung, A. Leung, B.-S. Han et al., "Wnt1-lmx1a forms a novel autoregulatory loop and controls midbrain dopaminergic differentiation synergistically with the SHH-FoxA2 pathway," *Cell Stem Cell*, vol. 5, no. 6, pp. 646–658, 2009.

[38] S. O. Castillo, J. S. Baffi, M. Palkovits et al., "Dopamine biosynthesis is selectively abolished in substantia nigra/ventral tegmental area but not in hypothalamic neurons in mice with targeted disruption of the Nurr1 gene," *Molecular and Cellular Neuroscience*, vol. 11, no. 1-2, pp. 36–46, 1998.

[39] M. P. Smidt and J. P. H. Burbach, "How to make a mesodiencephalic dopaminergic neuron," *Nature Reviews Neuroscience*, vol. 8, no. 1, p. 21, 2007.

[40] R. H. Zetterström, L. Solomin, L. Jansson, B. J. Hoffer, L. Olson, and T. Perlmann, "Dopamine neuron agenesis in Nurr1-deficient mice," *Science*, vol. 276, no. 5310, pp. 248–250, 1997.

[41] N. J. Van Eck and L. Waltman, "Visualizing bibliometric networks," in *Measuring Scholarly Impact*, Y. Ding, R. Rousseau, and D. Wolfram, Eds., Springer, Cham, 2014.

[42] N. van Eck and L. Waltman, "Software survey: VOSviewer, a computer program for bibliometric mapping," *Scientometrics*, vol. 84, no. 2, pp. 523–538, 2009.

[43] S. K. Pal and Y. Shukla, "Herbal medicine: current status and the future," *Asian Pacific Journal of Cancer Prevention*, vol. 4, no. 4, pp. 281–288, 2003.

[44] S.-Y. Pan, G. Litscher, S.-H. Gao et al., "Historical perspective of traditional indigenous medical practices: the current renaissance and conservation of herbal resources," *Evidence-based Complementary and Alternative Medicine*, vol. 2014, Article ID 525340, 20 pages, 2014.

[45] E. Lev, "Traditional healing with animals (zootherapy): medieval to present-day Levantine practice," *Journal of Ethnopharmacology*, vol. 85, no. 1, pp. 107–118, 2003.

[46] M. O. Adeola, "Importance of wild animals and their parts in the culture, religious festivals, and traditional medicine, of Nigeria," *Environmental Conservation*, vol. 19, no. 2, pp. 125–134, 1992.

[47] R. R. Alves and I. L. Rosa, "Why study the use of animal products in traditional medicines?," *Journal of Ethnobiology and Ethnomedicine*, vol. 1, no. 1, p. 5, 2005.

[48] O. Akerele, V. Heywood, and H. Synge, *Conservation of Medicinal Plants*, Cambridge University Press, 1991.

[49] Y.-P. Zhu, *Chinese Materia Medica: Chemistry, Pharmacology and Applications*, CRC press, 1998.

[50] K. M. Lohr, M. Chen, C. A. Hoffman et al., "Vesicular monoamine transporter 2 (VMAT2) level regulates MPTP vulnerability and clearance of excess dopamine in mouse striatal terminals," *Toxicological Sciences*, vol. 153, no. 1, pp. 79–88, 2016.

[51] G. W. Miller, R. R. Gainetdinov, A. I. Levey, and M. G. Caron, "Dopamine transporters and neuronal injury," *Trends in Pharmacological Sciences*, vol. 20, no. 10, pp. 424–429, 1999.

[52] T. Zhang, N. Jia, E. Fei et al., "Nurr1 is phosphorylated by ERK2 in vitro and its phosphorylation upregulates tyrosine hydroxylase expression in SH-SY5Y cells," *Neuroscience Letters*, vol. 423, no. 2, pp. 118–122, 2007.

[53] M. K. Lee and V. M. Nikodem, "Differential role of ERK in cAMP-induced Nurr1 expression in N2A and C6 cells," *Neuroreport*, vol. 15, no. 1, pp. 99–102, 2004.

[54] L. Lu, X. Sun, Y. Liu, H. Zhao, S. Zhao, and H. Yang, "DJ-1 upregulates tyrosine hydroxylase gene expression by activating its transcriptional factor Nurr1 via the ERK1/2 pathway," *The International Journal of Biochemistry & Cell Biology*, vol. 44, no. 1, pp. 65–71, 2012.

[55] J. Meiser, D. Weindl, and K. Hiller, "Complexity of dopamine metabolism," *Cell Communication and Signaling*, vol. 11, no. 1, p. 34, 2013.

[56] P. E. Jiang, Q. H. Lang, Q. Y. Yu et al., "Behavioral assessments of spontaneous locomotion in a murine MPTP-induced Parkinson's disease model," *Journal of Visualized Experiments*, vol. 143, article e58653, 2019.

[57] T. Asakawa, H. Fang, K. Sugiyama et al., "Animal behavioral assessments in current research of Parkinson's disease," *Neuroscience & Biobehavioral Reviews*, vol. 65, pp. 63–94, 2016.

[58] E. R. Kramer and B. Liss, "GDNF–Ret signaling in midbrain dopaminergic neurons and its implication for Parkinson disease," *FEBS Letters*, vol. 589, no. 24, PartA, pp. 3760–3772, 2015.

[59] A. Pascual, M. Hidalgo-Figueroa, J. I. Piruat, C. O. Pintado, R. Gómez-Díaz, and J. López-Barneo, "Absolute requirement of GDNF for adult catecholaminergic neuron survival," *Nature Neuroscience*, vol. 11, no. 7, p. 755, 2008.

[60] M. Decressac, B. Kadkhodaei, B. Mattsson, A. Laguna, T. Perlmann, and A. Björklund, "α-Synuclein–induced down-regulation of Nurr1 disrupts GDNF signaling in nigral dopamine neurons," *Science Translational Medicine*, vol. 4, no. 163, pp. 156–163, 2012.

[61] N. Volakakis, K. Tiklova, M. Decressac et al., "Nurr1 and retinoid X receptor ligands stimulate Ret signaling in dopamine neurons and can alleviate α-synuclein disrupted gene expression," *Journal of Neuroscience*, vol. 35, no. 42, pp. 14370–14385, 2015.

[62] J. Liu, W. Liu, Y. Lu et al., "Piperlongumine restores the balance of autophagy and apoptosis by increasing BCL2 phosphorylation in rotenone-induced Parkinson disease models," *Autophagy*, vol. 14, no. 5, pp. 845–861, 2018.

[63] A. Peña-Blanco and A. J. García-Sáez, "Bax, Bak and beyond — mitochondrial performance in apoptosis," *The FEBS Journal*, vol. 285, no. 3, pp. 416–431, 2018.

[64] T. Zhang, P. Wang, H. Ren, J. Fan, and G. Wang, "NGFI-B nuclear orphan receptor Nurr1 interacts with p53 and suppresses its transcriptional activity," *Molecular Cancer Research*, vol. 7, no. 8, pp. 1408–1415, 2009.

[65] K. M. Sousa, H. Mira, A. C. Hall, L. Jansson-Sjöstrand, M. Kusakabe, and E. Arenas, "Microarray analyses support a role for Nurr1 in resistance to oxidative stress and neuronal differentiation in neural stem cells," *Stem Cells*, vol. 25, no. 2, pp. 511–519, 2007.

[66] K. Sasaki, A. Ugajin, and K. I. Harano, "Caste-specific development of the dopaminergic system during metamorphosis in female honey bees," *PLoS One*, vol. 13, no. 10, article e0206624, 2018.

[67] G. Zega, R. Pennati, S. Groppelli, C. Sotgia, and F. De Bernardi, "Dopamine and serotonin modulate the onset of metamorphosis in the ascidian *Phallusia mammillata*," *Developmental Biology*, vol. 282, no. 1, pp. 246–256, 2005.

[68] K. Regna, P. T. Kurshan, B. N. Harwood et al., "A critical role for the *Drosophila* dopamine D_1-like receptor Dop1R2 at the onset of metamorphosis," *BMC Developmental Biology*, vol. 16, no. 1, p. 15, 2016.

Hindawi
Oxidative Medicine and Cellular Longevity
Volume 2019, Article ID 4174803, 14 pages
https://doi.org/10.1155/2019/4174803

Research Article

Chloramphenicol Mitigates Oxidative Stress by Inhibiting Translation of Mitochondrial Complex I in Dopaminergic Neurons of Toxin-Induced Parkinson's Disease Model

Jeongsu Han,[1,2] **Soo Jeong Kim**,[1,2] **Min Jeong Ryu**,[1] **Yunseon Jang**,[1,2,3] **Min Joung Lee**,[1,2,3] **Xianshu Ju**,[1,2,3] **Yu Lim Lee**,[1,2,3] **Jianchen Cui**,[1,2,3] **Minho Shong**,[4,5] **Jun Young Heo**,[1,2,3] **and Gi Ryang Kweon**[1,2]

[1]*Department of Biochemistry, Chungnam National University School of Medicine, Daejeon 35015, Republic of Korea*
[2]*Infection Control Convergence Research Center, Chungnam National University School of Medicine, Daejeon 35015, Republic of Korea*
[3]*Department of Medical Science, Chungnam National University School of Medicine, Daejeon 35015, Republic of Korea*
[4]*Department of Internal Medicine, Chungnam National University School of Medicine, Daejeon 35015, Republic of Korea*
[5]*Research Center for Endocrine and Metabolic Diseases, Chungnam National University Hospital, Daejeon 35015, Republic of Korea*

Correspondence should be addressed to Jun Young Heo; junyoung3@gmail.com and Gi Ryang Kweon; mitochondria@cnu.ac.kr

Jeongsu Han and Soo Jeong Kim contributed equally to this work and are co-first authors.

Received 18 April 2019; Accepted 18 June 2019; Published 26 August 2019

Guest Editor: Roberta Cascella

Paraquat (PQ), an herbicide considered an environmental contributor to the development of Parkinson's disease (PD), induces dopaminergic neuronal loss through reactive oxygen species (ROS) production and oxidative stress by mitochondrial complex I. Most patients with PQ-induced PD are affected by chronic exposure and require a preventive strategy for modulation of disease progression. To identify drugs that are effective in preventing PD, we screened more than 1000 drugs that are currently used in clinics and in studies employing PQ-treated cells. Of these, chloramphenicol (CP) showed the most powerful inhibitory effect. Pretreatment with CP increased the viability of PQ-treated SN4741 dopaminergic neuronal cells and rat primary cultured dopaminergic neurons compared with control cells treated with PQ only. CP pretreatment also reduced PQ-induced ROS production, implying that mitochondrial complex I is a target of CP. This effect of CP reflected downregulation of the mitochondrial complex I subunit ND1 and diminished PQ recycling, a major mechanism of ROS production, and resulted in the prevention of cell loss. Notably, these effects of CP were not observed in rotenone-pretreated SN4741 cells and Rho-negative cells, in which mitochondrial function is defective. Consistent with these results, CP pretreatment of MPTP-treated PD model mice also ameliorated dopaminergic neuronal cell loss. Our findings indicate that the inhibition of mitochondrial complex I with CP protects dopaminergic neurons and may provide a strategy for preventing neurotoxin-induced PD.

1. Introduction

Epidemiological studies have suggested that chemical pesticides are associated with the development of Parkinson's disease (PD) [1–3]. However, the underlying mechanism by which pesticides might contribute to PD pathogenesis remains unclear. A primary characteristic of PD is that clinical symptoms arise when a majority (~60–70%) of dopaminergic neurons in the substantia nigra pars compacta (SNpc) are lost. The exact cause of this cell loss, which is referred to as idiopathic Parkinson's disease and accounts for ~90% of the total burden of PD, is unknown. Typically, PD treatments, which include levodopa (L-DOPA), MAO-B inhibitors, and dopamine agonists, focus on maintaining

dopamine levels in the body [4]. L-DOPA, a dopamine precursor, is particularly effective in relieving short-term behavioral disturbances but does not prevent the death of dopaminergic neurons [5]. Ultimately, curing Parkinson's disease will require going beyond maintenance of the body's dopamine levels (symptomatic therapy) to the prevention of the death of dopamine neurons (causal therapy).

A meta-analysis of PD sought to establish a relationship between exposure to pesticides and the onset of idiopathic PD. Among the various pesticides examined, only paraquat (PQ), which increased the risk of PD by ~2.2-fold, showed a significant association with the onset of Parkinson's disease [6, 7]. PQ is classified as viologen, a family of very strong reducing agents, and produces large amounts of reactive oxygen species (ROS) through a continuous oxidation-reduction process in mitochondrial complex I [8, 9]. This excessive production of ROS damages cellular macromolecules, including proteins, nucleic acids, carbohydrates, and lipids, and constitutes the main cause of the death of dopaminergic neurons exposed to PQ. Clinical studies have shown that the total amount of reduced glutathione, an important cellular component that relieves oxidative stress, is decreased in patients with PD, leading to increased ROS and dysfunction of dopaminergic neurons [10, 11]. Consistent with this, it has been confirmed that the inhibition of excessive ROS production by treatment with antioxidants or by overexpression of antioxidant enzymes protects against the loss of dopaminergic neurons in a PD model [12, 13]. Collectively, these observations suggest that a mitochondrial-targeting strategy to inhibit ROS production might be quite effective in controlling the progression of PQ-induced PD.

To test this hypothesis, we screened 1040 therapeutic agents currently on the market for drugs that increase the viability of PQ-exposed dopaminergic neurons. Notably, the greatest protection against the PQ-induced loss of dopaminergic neurons was provided by chloramphenicol (CP), an antibiotic that inhibits mitochondrial protein synthesis. Other antibiotics, such as ceftriaxone, rapamycin, and rifampicin, exerted possible neuroprotective effects through attenuation of neuroinflammation [14–16]. Although the phenomenon of antibiotic-mediated protection against dopaminergic neuronal loss in PD has been reported, these previous studies mainly focused on inflammation and the primary effects of antibiotics; however, the metabolic effects of these drugs on mitochondria are not well known. In the current study, we sought to fill these gaps in our knowledge, investigating how CP affects the mitochondria of dopaminergic neurons and protects against dopaminergic neuronal cell loss induced by PQ.

2. Materials and Methods

2.1. MPTP-Induced PD Mouse Model. Male C57Bl/6 mice (21-25 g; age 8 weeks) were intraperitoneally injected 1-methyl-4-phenyl-1,2,3,6-tetrahydropyridine (MPTP, Sigma-Aldrich, M0896, MO, USA) as 4 times injections of 20 mg/kg at 2 h intervals and were sacrificed at day 7 after the final injection of MPTP. Control animals were injected an equal volume of 0.9% sterile saline. Mice were divided into three groups ($n = 5$): group 1, vehicle control; group 2, vehicle and MPTP 20 mg/kg i.p.; group 3 was treated MPTP 20 mg/kg i.p. with chloramphenicol at a dose of 50 mg/kg at 3 times by oral gavage (-1, 0, and 1 day based on MPTP injection).

2.2. Immunohistochemistry on MPTP-Induced PD Mouse Brain Tissues. Saline- and MPTP-injected mice were perfused with perfusion solution and postfixated with 4% paraformaldehyde for 1 day. The perfusion solution was made with NaCl, $NaNO_3$, and heparin (Sigma-Aldrich) in dissolving distilled water. The brains stored in 30% sucrose for cryoprotection were cut to a thickness of 30 μm. Dissection of the brain to obtain the SNpc and striatum regions was performed as previously described [17]. Brain slices were fixed with tissue stock solution and rinsed three times in phosphate-buffered saline (PBS pH 7.4). 0.3% Triton X-100 and 2% donkey serum (GeneTex, Irvine, CA, USA) in PBS were used for blocking for 90 min, then brain slices were incubated with primary antibodies against anti-tyrosine hydroxylase (Millipore, AB152) at 4°C overnight. For immunohistochemistry, brain slices were incubated with rabbit secondary antibodies (Dako EnVision$^+$ System-HRP, USA) for 90 min, and then, reacting with DAB$^+$ substrate buffer. After mounting by fluorescent mounting medium (Dako North America Inc., Santa Barbara, CA, USA) on cover slides, immunofluorescent images were acquired using an Olympus™ microscope (Olympus, Hachioji-shi, Tokyo, Japan).

2.3. Rat Primary Dopaminergic Neuron Culture and TH Immunofluorescence Staining. Primary dopaminergic neurons were prepared from E14 rat embryos obtained from pregnant dams using a previously described isolation method [18]. Isolated primary dopaminergic neurons in Minimal Essential Medium (MEM; Welgene, Dalseo-gu, Daegu, South Korea) supplemented with 10% fetal bovine serum (FBS; Thermo Fisher Scientific Inc., MA, USA), 2 mM glutamine, 10 units/ml penicillin, and 2 μM Ara-C (Invitrogen, Carlsbad, CA, USA) were plated in gelatin-coated coverslips in a 24-well plate and allowed to attach for 6–8 h. Thereafter, the medium was replaced with growth medium containing different concentrations of PQ (Sigma-Aldrich, 36541, MO, USA) or CP (Sigma-Aldrich, C0378), and cells were incubated as described in the text. For immunofluorescence staining, primary dopaminergic neurons were collected 24 h after pharmacological treatment, rinsed three times in phosphate-buffered saline (PBS; pH 7.4), and then blocked by incubating with PBS containing 0.3% Triton X-100 and 2% donkey serum (GeneTex, Irvine, CA, USA) for 90 min. After blocking, primary dopaminergic neurons were incubated first with primary anti-TH antibodies (EMD Millipore, AB152, Burlington, MA, USA) at 4°C overnight and then with Alexa Fluor 488-conjugated anti-rabbit secondary antibodies (Abcam, 150081, Cambridge, MA, USA) at room temperature for 90 min. Slides were coverslip-mounted using fluorescent mounting medium (Dako North America Inc.), and immunofluorescence images were acquired using a fluorescence microscope (Olympus).

2.4. Cell Culture. The dopaminergic neuronal progenitor cell line (SN4741) was cultured as described before [19–22].

SN4741 cells were grown in RF medium containing Dulbecco's modified Eagle's medium (DMEM, Welgene) supplemented with 10% fetal bovine serum (FBS, Thermo Fisher Scientific Inc.), 1% glucose (Amresco, Solon, OH, USA), 1% penicillin-streptomycin, and 2 mM L-glutamine (Invitrogen) at 33°C with 5% CO_2. And wild-type 143B, Rho-positive (Rho+), and Rho-negative (Rho0) cell lines were grown in medium containing DMEM (Welgene) supplemented with 10% FBS (Thermo Fisher Scientific Inc.), 1% glucose (Amresco), 1% penicillin-streptomycin, and 100 μg/ml sodium pyruvate (Invitrogen) at 37°C with 5% CO_2. In addition, Rho0 cells were supplemented with 200 μg/ml sodium pyruvate and 50 μM uridine (Invitrogen) to grow cells through the provision of exogenous electron acceptors. The Rho0 cell lines were generated as previously described [23]. CP (Sigma-Aldrich) was initially diluted from powder in EtOH (Millipore) to the stock concentration of 20 mM. PQ (Sigma-Aldrich) was initially diluted from powder in distilled water to the stock concentration of 10 mM. This stock was further diluted with medium to 100 μM, which was used for the cell treatments. All the used cell lines have been routinely checked in the laboratory for mycoplasma contamination with the MycoProbe detection kit (R&D Systems, MN, USA). Only cells negative for mycoplasma contamination were used.

2.5. Cell Viability Assay. Cell viability was determined by the Cell Counting Kit-8 (CCK-8) purchased from Dojindo (Rockville, MD, USA). The CCK-8 assay was used to measure cytotoxicity and SN4741, Rho+, and Rho0 cells were plated at 1×10^4 cells per well in 96-well culture plates in 37°C for 24 h under conditions at various concentrations of PQ and CP (Sigma-Aldrich). CCK-8 solution was added to each well, and the absorbance was measured at 450 nm wavelength by MultiSkan Ascent microplate spectrophotometer (Thermo Fisher Scientific Inc., MA, USA).

2.6. Protein Isolation and Western Blot. Proteins were extracted from SN4741 cells using RIPA lysis buffer (100 mM Tris-HCl (pH 8.5), 200 mM NaCl, 5 mM EDTA, 0.2% SDS, phosphatase, and a protease inhibitor cocktail) (iNtRON Biotechnology, Gyeonggi, South Korea). After centrifugation at 15000×g for 20 min at 4°C, supernatants were collected. Protein levels were measured using the Bradford (Bio-Rad, CA, USA) method. Isolated proteins (20 μg) were resolved using 10-12% SDS-PAGE and transferred onto polyvinylidene fluoride (PVDF, Millipore, ISEQ00010) membranes, which were blocked with 5% BSA in TBST (10 mM Tris-HCl (pH 7.6), 150 mM NaCl, and 0.1% Tween 20). The membranes were incubated overnight at 4°C with primary antibodies against NDUFA9 (Invitrogen, 459100), NDUFA8 (Invitrogen, 459210), SDHA (Invitrogen, 459200), UQCRC2 (Invitrogen, A11143), COX4 (Invitrogen, A21348), ATP5A1 (Invitrogen, A21350), Mn SOD (MA1-106), Cu-Zn SOD (Novus Biologicals, NBP2-24915), HSP60 (Santa Cruz, sc-1052), and actin (Santa Cruz, sc-8432) and then with a horseradish peroxidase-coupled secondary antibody for 1 h at room temperature (RT). Finally, the antibody-labeled proteins were detected using an ECL system (iNtRON Biotechnology, Gyeonggi, South Korea). All antibodies were validated by the manufacturer. Band quantification was performed with the ImageJ software (http://imagej.nih.gov/ij; v.1.47b).

2.7. Measurement of Cellular Oxygen Consumption Rate (OCR). Oxygen consumption rate (OCR) was measured using a Seahorse Bioscience XF24 analyzer (Seahorse Bioscience, MA, USA). The XF24 biosensor cartridge (Seahorse Bioscience) was activated overnight with 1 ml of XF24 calibration buffer per well and incubation at 37°C without CO_2. Thereafter, SN4741, Rho+, and Rho0 cells were seeded to the XF24 cell culture microplates (Seahorse Bioscience) at 2×10^4 cells in 4.5 ml DMEM medium per well and incubated at 37°C without CO_2 for at least 1 hour. For measurements, each port in the well of the XF24 biosensor cartridge was filled with 20 μg/ml oligomycin (an ATPase inhibitor, Sigma-Aldrich, O4876), 25 μM CCCP (an uncoupler, Sigma-Aldrich, C2759), and 20 μM rotenone (a mitochondrial complex I inhibitor, Sigma-Aldrich, R8875), and the XF24 analyzer was operated under the manufacturer's basal protocol at 37°C.

2.8. RNA Isolation and qPCR Analysis. Total RNA was extracted using TRIzol reagent (Invitrogen) according to the manufacturer's instructions, and real-time quantitative PCR was performed using cDNA, a Rotor-Gene 6000 real-time instrument (Qiagen, Valencia, CA, USA), and SYBR Green PCR Master Mix (iCycleriQ Real-Time PCR Detection System; Bio-Rad, Hercules, CA, USA). All primers were designed using the Primer3 program (http://bioinfo.ut.ee/primer3-0.4.0/) and are listed in Supplementary Table 2. Relative gene expression was quantified and normalized with respect to that of 18s ribosomal RNA (endogenous control) using Rotor-Gene 6000 real-time Rotary Analyzer software (Qiagen). Each experiment was repeated at least three times.

2.9. Mitochondrion Isolation. Mitochondria were isolated as previously described [24]. Briefly, SN4741 cells were suspended in buffer A (250 mM sucrose, 2 mM HEPES pH 7.4, and 0.1 mM EGTA) and centrifuged at 320 × g for 10 min. Cell pellets were homogenized in buffer A using a glass-Teflon homogenizer. The homogenate was centrifuged at 570 × g for 10 min, and the supernatant was retained. For crude mitochondrion preparation, the supernatant was centrifuged at 14000 × g for 10 min. The pellet (mitochondria) was resuspended in buffer B (25 mM potassium phosphate pH 7.2, 5 mM $MgCl_2$) and centrifuged at 15000 × g for 10 min. The mitochondrial pellet was used or stored at -70°C for BN-PAGE and assay of mitochondrial complex activity.

2.10. Blue Native Polyacrylamide Gel Electrophoresis (BN-PAGE). BN-PAGE analyses were performed as previously described [24] using isolated mitochondria lysed with n-dodecyl-β-D-maltoside using the Native PAGE Novex Bis-Tris Gel system (Invitrogen) according to the manufacturer's instructions. Briefly, 30 μg of isolated mitochondria was solubilized using sodium dodecyl maltoside. Digitonin

was included in the lysis buffer for detection of mitochondrial supercomplexes. The suspensions were centrifuged at 20000 × g for 10 min at 4°C, after which proteins in the resulting supernatants were resolved by PAGE on a native polyacrylamide Novex 3–12% Bis-Tris gel (Invitrogen) and then transferred to a polyvinylidene fluoride (PVDF) membrane. After fixing with 8% acetic acid, the membrane was blocked with 5% skim milk in TBS-T (10 mM Tris-HCl pH 7.6, 150 mM NaCl, 0.1% Tween 20) for 1 h and immunoblotted using Anti-OxPhos Blue Native WB Antibody Cocktail (Invitrogen, 457999).

2.11. Enzymatic Assay for Mitochondrial Complex Activity and PQ-Recycling Rate. Mitochondrial respiratory chain enzyme activity was measured as previously described [25]. Briefly, isolated mitochondrial pellets were suspended in hypotonic buffer (25 mM potassium phosphate pH 7.2, 5 mM $MgCl_2$) and then subjected to three freeze-thaw cycles. The concentration of mitochondrial proteins was measured by the Bradford assay using bovine serum albumin (BSA) as a standard. Complex I activity (NADH:CoQ oxidoreductase) was measured in the presence of decylubiquinone as the rotenone-sensitive decrease in NADH at 340 nm. The activity of complex II (succinate:DCIP oxidoreductase) was measured in the presence of decylubiquinone plus rotenone as the antimycin A-sensitive reduction of 2,6-DCIP at 600 nm, using 520 nm as the reference wavelength. Complex III activity (ubiquinol:cytochrome C oxidoreductase) was measured in the presence of rotenone and decylubiquinol by following the rate of reduction of cytochrome C at 550 nm, using 580 nm as the reference wavelength. Complex IV activity (cytochrome C oxidase) was measured as the disappearance of reduced cytochrome C at 550 nm. All absorbance measurements were performed in a Beckman DU650 (Beckman Coulter, Fullerton, CA, USA) spectrophotometer. The absorbance of mitochondrial complex I was determined with PQ-recycling assays, performed in the same manner as experiments for measuring the activity of mitochondrial complex I, using PQ instead of CoQ as the electron acceptor in isolated mitochondria.

2.12. ROS Quantification. ROS generation was analyzed using the fluorescent dyes, MitoSOX (Invitrogen, M36008), MitoTracker Red CM-H_2XRos (Invitrogen, M7513), and DCF-DA (Invitrogen, C6827), according to the manufacturers' instructions. SN4147 cells were incubated with MitoSOX (5 μM), MitoTracker Red CM-H_2XRos (1 μM), or DCF-DA (5 μM) in Krebs-HEPES buffer (pH 7.4) at 37°C for 25 min and then washed twice with Hank's Balanced Salt Solution (HBSS; pH 7.4, Welgene, Dalseo-gu, Daegu, South-Korea). ROS generation was measured using a FACScan flow cytometer (BD Biosciences, CA, USA) and a Twinkle LB 970 Microplate Fluorometer (Berthold Technologies, Oak Ridge, TN, USA) and analyzed using FACS-Diva software (BD Biosciences).

2.13. Ethics Approval and Consent to Participate. The mice were housed in an environment controlled at 22°C temperature, 50% humidity, and 12 h light/dark cycle. Mice were maintained at 3-4 per cage in an environment suitable for water and food ad libitum. All mouse experiments were performed in the animal facility according to institutional guidelines (SOP; standard operating procedure), and the experimental protocols were approved by the institutional review board of Chungnam National University (CNU-00356).

2.14. Statistical Analysis. All results are presented as mean values + SD (error bars). Data were analyzed using one-way analysis of variance (ANOVA) with Tukey's post hoc analysis or 2-tailed, unpaired Student's t-test, as appropriate for the experiment, using GraphPad Instat (GraphPad Software Inc., San Diego, CA, USA). A P value < 0.05 was considered statistically significant; individual P values are indicated in figure legends.

3. Results

3.1. CP Effectively Protects against PQ-Induced Dopaminergic Neuronal Loss. Dopaminergic neurons are well known to be susceptible to damage and loss of function upon exposure to exogenous harmful stimuli such as ROS [26]. In an attempt to find new applications of existing medicines in the prevention of PD, we screened 1040 drugs that had already demonstrated drug safety in clinical tests and that are expected to have direct and indirect effects on mitochondria. We sorted the candidate drugs according to how effectively they protected against the PQ-induced loss of cell viability using the MN9D dopaminergic neuronal cell line. Supplementary Table 1 lists the top 100 most effective drugs, which include antibiotics and NSAIDs (nonsteroidal anti-inflammatory drugs). In particular, antibiotics known to inhibit mitochondrial protein synthesis were detected in the top ranking in protecting the viability of dopaminergic neurons against PQ. Among all drugs tested, CP provided the strongest protective effect against PQ cytotoxicity, maintaining a 96.8% cell survival rate. Accordingly, CP was selected for use in subsequent experiments designed to test the efficacy of the mitochondrial-targeting strategy in protecting against PQ-induced dopaminergic neuronal damage.

To investigate the protective effect of CP on dopaminergic neuron loss, we examined the survival rate of rat primary dopaminergic neurons obtained from the ventromedial area of the mesencephalic region at embryonic day 14 (E14) following treatment with CP and/or PQ. In the group treated with PQ alone, the number of neurons positive for the dopaminergic marker, tyrosine hydroxylase (TH), started to decrease at a PQ concentration of 8 μM, which reduced viability to 45.5% ± 4.6%, less than 5% of cells survived at a PQ concentration of 16 μM. In contrast, the survival rate of TH-positive neurons in the group treated with PQ and 1 μg/ml CP remained as high as 80% (Figures 1(a) and 1(b)). Although the unique characteristics of the tissue are well preserved, the heterogeneous cell population and the lack of proliferation of the primary dopaminergic neuron are obstacles to the study of molecular mechanisms [18, 27–29]. We further validated the protective effect of

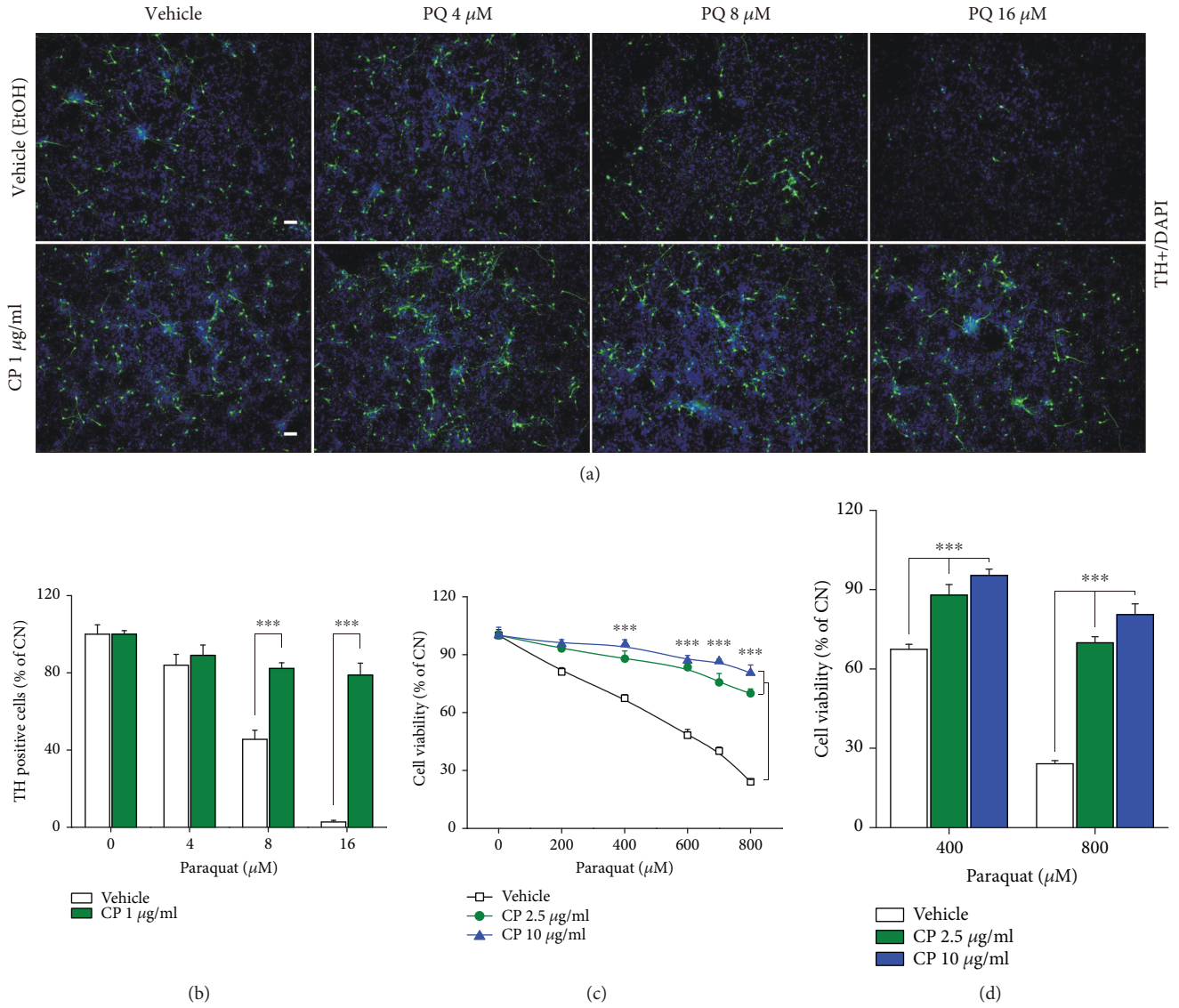

Figure 1: CP protects against neuronal cell loss induced by PQ in rat primary dopaminergic neurons and the SN4741 dopaminergic neuronal cell line. (a, b) Primary dopaminergic neurons isolated from the ventromedial area of the mesencephalic region of E14 rats were pretreated with 1 μg/ml CP for 24 h and then treated with 0–16 μM PQ for 24 h. Dopaminergic neurons were identified by immunofluorescence staining with an anti-TH antibody. (a) Immunofluorescence-stained TH+ cells were confirmed by fluorescence microscopy TH+ cells, green; nuclei, blue. Scale bars, 100 μm. (b) Bar graph showing quantification of TH+ cells, confirmed by fluorescence microscopy ($n = 12$). (c) SN4741 cells were pretreated with 2.5 or 10 μg/ml CP for 24 h. Cells were further treated with 0–800 μM PQ for 24 h, and the survival rate of dopaminergic neurons was confirmed using CCK8 ($n = 15$). (d) Bar graph showing cell viability ($n = 15$). All data are representative of three independent experiments. $^{***}P < 0.001$ by 2-tailed unpaired Student's t-test in (b) and by one-way ANOVA in (c, d). Error bars represent +SD.

CP in the SN4741 dopaminergic neuronal cell line, a previously used immature dopaminergic neuronal cell line that is easier to culture than primary cells and is suitable for mechanism studies [19–22]. To examine the toxicity of CP, we treated SN4741 cells with different concentrations of CP alone for 48 h and found no evidence for cytotoxicity at concentrations up to 80 μg/ml (Figure S1). Consistent with results obtained using primary embryonic dopaminergic neurons, PQ induced a concentration-dependent decrease in the survival rate of SN4741 cells; notably, treatment with 2.5 or 10 μg/ml of CP restored survival of PQ-treated cells to 75% and 90%, respectively (Figures 1(c) and 1(d)). Concentrations of CP greater than 10 μg/ml did not produce any additional survival benefit; accordingly, we used 10 μg/ml CP as an ideal concentration in subsequent mechanistic studies.

3.2. CP Reduces the Total Amount of Intracellular ROS Generated by PQ. ROS, produced as byproducts of the operation of the mitochondrial respiratory chain, are known to mediate PQ-induced neuronal toxic effects. Mitochondrial complexes I and III are involved in the oxidation-reduction process of PQ and sequentially generate superoxide and hydrogen peroxide (H_2O_2) as the primary ROS [30, 31]. To

determine whether the modulation of intracellular ROS is involved in CP-mediated protection of dopaminergic neurons from PQ-induced toxicity, we measured intracellular ROS generation using the ROS-detecting dye DCF-DA (as an indicator of total ROS), MitoTracker Red CM-H_2XRos, and MitoSOX (as an indicator of mitochondrial superoxide) in conjunction with fluorescence microscopy, microplate fluorometer, and fluorescence-activated cell sorting (FACS) analysis. The DCF-DA and MitoSOX intensities measured by fluorescence microscopy were significantly increased after treatment with 400 μM PQ for 16 h in the SN4741 cell line, while the DCF-DA and MitoSOX intensities were decreased to the control level in the PQ-treated group after CP pretreatment (Figure 2(a), Figure S2(a)). As a result of quantification of mitochondrial superoxide through FACS analysis and microplate fluorometer, median ROS values, expressed in arbitrary units (A.U.), were shifted to higher levels in the PQ-treated group ($14.62 \pm 0.2 \times 10^2$ A.U.) compared with the control group ($5.12 \pm 0.1 \times 10^2$ A.U.) but were restored to normal values in the CP pretreatment group ($10.84 \pm 0.3 \times 10^2$ A.U.), confirming that CP decreased ROS production (Figures 2(b) and 2(c) and Figure S2(b)). Thus, we conclude that CP decreases total intracellular ROS content, a key element in PQ-induced neuronal cell defects.

3.3. CP Reduces the Production of ROS through Inhibition of PQ Recycling. There are two mechanisms by which CP might reduce the total amount of ROS generated by PQ: inhibition of ROS production and increased capacity of antioxidants to remove ROS. To verify the ROS-lowering effect of CP, we first examined how CP affects intracellular antioxidant enzymes, focusing on superoxide dismutase (SOD) enzymes, which remove ROS by converting superoxide to H_2O_2 (Figures 2(d)–2(f)). Intracellular antioxidant capacity was assessed by Western blot analysis using antibodies against manganese SOD (MnSOD) and copper/zinc SOD (Cu/ZnSOD), which represent mitochondrial and cytosolic antioxidant enzymes, respectively. Interestingly, there was no change in the expression of MnSOD in the PQ-treated group compared with HSP60 or actin, endogenous controls for mitochondrial and cytosolic proteins. Contrary to our expectations, we found that the expression of Cu/ZnSOD in dopaminergic neurons treated with PQ administration was decreased slightly after CP pretreatment rather than increased. These results suggest that ROS removal by antioxidant enzymes is not involved in the protective effect of CP treatment. In addition, we examined whether CP was capable of preventing the loss of dopaminergic neurons treated exogenously with H_2O_2 (Figure 2(g)). In contrast to the effects of treatment with PQ alone, cotreatment with CP and H_2O_2 accelerated the decrease in the viability of dopaminergic neurons compared with H_2O_2 alone. Next, to determine whether CP inhibits ROS generation, we measured the rate of PQ recycling, a key step in the generation of ROS by PQ (Figure 2(h)). For this, we used isolated mitochondria from the SN4741 cell line, allowing us to focus on the mitochondrial respiratory chain as a specific target for PQ recycling. These experiments showed that the PQ-recycling rate in the group treated with CP decreased to ~20% of that in the control group. Taken together, these results indicate that, instead of reflecting an increase in ROS removal, the decrease in the total amount of intracellular ROS caused by CP treatment results from suppressing ROS generation through a reduction in PQ recycling.

3.4. CP Inhibits Mitochondrial Oxidative Phosphorylation (OxPhos) and Supercomplex Formation in Dopaminergic Neurons. CP is known to act as an antibacterial medicine by inhibiting protein synthesis through binding to the ribosomal 50S subunit, which has a structure similar to that of the corresponding mitochondrial ribosomal subunit in eukaryotes [32]. Since CP effectively inhibited PQ recycling in isolated mitochondria (Figure 2(h)), we hypothesized that CP could reduce the function of mitochondrial complex I in dopaminergic neurons. To investigate the effect of CP on the function of mitochondria, we measured the oxygen consumption rate (OCR) of SN4741 cells using an XF24 analyzer (Figures 3(a)–3(c)). We found that CP induced a concentration-dependent decrease in the overall oxygen uptake rate, including basal oxygen consumption. This reduction in oxygen consumption rate reflects a decrease in electron transfer to O_2 in the mitochondrial respiratory chain. Treatment with oligomycin, an inhibitor of ATPase, also decreased proton leak in the CP-treated group compared with the control group, consistent with a reduction in ROS production by CP (Figure 3(c)). Interestingly, an assessment of mitochondrial complex activity, performed to determine how CP decreased oxygen consumption, showed that complex I activity was decreased to ~50% of that in controls, whereas the activity of complexes II–V was not significantly changed (Figure 3(d)).

The maintenance of mitochondrial OxPhos function depends on the integrity of the composition of all respiratory chain complexes, which are produced within mitochondria by the operation of mitochondrial transcription and translation machinery. To assess changes in mitochondrial transcription induced by treatment with CP, we performed quantitative polymerase chain reaction (qPCR) for a subset of mitochondrial complexes (Figure 3(e)). For this, we selected ND1, SDHA, CytB, COX1, and ATP8 as representative subunits of mitochondrial complexes I, II, III, IV, and V, respectively. We found no change in mRNA expression levels for subunits belonging to complexes I–V in SN4741 cells. However, unlike the mRNA results, protein expression of the complex I subunit ND1 was dramatically reduced (~90%) compared with controls (Figures 3(f) and 3(g)). The loss of ND1, which acts as a column within the 42-subunit mitochondrial complex I, can lead to structural changes in this complex [33, 34]. To assess the formation of native mitochondrial complex I, we probed for supercomplexes using blue native polyacrylamide gel electrophoresis (BN-PAGE), which can identify proteins larger than 300 kDa. As expected, we found that treatment with CP decreased mitochondrial complex I formation without changing complex II formation (Figures 3(h) and 3(i)). These results demonstrate that CP inhibits the translation and formation of mitochondrial complex I, resulting in diminished mitochondrial function.

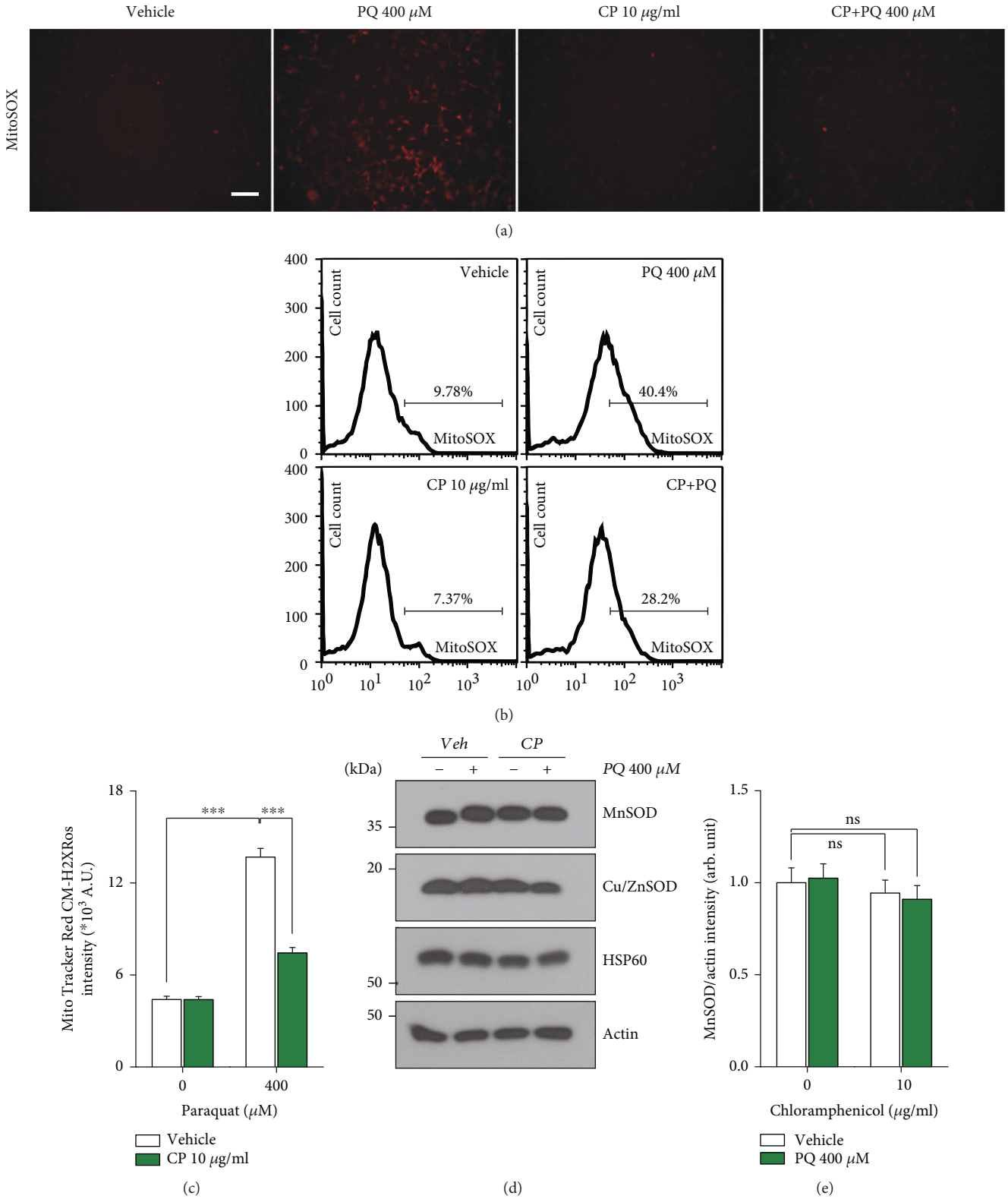

Figure 2: Continued.

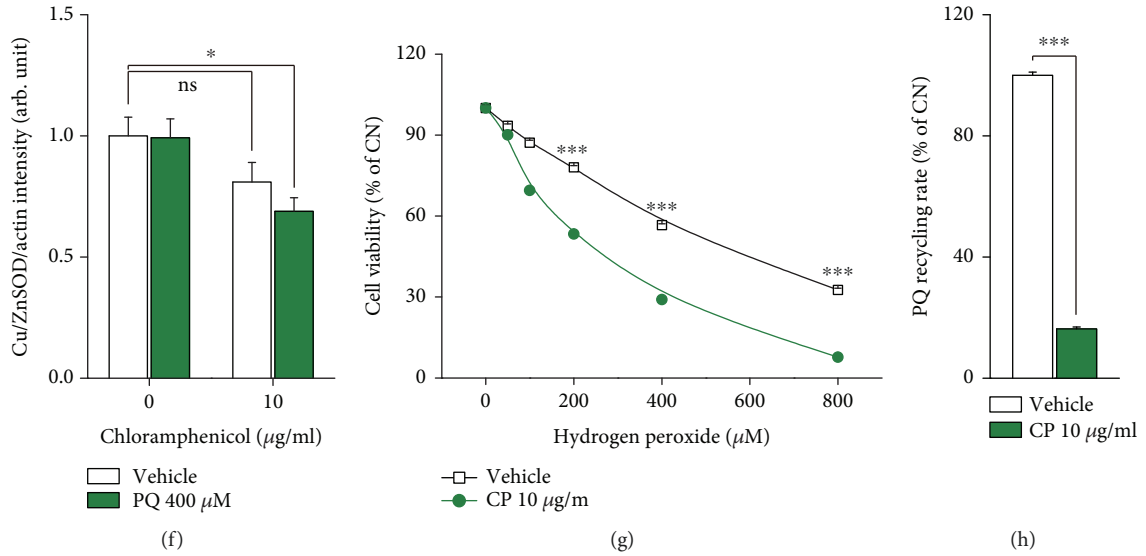

Figure 2: CP effectively reduced PQ recycling and decreased total ROS levels in SN4741 cells by inhibiting ROS production. (a–c) SN4147 cells were treated with 10 μg/ml CP and PQ, and mitochondrial superoxide was measured by staining with the fluorescent dye MitoSOX and MitoTracker Red CM-H_2XRos. (a) The amount of mitochondrial superoxide production was visually confirmed by fluorescence microscopy. Scale bars, 100 μm. (b) The total amount of fluorescently stained by MitoSOX was quantified by FACS analysis ($n = 15$). (c) MitoTracker Red CM-H_2XRos intensity was quantified by microplate fluorometer ($n = 12$). (d–f) SN4741 cells were treated with 10 μg/ml CP and 400 μM PQ for 24 h. (d) Western blotting revealed the expression of MnSOD and Cu/ZnSOD proteins, which can remove superoxide ($n = 9$). MnSOD: mitochondrial SOD; Cu/ZnSOD: cytosolic SOD. (e) Quantification of mitochondrial SOD ($n = 9$). (f) Quantification of cytosolic SOD ($n = 9$). (g) CP potentiated the dopaminergic neuron-killing effect of H_2O_2, an exogenous ROS, in SN4741 cells ($n = 15$). (h) The rate of PQ recycling, a key step in the production of ROS by PQ, was confirmed by enzymatic assay using mitochondria isolated from the SN4741 cell line ($n = 9$). All data are representative of three independent experiments. $^*P < 0.05$; $^{***}P < 0.001$ by 2-tailed unpaired Student's t-test in (c, h) and by one-way ANOVA in (e–g); ns: not significant. Error bars represent +SD.

3.5. Cells with Reduced Mitochondrial Function Exhibit Resistance to PQ Toxicity. To verify the involvement of mitochondrial respiration in the sensitivity to PQ toxicity, we tested the effects of PQ (1) in Rho-negative (Rho0) cells, characterized by a deficiency in mitochondrial protein and DNA, using prolonged treatment with a low concentration of ethidium bromide (EtBr), which depletes mitochondrial DNA and (2) in SN4741 cells treated with rotenone, which specifically inhibits mitochondrial complex I. We first treated wild-type Rho-positive (Rho+) and mitochondria-deficient Rho0 cell lines with CP and PQ alone or in combination. OCR measurement revealed that the mitochondrial function of the Rho0 cell line was reduced (Figure S3). The Rho0 cell line was more resistant to PQ toxicity than the Rho+ cell line following treatment with PQ alone. In Rho+ cells treated with PQ and CP in combination, the toxicity of PQ was decreased compared with that in PQ-treated (control) Rho+ cells, whereas Rho0 cells showed no difference between CP-treated and CP-untreated groups (Figures 4(a) and 4(b)). In a second experiment performed in the same manner, rotenone alone reduced PQ toxicity in the SN4741 cell line compared with the control group, but cotreatment with CP did not produce any additional protective effect (Figures 4(c) and 4(d)). If CP targeted cytosolic ROS or other mitochondrial complexes in exerting its protective effect against PQ, pretreatment with rotenone and CP would be predicted to exert synergetic effects on cell viability. However, the fact that there was no significant difference in PQ toxicity between CP-only treatment and the CP/rotenone-combination treatment groups implies that PQ and CP act on the same mitochondrial target. Taken together, these results indicate that PQ toxicity results from the disruption of mitochondrial respiration function and that CP protects dopaminergic neurons from PQ toxicity by inhibiting mitochondrial complex I.

3.6. CP Prevents Dopaminergic Neuronal Loss in the Nigral Pathway in the MPTP-Induced PD Mouse Model. Based on the above results, we evaluated whether CP protects against dopaminergic neuronal cell loss *in vivo* in a mouse model of MPTP-induced PD. MPTP (1-methyl-4-phenyl-1,2,3,6-tetrahydropyridine), which is converted to MPP+ by astrocytes, is known to cause dopaminergic neuronal loss by inducing ROS production and mitochondrial dysfunction [2]. After oral administration of CP into the MPTP mouse model, we monitored the survival of TH+ (dopaminergic) neurons. In these experiments, CP was injected three times before and after MPTP treatment (Figure 4(f)). After 7 days, mice were sacrificed and TH+ neurons were quantified. In the MPTP-treated group, the number of TH+ cells in the SNpc and the intensity of TH staining in the striatum decreased to 40% and 60%, respectively, compared with those in the control group; however, in mice treated with CP, the corresponding values were 60% and 85% (Figures 4(g)–4(i)). These results suggest that treatment of a MPTP-induced PD mouse model with CP attenuates

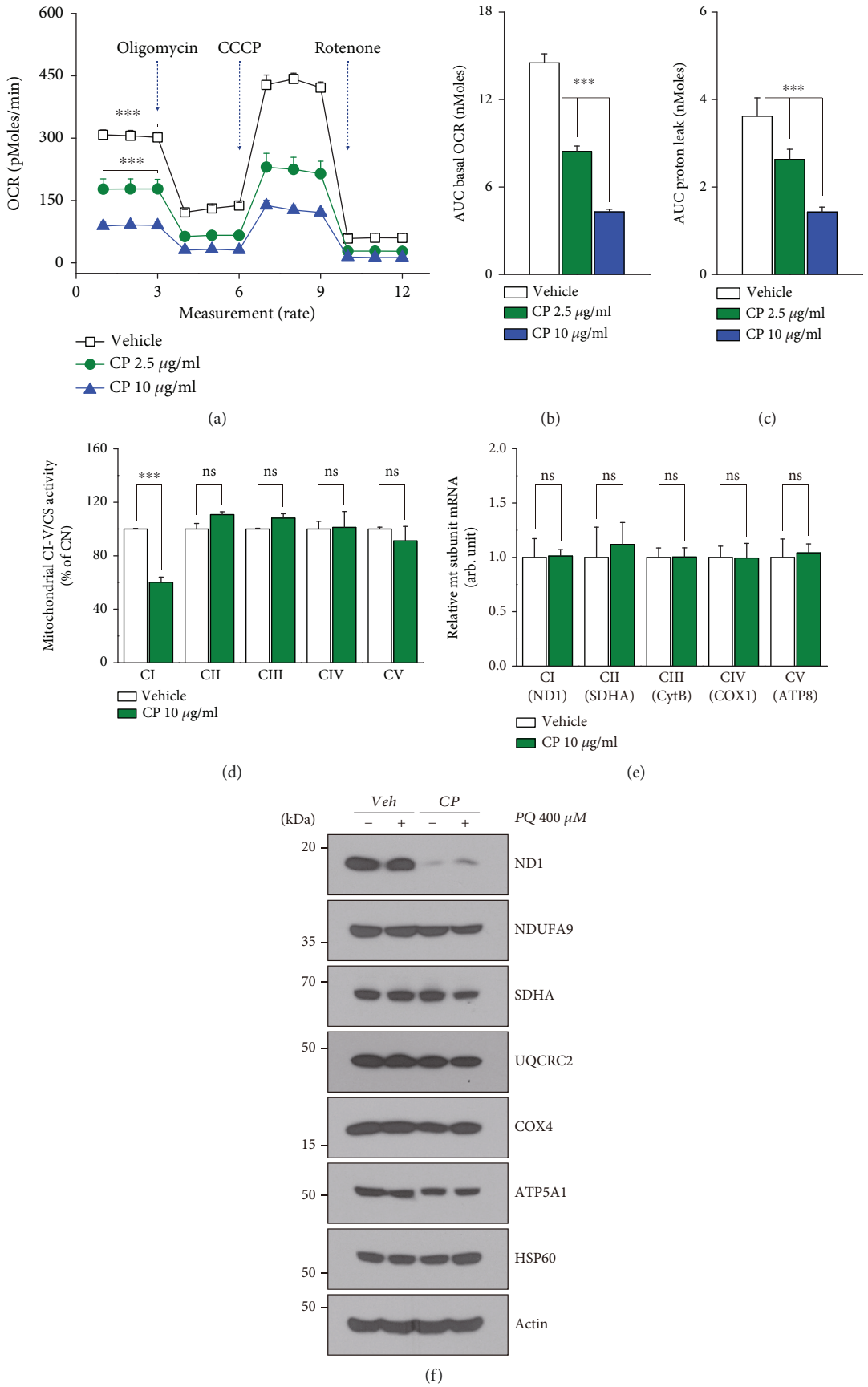

Figure 3: Continued.

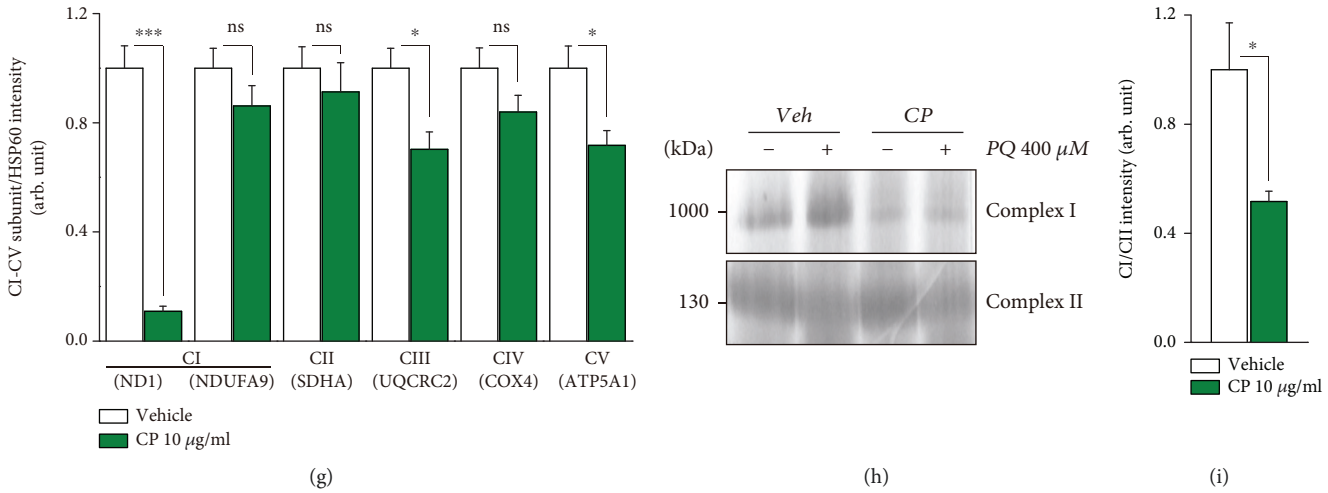

Figure 3: CP decreases mitochondrial function in SN4741 cells by reducing the amount of mitochondrial complex I. (a–c) Oxygen consumption rate (OCR), a direct indicator of mitochondrial function, was measured using an XF24 analyzer after treating SN4741 cells with 2.5 or 10 μg/ml CP for 24 h. (a) Measurement of changes in OCR ($n = 15$). (b) Bar graph showing basal OCR ($n = 15$). (c) Bar graph showing proton leak ($n = 15$). (d) Activity of mitochondrial complex I-V isolated from SN4741 cells, determined by enzymatic assay ($n = 9$). (e) The amount of mRNA for mitochondrial complex I–V subunits, determined by qPCR ($n = 12$). (f) Expression levels of mitochondrial complex I–V subunit proteins were measured by Western blotting ($n = 9$). (g) Bar graph showing quantification of mitochondrial complex I-V subunit expression, measured by Western blotting ($n = 9$). (h) Expression levels of mitochondrial supercomplex I, II proteins were measured by BN-PAGE ($n = 3$) (i) A bar graph ($n = 3$) showing quantification of mitochondrial supercomplex protein expression. All data are representative of three independent experiments. $^{***}P < 0.001$ by one-way ANOVA in (a–c) and by 2-tailed unpaired Student's t-test in (d, e, g, i); ns: not significant. Error bars represent +SD.

toxin-induced dopaminergic neuronal loss by blocking the target site of PQ action.

4. Discussion

Current treatments for PD, such as L-DOPA, MAO-B inhibitors, and dopamine agonists, cannot prevent the process of dopaminergic neuronal cell loss [5]. For this reason, ~80% of PD patients who have taken L-DOPA for 5 to 10 years will be faced with levodopa-induced dyskinesia (LID), termed a "wearing off" period. Because the pathogenesis of LID is considered to reflect a profound loss of the dopaminergic neurons that respond to L-DOPA, delaying or inhibiting dopaminergic neuronal cell loss is important for reducing the side effects of current PD drugs and extending their efficacy beyond 10 years. The production of ROS by defective or inhibited mitochondrial respiration is considered a causative factor for dopaminergic neuronal loss and the pathogenesis of PD [30, 31]. Unlike toxic environmental factors that inhibit mitochondrial complex I, CP does not induce mitochondrial ROS production. Moreover, it appears to be superior in preventing dopaminergic neuronal cell death, especially in a setting in which mitochondrial dysfunction is induced by an environmental toxin.

A key to the protective effect of CP on dopaminergic neuronal cell loss is its ability to effectively block the target of PQ toxicity in mitochondria without affecting cell viability. The administration of PQ after CP pretreatment increased the viability of SN4741 cells and rat primary cultured dopaminergic neurons compared with cells in the PQ-only control group. ROS production induced by PQ treatment was also reduced by CP pretreatment, implying that mitochondrial complex I is a target of CP. The decreased activity of mitochondrial complex I caused by the CP-induced reduction in the synthesis of ND1 protein decreased PQ recycling—a mechanism of ROS production—thereby preventing cell loss; notably, these CP effects were not observed in rotenone-pretreated SN4741 cells and mtDNA-deficient Rho0 cells. Treatment with exogenous ROS, H_2O_2, and CP caused greater cell loss than what was observed in the control group, and the expression of SOD, which is capable of removing ROS, was decreased in the CP treatment group. This implies that CP does not increase ROS-removal ability but instead suppresses ROS generation by inhibiting PQ recycling. Consistent with *in vitro* and *ex vivo* results, dopaminergic neuronal cell loss was also ameliorated by CP pretreatment in MPTP-treated PD model mice. Our findings indicate that the inhibitory effect of CP treatment on mitochondrial complex I may provide a strategy for protecting dopaminergic neurons and preventing neurotoxin-induced PD.

An important major difference between CP and drugs that induce PD is that CP effectively inhibits mitochondrial protein translation and complex formation but only to an extent that does not result in intracellular toxicity. This is exemplified by CP-induced reductions in mitochondrial functions, such as oxygen consumption rate, mitochondrial activity, mitochondrial super-complex formation, and subunit protein expression, in the absence of effects on the total amount of ATP (data not shown) in cells or cell viability. Although some previously published studies reported that CP induces mitochondrial dysfunction and causes

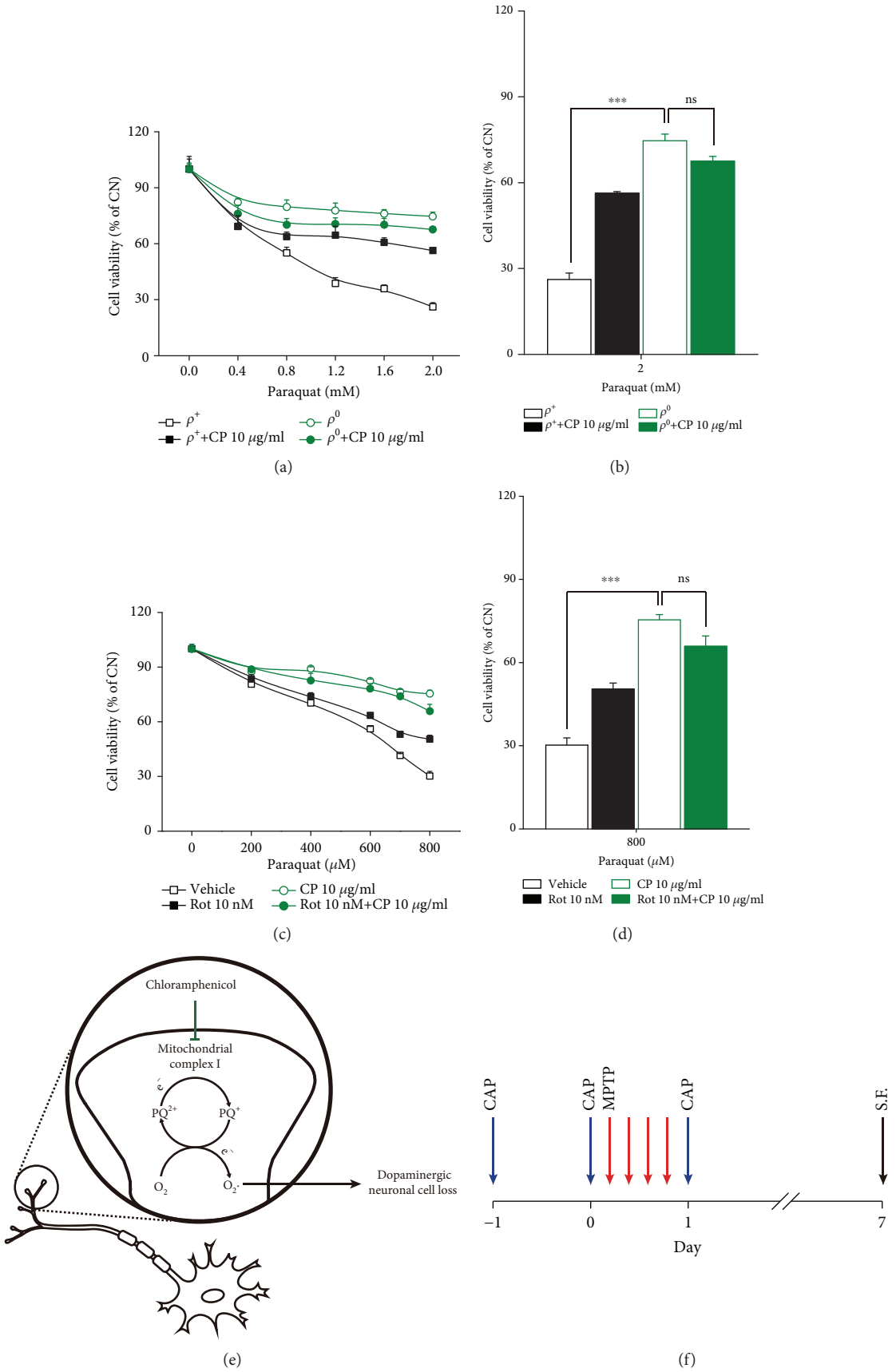

Figure 4: Continued.

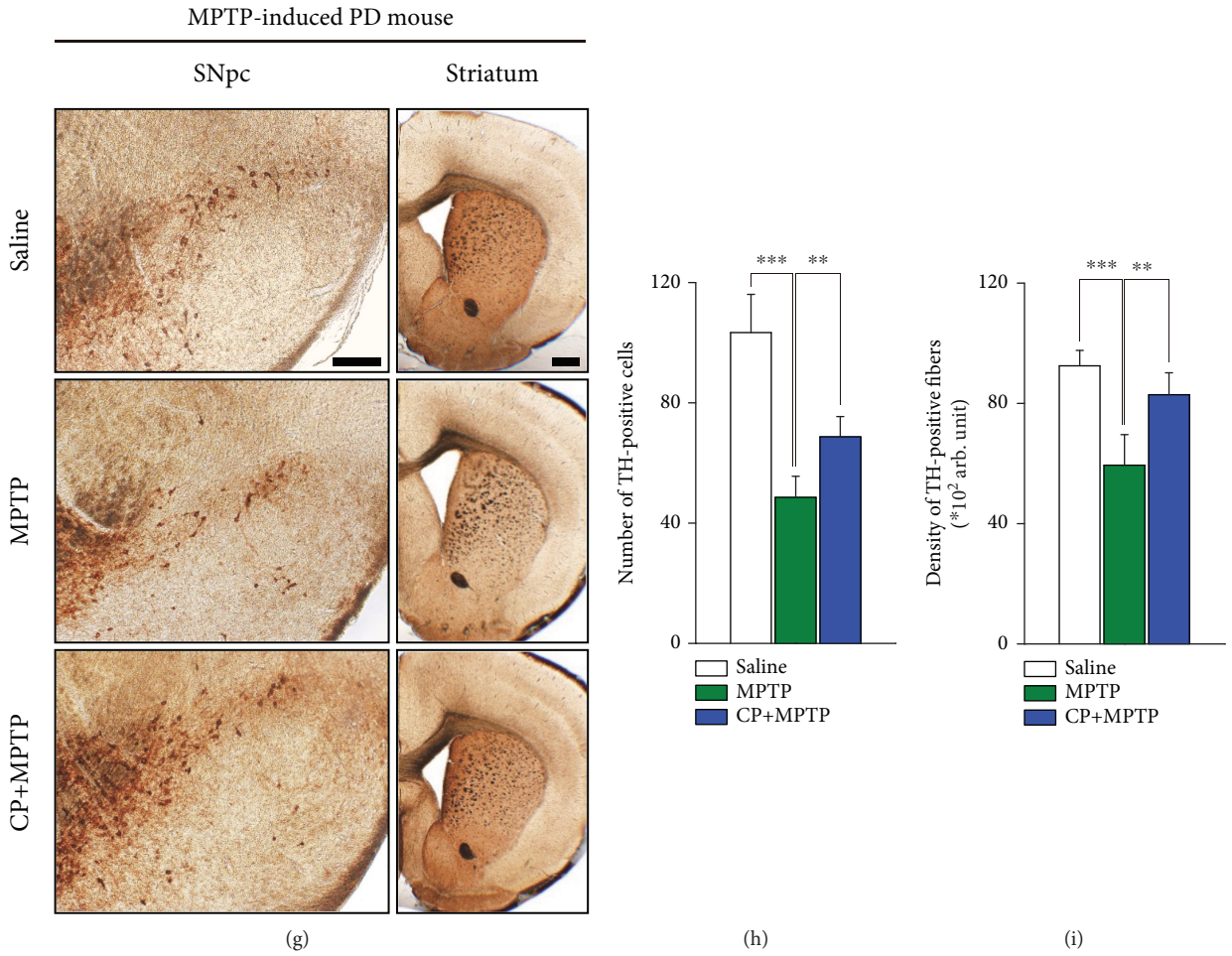

Figure 4: In vitro experimental models with reduced mitochondrial function exhibit higher resistance to PQ, and CP protects against dopaminergic neuronal loss in the MPTP-induced PD mouse model. (a, b) To confirm the mitochondrial dependence of PQ and the additional protective effects of CP, we examined the survival rates of wild-type Rho+ and mtDNA-deficient Rho0 cells following treatment with PQ or PQ plus CP. (a) Viability of Rho+ and Rho0 cell lines after treatment with 10 μg/ml CP and PQ was confirmed using CCK8 assays ($n = 15$). (b) Bar graphs showing quantification of cell viability following treatment with 2 mM PQ ($n = 15$). (c, d) Treatment with the mitochondrial complex I inhibitor, rotenone, decreased mitochondrial function and cell viability, as confirmed by PQ treatment in SN4741 cells. (c) Cell viability, determined using CCK8 assays ($n = 15$). (d) Bar graphs showing quantification of cell viability in 800 μM PQ ($n = 15$). (f–h) MPTP and CP treatment conditions used in MPTP-induced PD mouse model experiments ($n = 9$). (e) A schematic overview of the protective role of CP against PQ-induced neuronal cell loss on the basis of our results. (f) Mice were administered MPTP four times per day and CP (50 mg/kg) was orally administered three times. One week after MPTP administration, mice were sacrificed and the brain tissue was immunostained. (g) Dopaminergic neurons in the SNpc and striatum regions in brain tissue from MPTP-induced PD mouse models were confirmed by TH immunostaining ($n = 9$) (scale bars, left panel; 100 μm; right panel; 250 μm). (h, i) Bar graph showing quantification of the total number of dopaminergic neurons in the striatum region ($n = 9$). All data are representative of three independent experiments. $^{***}P < 0.001$ by one-way ANOVA in (c, e) and by 2-tailed unpaired Student's t-test in (h, i); ns: not significant. Error bars represent +SD.

neurotoxicity, they used a higher (cytotoxic) concentration of CP than that used in our study [35].

We used two types of experimental models of PD: an *in vitro* model using PQ-treated cell lines and an MPTP-treated mouse (*in vivo*) model of PD. Although these two experimental models are not identical, both PQ and MPTP cause toxicity by targeting the mitochondria of dopaminergic neurons [1, 36]. PQ produces ROS through PQ recycling in mitochondrial complex I, whereas MPTP is converted to MPP+ to generate ROS via mitochondria; in both cases, the result is neurotoxicity. Thus, both PQ and MPTP induce dopaminergic neuronal cell loss through the effects on mitochondria, and the protective effect of CP was evident in both models. Extending the effectiveness of CP to sporadic PD would require verification of our results using an animal model of PD-related gene mutants, such as the α-synuclein A53T mutant model.

Ongoing research seeks to identify new and efficacious drugs for the growing world market for PD therapeutics. One representative example is axitinib, a tyrosine kinase inhibitor identified as part of the "Discovering New Therapeutic Uses for Existing Molecules" program that has been

used to treat renal cell cancer [37]. Such drug repurposing, defined as the use of existing drugs that have passed numerous toxicity and clinical safety tests for new indications, can identify new uses for old compounds and facilitate the introduction of new treatment strategies. This approach has revealed that CP is a promising candidate for the treatment of PD. The development of new therapies is a time-consuming and extremely expensive process. By comparison, new therapeutic applications of commercially available therapeutic agents bypass extensive regulatory requirements since the safety of the therapeutic agent has already been demonstrated.

5. Conclusions

Some studies have shown that protection of neuronal cells by antibiotics, typically including ceftriaxone, rapamycin, and rifampicin, is effective in neurodegenerative diseases [14–16]. Although antibiotics are used in PD to protect neurons, previous studies have focused on inflammation-based mechanisms related to the known bactericidal/bacteriostatic actions of these antibiotics, but little is known in terms of their effects on intracellular metabolism, such as mitochondrial respiration. We have shown that CP effectively reduces mitochondrial damage within a concentration range that does not affect cell survival and thus effectively protects against drugs that cause toxicity through mitochondrial-dependent cell loss. PQ and MPTP are widely used in the third world as herbicides. Clinical statistics indicate that many patients with PD, especially in rural areas that use large amounts of pesticides, would benefit from a new treatment option that targeted mitochondrial dysfunction, highlighting the importance of the current study. If the diagnosis of presymptomatic PD patients is possible through the development of PD biomarkers in the future, CP could be beneficial in delaying disease progression and reducing the severity of behavioral symptoms.

Data Availability

The data used to support the findings of this study are available from the corresponding authors upon request.

Conflicts of Interest

The authors declare that they have no conflict of interest.

Authors' Contributions

JH, SJK, MS, JYH, and GRK made substantial contributions to the conception and design of the study. JH and SJK were responsible for the acquisition of data and provided materials for animal experiments. All authors helped with the analysis and interpretation of data. JH, SJK, JYH, and GRK wrote the manuscript. All authors contributed to the discussion and revised the article, and all approved the final version of the manuscript. GRK and JYH are responsible for the integrity of the work as a whole. Jeongsu Han and Soo Jeong Kim contributed equally to this work.

Acknowledgments

This work was funded by the National Research Foundation of Korea (NRF) grant, the Ministry of Science and ICT (MSIT) (2016R1A2B4010398, 2017R1A5A2015385, and 2019M3E5D1A02068575), the Ministry of Education (2014R1A6A1029617 and 2016R1D1A1B03932766), and the research fund of Chungnam National University.

Supplementary Materials

This article contains supplementary information, which is available to authorized users. *(Supplementary Materials)*

References

[1] S. Mostafalou and M. Abdollahi, "Pesticides and human chronic diseases: evidences, mechanisms, and perspectives," *Toxicology and Applied Pharmacology*, vol. 268, no. 2, pp. 157–177, 2013.

[2] K. Wirdefeldt, H. O. Adami, P. Cole, D. Trichopoulos, and J. Mandel, "Epidemiology and etiology of Parkinson's disease: a review of the evidence," *European Journal of Epidemiology*, vol. 26, Supplement 1, pp. 1–58, 2011.

[3] A. Elbaz, J. Clavel, P. J. Rathouz et al., "Professional exposure to pesticides and Parkinson disease," *Annals of Neurology*, vol. 66, no. 4, pp. 494–504, 2009.

[4] W. Oertel and J. B. Schulz, "Current and experimental treatments of Parkinson disease: a guide for neuroscientists," *Journal of Neurochemistry*, vol. 139, no. S1, pp. 325–337, 2016.

[5] S. Fahn, D. Oakes, I. Shoulson et al., "Levodopa and the progression of Parkinson's disease," *The New England Journal of Medicine*, vol. 351, no. 24, pp. 2498–2508, 2004.

[6] G. Pezzoli and E. Cereda, "Exposure to pesticides or solvents and risk of Parkinson disease," *Neurology*, vol. 80, no. 22, pp. 2035–2041, 2013.

[7] F. Kamel, "Paths from pesticides to Parkinson's," *Science*, vol. 341, no. 6147, pp. 722-723, 2013.

[8] T. Blanco-Ayala, A. C. Anderica-Romero, and J. Pedraza-Chaverri, "New insights into antioxidant strategies against paraquat toxicity," *Free Radical Research*, vol. 48, no. 6, pp. 623–640, 2014.

[9] H. M. Cocheme and M. P. Murphy, "The uptake and interactions of the redox cycler paraquat with mitochondria," *Methods in Enzymology*, vol. 456, pp. 395–417, 2009.

[10] P. Jenner, D. T. Dexter, J. Sian, A. H. V. Schapira, C. D. Marsden, and The Royal Kings And Queens Parkinson's Disease Research Group, "Oxidative stress as a cause of nigral cell death in Parkinson's disease and incidental lewy body disease," *Annals of Neurology*, vol. 32, no. S1, pp. S82–S87, 1992.

[11] J. Sian, D. T. Dexter, A. J. Lees, S. Daniel, P. Jenner, and C. D. Marsden, "Glutathione-related enzymes in brain in Parkinson's disease," *Annals of Neurology*, vol. 36, no. 3, pp. 356–361, 1994.

[12] M. Thiruchelvam, O. Prokopenko, D. A. Cory-Slechta, E. K. Richfield, B. Buckley, and O. Mirochnitchenko, "Overexpression of superoxide dismutase or glutathione peroxidase protects against the paraquat + maneb-induced Parkinson disease phenotype," *The Journal of Biological Chemistry*, vol. 280, no. 23, pp. 22530–22539, 2005.

[13] N. Nakao, E. M. Frodl, H. Widner et al., "Overexpressing Cu/Zn superoxide dismutase enhances survival of transplanted neurons in a rat model of Parkinson's disease," *Nature Medicine*, vol. 1, no. 3, pp. 226–231, 1995.

[14] R. Bisht, B. Kaur, H. Gupta, and A. Prakash, "Ceftriaxone mediated rescue of nigral oxidative damage and motor deficits in MPTP model of Parkinson's disease in rats," *Neurotoxicology*, vol. 44, pp. 71–79, 2014.

[15] E. D. Smith, G. A. Prieto, L. Tong et al., "Rapamycin and interleukin-1β impair brain-derived neurotrophic factor-dependent neuron survival by modulating autophagy," *The Journal of Biological Chemistry*, vol. 289, no. 30, pp. 20615–20629, 2014.

[16] Y. Liang, T. Zhou, Y. Chen et al., "Rifampicin inhibits rotenone-induced microglial inflammation via enhancement of autophagy," *Neurotoxicology*, vol. 63, pp. 137–145, 2017.

[17] V. Jackson-Lewis and S. Przedborski, "Protocol for the MPTP mouse model of Parkinson's disease," *Nature Protocols*, vol. 2, no. 1, pp. 141–151, 2007.

[18] T. Fath, Y. D. Ke, P. Gunning, J. Gotz, and L. M. Ittner, "Primary support cultures of hippocampal and substantia nigra neurons," *Nature Protocols*, vol. 4, no. 1, pp. 78–85, 2009.

[19] J. H. Son, H. S. Chun, T. H. Joh, S. Cho, B. Conti, and J. W. Lee, "Neuroprotection and neuronal differentiation studies using substantia nigra dopaminergic cells derived from transgenic mouse embryos," *The Journal of Neuroscience*, vol. 19, no. 1, pp. 10–20, 1999.

[20] H. S. Chun, G. E. Gibson, D. G. LA, H. Zhang, V. J. Kidd, and J. H. Son, "Dopaminergic cell death induced by MPP^+, oxidant and specific neurotoxicants shares the common molecular mechanism," *Journal of Neurochemistry*, vol. 76, no. 4, pp. 1010–1021, 2001.

[21] H. J. Lee, J. Han, Y. Jang et al., "Docosahexaenoic acid prevents paraquat-induced reactive oxygen species production in dopaminergic neurons via enhancement of glutathione homeostasis," *Biochemical and Biophysical Research Communications*, vol. 457, no. 1, pp. 95–100, 2015.

[22] S. J. Kim, M. J. Ryu, J. Han et al., "Activation of the HMGB1-RAGE axis upregulates TH expression in dopaminergic neurons via JNK phosphorylation," *Biochemical and Biophysical Research Communications*, vol. 493, no. 1, pp. 358–364, 2017.

[23] K. Hashiguchi and Q. M. Zhang-Akiyama, "Establishment of human cell lines lacking mitochondrial DNA," *Methods in Molecular Biology*, vol. 554, pp. 383–391, 2009.

[24] H. K. Chung, Y. K. Kim, J. H. Park et al., "The indole derivative NecroX-7 improves nonalcoholic steatohepatitis in *ob*/*ob* mice through suppression of mitochondrial ROS/RNS and inflammation," *Liver International*, vol. 35, no. 4, pp. 1341–1353, 2015.

[25] S. J. Kim, M. C. Kwon, M. J. Ryu et al., "CRIF1 is essential for the synthesis and insertion of oxidative phosphorylation polypeptides in the mammalian mitochondrial membrane," *Cell Metabolism*, vol. 16, no. 2, pp. 274–283, 2012.

[26] C. Henchcliffe and M. F. Beal, "Mitochondrial biology and oxidative stress in Parkinson disease pathogenesis," *Nature Clinical Practice. Neurology*, vol. 4, no. 11, pp. 600–609, 2008.

[27] S. Rayport, D. Sulzer, W. X. Shi et al., "Identified postnatal mesolimbic dopamine neurons in culture: morphology and electrophysiology," *The Journal of Neuroscience*, vol. 12, no. 11, pp. 4264–4280, 1992.

[28] D. L. Cardozo, "Midbrain dopaminergic neurons from postnatal rat in long-term primary culture," *Neuroscience*, vol. 56, no. 2, pp. 409–421, 1993.

[29] D. Sulzer, M. P. Joyce, L. Lin et al., "Dopamine neurons make glutamatergic synapses in vitro," *The Journal of Neuroscience*, vol. 18, no. 12, pp. 4588–4602, 1998.

[30] H. M. Cocheme and M. P. Murphy, "Complex I is the major site of mitochondrial superoxide production by paraquat," *The Journal of Biological Chemistry*, vol. 283, no. 4, pp. 1786–1798, 2008.

[31] P. R. Castello, D. A. Drechsel, and M. Patel, "Mitochondria are a major source of paraquat-induced reactive oxygen species production in the brain," *The Journal of Biological Chemistry*, vol. 282, no. 19, pp. 14186–14193, 2007.

[32] A. A. Yunis, "Chloramphenicol toxicity: 25 years of research," *The American Journal of Medicine*, vol. 87, no. 3N, pp. 44N–48N, 1989.

[33] R. O. Vogel, J. A. M. Smeitink, and L. G. J. Nijtmans, "Human mitochondrial complex I assembly: a dynamic and versatile process," *Biochimica et Biophysica Acta (BBA) - Bioenergetics*, vol. 1767, no. 10, pp. 1215–1227, 2007.

[34] D. A. Stroud, E. E. Surgenor, L. E. Formosa et al., "Accessory subunits are integral for assembly and function of human mitochondrial complex I," *Nature*, vol. 538, no. 7623, pp. 123–126, 2016.

[35] C. A. Guimaraes and R. Linden, "Chloramphenicol induces apoptosis in the developing brain," *Neuropharmacology*, vol. 39, no. 9, pp. 1673–1679, 2000.

[36] D. T. Dexter and P. Jenner, "Parkinson disease: from pathology to molecular disease mechanisms," *Free Radical Biology & Medicine*, vol. 62, pp. 132–144, 2013.

[37] T. Pemovska, E. Johnson, M. Kontro et al., "Axitinib effectively inhibits BCR-ABL1(T315I) with a distinct binding conformation," *Nature*, vol. 519, no. 7541, pp. 102–105, 2015.

Hindawi
Oxidative Medicine and Cellular Longevity
Volume 2019, Article ID 4578462, 11 pages
https://doi.org/10.1155/2019/4578462

Review Article

Current Progress of Mitochondrial Quality Control Pathways Underlying the Pathogenesis of Parkinson's Disease

Xue Jiang, Tao Jin, Haining Zhang, Jing Miao, Xiuzhen Zhao, Yana Su, and Ying Zhang

Department of Neurology and Neuroscience Center, First Hospital of Jilin University, Xinmin Street No. 71, Changchun 130000, China

Correspondence should be addressed to Ying Zhang; zhang_ying99@jlu.edu.cn

Received 5 March 2019; Revised 5 June 2019; Accepted 11 July 2019; Published 14 August 2019

Academic Editor: Ana Lloret

Parkinson's disease (PD), clinically characterized by motor and nonmotor symptoms, is a common progressive and multisystem neurodegenerative disorder, which is caused by both genetic and environmental risk factors. The main pathological features of PD are the loss of dopaminergic (DA) neurons and the accumulation of alpha-synuclein (α-syn) in the residual DA neurons in the substantia nigra pars compacta (SNpc). In recent years, substantial progress has been made in discovering the genetic factors of PD. In particular, a total of 19 PD-causing genes have been unraveled, among which some members have been regarded to be related to mitochondrial dysfunction. Mitochondria are key regulators of cellular metabolic activity and are critical for many important cellular processes including energy metabolism and even cell death. Their normal function is basically maintained by the mitochondrial quality control (MQC) mechanism. Accordingly, 1-methyl-4-phenyl-1,2,3,6-tetrahydropyridine (MPTP), a kind of neurotoxin, exerts its neurotoxic effects at least partially by producing its toxic metabolite, namely, 1-methyl-4-phenylpyridine (MPP+), which in turn causes mitochondrial dysfunction by inhibiting complex I and mimicking the key features of PD pathogenesis. This review focused on three main aspects of the MQC signaling pathways, that is, mitochondrial biogenesis, mitochondrial dynamics, and mitochondrial autophagy; hence, it demonstrates in detail how genetic and environmental factors result in PD pathogenesis by interfering with MQC pathways, thereby hopefully contributing to the discovery of novel potential therapeutic targets for PD.

1. Introduction

Parkinson's disease (PD) is the second most common neurodegenerative disorder after Alzheimer's disease (AD), from which over 1% of the population older than 60 years of age worldwide has suffered from related serious and even fatal illness [1]. The progressive loss of dopaminergic (DA) neurons and the accumulation of α-synuclein (α-syn) in the residual DA neurons in the substantia nigra pars compacta (SNpc) are the main pathological features of the disease [2]. The clinical features of PD are generally subdivided into motor and nonmotor symptoms. Motor symptoms mainly include muscle rigidity, bradykinesia, posture disorders, and resting tremors. These symptoms are traditionally considered to largely result from the loss of DA neurons in the SNpc [3]. Comparatively, the nonmotor symptoms of PD include depression, cognitive impairment, hallucinations, sleep disorders, olfactory disorders, and autonomic dysfunction. Besides the fact that some of these nonmotor symptoms may appear as early as one decade prior to the appearance of motor dysfunction [1], more intriguingly, some of these nonmotor symptoms in PD cannot be simply ascribed to the loss of DA neurons in the SNpc. As a matter of fact, the etiology of PD is yet to be fully defined, which is generally related to either genetic or environmental factors [4].

During the past two decades, substantial progress has been made in genetic mapping and understanding the roles of related genes in PD pathogenesis, especially single-gene causative genes. About 15% of the patients with PD have a family history, and 5-10% have been identified to have genetic susceptibility factors known as Mendelian forms [5]. To date, 19 pathogenic genes have been uncovered to be involved in PD pathogenesis, including 10 autosomal dominant genes and 9 autosomal recessive ones [6]. At

present, SNCA (PARK1), LRRK2 (PARK8), CHCHD2 (PARK22), Parkin (PARK2), PINK1 (PARK6), and other gene mutations are widely studied in PD pathogenesis [7, 8].

Although PD pathogenesis remains elusive, multiple essential processes have been found to contribute to the higher incidence among patients, including protein aggregation, impairment of the ubiquitin-proteasome pathway, oxidative stress, mitochondrial dysfunction, and neuroinflammation [9]. Accumulated evidence from PD models *in vitro* and *in vivo* suggested that mitochondrial dysfunction plays a major role in the pathogenesis of PD [8, 10–12]. The connection between mitochondrial dysfunction and PD was originally inspired by the administration of the neurotoxin 1-methyl-4-phenyl-1,2,3,6-tetrahydropyridine (MPTP), a by-product of the chemical synthesis of pethidine that may induce syndromes of PD [13, 14]. The neurotoxicity of MPTP is derived from its toxic metabolite 1-methyl-4-phenylpyridine (MPP+), which has a suppressive capacity over the electron transport chain by inhibiting the accumulation of complex I in the mitochondria, thus leading to mitochondrial dysfunction [15, 16]. Toxicants such as rotenone and paraquat, which are structurally similar to MPTP, further demonstrated the vital role of MPTP in mitochondrial dysfunction [17]. Given the indispensability of mitochondria within eukaryotic cells for energy metabolism, which is mainly driven by oxidative phosphorylation (OXPHOS), along with their involvements in many other physiological processes such as programmed cell death, innate immunity, autophagy, redox signaling, calcium homeostasis, and stem cell reprogramming, the role of mitochondria has received increasing attention during the pathogenesis of PD. Accordingly, its proper functioning is basically maintained by the mitochondrial quality control (MQC) machinery, a highly integrated network of signaling pathways, which is constantly involved in mitochondrial dynamics, biogenesis, and mitophagy [18]. Conversely, a variety of key biosynthetic processes such as ATP production, Ca^{2+} buffering, and apoptosis can be drastically undermined by impaired mitochondrial quality control pathways, which may in turn interfere with overall cellular homeostasis [19]. Reactive oxygen species (ROS) are by-products of biological aerobic metabolism, which include oxygen free radicals (such as superoxide anion radical ($O_2^{\cdot}$) and hydroxyl radical ($^{\cdot}OH$)), nonradical oxidants (such as hydrogen peroxide (H_2O_2)), and oxygen-containing free radicals (such as nitric oxide (NO) and peroxyl radical ($^{\cdot}OOH$)) [20]. ROS are mainly produced by mitochondria, and maintaining low levels of ROS is critical for normal cellular function [21]. When the steady state equilibrium between ROS and the antioxidant defense system is destroyed, oxidative stress occurs, which not only causes harmful oxidation of biological macromolecules such as lipids, DNA, and proteins, but also causes the destruction of dopaminergic neurons [20–23]. Antioxidants include antioxidant enzymes (e.g., superoxide dismutase (SOD), catalase (CAT), glutathione peroxidase, and glutathione-S-transferase) and nonenzymatic antioxidant factors (e.g., melatonin, carotenoid and some microelements) [24]. Thus, ROS homeostasis plays a key role in maintaining the stability of mitochondrial quality control. Therefore, a detailed understanding of the precise role of the mitochondrial quality control pathways that underlie the pathogenesis of PD is conducive to the discovery of novel therapeutic targets for PD. In this review, we mainly focused on mitochondrial biogenesis, mitochondrial dynamics, and mitochondrial autophagy in order to gain a better understanding of the latest advances in mitochondrial quality control in PD pathogenesis, based on both genetic and environmental risk factors (see Figure 1).

2. Mitochondrial Biogenesis and PD

2.1. Mitochondrial Biogenesis. Mitochondrial biosynthesis plays an important role in mitochondrial quality control by creating new mitochondria to replace damaged mitochondria. Mammalian mitochondria are semiautonomous organelles containing products expressed from both mitochondrial genomes and nuclear genomes [25–27]. Despite the fact that the mitochondrial genome consists of circular double-stranded DNA (mtDNA), mitochondria still rely heavily on the expression of the nuclear genome to achieve most of its biological functions, possibly due to the limited coding capacity of mtDNA [28]. Mitochondrial biogenesis is activated by numerous different signals at the time of cellular stress or in response to environmental stimuli (nutrient availability, growth factors and hormones, toxins, temperature and oxygen fluctuations, among others) to form new mitochondria to maintain and restore mitochondrial structure, quantity, and function. Mitochondrial biogenesis is a complex and multistep cellular process, which not only involves the synthesis of either the inner or outer mitochondrial membrane but also involves the synthesis of mitochondrial-encoded proteins, the synthesis and import of nuclear-encoded mitochondrial proteins, and the replication of mtDNA [29]. Furthermore, the normal development of mitochondria requires coordinated expression of both the mitochondrial genome and the nuclear genome [30]. Currently, the mitochondrial biogenesis process is considered to be mainly regulated by peroxisome proliferator-activated receptor-gamma (PPARγ) coactivator-1 alpha (PGC-1α) [31]. Adenosine monophosphate protein kinase (AMPK) and silent information regulator 1 (Sirt1) act as upstream regulators of PGC-1α, which activate PGC-1α by phosphorylation and deacetylation, respectively [32]. Upon activation of PGC-1α by phosphorylation or deacetylation, activated PGC-1α in turn activates nuclear respiratory factors 1 and 2 (NRF1 and NRF2), resulting in increased levels of NRF1 and NRF2 expression and their activities [33]. Subsequently, NRF1 and NRF2 activate mitochondrial transcription factor A (Tfam) to drive the transcription and replication of mitochondrial DNA, inducing mitochondrial biogenesis [34]. ROS, functioning as intracellular signaling messengers, play a key role in cell proliferation, apoptosis, and cellular oxidative damage [35]. Studies have shown that PGC-1α expression is regulated by ROS, thereby forming a potential network between PGC-1α and ROS [36–38]. It was found that NO can increase the expression of PGC-1α by activating AMPK and SIRT1, and H_2O_2 can also regulate the expression of PGC-1α through the AMPK pathway [32, 39]. At the same

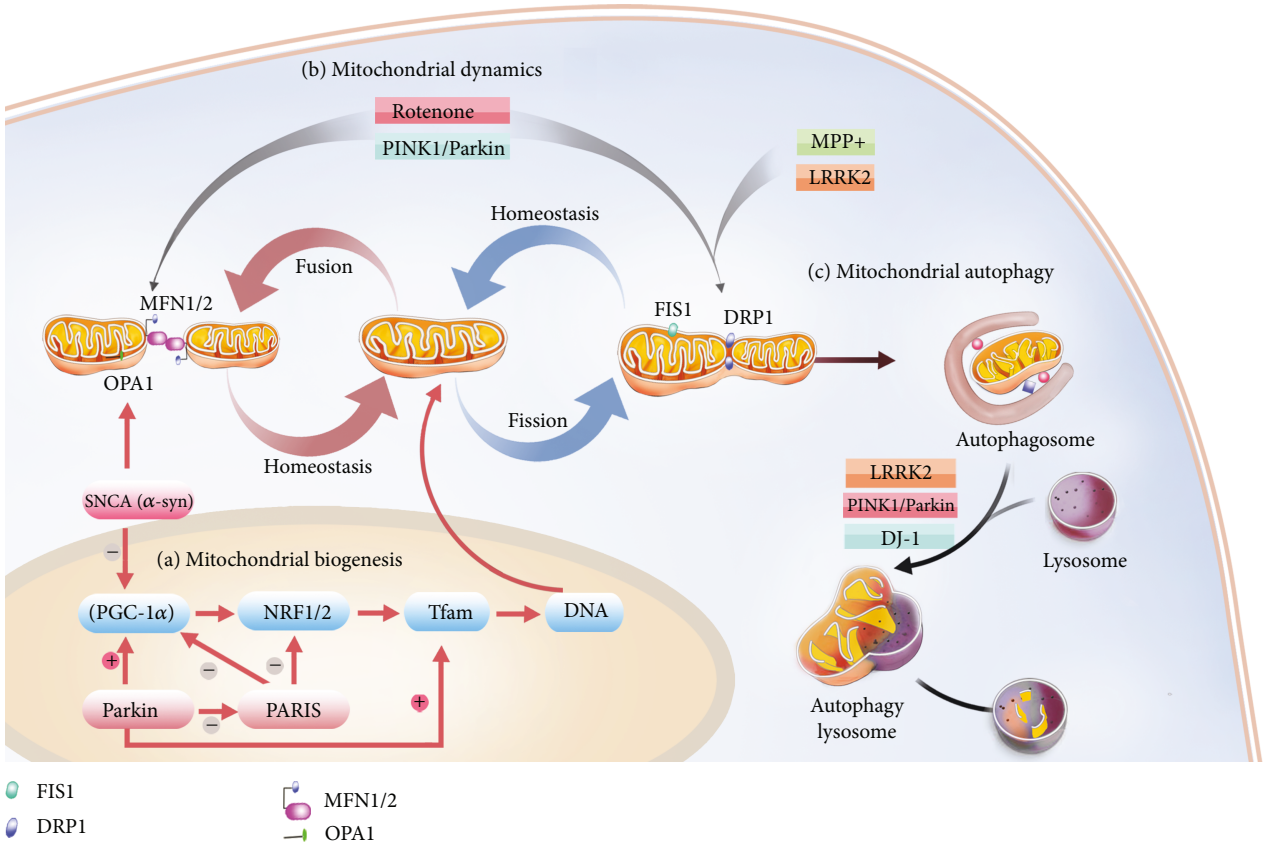

Figure 1: A schematic illustration of mitochondrial quality control in Parkinson's disease. (a) Mitochondrial biosynthesis plays an important role in mitochondrial quality control by creating new mitochondria to replace damaged mitochondria. (b) Mitochondrial dynamics include both mitochondrial division and mitochondrial fusion, which are critical for maintaining mitochondrial homeostasis and normal function. (c) Autophagy is generally a process by which cells degrade harmful or excessive cellular components and thus recycling components to maintain the homeostasis.

time, PGC-1α can also potently reduce the generation of mitochondrial-driven ROS, and loss of PGC-1α activity will lead to an increase in ROS [36, 40]. These regulatory factors play an important role in the maintenance of organelles and the expression of nuclear and mitochondrial genes required for biogenesis.

2.2. Abnormalities in Mitochondrial Biogenesis and Their Implications for PD. PGC-1α dysregulation affects mitochondrial biogenesis, leading to mitochondrial dysfunction, which will cause disease. Next, we will mainly discuss the relationship between PD and PGC-1α imbalance. A decrease in PGC-1α and the downregulation of various PGC-1α target genes were observed in DA neurons of PD [11, 41], suggesting that dysfunctional PGC-1α is involved in the clinical pathogenesis of PD. DA neurons in PGC-1α knockout mice are more sensitive to the neurodegenerative effects of MPTP and other stressors [36]. The importance of PGC-1α in the pathogenesis of PD was further revealed by the generation of PGC-1α deficient mice. PARIS is a transcriptional repressor that inhibits the expression of PGC-1α and its target gene NRF1 [42, 43]. PINK1/Parkin not only promotes mitochondrial biosynthesis by inducing the proteasomal degradation of PARIS to enhance PGC-1α transcription, but also directly interacts with Tfam to induce mtDNA replication and transcription of mitochondrial genes [44]. It has been widely accepted that the PINK1/Parkin gene acts as a major neuroprotective gene whose mutation is most likely to result in abnormal mitochondrial biogenesis. Besides, its mutation is the most common autosomal recessive form of PD. Quite a few studies have shown that α-syn binds to the PGC-1α promoter under oxidative stress and leads to PGC-1α suppression, for which mitochondrial biogenesis is in turn compromised [45]. In fact, it has been demonstrated in animal models that the inhibition of PGC-1α may sensitize experimental models to the neurodegenerative effects of MPTP, α-syn, and other stressors [36, 46], whereas the overexpression of PGC-1α has been shown to rescue either synaptic abnormalities caused by α-syn mutations or dopaminergic neuron loss induced by acute MPTP administration [36, 47, 48]. Studies have reported that PGC-1α is a broad and powerful regulator of ROS metabolism, and the expression of ROS antioxidant enzymes increases with the increase of PGC-1α [37–39]. Oxidative damage caused by the deletion of PGC-1α aggravates the degeneration of dopaminergic neurons [36]. Epidemiological studies have shown that high saturated fat diet is a risk factor for sporadic PD [49, 50]. The administration of palmitate to ICV in alpha-synuclein

transgenic mice results in the hypermethylation of the PGC-1α promoter in the substantia nigra (SN), which in turn reduces PGC-1α gene expression and decreases mitochondrial content [51]. This further provides evidence that PGC-1α inhibition can promote sporadic PD. At the same time, research on PGC-1α is increasing in the search for PD treatment methods. cAMP response element binding protein (CREB) and activating transcription factor 2 (ATF2) are transcriptional activators of PGC-1α. Studies have found that metformin acts as a potential upstream regulator of mitochondrial gene transcription, stimulating PGC-1α promoter activity via the CREB and ATF2 pathways [52]. Collectively, previous studies indicated that PGC-1α, as a major regulator of mitochondrial biogenesis, is indeed a pivotal component involved in the pathogenesis of PD and may become a potential therapeutic target for PD.

3. Mitochondrial Dynamics and PD

3.1. Mitochondrial Dynamics. Mitochondria are dynamic organelles that are continuously undergoing fission and fusion in addition to organelle redistribution within the cytosol [53]. This property of mitochondria is collectively referred to as mitochondrial dynamics, which is essential for maintaining mitochondrial homeostasis and normal function. For instance, the length, shape, size, and number of mitochondria are basically controlled by their fusion and fission [54]. Mitochondria normally comprise the outer mitochondrial membranes (OMM) and the inner mitochondrial membranes (IMM), which constitute the border of the intermembrane space (IMS) and the matrix [55]. Mitochondrial fusion is a dynamic process in which two mitochondria not only fuse to form elongated mitochondria but also undergo component exchange, resulting in the renewal of the macromolecule as well as the ions [56, 57]. Furthermore, mitochondrial fusion requires a coordinated operation between the outer and inner membranes. In particular, mitochondrial fusion proteins in mammals are primarily composed of three members of the actin-related guanosine triphosphatase (GTPases) family, i.e., mitochondrial proteins (MFN) 1 and 2 and optic atrophy 1 (OPA1) [58]. MFN1 and MFN2 are involved in OMM fusion, while OPA1 is involved in IMM fusion [53, 59].

Mitochondrial division refers to the process of redistributing the mitochondrial matrix and mitochondrial DNA into two new mitochondria by separating the mitochondrial membrane, thereby isolating severely damaged mitochondria or protecting mitochondria against irreversible damages [60]. The dynein-related GTPase protein (DRP1) and mitochondrial fission (FIS1) are the major proteins responsible for fission [56].

Moreover, mitochondrial dynamics not only maintains the integrity of mitochondrial DNA and the balance of oxidative respiration, intracellular biosynthesis, and intracellular calcium signaling pathways but also underlies many essential processes, including neuronal remodeling and apoptosis. Imbalances of mitochondrial division and fusion often lead to structural alterations and dysfunction of mitochondria. Abnormalities in mitochondrial fusion often cause mitochondrial fragmentation, whereas the formation of megamitochondria usually results from defects in mitochondrial division. One of the most basic functions of mitochondrial fusion is the functional complementarity between mitochondria through the exchange of key components such as proteins from respiratory complexes as well as mtDNA [61–64]. Drastic alterations in mitochondrial fusion are most likely to lead to an increased mutation rate and genomic loss, which are definitely not conducive to maintaining the integrity of mtDNA [65].

3.2. Environmental Factors for Mitochondrial Dynamics. The kinetic defects within mitochondria usually become increasingly prominent during neurodegeneration, especially in the pathogenesis of PD [66, 67]. In particular, imbalances in the kinetic properties of neuronal mitochondria show strong association with PD through both environmental and genetic factors. For instance, an *in vitro* study using primary neurons showed that high concentrations of *rotenone* effectively induce mitochondrial division, whereas either exogenous overexpression of MFN1 or dominant inactivation of DRP1 results in a higher incidence of mitochondrial fusion, thus potentially preventing mitochondrial rupture as well as rescuing neurons from injury-induced dendrite degeneration and even neuronal death [68]. Similarly, Wang et al. established a PD model by MPP+ administration in order to determine the effect of MPP+ on mitochondrial dynamics. Their results have revealed that in neuron-derived SH-SY5Y cells, MPP+ accelerates mitochondrial fragmentation by increasing DRP1 expression levels and promoting the recruitment of DRP1 within mitochondria [69]. This study also showed that genetic inactivation of DRP1 completely blocks MPP+-induced mitochondrial fragmentation, and hence almost completely blocks downstream events such as MPP+-induced bioenergy homeostatic disruption, ROS production, and neuronal death, suggesting that DRP1-dependent mitochondrial fragmentation is mediated by MPP+-induced mitochondrial abnormalities. Excessive mitochondrial fragmentation is associated with the pathology of sporadic PD. Santos et al. demonstrated that only the inhibition of Drp1-induced fission and not Opa1-induced fusion rescues mitochondrial deficits in sporadic cases [70]. Thus, cellular dysfunction caused by kinetic defects within mitochondria plays a crucial role and may become a novel therapeutic target for PD.

3.3. Genetic Risk Factors for Mitochondrial Dynamics. In addition to toxins, specific mutations in the PD-related gene also play a role in the imbalance of mitochondrial dynamics. The α-syn protein is normally encoded by the SNCA gene, while alterations in the genetic locus of the SNCA gene have been found to encode dominant α-syn mutations (A53T, A30P, and E46K) besides having SNCA gene duplication and triplication. Furthermore, the overexpression of pathogenic α-syn (A53T or A30P) induces mitochondrial fragmentation by increasing the cleavage of OPA1 to inhibit mitochondrial fusion, which either MFN2 overexpression or DRP1 inhibition/elimination does not improve, suggesting that pathogenic α-syn-

mediated mitochondrial fragmentation is possibly caused by defects in mitochondrial fusion/fission [71]. However, other studies have shown that, by synthesizing PINK1, Parkin, and DJ-1, fragmentation induced by pathogenic α-syn can be successfully rescued [72]. In addition, a recent study of rats overexpressing human A53T-α-synuclein (hA53T-α-syn) in the nigrostriatal pathway showed that, consistent with the findings of Guardia-Laguarta et al. [71], mitochondrial fragmentation induced by α-syn overexpression is at least partially reversed as well via the administration of small molecule mitochondrial division inhibitor-1 (mdivi-1) [73]. Nevertheless, whether mdivi-1 has a therapeutic potential for PD is poorly understood; hence, further exploration is needed.

Given that PINK1 and Parkin genes, as autosomal recessive genes, encode a mitochondrial serine/threonine protein kinase and a cytosolic E3 ubiquitin-protein ligase, respectively, they are currently regarded as being commonly associated with susceptibility to PD [74, 75]. Under normal conditions, the PINK1/Parkin signaling pathway regulates mitochondrial homeostasis by promoting DRP1-dependent mitochondrial division [76]. Based on the fact that MFN1, MFN2, and DRP1 are substrates for the ubiquitination of Parkin [77], mitochondrial fragmentation can be abolished simply by interfering with the calcium/-calmodulin/calcineurin pathway, through which the involvement of Parkin signaling is indeed required for the dephosphorylation of DRP1 at serine 637 [78]. Moreover, the overexpression of PINK1/Parkin promotes mitochondrial division, resulting in an increase in the number of mitochondria, whereas the inactivation of PINK1/Parkin suppresses MFN ubiquitination, leading to the formation of megamitochondria [79]. The mutation of the PARK7 gene encoding DJ-1 is associated with the autosomal recessive form of early-onset PD [80, 81]. For instance, the loss of the normal DJ-1 function may result in mitochondrial fragmentation by an apparent decrease in the level of mitochondrial fusion. Conversely, mitochondrial rupture caused by DJ-1 deficiency is effectively rescued by the overexpression of PINK1/Parkin [82]. These findings suggested that DJ-1 is most likely to be directly involved in the PINK1/Parkin pathway, or at least regulates their corresponding activity. The LRRK2 mutation is one of the most common genetic factors for autosomal dominant parkinsonism, based on the fact that the LRRK2 mutant generally increases the level of mitochondrial DRP1 through mutual interaction with DRP1, thereby leading to severe mitochondrial rupture [83]. Together, alterations in mitochondrial dynamics are highly likely to be involved in a common pathogenic pathway for various genetic risk factors for PD, and may thus have great potential to become novel therapeutic goals.

4. Mitochondrial Autophagy and PD

4.1. Mitochondrial Autophagy. Autophagy is generally a process by which cells degrade harmful or excessive cellular components and thus recycle components to maintain homeostasis. Similarly, the removal of damaged mitochondria by autophagy is defined as mitochondrial autophagy (mitophagy) [84]. On the other hand, autophagy is also subdivided into three categories as follows: macroautophagy, microautophagy, and chaperone-mediated autophagy [85, 86]. Among them, macroautophagy is currently regarded as being the most essential subtype of autophagy, which is mainly composed of endoplasmic reticulum membranes, in order for the formation of cellular components, e.g. the cytoplasm, organelles, and protein aggregates. Thus, autophagosomes are basically a result of their recruitment, and then autophagosomes are normally transported to lysosomes for further degradation [87–89]. Autophagy can be induced by various forms of stress outside the cells such as starvation, growth factor deprivation, hypoxia, DNA damage, protein aggregates, damaged organelles, and intracellular pathogens [90, 91]. Autophagy can simply be subdivided into selective autophagy and nonselective autophagy depending on the selectivity of degraded subjects. Mitochondrial autophagy is a type of selective autophagy, meaning that mitochondria are selectively recruited into isolation membranes, which are sealed and then fused with lysosomes to eliminate the trapped mitochondria [92, 93]. Different steps of autophagy, including the amplification of the separation membrane and the production of autophagosomes, are mediated by autophagy-associated (Atg) proteins. More than 30 Atg proteins have so far been identified in yeast, among which Atg1-10, 12-14, 16, and 18 are regarded as "core Atg proteins," and are hence required for autophagosome formation [94–96]. The autophagosome marker MAP1 light chain 3 (LC3; a homolog of yeast Atg8) in mammals is an ubiquitin-like protein covalently linked to phosphatidylethanolamine [97, 98]. LC3, normally located on the separating membrane and autophagosome, is definitively required for the formation of autophagosomes [99]. In yeast, Atg32 positioned on the OMM can be directly (the cytosolic domain of Atg32 contains a WXXL-like Atg8-binding motif) or indirectly (when bridged by Atg11) associated with Atg8 bound to the separation membrane to recruit mitochondria into the autophagosome [87, 100]. The homolog of Atg32 in mammals is BCL-2-like protein 13 (BCL2L13), which binds to LC3 during mitochondrial stress [101]. Mitochondrial autophagy is a type of macroautophagy that selectively removes damaged or nonessential mitochondria and hence plays an important role in mitochondrial quality control. Impaired mitochondrial autophagy disrupts mitochondrial function and results in the accumulation of defective organelles, inevitably leading to cell and tissue damages.

4.2. PINK1/Parkin Pathway and Mitochondrial Autophagy. Among the identified signaling pathways that underlie mitochondrial autophagy, the PINK1/Parkin pathway and receptor-mediated mitochondrial autophagy are more closely related to PINK1/Parkin [102]. The PINK1 protein encoded by PINK1 (PARK6) is a serine/threonine kinase, and the Parkin protein encoded by the Parkin (PARK2) gene is a RING finger containing the E3 ligase, which ubiquitinates many mitochondrial outer membrane proteins [75, 103].

Mitochondrial depolarization-induced mitochondrial autophagy is dependent on the PINK1/Parkin pathway,

which is mediated by mitochondrial ubiquitination, which allows mitochondria-induced ubiquitination and adaptor proteins (p62, OPTN, and NDP52) to recognize each other and recruit adaptor proteins to mitochondria [104–107]. LC3 then recognizes and interacts with the adaptor protein to recruit ubiquitinated mitochondria to LC3-conjugated phagocytic cells (precursors of autophagosomes) to initiate autophagosome formation, and the depolarized mitochondria are ultimately degraded by lysosomal hydrolase [108]. Regarding normal mitochondrial function, PINK1 is expressed and introduced into the mitochondria and then rapidly passes through proteolysis; its expression level is maintained at a rather low level. When mitochondria are damaged, PINK1 proteolysis is inhibited, leading to the accumulation of PINK1 in damaged mitochondria, followed by specific recruitment of Parkin from the cytoplasm into damaged mitochondria in order for ubiquitinated mitochondria to initiate mitochondrial autophagy [109–112]. Therefore, mitochondrial depolarization, ROS production, and protein misfolding can trigger PINK1-mediated mitochondrial autophagy [113].

Receptor-mediated mitochondrial autophagy is mediated by mitochondrial autophagy receptors (BNIP3, NIX, and FUNDC1), and mitochondrial autophagy receptors localized on OMM interact directly with LC3 to mediate mitochondrial elimination [102]. Among them, Parkin-dependent ubiquitination of NIX and BNIP3 highlights the intricate crosstalk between receptor-mediated mitochondrial autophagy and the PINK1/Parkin pathway [108]. Mutations in PINK1 or Parkin cause defects in mitochondrial autophagy, and accumulation of damaged mitochondria causes oxidative stress and loss of nerve cells, which may be closely related to the pathogenesis of PD [107, 109, 114–116]. Chen et al. confirmed the role of Parkin and PINK1 in mitochondrial autophagy by the α-synuclein (A53T) transgenic mouse model [117]. When PINK1 or Parkin is deleted, these mice have increased the size and number of inclusion bodies, including neuronal inclusions of mitochondrial residual DA neurons and autophagosome, accumulated in the early stages prior to neurodegeneration, which further confirms the involvement of PINK1 and Parkin in mitochondrial clearance *in vivo* [117]. The PINK1/Parkin pathway is involved in mitochondrial autophagy, so neurons lacking PINK1 or Parkin are most likely to have defects in mitochondrial clearance and easily result in neuronal degeneration.

4.3. Other Genetic Risk Factors and Mitochondrial Autophagy. ERK signaling regulates mitochondrial autophagy, and DJ-1 activates ERK2 independently of the PINK1/Parkin pathway [118]. Previous studies have shown that the loss of DJ-1 leads to a decrease in basal autophagy, which is associated with decreased levels of phosphate-activated ERK2 [119]. The LRRK2 encoded by the PARK8 gene is a member of the leucine-rich repeat kinase family whose mutations are associated with autosomal dominant PD [120, 121]. Mutations in LRRK2 are a common cause of familial and sporadic PD [122]. Miro is an outer mitochondrial membrane protein, which serves to anchor mitochondria to microtubule motors [123, 124]. Mitochondria are highly mobile organelles whose movement should stop before mitochondrial autophagy begins [125]. In the early stages of clearance of damaged mitochondria, Miro is removed from the mitochondrial outer membrane, causing mitochondrial motion to cease, preparing for subsequent mitochondrial autophagy [126]. Some studies have previously shown that the PINK1/Parkin pathway induces Miro degradation and releases kinesins from mitochondria [125]. Others have shown that LRRK2 promotes the removal of Miro from damaged mitochondria by the formation of a complex with Miro, whereas the pathogenic LRRK2 mutation, mainly LRRK2G2019S, disrupts the structural integrity of the complex, thereby slowing Miro removal and causing mitochondrial stagnation as well as delaying subsequent mitochondrial autophagy [127].

4.4. Sporadic PD and Mitochondrial Autophagy. At present, the research on the mitochondrial autophagy of PD mainly focuses on familial PD, and there are few reports on sporadic PD and mitochondrial autophagy. Since sporadic PD accounts for 80%-85% of PD patients [128], it is particularly important to further explore the link between sporadic PD and mitochondrial autophagy. Many studies have already mentioned that Miro-related mitochondrial clearance disorders have a strong relationship with mutations in the PINK1/Parkin and LRRK2 genes. Recent studies have found that there is some correlation between mitochondrial autophagy and Miro in sporadic PD. Hsieh et al. found that Miro deficiency also causes mitochondrial autophagy defects in sporadic PD cases [127]. Studies have shown that lipid synthesis plays a role in PINK1-PARK2-mediated mitochondrial autophagy, and SREBF1, which is part of the lipogenesis pathway, has been shown to be a risk locus for sporadic PD [129]. Miro and SREBF1 link the pathogenesis of familial PD and sporadic PD, providing new ideas for exploring the pathogenesis of PD, especially the pathogenesis of sporadic PD. Miro and SREBF1 have also become potential targets for PD therapy. At the same time, more and more scientists have realized the importance of exploring the pathogenesis of sporadic PD for PD prevention and treatment, and more and more research will be done in this area.

5. Conclusions

Both environmental and genetic risk factors are involved in various aspects of mitochondrial quality control (mitochondrial biogenesis, kinetics, and autophagy) during the pathogenesis of PD. Although its complexity is not fully understood, recent studies have started to unravel the role of specific signaling pathways (e.g., the PINK1/Parkin pathway) in biosynthesis, kinetics, and autophagy during the regulation of mitochondrial quality control processes. This review summarized the current understanding of the mitochondrial quality control pathways that underlie the pathogenesis of Parkinson's disease and evaluated whether each signaling pathway and the related components could be potential targets of the prevention, diagnosis, and treatment of PD, based on both environmental and genetic risk factors for the mitochondrial quality control pathways at the forefront of translational research in PD. Hopefully, our study

provides researchers with insightful opinions, and even points out promising general research directions, since each potential target has not been explained in detail in each section. Given the continuous progress in understanding the basic mechanism underlying the involvement of mitochondrial quality control pathways, it is widely believed that precision therapy in PD is most likely to precede breakthrough in the near future.

Conflicts of Interest

The authors have no conflicts of interest to declare.

Authors' Contributions

Xue Jiang and Tao Jin equally contributed to this study.

Acknowledgments

This work was supported by the crosswise project from the Natural Science Foundation of Jilin Province (Grant No. 20180101154JC) and the Health and Wellness Technology Innovation Project of Jilin Province (Grant No. 2018J045).

References

[1] L. V. Kalia and A. E. Lang, "Parkinson's disease," *The Lancet*, vol. 386, no. 9996, pp. 896–912, 2015.

[2] J. M. Shulman, P. L. De Jager, and M. B. Feany, "Parkinson's disease: genetics and pathogenesis," *Annual Review of Pathology*, vol. 6, no. 1, pp. 193–222, 2011.

[3] J. Jankovic, "Parkinson's disease: clinical features and diagnosis," *Journal of Neurology, Neurosurgery, and Psychiatry*, vol. 79, no. 4, pp. 368–376, 2008.

[4] N. Tambasco, P. Nigro, M. Romoli, P. Prontera, S. Simoni, and P. Calabresi, "A53T in a parkinsonian family: a clinical update of the SNCA phenotypes," *Journal of Neural Transmission (Vienna)*, vol. 123, no. 11, pp. 1301–1307, 2016.

[5] K. Kalinderi, S. Bostantjopoulou, and L. Fidani, "The genetic background of Parkinson's disease: current progress and future prospects," *Acta Neurologica Scandinavica*, vol. 134, no. 5, pp. 314–326, 2016.

[6] H. Deng, P. Wang, and J. Jankovic, "The genetics of Parkinson disease," *Ageing Research Reviews*, vol. 42, pp. 72–85, 2018.

[7] K. R. Kumar, A. Djarmati-Westenberger, and A. Grunewald, "Genetics of Parkinson's disease," *Seminars in Neurology*, vol. 31, no. 5, pp. 433–440, 2011.

[8] Q. Hu and G. Wang, "Mitochondrial dysfunction in Parkinson's disease," *Translational Neurodegeneration*, vol. 5, no. 1, article 14, 2016.

[9] A. Bose and M. F. Beal, "Mitochondrial dysfunction in Parkinson's disease," *Journal of Neurochemistry*, vol. 139, pp. 216–231, 2016.

[10] B. Wang, N. Abraham, G. Gao, and Q. Yang, "Dysregulation of autophagy and mitochondrial function in Parkinson's disease," *Translational Neurodegeneration*, vol. 5, no. 1, p. 19, 2016.

[11] B. Zheng, Z. Liao, J. J. Locascio et al., "*PGC-1α*, a potential therapeutic target for early intervention in Parkinson's disease," *Science Translational Medicine*, vol. 2, no. 52, article 52ra73, 2010.

[12] M. C. Zanellati, V. Monti, C. Barzaghi et al., "Mitochondrial dysfunction in Parkinson disease: evidence in mutant *PARK2* fibroblasts," *Frontiers in Genetics*, vol. 6, p. 78, 2015.

[13] G. C. Davis, A. C. Williams, S. P. Markey et al., "Chronic Parkinsonism secondary to intravenous injection of meperidine analogues," *Psychiatry Research*, vol. 1, no. 3, pp. 249–254, 1979.

[14] J. W. Langston, P. Ballard, J. W. Tetrud, and I. Irwin, "Chronic Parkinsonism in humans due to a product of meperidine-analog synthesis," *Science*, vol. 219, no. 4587, pp. 979-980, 1983.

[15] Y. Mizuno, K. Suzuki, and N. Sone, "Inhibition of ATP synthesis by 1-methyl-4-phenylpyridinium ion (MPP+) in mouse brain in vitro and in vivo," *Advances in Neurology*, vol. 53, pp. 197–200, 1990.

[16] S. Przedborski, K. Tieu, C. Perier, and M. Vila, "MPTP as a mitochondrial neurotoxic model of Parkinson's disease," *Journal of Bioenergetics and Biomembranes*, vol. 36, no. 4, pp. 375–379, 2004.

[17] K. Tieu, "A guide to neurotoxic animal models of Parkinson's disease," *Cold Spring Harbor Perspectives in Medicine*, vol. 1, no. 1, article a009316, 2011.

[18] K. Palikaras, E. Lionaki, and N. Tavernarakis, "Balancing mitochondrial biogenesis and mitophagy to maintain energy metabolism homeostasis," *Cell Death and Differentiation*, vol. 22, no. 9, pp. 1399–1401, 2015.

[19] J. Nunnari and A. Suomalainen, "Mitochondria: in sickness and in health," *Cell*, vol. 148, no. 6, pp. 1145–1159, 2012.

[20] D. B. Zorov, M. Juhaszova, and S. J. Sollott, "Mitochondrial reactive oxygen species (ROS) and ROS-induced ROS release," *Physiological Reviews*, vol. 94, no. 3, pp. 909–950, 2014.

[21] R. S. Balaban, S. Nemoto, and T. Finkel, "Mitochondria, oxidants, and aging," *Cell*, vol. 120, no. 4, pp. 483–495, 2005.

[22] S. Franco-Iborra, M. Vila, and C. Perier, "Mitochondrial quality control in neurodegenerative diseases: focus on Parkinson's disease and Huntington's disease," *Frontiers in Neuroscience*, vol. 12, p. 342, 2018.

[23] A. Umeno, V. Biju, and Y. Yoshida, "In vivo ROS production and use of oxidative stress-derived biomarkers to detect the onset of diseases such as Alzheimer's disease, Parkinson's disease, and diabetes," *Free Radical Research*, vol. 51, no. 4, pp. 413–427, 2017.

[24] T. Jiang, Q. Sun, and S. Chen, "Oxidative stress: a major pathogenesis and potential therapeutic target of antioxidative agents in Parkinson's disease and Alzheimer's disease," *Progress in Neurobiology*, vol. 147, pp. 1–19, 2016.

[25] T. G. McDonald and J. E. Van Eyk, "Mitochondrial proteomics. Undercover in the lipid bilayer," *Basic Research in Cardiology*, vol. 98, no. 4, pp. 219–227, 2003.

[26] M. F. Lopez, B. S. Kristal, E. Chernokalskaya et al., "High-throughput profiling of the mitochondrial proteome using affinity fractionation and automation," *Electrophoresis*, vol. 21, no. 16, pp. 3427–3440, 2000.

[27] S. E. Calvo, K. R. Clauser, and V. K. Mootha, "MitoCarta2.0: an updated inventory of mammalian mitochondrial proteins," *Nucleic Acids Research*, vol. 44, no. D1, pp. D1251–D1257, 2016.

[28] R. C. Scarpulla, "Transcriptional paradigms in mammalian mitochondrial biogenesis and function," *Physiological Reviews*, vol. 88, no. 2, pp. 611–638, 2008.

[29] M. Uittenbogaard and A. Chiaramello, "Mitochondrial biogenesis: a therapeutic target for neurodevelopmental disorders and neurodegenerative diseases," *Current Pharmaceutical Design*, vol. 20, no. 35, pp. 5574–5593, 2014.

[30] G. López-Lluch, P. M. Irusta, P. Navas, and R. de Cabo, "Mitochondrial biogenesis and healthy aging," *Experimental Gerontology*, vol. 43, no. 9, pp. 813–819, 2008.

[31] P. Puigserver, Z. Wu, C. W. Park, R. Graves, M. Wright, and B. M. Spiegelman, "A cold-inducible coactivator of nuclear receptors linked to adaptive thermogenesis," *Cell*, vol. 92, no. 6, pp. 829–839, 1998.

[32] A. Thirupathi and C. T. de Souza, "Multi-regulatory network of ROS: the interconnection of ROS, PGC-1 alpha, and AMPK-SIRT1 during exercise," *Journal of Physiology and Biochemistry*, vol. 73, no. 4, pp. 487–494, 2017.

[33] P. A. Li, X. Hou, and S. Hao, "Mitochondrial biogenesis in neurodegeneration," *Journal of Neuroscience Research*, vol. 95, no. 10, pp. 2025–2029, 2017.

[34] F. R. Jornayvaz and G. I. Shulman, "Regulation of mitochondrial biogenesis," *Essays in Biochemistry*, vol. 47, pp. 69–84, 2010.

[35] B. D'Autreaux and M. B. Toledano, "ROS as signalling molecules: mechanisms that generate specificity in ROS homeostasis," *Nature Reviews. Molecular Cell Biology*, vol. 8, no. 10, pp. 813–824, 2007.

[36] J. St-Pierre, S. Drori, M. Uldry et al., "Suppression of reactive oxygen species and neurodegeneration by the PGC-1 transcriptional coactivators," *Cell*, vol. 127, no. 2, pp. 397–408, 2006.

[37] J. St-Pierre, J. Lin, S. Krauss et al., "Bioenergetic analysis of peroxisome proliferator-activated receptor gamma coactivators 1alpha and 1beta (PGC-1alpha and PGC-1beta) in muscle cells," *The Journal of Biological Chemistry*, vol. 278, no. 29, pp. 26597–26603, 2003.

[38] I. Valle, A. Alvarezbarrientos, E. Arza, S. Lamas, and M. Monsalve, "PGC-1α regulates the mitochondrial antioxidant defense system in vascular endothelial cells," *Cardiovascular Research*, vol. 66, no. 3, pp. 562–573, 2005.

[39] D. Kukidome, T. Nishikawa, K. Sonoda et al., "Activation of AMP-activated protein kinase reduces hyperglycemia-induced mitochondrial reactive oxygen species production and promotes mitochondrial biogenesis in human umbilical vein endothelial cells," *Diabetes*, vol. 55, no. 1, pp. 120–127, 2006.

[40] Y. Olmos, I. Valle, S. Borniquel et al., "Mutual dependence of Foxo3a and PGC-1alpha in the induction of oxidative stress genes," *The Journal of Biological Chemistry*, vol. 284, no. 21, pp. 14476–14484, 2009.

[41] M. Elstner, C. M. Morris, K. Heim et al., "Expression analysis of dopaminergic neurons in Parkinson's disease and aging links transcriptional dysregulation of energy metabolism to cell death," *Acta Neuropathologica*, vol. 122, no. 1, pp. 75–86, 2011.

[42] D. A. Stevens, Y. Lee, H. C. Kang et al., "Parkin loss leads to PARIS-dependent declines in mitochondrial mass and respiration," *Proceedings of the National Academy of Sciences of the United States of America*, vol. 112, no. 37, pp. 11696–11701, 2015.

[43] J. H. Shin, H. S. Ko, H. Kang et al., "PARIS (ZNF746) repression of PGC-1alpha contributes to neurodegeneration in Parkinson's disease," *Cell*, vol. 144, no. 5, pp. 689–702, 2011.

[44] L. Zheng, N. Bernard-Marissal, N. Moullan et al., "Parkin functionally interacts with PGC-1α to preserve mitochondria and protect dopaminergic neurons," *Human Molecular Genetics*, vol. 26, no. 3, pp. 582–598, 2017.

[45] A. Siddiqui, S. J. Chinta, J. K. Mallajosyula et al., "Selective binding of nuclear alpha-synuclein to the PGC1alpha promoter under conditions of oxidative stress may contribute to losses in mitochondrial function: implications for Parkinson's disease," *Free Radical Biology & Medicine*, vol. 53, no. 4, pp. 993–1003, 2012.

[46] C. Ciron, L. Zheng, W. Bobela et al., "PGC-1α activity in nigral dopamine neurons determines vulnerability to α-synuclein," *Acta Neuropathologica Communications*, vol. 3, no. 1, p. 16, 2015.

[47] J. Eschbach, B. von Einem, K. Müller et al., "Mutual exacerbation of peroxisome proliferator-activated receptor γ coactivator 1α deregulation and α-synuclein oligomerization," *Annals of Neurology*, vol. 77, no. 1, pp. 15–32, 2015.

[48] G. Mudò, J. Mäkelä, V. Di Liberto et al., "Transgenic expression and activation of PGC-1α protect dopaminergic neurons in the MPTP mouse model of Parkinson's disease," *Cellular and Molecular Life Sciences*, vol. 69, no. 7, pp. 1153–1165, 2012.

[49] H. Chen, S. M. Zhang, M. A. Hernán, W. C. Willett, and A. Ascherio, "Dietary intakes of fat and risk of Parkinson's disease," *American Journal of Epidemiology*, vol. 157, no. 11, pp. 1007–1014, 2003.

[50] G. Logroscino, K. Marder, L. Cote, M. X. Tang, S. Shea, and R. Mayeux, "Dietary lipids and antioxidants in Parkinson's disease: a population-based, case-control study," *Annals of Neurology*, vol. 39, no. 1, pp. 89–94, 1996.

[51] X. Su, Y. Chu, J. H. Kordower et al., "PGC-1α promoter methylation in Parkinson's disease," *PLoS One*, vol. 10, no. 8, article e0134087, 2015.

[52] H. Kang, R. Khang, S. Ham et al., "Activation of the ATF2/-CREB-PGC-1α pathway by metformin leads to dopaminergic neuroprotection," *Oncotarget*, vol. 8, no. 30, pp. 48603–48618, 2017.

[53] A. S. Rambold and E. L. Pearce, "Mitochondrial dynamics at the interface of immune cell metabolism and function," *Trends in Immunology*, vol. 39, no. 1, pp. 6–18, 2018.

[54] N. Zemirli, E. Morel, and D. Molino, "Mitochondrial dynamics in basal and stressful conditions," *International Journal of Molecular Sciences*, vol. 19, no. 2, p. 564, 2018.

[55] V. Eisner, M. Picard, and G. Hajnoczky, "Mitochondrial dynamics in adaptive and maladaptive cellular stress responses," *Nature Cell Biology*, vol. 20, no. 7, pp. 755–765, 2018.

[56] V. M. Pozo Devoto and T. L. Falzone, "Mitochondrial dynamics in Parkinson's disease: a role for alpha-synuclein?," *Disease Models & Mechanisms*, vol. 10, no. 9, pp. 1075–1087, 2017.

[57] H. Chen, J. M. McCaffery, and D. C. Chan, "Mitochondrial fusion protects against neurodegeneration in the cerebellum," *Cell*, vol. 130, no. 3, pp. 548–562, 2007.

[58] G. W. Dorn, "Evolving concepts of mitochondrial dynamics," *Annual Review of Physiology*, vol. 81, no. 1, pp. 1–17, 2018.

[59] C. Frezza, S. Cipolat, O. Martins de Brito et al., "OPA1 controls apoptotic cristae remodeling independently from mitochondrial fusion," *Cell*, vol. 126, no. 1, pp. 177–189, 2006.

[60] G. Twig, A. Elorza, A. J. A. Molina et al., "Fission and selective fusion govern mitochondrial segregation and elimination by autophagy," *The EMBO Journal*, vol. 27, no. 2, pp. 433–446, 2008.

[61] L. Yang, Q. Long, J. Liu et al., "Mitochondrial fusion provides an "initial metabolic complementation" controlled by mtDNA," *Cellular and Molecular Life Sciences*, vol. 72, no. 13, pp. 2585–2598, 2015.

[62] F. Legros, A. Lombès, P. Frachon, and M. Rojo, "Mitochondrial fusion in human cells is efficient, requires the inner membrane potential, and is mediated by mitofusins," *Molecular Biology of the Cell*, vol. 13, no. 12, pp. 4343–4354, 2002.

[63] F. Legros, F. Malka, P. Frachon, A. Lombès, and M. Rojo, "Organization and dynamics of human mitochondrial DNA," *Journal of Cell Science*, vol. 117, no. 13, pp. 2653–2662, 2004.

[64] V. Wilkens, W. Kohl, and K. Busch, "Restricted diffusion of OXPHOS complexes in dynamic mitochondria delays their exchange between cristae and engenders a transitory mosaic distribution," *Journal of Cell Science*, vol. 126, no. 1, pp. 103–116, 2013.

[65] A. M. Bertholet, T. Delerue, A. M. Millet et al., "Mitochondrial fusion/fission dynamics in neurodegeneration and neuronal plasticity," *Neurobiology of Disease*, vol. 90, pp. 3–19, 2016.

[66] J. Gao, L. Wang, J. Liu, F. Xie, B. Su, and X. Wang, "Abnormalities of mitochondrial dynamics in neurodegenerative diseases," *Antioxidants*, vol. 6, no. 2, p. 25, 2017.

[67] V. S. Van Laar and S. B. Berman, "The interplay of neuronal mitochondrial dynamics and bioenergetics: implications for Parkinson's disease," *Neurobiology of Disease*, vol. 51, pp. 43–55, 2013.

[68] M. J. Barsoum, H. Yuan, A. A. Gerencser et al., "Nitric oxide-induced mitochondrial fission is regulated by dynamin-related GTPases in neurons," *The EMBO Journal*, vol. 25, no. 16, pp. 3900–3911, 2006.

[69] X. Wang, B. Su, W. Liu et al., "DLP1-dependent mitochondrial fragmentation mediates 1-methyl-4-phenylpyridinium toxicity in neurons: implications for Parkinson's disease," *Aging Cell*, vol. 10, no. 5, pp. 807–823, 2011.

[70] D. Santos, A. R. Esteves, D. F. Silva, C. Januário, and S. M. Cardoso, "The impact of mitochondrial fusion and fission modulation in sporadic Parkinson's disease," *Molecular Neurobiology*, vol. 52, no. 1, pp. 573–586, 2015.

[71] C. Guardia-Laguarta, E. Area-Gomez, C. Rub et al., "α-Synuclein is localized to mitochondria-associated ER membranes," *The Journal of Neuroscience*, vol. 34, no. 1, pp. 249–259, 2014.

[72] F. Kamp, N. Exner, A. K. Lutz et al., "Inhibition of mitochondrial fusion by α-synuclein is rescued by PINK1, Parkin and DJ-1," *The EMBO Journal*, vol. 29, no. 20, pp. 3571–3589, 2010.

[73] S. Bido, F. N. Soria, R. Z. Fan, E. Bezard, and K. Tieu, "Mitochondrial division inhibitor-1 is neuroprotective in the A53T-α-synuclein rat model of Parkinson's disease," *Scientific Reports*, vol. 7, no. 1, article 7495, 2017.

[74] L. Silvestri, V. Caputo, E. Bellacchio et al., "Mitochondrial import and enzymatic activity of PINK1 mutants associated to recessive parkinsonism," *Human Molecular Genetics*, vol. 14, no. 22, pp. 3477–3492, 2005.

[75] H. Shimura, N. Hattori, S. I. Kubo et al., "Familial Parkinson disease gene product, parkin, is a ubiquitin-protein ligase," *Nature Genetics*, vol. 25, no. 3, pp. 302–305, 2000.

[76] A. M. Pickrell and R. J. Youle, "The roles of PINK1, parkin, and mitochondrial fidelity in Parkinson's disease," *Neuron*, vol. 85, no. 2, pp. 257–273, 2015.

[77] M. E. Gegg, J. M. Cooper, K. Y. Chau, M. Rojo, A. H. V. Schapira, and J. W. Taanman, "Mitofusin 1 and mitofusin 2 are ubiquitinated in a PINK1/parkin-dependent manner upon induction of mitophagy," *Human Molecular Genetics*, vol. 19, no. 24, pp. 4861–4870, 2010.

[78] L. Buhlman, M. Damiano, G. Bertolin et al., "Functional interplay between Parkin and Drp1 in mitochondrial fission and clearance," *Biochimica et Biophysica Acta (BBA) - Molecular Cell Research*, vol. 1843, no. 9, pp. 2012–2026, 2014.

[79] E. Ziviani, R. N. Tao, and A. J. Whitworth, "Drosophila parkin requires PINK1 for mitochondrial translocation and ubiquitinates mitofusin," *Proceedings of the National Academy of Sciences of the United States of America*, vol. 107, no. 11, pp. 5018–5023, 2010.

[80] V. Bonifati, P. Rizzu, M. van Baren et al., "Mutations in the *DJ-1* gene associated with autosomal recessive early-onset parkinsonism," *Science*, vol. 299, no. 5604, pp. 256–259, 2003.

[81] S. Hague, E. Rogaeva, D. Hernandez et al., "Early-onset Parkinson's disease caused by a compound heterozygous DJ-1 mutation," *Annals of Neurology*, vol. 54, no. 2, pp. 271–274, 2003.

[82] I. Irrcher, H. Aleyasin, E. L. Seifert et al., "Loss of the Parkinson's disease-linked gene DJ-1 perturbs mitochondrial dynamics," *Human Molecular Genetics*, vol. 19, no. 19, pp. 3734–3746, 2010.

[83] X. Wang, M. H. Yan, H. Fujioka et al., "LRRK2 regulates mitochondrial dynamics and function through direct interaction with DLP1," *Human Molecular Genetics*, vol. 21, no. 9, pp. 1931–1944, 2012.

[84] S. B. Yu and G. Pekkurnaz, "Mechanisms orchestrating mitochondrial dynamics for energy homeostasis," *Journal of Molecular Biology*, vol. 430, no. 21, pp. 3922–3941, 2018.

[85] L. Galluzzi, E. H. Baehrecke, A. Ballabio et al., "Molecular definitions of autophagy and related processes," *The EMBO Journal*, vol. 36, no. 13, pp. 1811–1836, 2017.

[86] F. Gao, J. Yang, D. Wang et al., "Mitophagy in Parkinson's disease: pathogenic and therapeutic implications," *Frontiers in Neurology*, vol. 8, p. 527, 2017.

[87] N. Mizushima and M. Komatsu, "Autophagy: renovation of cells and tissues," *Cell*, vol. 147, no. 4, pp. 728–741, 2011.

[88] N. Mizushima, T. Yoshimori, and Y. Ohsumi, "The role of Atg proteins in autophagosome formation," *Annual Review of Cell and Developmental Biology*, vol. 27, no. 1, pp. 107–132, 2011.

[89] S. A. Tooze and T. Yoshimori, "The origin of the autophagosomal membrane," *Nature Cell Biology*, vol. 12, no. 9, pp. 831–835, 2010.

[90] C. He and D. J. Klionsky, "Regulation mechanisms and signaling pathways of autophagy," *Annual Review of Genetics*, vol. 43, no. 1, pp. 67–93, 2009.

[91] G. Kroemer, G. Marino, and B. Levine, "Autophagy and the integrated stress response," *Molecular Cell*, vol. 40, no. 2, pp. 280–293, 2010.

[92] I. Kim, S. Rodriguez-Enriquez, and J. J. Lemasters, "Selective degradation of mitochondria by mitophagy," *Archives of Biochemistry and Biophysics*, vol. 462, no. 2, pp. 245–253, 2007.

[93] R. J. Youle and D. P. Narendra, "Mechanisms of mitophagy," *Nature Reviews. Molecular Cell Biology*, vol. 12, no. 1, pp. 9–14, 2011.

[94] H. Nakatogawa, K. Suzuki, Y. Kamada, and Y. Ohsumi, "Dynamics and diversity in autophagy mechanisms: lessons from yeast," *Nature Reviews Molecular Cell Biology*, vol. 10, no. 7, pp. 458–467, 2009.

[95] N. Mizushima, T. Noda, T. Yoshimori et al., "A protein conjugation system essential for autophagy," *Nature*, vol. 395, no. 6700, pp. 395–398, 1998.

[96] Y. Ichimura, T. Kirisako, T. Takao et al., "A ubiquitin-like system mediates protein lipidation," *Nature*, vol. 408, no. 6811, pp. 488–492, 2000.

[97] Y. Kabeya, N. Mizushima, T. Ueno et al., "LC3, a mammalian homologue of yeast Apg8p, is localized in autophagosome membranes after processing," *The EMBO Journal*, vol. 19, no. 21, pp. 5720–5728, 2000.

[98] K. Yoshimoto, H. Hanaoka, S. Sato et al., "Processing of ATG8s, ubiquitin-like proteins, and their deconjugation by ATG4s are essential for plant autophagy," *Plant Cell*, vol. 16, no. 11, pp. 2967–2983, 2004.

[99] H. Nakatogawa, Y. Ichimura, and Y. Ohsumi, "Atg8, a ubiquitin-like protein required for autophagosome formation, mediates membrane tethering and hemifusion," *Cell*, vol. 130, no. 1, pp. 165–178, 2007.

[100] D. Gatica, V. Lahiri, and D. J. Klionsky, "Cargo recognition and degradation by selective autophagy," *Nature Cell Biology*, vol. 20, no. 3, pp. 233–242, 2018.

[101] T. Murakawa, O. Yamaguchi, A. Hashimoto et al., "Bcl-2-like protein 13 is a mammalian Atg32 homologue that mediates mitophagy and mitochondrial fragmentation," *Nature Communications*, vol. 6, no. 1, p. 7527, 2015.

[102] K. Palikaras, I. Daskalaki, M. Markaki, and N. Tavernarakis, "Mitophagy and age-related pathologies: development of new therapeutics by targeting mitochondrial turnover," *Pharmacology & Therapeutics*, vol. 178, pp. 157–174, 2017.

[103] E. M. Valente, P. M. Abou-Sleiman, V. Caputo et al., "Hereditary early-onset Parkinson's disease caused by mutations in PINK1," *Science*, vol. 304, no. 5674, pp. 1158–1160, 2004.

[104] J. W. Harper, A. Ordureau, and J. M. Heo, "Building and decoding ubiquitin chains for mitophagy," *Nature Reviews. Molecular Cell Biology*, vol. 19, no. 2, pp. 93–108, 2018.

[105] J. M. Heo, A. Ordureau, J. A. Paulo, J. Rinehart, and J. W. Harper, "The PINK1-PARKIN mitochondrial ubiquitylation pathway drives a program of OPTN/NDP52 recruitment and TBK1 activation to promote mitophagy," *Molecular Cell*, vol. 60, no. 1, pp. 7–20, 2015.

[106] S. Pankiv, T. H. Clausen, T. Lamark et al., "p62/SQSTM1 binds directly to Atg8/LC3 to facilitate degradation of ubiquitinated protein aggregates by autophagy," *Journal of Biological Chemistry*, vol. 282, no. 33, pp. 24131–24145, 2007.

[107] S. Geisler, K. M. Holmström, D. Skujat et al., "PINK1/Parkin-mediated mitophagy is dependent on VDAC1 and p62/SQSTM1," *Nature Cell Biology*, vol. 12, no. 2, pp. 119–131, 2010.

[108] K. Palikaras, E. Lionaki, and N. Tavernarakis, "Mechanisms of mitophagy in cellular homeostasis, physiology and pathology," *Nature Cell Biology*, vol. 20, no. 9, pp. 1013–1022, 2018.

[109] D. P. Narendra, S. M. Jin, A. Tanaka et al., "PINK1 is selectively stabilized on impaired mitochondria to activate Parkin," *PLoS Biology*, vol. 8, no. 1, article e1000298, 2010.

[110] M. Lazarou, S. M. Jin, L. A. Kane, and R. J. Youle, "Role of PINK1 binding to the TOM complex and alternate intracellular membranes in recruitment and activation of the E3 ligase Parkin," *Developmental Cell*, vol. 22, no. 2, pp. 320–333, 2012.

[111] N. Matsuda, S. Sato, K. Shiba et al., "PINK1 stabilized by mitochondrial depolarization recruits Parkin to damaged mitochondria and activates latent Parkin for mitophagy," *The Journal of Cell Biology*, vol. 189, no. 2, pp. 211–221, 2010.

[112] D. Narendra, A. Tanaka, D. F. Suen, and R. J. Youle, "Parkin is recruited selectively to impaired mitochondria and promotes their autophagy," *Journal of Cell Biology*, vol. 183, no. 5, pp. 795–803, 2008.

[113] O. S. Shirihai, M. Song, and G. W. Dorn 2nd, "How mitochondrial dynamism orchestrates mitophagy," *Circulation Research*, vol. 116, no. 11, pp. 1835–1849, 2015.

[114] J. Y. Lee, Y. Nagano, J. P. Taylor, K. L. Lim, and T. P. Yao, "Disease-causing mutations in parkin impair mitochondrial ubiquitination, aggregation, and HDAC6-dependent mitophagy," *Journal of Cell Biology*, vol. 189, no. 4, pp. 671–679, 2010.

[115] S. Gandhi, A. Wood-Kaczmar, Z. Yao et al., "PINK1-associated Parkinson's disease is caused by neuronal vulnerability to calcium-induced cell death," *Molecular Cell*, vol. 33, no. 5, pp. 627–638, 2009.

[116] D. J. Surmeier, J. N. Guzman, J. Sanchez-Padilla, and J. A. Goldberg, "What causes the death of dopaminergic neurons in Parkinson's disease?," *Progress in Brain Research*, vol. 183, pp. 59–77, 2010.

[117] L. Chen, Z. Xie, S. Turkson, and X. Zhuang, "A53T human alpha-synuclein overexpression in transgenic mice induces pervasive mitochondria macroautophagy defects preceding dopamine neuron degeneration," *The Journal of Neuroscience*, vol. 35, no. 3, pp. 890–905, 2015.

[118] Y. Hirota, S. I. Yamashita, Y. Kurihara et al., "Mitophagy is primarily due to alternative autophagy and requires the MAPK1 and MAPK14 signaling pathways," *Autophagy*, vol. 11, no. 2, pp. 332–343, 2015.

[119] G. Krebiehl, S. Ruckerbauer, L. F. Burbulla et al., "Reduced basal autophagy and impaired mitochondrial dynamics due to loss of Parkinson's disease-associated protein DJ-1," *PLoS One*, vol. 5, no. 2, article e9367, 2010.

[120] C. Paisán-Ruíz, S. Jain, E. W. Evans et al., "Cloning of the gene containing mutations that cause PARK8-linked Parkinson's disease," *Neuron*, vol. 44, no. 4, pp. 595–600, 2004.

[121] International Parkinson Disease Genomics Consortium, "Imputation of sequence variants for identification of genetic risks for Parkinson's disease: a meta-analysis of genome-wide association studies," *The Lancet*, vol. 377, no. 9766, pp. 641–649, 2011.

[122] D. G. Healy, M. Falchi, S. S. O'Sullivan et al., "Phenotype, genotype, and worldwide genetic penetrance of LRRK2-associated Parkinson's disease: a case-control study," *Lancet Neurology*, vol. 7, no. 7, pp. 583–590, 2008.

[123] S. Fransson, A. Ruusala, and P. Aspenstrom, "The atypical Rho GTPases Miro-1 and Miro-2 have essential roles in mitochondrial trafficking," *Biochemical and Biophysical Research Communications*, vol. 344, no. 2, pp. 500–510, 2006.

[124] E. E. Glater, L. J. Megeath, R. S. Stowers, and T. L. Schwarz, "Axonal transport of mitochondria requires milton to recruit kinesin heavy chain and is light chain independent," *The Journal of Cell Biology*, vol. 173, no. 4, pp. 545–557, 2006.

[125] X. Wang, D. Winter, G. Ashrafi et al., "PINK1 and Parkin target Miro for phosphorylation and degradation to arrest mitochondrial motility," *Cell*, vol. 147, no. 4, pp. 893–906, 2011.

[126] S. Liu, T. Sawada, S. Lee et al., "Parkinson's disease-associated kinase PINK1 regulates Miro protein level and axonal transport of mitochondria," *PLoS Genetics*, vol. 8, no. 3, article e1002537, 2012.

[127] C. H. Hsieh, A. Shaltouki, A. E. Gonzalez et al., "Functional impairment in Miro degradation and mitophagy is a shared feature in familial and sporadic Parkinson's disease," *Cell Stem Cell*, vol. 19, no. 6, pp. 709–724, 2016.

[128] L. M. de Lau and M. M. Breteler, "Epidemiology of Parkinson's disease," *Lancet Neurology*, vol. 5, no. 6, pp. 525–535, 2006.

[129] R. M. Ivatt and A. J. Whitworth, "SREBF1 links lipogenesis to mitophagy and sporadic Parkinson disease," *Autophagy*, vol. 10, no. 8, pp. 1476-1477, 2014.

Hindawi
Oxidative Medicine and Cellular Longevity
Volume 2019, Article ID 5410657, 9 pages
https://doi.org/10.1155/2019/5410657

Review Article

Alpha-2-Macroglobulin, a Hypochlorite-Regulated Chaperone and Immune System Modulator

Jordan H. Cater,[1] Mark R. Wilson,[1] and Amy R. Wyatt[1,2,3]

[1]*Illawarra Health and Medical Research Institute and School of Chemistry and Molecular Bioscience, University of Wollongong, New South Wales 2522, Australia*
[2]*College of Medicine and Public Health, Flinders University, South Australia 4052, Australia*
[3]*Centre for Neuroscience, Flinders University, South Australia 4052, Australia*

Correspondence should be addressed to Amy R. Wyatt; amy.wyatt@flinders.edu.au

Received 5 April 2019; Accepted 2 June 2019; Published 22 July 2019

Academic Editor: Sander Bekeschus

Alpha-macroglobulins are ancient proteins that include monomeric, dimeric, and tetrameric family members. In humans, and many other mammals, the predominant alpha-macroglobulin is alpha-2-macroglobulin (α_2M), a tetrameric protein that is constitutively abundant in biological fluids (e.g., blood plasma, cerebral spinal fluid, synovial fluid, ocular fluid, and interstitial fluid). α_2M is best known for its remarkable ability to inhibit a broad spectrum of proteases, but the full gamut of its activities affects diverse biological processes. For example, α_2M can stabilise and facilitate the clearance of the Alzheimer's disease-associated amyloid beta (Aβ) peptide. Additionally, α_2M can influence the signalling of cytokines and growth factors including neurotrophins. The results of several studies support the idea that the functions of α_2M are uniquely regulated by hypochlorite, an oxidant that is generated during inflammation, which induces the native α_2M tetramer to dissociate into dimers. This review will discuss the evidence for hypochlorite-induced regulation of α_2M and the possible implications of this in neuroinflammation and neurodegeneration.

1. Structure and Function

α_2M is a secreted protein that is present at 1.5–2 mg mL^{-1} and 1.0–3.6 μg mL^{-1} in human blood plasma and cerebral spinal fluid, respectively [1, 2]. The cage-like structure of α_2M (720 kDa) is formed by the assembly of four 180 kDa subunits into two disulfide-linked dimers, which noncovalently associate to complete the tetrameric quaternary structure of the protein [3]. A bait region that contains a large number of protease cleavage sites is responsible for the incredibly diverse range of proteases that interact with α_2M [4]. Cleavage of the α_2M bait region, which is in close physical proximity to a reactive thioester bond, results in covalent trapping of proteases within a steric cage [5]. This process involves a substantial conformational change that generates a compact tetrameric form [6] and reveals the binding site for the low-density lipoprotein receptor-related protein-1 (LRP1) [7, 8] (Figure 1(a)). For the purpose of this review, the compact tetrameric protease-bound form of α_2M is referred to as transformed α_2M. Transformed α_2M (covalently bound to up to two protease molecules) is rapidly cleared from the circulation via LRP1-facilitated endocytosis (Figure 1(a)). As such, α_2M can efficiently inhibit a myriad of extracellular processes that are dependent on proteolysis.

Consistent with having an ancient origin in innate immunity, α_2M is a promiscuous protein that noncovalently binds to a diverse range of nonprotease ligands including cytokines [9, 10], growth factors [9–14], apolipoproteins [15], and misfolded proteins [16–20]. Many noncovalent ligands of α_2M including the Alzheimer's disease-associated Aβ peptide [21], neurotrophins [14], and tumour necrosis factor-alpha (TNF-α) preferentially bind to transformed α_2M which is generated following the reaction of native α_2M with a protease or with small nucleophilic compounds that also target the α_2M thioester bond [6]. In these cases, it is proposed that transformed α_2M acts to limit the activities of noncovalently bound ligands by facilitating their disposal via LRP1 [10, 22] (Figure 1(a)). On the other hand, α_2M can control signalling

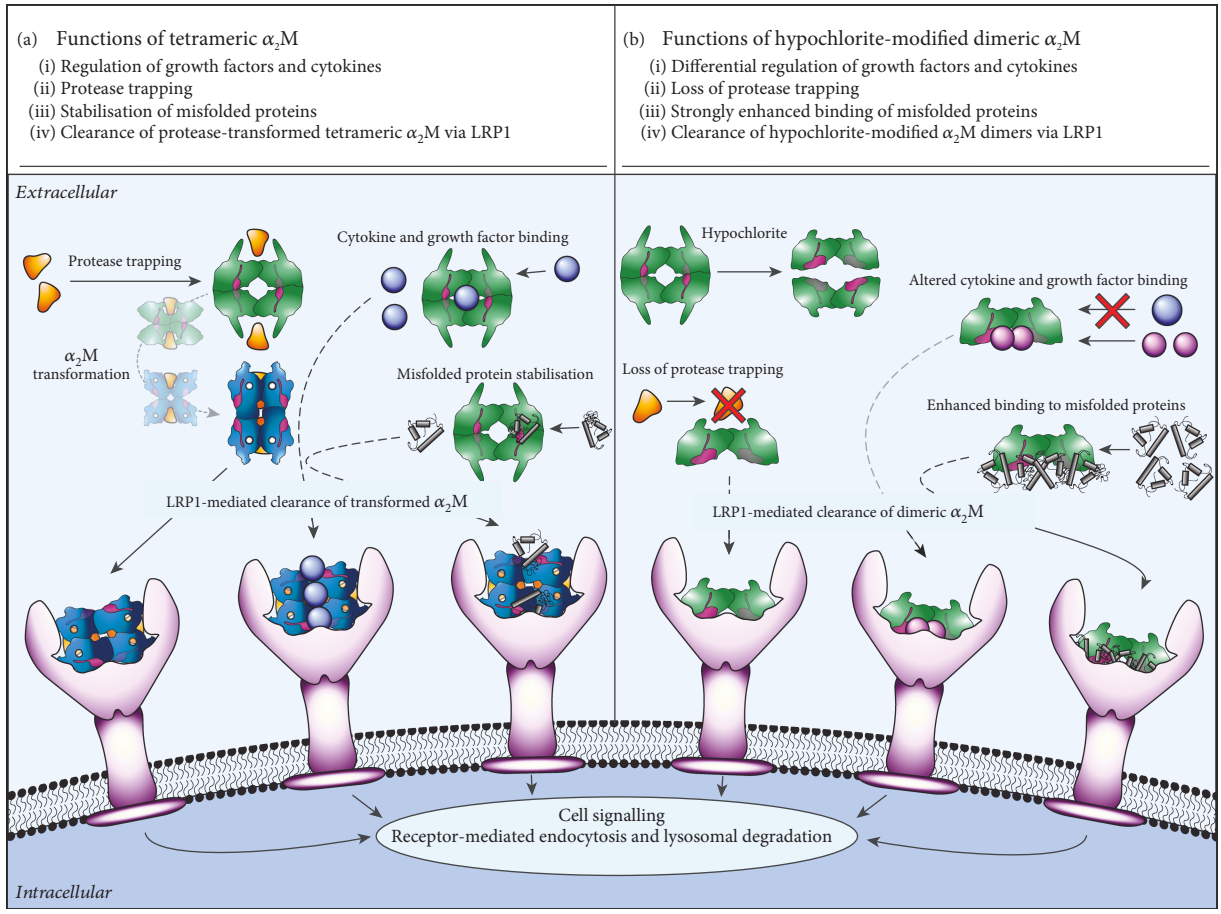

Figure 1: Schematic diagram showing the function consequences of hypochlorite-induced modification of α_2M. (a) Native α_2M, a tetramer (shown in green), is constitutively present in biological fluids and covalently binds to a broad range of proteases. Binding to proteases results in a conformational change that exposes the binding site on α_2M for LRP1, which is responsible for the clearance of the protease-transformed α_2M complex (shown in dark blue). α_2M also binds to a large number of noncovalent ligands including cytokines and misfolded proteins. In many cases, noncovalent binding of ligands occurs preferentially to the protease-transformed conformation (not shown). In the instance that native α_2M binds noncovalently to a nonprotease substrate, protease interaction is required to enable clearance of the complex via LRP1. (b) Reaction with hypochlorite induces the dissociation of the native α_2M tetramer into dimers. This process abolishes the protease-trapping activity of α_2M; however, the binding to some cytokines (i.e., TNF-α, IL-2, and IL-6) and misfolded proteins is enhanced. On the other hand, the binding of α_2M to other noncovalent ligands (i.e., β-NGF, PDGF-BB, TGF-β1, and TGF-β2) is reduced. The dissociation of the native α_2M tetramer into dimers reveals the binding site on α_2M for LRP1. Therefore, α_2M dimers can facilitate the clearance of substrates in a protease-independent manner. N.B.: Inflammatory processes potentially elevate levels of protease-transformed α_2M and hypochlorite-modified α_2M dimers, concomitantly.

pathways via alternative mechanisms. For example, the binding of α_2M to phosphorylated insulin-like growth factor binding protein-1 abrogates its inhibitory effects on insulin-like growth factor-1 (IGF-1); therefore, in some scenarios, α_2M can potentiate growth factor signalling [13]. Another example whereby α_2M is reported to potentiate growth factor signalling involves the pronerve growth factor (pro-NGF), which induces the expression of TNF-α via stimulating the neurotrophin receptor p75 [11]. Although α_2M potentiates pro-NGF signalling *in vitro*, α_2M is reported to inhibit the activity of mature NGF by binding either to NGF or to Trk receptors [12, 23, 24].

The accumulation of misfolded proteins is inherently deleterious to living organisms and underlies the pathology of many human diseases including Alzheimer's disease, Parkinson's disease, and motor neuron disease. α_2M is one of a small number of secreted proteins that are known to possess holdase-type chaperone activity, which is the ability to stabilise misfolded proteins and prevent their aberrant aggregation [16–20, 25]. The chaperone function of α_2M has been demonstrated *in vitro* using a broad range of misfolded clients including denatured globular proteins and aggregation prone, intrinsically disordered substrates (e.g., Aβ peptide and Parkinson's disease-associated alpha-synuclein). Furthermore, it has been shown that α_2M preferentially binds several plasma proteins *in situ* following experimentally-induced shear stress which causes plasma protein aggregation [18, 19]. The likely fate for complexes formed between native α_2M and misfolded proteins is clearance via LRP1 following interaction with a

protease [16, 22, 25–27] (Figure 1(a)). However, protease-transformed α_2M can also inhibit Aβ aggregation via degrading the peptide because trapped proteases remain active following covalent binding to α_2M [18, 19]. The neuroprotective activity of α_2M against the toxicity induced by misfolded proteins has been demonstrated using several *in vitro* models [17, 25, 27, 28] and has also been demonstrated in rats directly injected with toxic Aβ oligomers [29]. Taken together, the results of these studies support the conclusion that the functions of α_2M are broadly important to extracellular proteostasis.

2. α_2M and Neurodegenerative Diseases

Interest in the role of α_2M in Alzheimer's disease spans several decades. In part, this stems from early reports that polymorphisms in α_2M are associated with increased risk of Alzheimer's disease in some populations [30–36]. However, opposing results have also been presented [37, 38], and more recent genome-wide association studies have not found any association [39]. It has recently been reported that serum α_2M is elevated in men with preclinical Alzheimer's disease, which potentially represents a general response to neuronal injury [40]. The significance of elevated levels of α_2M is hard to determine, because aside from influencing Aβ aggregation and clearance, there are many other relevant biological processes that α_2M potentially influences. For example, apolipoprotein E (ApoE) is an endogenous ligand of α_2M in blood plasma, and the binding of α_2M to the ε4 isoform (the strongest known genetic risk factor for Alzheimer's disease) is much less compared to the binding of α_2M to the ε2 and ε3 ApoE isoforms [15]. The functional importance of this interaction has yet to be solved.

There is strong evidence that native α_2M can inhibit the aggregation and toxicity of Aβ peptide (the major constituent of extracellular plaques in Alzheimer's disease). Furthermore, the widely documented ability of α_2M to facilitate the clearance of the Aβ peptide is central to its neuroprotective action [17, 25, 27–29]. α_2M is found colocalised with the Aβ peptide in the brain in Alzheimer's disease [41, 42], which supports the idea that the LRP1-mediated clearance of α_2M-Aβ complexes is impaired or overwhelmed. Similar to α_2M, there are conflicting reports regarding an association between polymorphisms in LRP1 and the risk of Alzheimer's disease (reviewed in [43]). Given that the accumulation of the Aβ peptide in the brain in Alzheimer's disease appears to be the result of a defect in clearance, rather than elevated production of the peptide [44], it is important to understand the contribution of α_2M to the clearance of the Aβ peptide in greater detail.

Roles for α_2M in preventing or promoting neurodegeneration independent of Alzheimer's disease are less clear. Nevertheless, α_2M is reported to bind to a broad range of misfolded proteins including the infectious prion protein that is responsible for transmissible spongiform encephalopathies [45] and α-synuclein, the major constituent of misfolded protein deposits in Parkinson's disease [17]. In the case of the prion protein, it has been reported that binding to α_2M *in vitro* facilitates the conformational change in the prion protein that is responsible for its infectious characteristics [45]. On the other hand, similar to the protective effect of α_2M on Aβ toxicity, the binding of α_2M to α-synuclein is cytoprotective [17]. α_2M also potentially inhibits neurodegeneration by influencing the activity of neurotrophins such as NGF and pro-NGF or by inhibiting the activity of neurotrophin receptors directly [12, 23, 24]. The latter could have relevance in a range of neurodegenerative diseases including Alzheimer's disease, Parkinson's disease, and Huntington's disease in which aberrant neurotrophin signalling is implicated [46]. Moreover, the ability of α_2M to bind to proinflammatory mediators such as TNF-α, IL-6, and IL-1β [47–49] supports the idea that α_2M has generalised importance in controlling inflammatory processes including in the central nervous system.

3. Hypochlorite, a Novel Regulator of α_2M Functions

Hypochlorite (OCl^-) is a powerful oxidant that is produced by the action of the enzyme myeloperoxidase during inflammation. Myeloperoxidase is not detected in the brains of healthy individuals; however, in neuroinflammatory disorders, myeloperoxidase is generated by activated microglia and astrocytes [50–54]. Infiltrating monocytes/macrophages and neutrophils can also contribute to myeloperoxidase production in the brain [50, 55]. Although the reasons for this are unclear, myeloperoxidase-immunoreactivity is also detected in neurons in Alzheimer's disease [50, 51]. Interestingly, in a mouse model of Parkinson's disease, ablation of the myeloperoxidase gene is protective, which supports the conclusion that myeloperoxidase is a major contributor to the oxidative damage generated by pathological neuroinflammatory processes [56].

Hypochlorite production is primarily considered important for defence against invading microbes [57]. The effectiveness of hypochlorite as a microbicidal agent is linked to the potency with which hypochlorite damages proteins, inducing their misfolding [58, 59]. Given that reaction with hypochlorite is not specific to molecules of microbial origin, the generation of hypochlorite is associated with collateral damage to the host organism. As a result of aberrant inflammatory activity, hypochlorite-modified proteins accumulate in a large number of pathologies including Alzheimer's disease [51], atherosclerosis [60], kidney disease [61], rheumatoid arthritis [52] and in experimental animal models of Parkinson's disease [56] and multiple sclerosis [62]. Hypochlorite-induced modification can directly cause proteins to adopt immunostimulatory and cytotoxic properties. For example, hypochlorite-induced modification of apolipoprotein B-100, the major protein component of low-density lipoprotein particles, promotes macrophage foam cell formation and triggers platelet aggregation [63]. Additionally, hypochlorite-modified albumin is known to promote proinflammatory signalling [64], endothelial cell dysfunction [65], and apoptosis [66].

It is well-known that antioxidants are the first line of defence that protects the host from excessive oxidative damage during inflammation. However, evidence has emerged

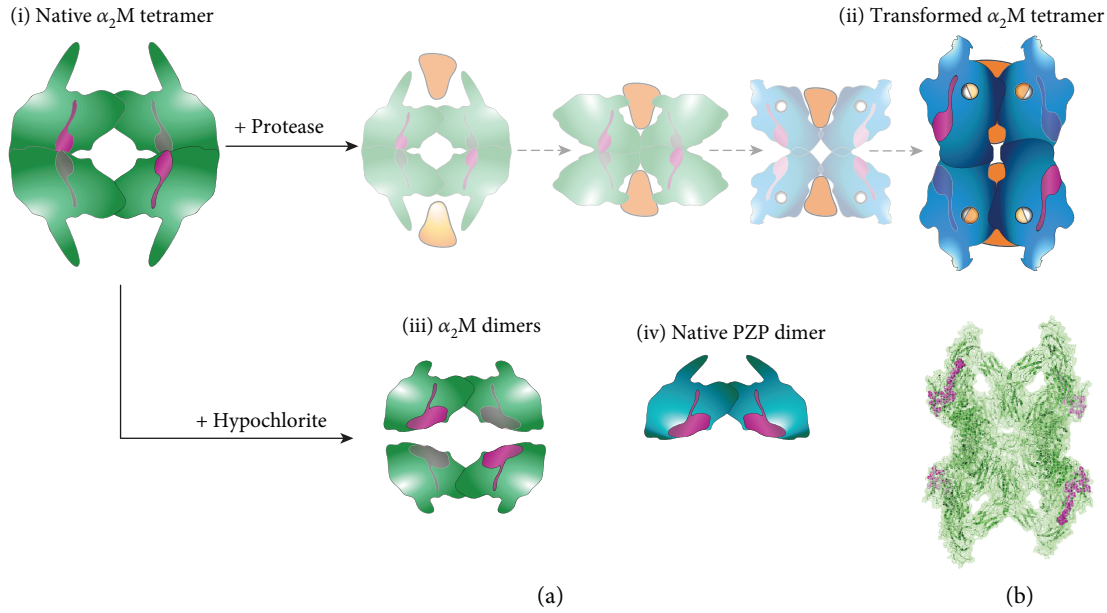

Figure 2: Theoretical model showing the binding sites for monomeric Aβ on native α_2M and PZP. (a) The binding sites for monomeric Aβ (magenta; centred at amino acids 1314–1365 according to [21]) are normally concealed at the noncovalent interface of the (i) native α_2M tetramer. (ii) Binding to proteases (yellow triangles) results in the partial opening of the noncovalent interface between α_2M dimers and exposes the binding sites for monomeric Aβ on each subunit of transformed α_2M. (iii) The binding sites for monomeric Aβ are also exposed by hypochlorite-induced dissociation of the native α_2M tetramer into dimers. (iv) Native PZP (a disulfide-linked dimer) shares 82.7% sequence identity with α_2M in the Aβ binding region (magenta). The dimeric quaternary structure of native PZP results in surface exposure of the binding sites for monomeric Aβ. Although the binding sites for other misfolded proteins are not known, intuitively, they are also located at the normally buried hydrophobic interface of noncovalently associated α_2M dimers. (b) Image of the crystal structure of the transformed α_2M tetramer from PBD 4ACQ [3] with the binding sites for monomeric Aβ shown in magenta, which is comparable to the model shown in (a (ii)). The crystal structures of native α_2M or hypochlorite-modified α_2M dimers have not been solved.

that supports the conclusion that specialised hypochlorite-inducible systems are also important. Around a decade ago, it was demonstrated that the activity of the bacterial chaperone Hsp33 is directly enhanced following reaction with hypochlorite and the chaperone activity of hypochlorite-modified Hsp33 protects bacteria from hypochlorite-induced death [59]. More recently, it has been demonstrated that reaction with hypochlorite induces the dissociation of the native α_2M tetramer into dimers that have dramatically enhanced chaperone activity compared to the native α_2M tetramer [25] (Figure 1(b)). The mechanism responsible for the enhanced chaperone activity of hypochlorite-modified α_2M dimers involves the exposure of the normally buried hydrophobic surfaces that are situated at the interface of noncovalently-associated dimers in the native α_2M tetramer [25] (Figure 2). It has been reported that methionine oxidation is largely responsible for the hypochlorite-induced dissociation of α_2M into dimers [67]; however, aromatic amino acids are also modified by physiologically relevant levels of hypochlorite [25, 68, 69]. The results of biophysical analyses show that physiologically-relevant levels of hypochlorite also alter the secondary structure of α_2M subunits [25, 68]. Precisely how hypochlorite-induced modification of the secondary structure of α_2M influences its functions is not known.

During inflammation, extracellular protease activity and the generation of hypochlorite are both elevated; therefore, it is plausible that protease-transformed α_2M and hypochlorite-induced α_2M dimers are concomitantly generated *in vivo*. Hypochlorite-induced modification of native α_2M exposes its LRP1 binding sites ([25, 70]); therefore, during inflammation, α_2M and its cargoes are potentially cleared via two distinct mechanisms involving LRP1 (Figure 1(a): protease-transformed α_2M and Figure 1(b): hypochlorite-induced α_2M dimers). The dissociation constant for the binding of hypochlorite-modified α_2M to LRP1 is reportedly ~0.7 nM [70] compared to 40 pM—2 nM for the transformed α_2M [71]. Unlike native α_2M, reaction with hypochlorite does not induce transformed α_2M (generated using methylamine) to dissociate into dimers, and the resultant hypochlorite-induced damage reduces the binding of transformed α_2M to LRP1 [70]. Therefore, during inflammation, the generation of hypochlorite potentially enhances the delivery of hypochlorite-modified α_2M dimers that are generated from the native α_2M tetramer to LRP1, while impeding the delivery of transformed α_2M to the same receptor.

Although the chaperone activity of native α_2M is enhanced following hypochlorite-induced modification, similar levels of hypochlorite-induced modification abolish the protease trapping function of α_2M [72, 73]. Collectively, the evidence suggests that reaction with hypochlorite is a rapid switch that regulates the activities of α_2M during inflammation. Supporting this idea, it has been reported that hypochlorite-induced modification of α_2M also regulates its binding to cytokines and growth factors in a manner that increases its binding to TNF-α, IL-2, and IL-6 (involving

preferential binding to hypochlorite-induced α_2M dimers) and decreases its binding to β-NGF, PDGF-BB, TGF-β1, and TGF-β2 *in vitro* [74] (Figure 1(b)). Furthermore, hypochlorite-induced dissociation of α_2M enhances its cytoprotective effect against TNF-α *in vitro* [74]. Interestingly, it has been reported that the complement system, which includes several proteins that are closely related to α_2M, is also activated by reaction with hypochlorite [75, 76]. Therefore, it is tempting to speculate that hypochlorite-induced regulation is a characteristic that is shared by this family of proteins.

Studies of the hypochlorite-induced regulation of α_2M are currently limited to *in vitro* systems; however, using the specific marker for reaction with hypochlorite 3-chlorotyrosine, it has been shown that α_2M is modified by hypochlorite in synovial fluid from inflamed joints [69]. Moreover, considering that hypochlorite levels are predicted to reach the low millimolar range in tissues during inflammation [77], it is plausible that hypochlorite-modified α_2M dimers are generated in biological fluids during inflammation. Of the studies reporting an association between mutation in α_2M and risk of Alzheimer's disease, one study has reported that there is a synergistic effect between polymorphisms in α_2M and myeloperoxidase and an increased risk of Alzheimer's disease [36]. The results of the latter study support the idea that the functions of these two proteins might interrelate in a way that is important to neurodegeneration. It is not currently known if any of the other identified extracellular chaperones (e.g., clusterin and haptoglobin) might also have their activities regulated by hypochlorite-induced modification, but this is an area worthy of future investigation.

4. PZP, a Dimeric α_2M-like Molecule

The major structural modification induced by reaction with hypochlorite that is responsible for functionally controlling α_2M is the dissociation of the native α_2M tetramer into dimers. Strikingly, many mammals are capable of generating large amounts of a dimeric α_2M-like protein known as pregnancy zone protein (PZP). In humans, α_2M and PZP share very high sequence homology in all domains (71% amino acid identity), with the exception of the bait region [4, 78]. As a result, the ability of PZP to inhibit proteases is much more restricted compared to that of α_2M. Few *in vitro* studies have focused on characterising the functions of PZP; however, it has been proposed that PZP contributes to regulating glycodelin-A (a paracrine mediator in early pregnancy) and TGF-β2 (important for embryonic development) [12, 79–81]. Consistent with this idea, PZP is usually lowly abundant in biological fluids but is markedly upregulated in pregnancy [82]. On the other hand, glycodelin-A and TGF-β2 are also ligands for constitutively abundant α_2M ([12, 79–81]); therefore, the precise importance of PZP as a modulator of these signalling pathways remains unclear. Similarly, several neurotrophins are shared ligands of PZP and α_2M, but the precise biological importance of these interactions is not known [12]. Pregnancy-independent expression of PZP is widely reported in diseases such as Alzheimer's disease [83, 84], Parkinson's disease [85], rheumatoid arthritis [86], Behcet's syndrome [87], psoriasis [88, 89], Chagas disease [90], viral infection [91, 92], inflammatory bowel disease [93], and cancers [94, 95]. The latter observations support the idea that the upregulation of PZP could be a general stress response that is related to chronic inflammation. This limits the usefulness of PZP as a diagnostic marker; however, the results of studies of lymphoma and arthritis patients suggest that PZP levels are potentially useful for monitoring disease progression [95, 96].

The ability of native tetrameric α_2M to inhibit Aβ aggregation is restricted to binding to soluble Aβ oligomers formed early during the aggregation pathway [20]. In contrast, transformed α_2M and hypochlorite-modified α_2M dimers bind to monomeric Aβ [21, 25], presumably via the hydrophobic binding site (centred at amino acids 1314–1365) identified by [21] (Figure 2). Intuitively, surface exposure of this site contributes to the efficiency with which hypochlorite-modified α_2M dimers inhibit Aβ amyloid formation compared to native α_2M [25]. Similarly, the results of recent studies show that PZP binds to the monomeric Aβ peptide and prevents the aggregation of the Aβ peptide much more efficiently than native α_2M [97]. Whether or not PZP contributes to the clearance of the Aβ peptide *in vivo* is currently unknown; however, it has been demonstrated that PZP levels are elevated in women with presymptomatic Alzheimer's disease and PZP is found colocalised with microglia around Aβ plaques in the brain in Alzheimer's disease [83, 84]. Combined, these observations suggest that PZP is likely to participate in Aβ homeostasis. Whether or not the role of PZP overlaps with or is discrete from that of α_2M remains to be determined.

5. Concluding Remarks

α_2M is a remarkably multifunctional protein that can influence a broad range of biological processes. Direct injection of α_2M into inflamed joints has been shown to have protective effects in a rodent model of osteoarthritis ([98]); however, the efficacy and safety of this as a human therapy is not yet known. An alternative α_2M-based anti-inflammatory strategy involves the oral administration of proteases, which is proposed to increase levels of transformed α_2M in blood plasma [99, 100]. This strategy is clearly limited by the poor bioavailability of orally administered proteases, but this problem could potentially be overcome by the identification of bioavailable small molecule modifiers of α_2M function.

Growing evidence suggests that hypochlorite-induced dissociation of α_2M into dimers is a rapid switch that enhances the ability of α_2M to facilitate the clearance of disease-associated misfolded proteins and proinflammatory cytokines during inflammation. This is potentially a broadly important process that occurs in response to inflammation, including in neurodegenerative disorders in which neuroinflammation is known to be an early event that precedes other pathological changes (reviewed in [101]). A deeper understanding of the physiological relevance of hypochlorite-induced α_2M dimers has the potential to shed much needed light on the participation of α_2M in controlling inflammatory processes and extracellular protein homeostasis during neuroinflammation.

Conflicts of Interest

The authors declare that there is no conflict of interest regarding the publication of this paper.

Acknowledgments

JHC is supported by an Australian Institute of Nuclear Science and Engineering (AINSE) postdoctoral award and an Australian Postgraduate Award (Commonwealth Government of Australia). This work was also supported by funding from the Australian Research Council (DP160100011 awarded to MRW), the National Health and Medical Research Council of Australia (APP1099991; awarded to ARW), and the Flinders Foundation (awarded to ARW).

References

[1] M. J. Garton, G. Keir, M. V. Lakshmi, and E. J. Thompson, "Age-related changes in cerebrospinal fluid protein concentrations," *Journal of the Neurological Sciences*, vol. 104, no. 1, pp. 74–80, 1991.

[2] L. Sottrup-Jensen, "Alpha-macroglobulins: structure, shape, and mechanism of proteinase complex formation," *The Journal of Biological Chemistry*, vol. 264, no. 20, pp. 11539–11542, 1989.

[3] A. Marrero, S. Duquerroy, S. Trapani et al., "The Crystal Structure of Human α2-Macroglobulin Reveals a Unique Molecular Cage," *Angewandte Chemie (International Ed. in English)*, vol. 51, no. 14, pp. 3340–3344, 2012.

[4] L. Sottrup-Jensen, O. Sand, L. Kristensen, and G. H. Fey, "The alpha-macroglobulin bait region. Sequence diversity and localization of cleavage sites for proteinases in five mammalian alpha-macroglobulins," *The Journal of Biological Chemistry*, vol. 264, no. 27, pp. 15781–15789, 1989.

[5] A. J. Barrett and P. M. Starkey, "The interaction of alpha 2-macroglobulin with proteinases. Characteristics and specificity of the reaction, and a hypothesis concerning its molecular mechanism," *The Biochemical Journal*, vol. 133, no. 4, pp. 709–724, 1973.

[6] A. J. Barrett, M. A. Brown, and C. A. Sayers, "The electrophoretically 'slow' and 'fast' forms of the alpha 2-macroglobulin molecule," *The Biochemical Journal*, vol. 181, no. 2, pp. 401–418, 1979.

[7] J. D. Ashcom, S. E. Tiller, K. Dickerson, J. L. Cravens, W. S. Argraves, and D. K. Strickland, "The human alpha 2-macroglobulin receptor: identification of a 420-kD cell surface glycoprotein specific for the activated conformation of alpha 2-macroglobulin," *The Journal of Cell Biology*, vol. 110, no. 4, pp. 1041–1048, 1990.

[8] T. Kristensen, S. K. Moestrup, J. Gliemann, L. Bendtsen, O. Sand, and L. Sottrup-Jensen, "Evidence that the newly cloned low-density-lipoprotein receptor related protein (LRP) is the alpha 2-macroglobulin receptor," *FEBS Letters*, vol. 276, no. 1-2, pp. 151–155, 1990.

[9] S. L. Gonias, A. Carmichael, J. M. Mettenburg, D. W. Roadcap, W. P. Irvin, and D. J. Webb, "Identical or overlapping sequences in the primary structure of human alpha(2)-macroglobulin are responsible for the binding of nerve growth factor-beta, platelet-derived growth factor-BB, and transforming growth factor-beta," *The Journal of Biological Chemistry*, vol. 275, no. 8, pp. 5826–5831, 2000.

[10] J. LaMarre, G. K. Wollenberg, S. L. Gonias, and M. A. Hayes, "Cytokine binding and clearance properties of proteinase-activated alpha 2-macroglobulins," *Laboratory Investigation*, vol. 65, no. 1, pp. 3–14, 1991.

[11] P. F. Barcelona and H. U. Saragovi, "A pro-nerve growth factor (proNGF) and NGF binding protein, α2-macroglobulin, differentially regulates p75 and TrkA receptors and is relevant to neurodegeneration ex vivo and in vivo," *Molecular and Cellular Biology*, vol. 35, no. 19, pp. 3396–3408, 2015.

[12] E. L. Skornicka, X. Shi, and P. H. Koo, "Comparative binding of biotinylated neurotrophins to alpha(2)-macroglobulin family of proteins: relationship between cytokine-binding and neuro-modulatory activities of the macroglobulins," *Journal of Neuroscience Research*, vol. 67, no. 3, pp. 346–353, 2002.

[13] M. Westwood, J. D. Aplin, I. A. Collinge, A. Gill, A. White, and J. M. Gibson, "Alpha 2-macroglobulin: a new component in the insulin-like growth factor/insulin-like growth factor binding protein-1 axis," *The Journal of Biological Chemistry*, vol. 276, no. 45, pp. 41668–41674, 2001.

[14] B. B. Wolf and S. L. Gonias, "Neurotrophin binding to human alpha 2-macroglobulin under apparent equilibrium conditions," *Biochemistry*, vol. 33, no. 37, pp. 11270–11277, 1994.

[15] L. Krimbou, M. Tremblay, J. Davignon, and J. S. Cohn, "Association of apolipoprotein E with alpha2-macroglobulin in human plasma," *Journal of Lipid Research*, vol. 39, no. 12, pp. 2373–2386, 1998.

[16] K. French, J. J. Yerbury, and M. R. Wilson, "Protease activation of alpha2-macroglobulin modulates a chaperone-like action with broad specificity," *Biochemistry*, vol. 47, no. 4, pp. 1176–1185, 2008.

[17] D. R. Whiten, D. Cox, M. H. Horrocks et al., "Single-Molecule Characterization of the Interactions between Extracellular Chaperones and Toxic α-Synuclein Oligomers," *Cell Reports*, vol. 23, no. 12, pp. 3492–3500, 2018.

[18] A. R. Wyatt, P. Constantinescu, H. Ecroyd et al., "Protease-activated alpha-2-macroglobulin can inhibit amyloid formation via two distinct mechanisms," *FEBS Letters*, vol. 587, no. 5, pp. 398–403, 2013.

[19] A. R. Wyatt, N. W. Zammit, and M. R. Wilson, "Acute phase proteins are major clients for the chaperone action of α2-macroglobulin in human plasma," *Cell Stress & Chaperones*, vol. 18, no. 2, pp. 161–170, 2013.

[20] J. J. Yerbury, J. R. Kumita, S. Meehan, C. M. Dobson, and M. R. Wilson, "Alpha2-macroglobulin and haptoglobin suppress amyloid formation by interacting with prefibrillar protein species," *The Journal of Biological Chemistry*, vol. 284, no. 7, pp. 4246–4254, 2009.

[21] J. M. Mettenburg, D. J. Webb, and S. L. Gonias, "Distinct binding sites in the structure of alpha 2-macroglobulin mediate the interaction with beta-amyloid peptide and growth factors," *The Journal of Biological Chemistry*, vol. 277, no. 15, pp. 13338–13345, 2002.

[22] M. Narita, D. M. Holtzman, A. L. Schwartz, and G. Bu, "α2-Macroglobulin complexes with and mediates the endocytosis of β-amyloid peptide via cell surface low-density lipoprotein receptor-related protein," *Journal of Neurochemistry*, vol. 69, no. 5, pp. 1904–1911, 2002.

[23] P. H. Koo and W. S. Qiu, "Monoamine-activated alpha 2-macroglobulin binds trk receptor and inhibits nerve growth factor-stimulated trk phosphorylation and signal

transduction," *The Journal of Biological Chemistry*, vol. 269, no. 7, pp. 5369–5376, 1994.

[24] D. J. Liebl and P. H. Koo, "Serotonin-activated alpha 2-macroglobulin inhibits neurite outgrowth and survival of embryonic sensory and cerebral cortical neurons," *Journal of Neuroscience Research*, vol. 35, no. 2, pp. 170–182, 1993.

[25] A. R. Wyatt, J. R. Kumita, R. W. Mifsud, C. A. Gooden, M. R. Wilson, and C. M. Dobson, "Hypochlorite-induced structural modifications enhance the chaperone activity of human 2-macroglobulin," *Proceedings of the National Academy of Sciences of the United States of America*, vol. 111, no. 20, pp. E2081–E2090, 2014.

[26] Z. Qiu, D. K. Strickland, B. T. Hyman, and G. W. Rebeck, "Alpha2-macroglobulin enhances the clearance of endogenous soluble beta-amyloid peptide via low-density lipoprotein receptor-related protein in cortical neurons," *Journal of Neurochemistry*, vol. 73, no. 4, pp. 1393–1398, 1999.

[27] J. J. Yerbury and M. R. Wilson, "Extracellular chaperones modulate the effects of Alzheimer's patient cerebrospinal fluid on Abeta(1-42) toxicity and uptake," *Cell Stress & Chaperones*, vol. 15, no. 1, pp. 115–121, 2010.

[28] C. Fabrizi, R. Businaro, G. M. Lauro, and L. Fumagalli, "Role of alpha2-macroglobulin in regulating amyloid beta-protein neurotoxicity: protective or detrimental factor?," *Journal of Neurochemistry*, vol. 78, no. 2, pp. 406–412, 2001.

[29] R. Cascella, S. Conti, F. Tatini et al., "Extracellular chaperones prevent Aβ42-induced toxicity in rat brains," *Biochimica et Biophysica Acta*, vol. 1832, no. 8, pp. 1217–1226, 2013.

[30] V. Alvarez, R. Alvarez, C. H. Lahoz et al., "Association between an alpha(2) macroglobulin DNA polymorphism and late-onset Alzheimer's disease," *Biochemical and Biophysical Research Communications*, vol. 264, no. 1, pp. 48–50, 1999.

[31] D. Blacker, M. A. Wilcox, N. M. Laird et al., "Alpha-2 macroglobulin is genetically associated with Alzheimer disease," *Nature Genetics*, vol. 19, no. 4, pp. 357–360, 1998.

[32] A. Liao, R. M. Nitsch, S. M. Greenberg et al., "Genetic association of an alpha2-macroglobulin (Val1000Ile) polymorphism and Alzheimer's disease," *Human Molecular Genetics*, vol. 7, no. 12, pp. 1953–1956, 1998.

[33] E. Mariani, D. Seripa, T. Ingegni et al., "Interaction of CTSD and A2M polymorphisms in the risk for Alzheimer's disease," *Journal of the Neurological Sciences*, vol. 247, no. 2, pp. 187–191, 2006.

[34] A. J. Saunders, L. Bertram, K. Mullin et al., "Genetic association of Alzheimer's disease with multiple polymorphisms in alpha-2-macroglobulin," *Human Molecular Genetics*, vol. 12, no. 21, pp. 2765–2776, 2003.

[35] X. Xu, Y. Wang, L. Wang et al., "Meta-analyses of 8 polymorphisms associated with the risk of the Alzheimer's disease," *PLoS One*, vol. 8, no. 9, article e73129, 2013.

[36] M. Zappia, I. Manna, P. Serra et al., "Increased risk for Alzheimer disease with the interaction of MPO and A2M polymorphisms," *Archives of Neurology*, vol. 61, no. 3, pp. 341–344, 2004.

[37] L. Chen, L. Baum, H. K. Ng et al., "Apolipoprotein E promoter and α2-macroglobulin polymorphisms are not genetically associated with Chinese late onset Alzheimer's disease," *Neuroscience Letters*, vol. 269, no. 3, pp. 173–177, 1999.

[38] F. Wavrant-DeVrièze, V. Rudrasingham, J. C. Lambert et al., "No association between the alpha-2 macroglobulin I1000V polymorphism and Alzheimer's disease," *Neuroscience Letters*, vol. 262, no. 2, pp. 137–139, 1999.

[39] L. Shen and J. Jia, "An overview of genome-wide association studies in Alzheimer's disease," *Neuroscience Bulletin*, vol. 32, no. 2, pp. 183–190, 2016.

[40] V. R. Varma, Predictors of Cognitive Decline Among Normal Individuals (BIOCARD) and the Alzheimer's Disease Neuroimaging Initiative (ADNI) studies, S. Varma et al., "Alpha-2 macroglobulin in Alzheimer's disease: a marker of neuronal injury through the RCAN1 pathway," *Molecular Psychiatry*, vol. 22, no. 1, pp. 13–23, 2017.

[41] D. R. Thal, R. Schober, and G. Birkenmeier, "The subunits of alpha2-macroglobulin receptor/low density lipoprotein receptor-related protein, native and transformed alpha2-macroglobulin and interleukin 6 in Alzheimer's disease," *Brain Research*, vol. 777, no. 1-2, pp. 223–227, 1997.

[42] D. Van Gool, B. de Strooper, F. Van Leuven, E. Triau, and R. Dom, "α2-macroglobulin expression in neuritic-type plaques in patients with Alzheimer's disease," *Neurobiology of Aging*, vol. 14, no. 3, pp. 233–237, 1993.

[43] M. Shinohara, M. Tachibana, T. Kanekiyo, and G. Bu, "Role of LRP1 in the pathogenesis of Alzheimer's disease: evidence from clinical and preclinical studies," *Journal of Lipid Research*, vol. 58, no. 7, pp. 1267–1281, 2017.

[44] R. Deane, R. Bell, A. Sagare, and B. Zlokovic, "Clearance of amyloid-beta peptide across the blood-brain barrier: implication for therapies in Alzheimer's disease," *CNS & Neurological Disorders Drug Targets*, vol. 8, no. 1, pp. 16–30, 2009.

[45] V. Adler, E. Davidowitz, P. Tamburi, P. Rojas, and A. Grossman, "α2-Macroglobulin is a potential facilitator of prion protein transformation," *Amyloid*, vol. 14, no. 1, pp. 1–10, 2007.

[46] J. Meldolesi, "Neurotrophin receptors in the pathogenesis, diagnosis and therapy of neurodegenerative diseases," *Pharmacological Research*, vol. 121, pp. 129–137, 2017.

[47] W. Borth, A. Urbanski, R. Prohaska, M. Susanj, and T. A. Luger, "Binding of recombinant interleukin-1 beta to the third complement component and alpha 2-macroglobulin after activation of serum by immune complexes," *Blood*, vol. 75, no. 12, pp. 2388–2395, 1990.

[48] T. Matsuda, T. Hirano, S. Nagasawa, and T. Kishimoto, "Identification of alpha 2-macroglobulin as a carrier protein for IL-6," *The Journal of Immunology*, vol. 142, no. 1, pp. 148–152, 1989.

[49] G. K. Wollenberg, J. LaMarre, S. Rosendal, S. L. Gonias, and M. A. Hayes, "Binding of tumor necrosis factor alpha to activated forms of human plasma alpha 2 macroglobulin," *The American Journal of Pathology*, vol. 138, no. 2, pp. 265–272, 1991.

[50] S. Gellhaar, D. Sunnemark, H. Eriksson, L. Olson, and D. Galter, "Myeloperoxidase-immunoreactive cells are significantly increased in brain areas affected by neurodegeneration in Parkinson's and Alzheimer's disease," *Cell and Tissue Research*, vol. 369, no. 3, pp. 445–454, 2017.

[51] P. S. Green, A. J. Mendez, J. S. Jacob et al., "Neuronal expression of myeloperoxidase is increased in Alzheimer's disease," *Journal of Neurochemistry*, vol. 90, no. 3, pp. 724–733, 2004.

[52] L. K. Stamp, I. Khalilova, J. M. Tarr et al., "Myeloperoxidase and oxidative stress in rheumatoid arthritis," *Rheumatology*, vol. 51, no. 10, pp. 1796–1803, 2012.

[53] D. L. Lefkowitz and S. S. Lefkowitz, "Microglia and myeloperoxidase: a deadly partnership in neurodegenerative disease," *Free Radical Biology & Medicine*, vol. 45, no. 5, pp. 726–731, 2008.

[54] R. A. Maki, V. A. Tyurin, R. C. Lyon et al., "Aberrant expression of myeloperoxidase in astrocytes promotes phospholipid oxidation and memory deficits in a mouse model of Alzheimer disease," *The Journal of Biological Chemistry*, vol. 284, no. 5, pp. 3158–3169, 2009.

[55] Y. Matsuo, H. Onodera, Y. Shiga et al., "Correlation between myeloperoxidase-quantified neutrophil accumulation and ischemic brain injury in the rat. Effects of neutrophil depletion," *Stroke*, vol. 25, no. 7, pp. 1469–1475, 1994.

[56] D. K. Choi, S. Pennathur, C. Perier et al., "Ablation of the inflammatory enzyme myeloperoxidase mitigates features of Parkinson's disease in mice," *The Journal of Neuroscience*, vol. 25, no. 28, pp. 6594–6600, 2005.

[57] F. Lanza, "Clinical manifestation of myeloperoxidase deficiency," *Journal of Molecular Medicine (Berlin, Germany)*, vol. 76, no. 10, pp. 676–681, 1998.

[58] D. I. Pattison and M. J. Davies, "Absolute rate constants for the reaction of hypochlorous acid with protein side chains and peptide bonds," *Chemical Research in Toxicology*, vol. 14, no. 10, pp. 1453–1464, 2001.

[59] J. Winter, M. Ilbert, P. C. F. Graf, D. Özcelik, and U. Jakob, "Bleach activates a redox-regulated chaperone by oxidative protein unfolding," *Cell*, vol. 135, no. 4, pp. 691–701, 2008.

[60] L. J. Hazell, J. J. M. van den Berg, and R. Stocker, "Oxidation of low-density lipoprotein by hypochlorite causes aggregation that is mediated by modification of lysine residues rather than lipid oxidation," *The Biochemical Journal*, vol. 302, no. 1, pp. 297–304, 1994, Pt 1.

[61] E. Malle, C. Woenckhaus, G. Waeg, H. Esterbauer, E. F. Gröne, and H. J. Gröne, "Immunological evidence for hypochlorite-modified proteins in human kidney," *The American Journal of Pathology*, vol. 150, no. 2, pp. 603–615, 1997.

[62] G. Yu, S. Zheng, and H. Zhang, "Inhibition of myeloperoxidase by N-acetyl lysyltyrosylcysteine amide reduces experimental autoimmune encephalomyelitis-induced injury and promotes oligodendrocyte regeneration and neurogenesis in a murine model of progressive multiple sclerosis," *Neuroreport*, vol. 29, no. 3, pp. 208–213, 2018.

[63] I. Volf, A. Roth, J. Cooper, T. Moeslinger, and E. Koller, "Hypochlorite modified LDL are a stronger agonist for platelets than copper oxidized LDL," *FEBS Letters*, vol. 483, no. 2-3, pp. 155–159, 2000.

[64] G. Marsche, M. Semlitsch, A. Hammer et al., "Hypochlorite-modified albumin colocalizes with RAGE in the artery wall and promotes MCP-1 expression via the RAGE-Erk1/2 MAP-kinase pathway," *The FASEB Journal*, vol. 21, no. 4, pp. 1145–1152, 2007.

[65] D. D. Tang, H. X. Niu, F. F. Peng et al., "Hypochlorite-Modified Albumin Upregulates ICAM-1 Expressionviaa MAPK–NF-κB Signaling Cascade: Protective Effects of Apocynin," *Oxidative Medicine and Cellular Longevity*, vol. 2016, Article ID 1852340, 14 pages, 2016.

[66] L. Li Zhou, F. F. Hou, G. B. Wang et al., "Accumulation of advanced oxidation protein products induces podocyte apoptosis and deletion through NADPH-dependent mechanisms," *Kidney International*, vol. 76, no. 11, pp. 1148–1160, 2009.

[67] V. Y. Reddy, P. E. Desorchers, S. V. Pizzo et al., "Oxidative dissociation of human alpha 2-macroglobulin tetramers into dysfunctional dimers," *The Journal of Biological Chemistry*, vol. 269, no. 6, pp. 4683–4691, 1994.

[68] T. Siddiqui, M. K. Zia, S. S. Ali, H. Ahsan, and F. H. Khan, "Insight into the interactions of proteinase inhibitor- alpha-2-macroglobulin with hypochlorite," *International Journal of Biological Macromolecules*, vol. 117, pp. 401–406, 2018.

[69] S. M. Wu and S. V. Pizzo, "Alpha(2)-macroglobulin from rheumatoid arthritis synovial fluid: functional analysis defines a role for oxidation in inflammation," *Archives of Biochemistry and Biophysics*, vol. 391, no. 1, pp. 119–126, 2001.

[70] S. M. Wu, C. M. Boyer, and S. V. Pizzo, "The binding of receptor-recognized alpha2-macroglobulin to the low density lipoprotein receptor-related protein and the alpha2M signaling receptor is decoupled by oxidation," *The Journal of Biological Chemistry*, vol. 272, no. 33, pp. 20627–20635, 1997.

[71] S. K. Moestrup and J. Gliemann, "Analysis of ligand recognition by the purified alpha 2-macroglobulin receptor (low density lipoprotein receptor-related protein) Evidence that high affinity of alpha 2-macroglobulin-proteinase complex is achieved by binding to adjacent receptors," *The Journal of Biological Chemistry*, vol. 266, no. 21, pp. 14011–14017, 1991.

[72] J. J. Abbink, A. M. Kamp, E. J. Nieuwenhuys, J. H. Nuijens, A. J. G. Swaak, and C. E. Hack, "Predominant role of neutrophils in the inactivation of alpha 2-macroglobulin in arthritic joints," *Arthritis and Rheumatism*, vol. 34, no. 9, pp. 1139–1150, 1991.

[73] S. M. Wu and S. V. Pizzo, "Mechanism of hypochlorite-mediated inactivation of proteinase inhibition by alpha 2-macroglobulin," *Biochemistry*, vol. 38, no. 42, pp. 13983–13990, 1999.

[74] S. M. Wu, D. D. Patel, and S. V. Pizzo, "Oxidized α2-Macroglobulin (α2M) Differentially Regulates Receptor Binding by Cytokines/Growth Factors: Implications for Tissue Injury and Repair Mechanisms in Inflammation," *Journal of Immunology*, vol. 161, no. 8, pp. 4356–4365, 1998.

[75] M. Shingu, S. Nonaka, H. Nishimukai, M. Nobunaga, H. Kitamura, and K. Tomo-Oka, "Activation of complement in normal serum by hydrogen peroxide and hydrogen peroxide-related oxygen radicals produced by activated neutrophils," *Clinical and Experimental Immunology*, vol. 90, no. 1, pp. 72–78, 1992.

[76] W. Vogt, "Complement activation by myeloperoxidase products released from stimulated human polymorphonuclear leukocytes," *Immunobiology*, vol. 195, no. 3, pp. 334–346, 1996.

[77] S. J. Weiss, "Tissue destruction by neutrophils," *The New England Journal of Medicine*, vol. 320, no. 6, pp. 365–376, 1989.

[78] K. Devriendt, H. van den Berghe, J. J. Cassiman, and P. Marynen, "Primary structure of pregnancy zone protein. Molecular cloning of a full-length PZP cDNA clone by the polymerase chain reaction," *Biochimica et Biophysica Acta*, vol. 1088, no. 1, pp. 95–103, 1991.

[79] G. A. Chiabrando, M. C. Sánchez, E. L. Skornicka, and P. H. Koo, "Low-density lipoprotein receptor-related protein mediates in PC12 cell cultures the inhibition of nerve growth factor-promoted neurite outgrowth by pregnancy zone protein and alpha2-macroglobulin," *Journal of Neuroscience Research*, vol. 70, no. 1, pp. 57–64, 2002.

[80] A. Philip, L. Bostedt, T. Stigbrand, and M. D. O'connor-McCourt, "Binding of transforming growth factor-β (TGF-β) to pregnancy zone protein (PZP)," *European Journal of Biochemistry*, vol. 221, no. 2, pp. 687–693, 1994.

[81] E. L. Skornicka, N. Kiyatkina, M. C. Weber, M. L. Tykocinski, and P. H. Koo, "Pregnancy zone protein is a carrier and modulator of placental protein-14 in T-cell growth and cytokine production," *Cellular Immunology*, vol. 232, no. 1-2, pp. 144–156, 2004.

[82] L. Ekelund and C. . B. Laurell, "The pregnancy zone protein response during gestation: a metabolic challenge," *Scandinavian Journal of Clinical and Laboratory Investigation*, vol. 54, no. 8, pp. 623–629, 1994.

[83] L. IJsselstijn, L. J. M. Dekker, C. Stingl et al., "Serum levels of pregnancy zone protein are elevated in presymptomatic Alzheimer's disease," *Journal of Proteome Research*, vol. 10, no. 11, pp. 4902–4910, 2011.

[84] D. A. T. Nijholt, L. Ijsselstijn, M. M. van der Weiden et al., "Pregnancy zone protein is increased in the Alzheimer's disease brain and associates with senile plaques," *Journal of Alzheimer's Disease*, vol. 46, no. 1, pp. 227–238, 2015.

[85] A. Henderson-Smith, J. J. Corneveaux, M. de Both et al., "Next-generation profiling to identify the molecular etiology of Parkinson dementia," *Neurology Genetics*, vol. 2, no. 3, p. e75, 2016.

[86] C. Horne, A. W. Thomson, C. B. Hunter, A. M. Tunstall, C. M. Towler, and M. E. Billingham, "Pregnancy-associated alpha 2-glycoprotein (alpha 2-PAG) and various acute phase reactants in rheumatoid arthritis and osteoarthritis," *Biomedicine*, vol. 30, no. 2, pp. 90–94, 1979.

[87] A. W. Thomson, T. Lehner, M. Adinolfi, and C. H. W. Horne, "Pregnancy-associated alpha-2-glycoprotein in recurrent oral ulceration and Behçet's syndrome," *International Archives of Allergy and Immunology*, vol. 66, no. 1, pp. 33–39, 1981.

[88] L. Beckman, K. Bergdahl, B. Cedergren et al., "Increased serum levels of the pregnancy zone protein in psoriasis," *Acta Dermato-Venereologica*, vol. 57, no. 5, pp. 403–406, 1977.

[89] L. Beckman, K. Bergdahl, B. Cedergren et al., "Association between Duffy blood groups and serum level of the pregnancy zone protein," *Human Heredity*, vol. 29, no. 5, pp. 257–260, 1979.

[90] A. Ramos et al., "Trypanosoma cruzi: cruzipain and membrane-bound cysteine proteinase isoform(s) interacts with human alpha(2)-macroglobulin and pregnancy zone protein," *Experimental Parasitology*, vol. 100, no. 2, pp. 121–130, 2002.

[91] E. J. Sarcione and W. C. Biddle, "Elevated serum pregnancy zone protein levels in HIV-1-infected men," *AIDS*, vol. 15, no. 18, pp. 2467–2469, 2001.

[92] J. A. Zarzur, M. Aldao, S. Sileoni, and M. A. Vides, "Serum pregnancy-associated alpha 2-glycoprotein levels in the evolution of hepatitis B virus infection," *Journal of Clinical Laboratory Analysis*, vol. 3, no. 2, pp. 73–77, 1989.

[93] E. Viennois, M. T. Baker, B. Xiao, L. Wang, H. Laroui, and D. Merlin, "Longitudinal study of circulating protein biomarkers in inflammatory bowel disease," *Journal of Proteomics*, vol. 112, pp. 166–179, 2015.

[94] W. H. Stimson, "Variations in the level of a pregnancy-associated alpha-macroglobulin in patients with cancer," *Journal of Clinical Pathology*, vol. 28, no. 11, pp. 868–871, 1975.

[95] F. E. Zalazar, G. A. Chiabrando, N. A. de Aldao, F. Ojeda, M. A. Vides, and M. A. J. Aldao, "Pregnancy-associated α2-glycoprotein in children with acute lymphocytic leukemia, Hodgkin's disease and non-Hodgkin's lymphomas," *Clinica Chimica Acta*, vol. 210, no. 1-2, pp. 133–138, 1992.

[96] A. Unger, A. Kay, A. J. Griffin, and G. S. Panayi, "Disease activity and pregnancy associated alpha 2-glycoprotein in rheumatoid arthritis during pregnancy," *British Medical Journal (Clinical Research Ed.)*, vol. 286, no. 6367, pp. 750–752, 1983.

[97] J. H. Cater, J. R. Kumita, R. Zeineddine Abdallah et al., "Human pregnancy zone protein stabilizes misfolded proteins including preeclampsia- and Alzheimer's-associated amyloid beta peptide," *Proceedings of the National Academy of Sciences*, vol. 116, no. 13, pp. 6101–6110, 2019.

[98] Y. Zhang, X. Wei, S. Browning, G. Scuderi, L. S. Hanna, and L. Wei, "Targeted designed variants of alpha-2-macroglobulin (A2M) attenuate cartilage degeneration in a rat model of osteoarthritis induced by anterior cruciate ligament transection," *Arthritis Research & Therapy*, vol. 19, no. 1, pp. 175–175, 2017.

[99] J. Leipner and R. Saller, "Systemic enzyme therapy in oncology," *Drugs*, vol. 59, no. 4, pp. 769–780, 2000.

[100] G. Lorkowski, "Gastrointestinal absorption and biological activities of serine and cysteine proteases of animal and plant origin: review on absorption of serine and cysteine proteases," *International Journal of Physiology, Pathophysiology and Pharmacology*, vol. 4, no. 1, pp. 10–27, 2012.

[101] M. T. Heneka, M. J. Carson, J. E. Khoury et al., "Neuroinflammation in Alzheimer's disease," *The Lancet Neurology*, vol. 14, no. 4, pp. 388–405, 2015.

Hindawi
Oxidative Medicine and Cellular Longevity
Volume 2019, Article ID 9693726, 13 pages
https://doi.org/10.1155/2019/9693726

Research Article

Nickel Enhances Zinc-Induced Neuronal Cell Death by Priming the Endoplasmic Reticulum Stress Response

Ken-ichiro Tanaka, Misato Kasai, Mikako Shimoda, Ayane Shimizu, Maho Kubota, and Masahiro Kawahara

Department of Bio-Analytical Chemistry, Faculty of Pharmacy, Musashino University, 1-1-20 Shinmachi, Nishitokyo-shi, Tokyo 202-8585, Japan

Correspondence should be addressed to Ken-ichiro Tanaka; k-tana@musashino-u.ac.jp
and Masahiro Kawahara; makawa@musashino-u.ac.jp

Received 15 February 2019; Revised 16 May 2019; Accepted 29 May 2019; Published 17 June 2019

Guest Editor: Roberta Cascella

Trace metals such as zinc (Zn), copper (Cu), and nickel (Ni) play important roles in various physiological functions such as immunity, cell division, and protein synthesis in a wide variety of species. However, excessive amounts of these trace metals cause disorders in various tissues of the central nervous system, respiratory system, and other vital organs. Our previous analysis focusing on neurotoxicity resulting from interactions between Zn and Cu revealed that Cu^{2+} markedly enhances Zn^{2+}-induced neuronal cell death by activating oxidative stress and the endoplasmic reticulum (ER) stress response. However, neurotoxicity arising from interactions between zinc and metals other than copper has not been examined. Thus, in the current study, we examined the effect of Ni^{2+} on Zn^{2+}-induced neurotoxicity. Initially, we found that nontoxic concentrations (0–60 μM) of Ni^{2+} enhance Zn^{2+}-induced neurotoxicity in an immortalized hypothalamic neuronal cell line (GT1-7) in a dose-dependent manner. Next, we analyzed the mechanism enhancing neuronal cell death, focusing on the ER stress response. Our results revealed that Ni^{2+} treatment significantly primed the Zn^{2+}-induced ER stress response, especially expression of the CCAAT-enhancer-binding protein homologous protein (CHOP). Finally, we examined the effect of carnosine (an endogenous peptide) on Ni^{2+}/Zn^{2+}-induced neurotoxicity and found that carnosine attenuated Ni^{2+}/Zn^{2+}-induced neuronal cell death and ER stress occurring before cell death. Based on our results, Ni^{2+} treatment significantly enhances Zn^{2+}-induced neuronal cell death by priming the ER stress response. Thus, compounds that decrease the ER stress response, such as carnosine, may be beneficial for neurological diseases.

1. Introduction

In many organisms, trace metals such as zinc (Zn), copper (Cu), and nickel (Ni) play important roles in various physiological functions such as immunity, cell division, and protein synthesis. Indeed, these trace metals are well-known cofactors for hundreds of enzyme proteins [1]. Thus, deficiency of these trace metals causes immune system dysfunction, physical development retardation, dwarfism, learning disabilities, and taste and olfaction disorders in humans [2, 3]. However, excessive amounts of these trace metals cause disorders of various organs, such as the central nervous system and respiratory system.

In particular, disorders involving excessive amounts of zinc in the central nervous system have been attracting keen attention. Zn binds firmly to certain metalloproteins and enzymes in their steady state but has also been shown to exist in the form of free Zn ions (Zn^{2+}) or loosely bound to proteins in a subset of excitatory neurons [4]. In pathological situations such as stroke or transient global ischemia, interrupted blood flow induces excessive release of Zn via long-lasting membrane depolarization [5]. The released Zn accumulates in neurons and induces neuronal cell death [6, 7]. These findings suggest that Zn is a key modulator of delayed neuronal cell death after ischemic injury, and moreover, Zn neurotoxicity is central to the pathogenesis of

poststroke dementia [8]. Furthermore, Zn is reportedly involved in the progression of Alzheimer's disease [9].

We previously examined molecular mechanisms underlying Zn^{2+}-induced neurotoxicity using an immortalized hypothalamic neuronal cell line (GT1-7) and found that Zn^{2+} induced a marked upregulation of endoplasmic reticulum (ER) stress-related genes, especially CCAAT-enhancer-binding protein homologous protein (CHOP) and growth arrest and DNA damage-inducible gene 34 (GADD34), and loss of mitochondrial membrane potential (mitochondrial injury) [10]. These results suggested that Zn^{2+} induces neuronal cell death via the ER stress response and mitochondrial injury. We also identified compounds capable of decreasing Zn^{2+}-induced neurotoxicity and neuronal cell death, including carnosine (an endogenous dipeptide), pyruvic acid (an organic acid involved in glycolysis and the tricarboxylic acid cycle), and thioredoxin-albumin fusion protein (HSA-Trx; an antioxidative protein) [10–12].

Other trace metals, such as Cu^{2+}, Ni^{2+}, iron (Fe^{2+}, Fe^{3+}), and manganese (Mn^{2+}), are also present in the brain and/or cerebrospinal fluid [13, 14]. Recent studies suggest that intracellular Cu^{2+} accumulates in synaptic vesicles and is then released into the synaptic cleft during neuronal excitation, with a reported concentration of Cu^{2+} in the synaptic cleft of 2–15 μM [15–17]. The translocated Cu^{2+} influences various receptors, including AMPA-type glutamate and GABA receptors, and contributes to the modulation of neuronal excitability [16]. Mn^{2+} is important both for neurotransmitter synthesis and as a component of superoxide dismutase 2 in mitochondria [18]. However, excessive amounts of Mn^{2+} are thought to induce neurotoxicity and cause a Parkinson's-like syndrome [19]. Ni^{2+} also reportedly causes neurotoxicity, reactive oxygen species (ROS) production, and mitochondrial dysfunction in neuronal cells [20]. Considering these reports, other trace metals may interact with Zn^{2+} in brain tissue and synaptic clefts, to act together in neuronal cells. Therefore, we recently examined the effects of various metal ions on Zn^{2+}-induced neurotoxicity in GT1-7 cells and found that Cu^{2+} or Ni^{2+} enhanced Zn^{2+}-induced neurotoxicity [21]. Moreover, we found that Cu^{2+} enhanced Zn^{2+}-induced neurotoxicity by activating oxidative stress, the ER stress response, and mitochondrial injury [11, 21, 22]. However, the mechanisms by which Ni^{2+} enhanced Zn^{2+}-induced neurotoxicity have not been examined.

Based on the results of our previous study [21], we first examined whether Ni^{2+} enhanced Zn^{2+}-induced neurotoxicity using GT1-7 cells in the current investigation. As a result, we found that Ni^{2+} (nontoxic concentrations by single treatment) enhanced Zn^{2+}-induced neurotoxicity in GT1-7 cells via a mechanism involving the ER stress response. Furthermore, we examined the effect of carnosine, an endogenous peptide, on neuronal cell death induced by cotreatment with Ni^{2+} and Zn^{2+}.

2. Materials and Methods

2.1. Chemicals and Reagents. An antibody against actin (SC-47778) was purchased from Santa Cruz Biotechnology (Santa Cruz, CA). Antibodies against CHOP (#5554) and goat anti-rabbit IgG (horseradish peroxidase- (HRP-) conjugated, #7074) were purchased from Cell Signaling Technology Japan (Tokyo, Japan). Tauroursodeoxycholic acid (TUDCA) was purchased from Tokyo Chemical Industry (Tokyo, Japan). The Zinc Assay Kit was purchased from Metallogenics Co. Ltd. (Chiba, Japan). HRP-conjugated donkey anti-mouse IgG was purchased from GE Healthcare Japan (Tokyo, Japan). Carnosine, $ZnCl_2$, $NiCl_2$, and RIPA buffer (20 mmol/L Tris-HCl (pH 7.4), 0.05 *w*/*v*% NP-40 substitute, 2.5 mmol/L $MgCl_2$, and 200 mmol/L NaCl) were purchased from Wako Pure Chemicals (Tokyo, Japan). Protease and phosphatase inhibitors (87786 and 78420), NuPAGE® Novex 4–12% Bis-Tris Protein Gel, iBlot™ Transfer Stack, and SuperSignal™ West Dura Extended Duration Substrate were from Thermo Fisher Scientific K.K. (Tokyo, Japan).

2.2. Cell Culture. GT1-7 cells, which were provided by Dr. R. Weiner, University of California San Francisco, were grown in Dulbecco's Modified Eagle's Medium/Ham's Nutrient Mixture F-12 supplemented with 10% fetal bovine serum. After trypsin digestion, cells were resuspended in serum-free medium, distributed into culture dishes, and cultured in a humidified incubator (7% CO_2) at 37°C [12].

2.3. Measurement of Cell Viability, Cytotoxicity, and Reactive Oxygen Species (ROS) Levels. Cell viability was measured as described previously [21, 23]. Briefly, dissociated GT1-7 cells were distributed into 96-well culture plates at a density of 3×10^4 cells per well in 200 μL of culture medium. After 24 h incubation, cells were treated with or without N-acetylcysteine (NAC: 0–250 μM), carnosine (0–4 mM), or TUDCA (0–100 mM) prior to the addition of $NiCl_2$ and $ZnCl_2$ to the medium. After 24 h exposure, cell viability was quantified using CellTiter-Glo® 2.0 (Promega Corporation, Madison, WI). Cytotoxicity was quantified using an LDH-Glo™ Cytotoxicity Assay kit (Promega Corporation, Madison, WI) after exposure for 24 h.

GT1-7 cells were precultured in black 96-well microplates (3×10^4 cells/well). After incubation for 24 h, cells were incubated with 2′,7′-dichlorodihydrofluorescein diacetate (DCFHDA, 100 μM), an indicator of ROS, in the absence (control) or presence of $NiCl_2$ and/or $ZnCl_2$ for 2 h. ROS levels were then measured using a microplate reader (Tecan, Kawasaki, Japan) (Ex: 480 nm; Em: 530 nm).

2.4. Real-Time RT-PCR. Dissociated GT1-7 cells were distributed into 6-well culture plates at a density of 7.5×10^5 cells per well in 1.5 mL of culture medium. After 24 h incubation, cells were treated with or without carnosine (0–4 mM) prior to the addition of $NiCl_2$ and $ZnCl_2$ to the medium. After 4 h exposure, total RNA was extracted using an RNeasy kit (QIAGEN, Hilden, Germany) according to the manufacturer's protocol. Samples were reverse-transcribed using a PrimeScript® First Strand cDNA Synthesis Kit (Takara Bio, Otsu, Japan). Synthesized cDNA was used in real-time RT-PCR experiments with Thunderbird® SYBR qPCR Mix (Toyobo, Osaka, Japan) and analyzed with a CFX96™ Real-Time System and CFX Manager™ software (Bio-Rad, Hercules, CA). Specificity was confirmed by electrophoretic

Table 1: Sequences of primers.

Name	Forward	Reverse
Gapdh	AACTTTGGCATTGTGGAAGG	ACACATTGGGGGTAGGAACA
Chop	CCACCACACCTGAAAGCAGAA	AGGTGAAAGGCAGGGACTCA
Gadd34	TCCCTCATGGGGAGACTGAA	AGCTGTGCGTTCCATTTCCT
Grp78	TTCAGCCAATTATCAGCAAACTCT	TTTTCTGATGTATCCTCTTCACCAGT
Edem	CTACCTGCGAAGAGGCCG	GTTCATGAGCTGCCCACTGA
Atf4	GGGTTCTGTCTTCCACTCCA	AAGCAGCAGAGTCAGGCTTTC
Grp94	AAGAATGAAGGAAAAACAGGACAAAA	CAAATGGAGAAGATTCCGCC
Pdi	GGATTGCACTGCCAACACAA	AGCTGGTCCTGCTTGTTTCT
Hif1a	CAAGATCTCGGCGAAGCAA	GGTGAGCCTCATAACAGAAGCTTT
Nrf2	TGGAGAACATTGTCGAGCTG	CTGAGCCGCCTTTTCAGTAG
Ho1	GAACCCAGTCTATGCCCCAC	GGCGTGCAAGGGATGATTTC
Gstm1	GCTCATCATGCTCTGTTACAACC	GCCCAGGAACTCAGAGTAGAG

analysis of reaction products and template- or reverse transcriptase-free controls. To normalize the amount of total RNA present in each reaction, glyceraldehyde-3-phosphate dehydrogenase (*Gapdh*) mRNA was used as an internal standard. Primers were designed using Primer-BLAST. Primer sequences are listed in Table 1.

2.5. Western Blotting Analysis. Zn-induced expression of CHOP and actin was assessed by Western blotting analysis. GT1-7 cells grown in 6-well culture plates (7.5×10^5 cells per well) were lysed with RIPA buffer containing protease and phosphatase inhibitors. Protein concentrations were measured using a Bradford Protein Assay Kit (Takara Bio). Samples were applied to a NuPAGE® Novex 4–12% Bis-Tris Protein Gel and electrophoresed at a constant voltage of 180 V, and then, proteins were transferred to an iBlot™ Transfer Stack (PVDF membranes) using the iBlot® 7-Minute Blotting System (Thermo Fisher Scientific K.K.). Membranes were blocked with 5% nonfat dry milk at room temperature for 1 h and then incubated with rabbit anti-CHOP antibody (1 : 1000 dilution) or mouse anti-actin antibody (1 : 1000 dilution) in 5% BSA, 1x Tris-buffered saline (TBS), and 0.1% Tween-20 overnight. The following day, membranes were incubated with goat anti-rabbit IgG (1 : 2000 dilution) or donkey anti-mouse IgG (1 : 4000 dilution) HRP-conjugated secondary antibodies in 1x TBS containing 0.1% Tween-20 for 1 h, and finally, bands were visualized using SuperSignal™ West Dura Extended Duration Substrate. Band intensities were quantitated using ImageJ software (version 1.39u), and the band intensity of each protein was determined and normalized with respect to actin intensity.

2.6. Statistical Analysis. All data are expressed as mean ± S.E.M. Significant differences among groups were examined using a one-way of analysis of variance (ANOVA) followed by Tukey's multiple comparison. SPSS 24 software was used for all statistical analyses. A probability value of $P < 0.05$ was considered to indicate statistical significance.

3. Results

3.1. Ni^{2+} Enhanced Zn^{2+}-Induced Neuronal Cell Death. We previously examined the effect of various metal ions on Zn^{2+}-induced neurotoxicity in GT1-7 cells and revealed that sublethal concentrations of Cu^{2+} markedly enhanced Zn^{2+}-induced neurotoxicity [21]. We also discovered that Ni^{2+} enhances Zn^{2+}-induced neurotoxicity, but its mechanism was not determined. In this study, we therefore examined the effect of Ni^{2+} on Zn^{2+}-induced neurotoxicity in GT1-7 cells. As shown in Figure 1(a), Zn^{2+} induced neurotoxicity in GT1-7 cells in a dose-dependent manner. The viability of cells exposed to 20, 30, or 40 μM of Zn^{2+} was 98.4% ± 0.6%, 79.8% ± 2.0%, and 48.0% ± 2.7% (mean ± S.E.M., $n = 4$) of the control, respectively. In contrast, the indicated concentrations of Ni^{2+} (0–40 μM) in Figure 1(b) did not reduce the viability of GT1-7 cells.

The effect of Ni^{2+} on Zn^{2+}-induced neurotoxicity in GT1-7 cells is shown in Figure 1(c). At a constant Zn^{2+} concentration of 25 μM, Ni^{2+} enhanced Zn^{2+}-induced neurotoxicity in GT1-7 cells in a dose-dependent manner within the tested Ni^{2+} concentration range (0–60 μM), whereas Ni^{2+} treatment alone did not cause any neurotoxicity. The viability of cells exposed to 0, 20, 40, or 60 μM of Ni^{2+} in the presence of 25 μM Zn^{2+} was 95.9% ± 0.8%, 72.0% ± 1.5%, 39.7% ± 1.6%, and 7.1% ± 3.2% (mean ± S.E.M., $n = 4$) of the control, respectively. We then measured LDH release from GT1-7 cells to monitor cytotoxicity. As shown in Figure 1(e), Ni^{2+} enhanced Zn^{2+}-induced LDH release from GT1-7 cells in a dose-dependent manner within the tested Ni^{2+} concentration range (0–60 μM). Based on the results shown in Figure 1, Ni^{2+} exacerbated Zn^{2+}-induced neuronal cell death.

3.2. Activation of the ER Stress Response by Cotreatment with $NiCl_2$ and $ZnCl_2$. We previously showed that Zn^{2+} and Cu^{2+} increase the expression of ER stress-related genes in GT1-7 cells and that Cu^{2+} enhances Zn^{2+} induced neurotoxicity by activating the ER stress response [21]. Thus, we monitored whether Ni^{2+} primes Zn^{2+}-induced ER stress-related gene expression using real-time RT-PCR. $ZnCl_2$

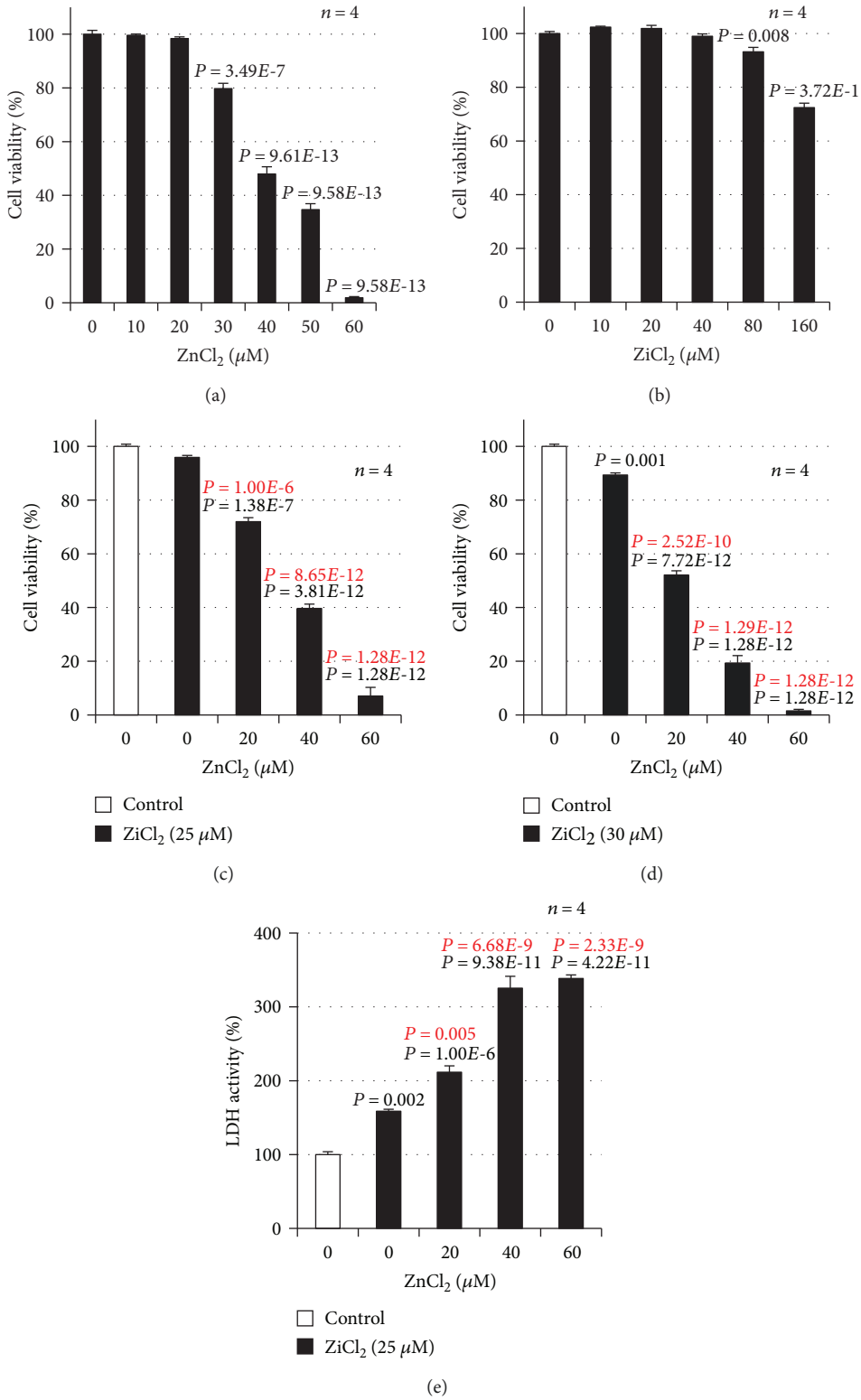

Figure 1: GT1-7 cells (96-well culture plates at a density of 3×10^4 cells per well) were incubated with the indicated concentrations (μM) of $ZnCl_2$ (a) or $NiCl_2$ (b) for 24 h. GT1-7 cells (96-well culture plates at a density of 3×10^4 cells per well) were incubated with the indicated concentrations (μM) of $NiCl_2$ in the absence (control) or presence of $ZnCl_2$ (25 μM) for 24 h (c). Cell viability was determined using CellTiter-Glo® 2.0. Values represent mean ± S.E.M. P values are described in the figure when $P < 0.05$ (black: vs. control, red: vs. $ZnCl_2$ alone).

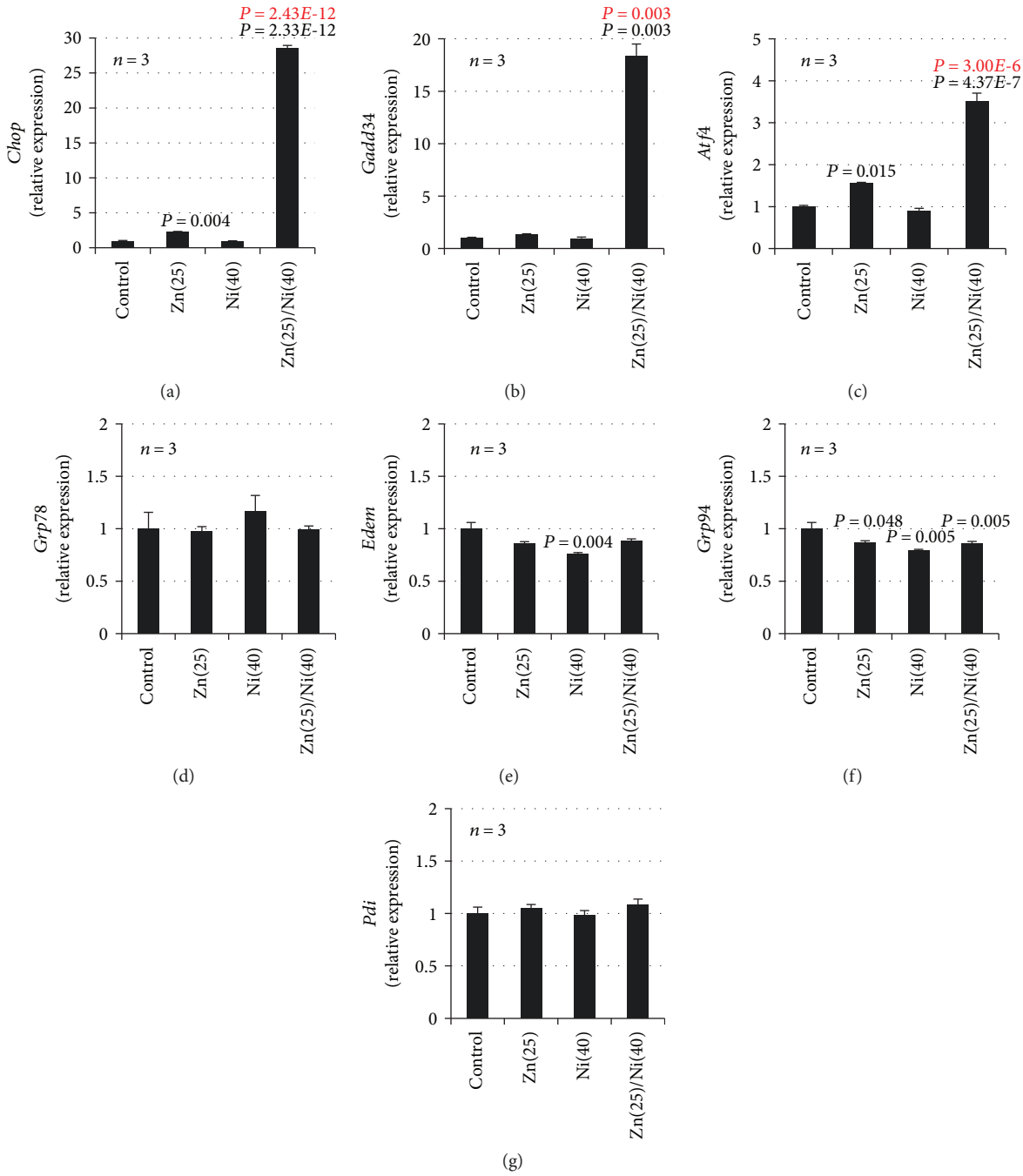

Figure 2: GT1-7 cells (6-well culture plates at a density of 7.5×10^5 cells per well) were incubated with $NiCl_2$ (Ni, 40 μM) in the absence (control) or presence of $ZnCl_2$ (Zn, 25 μM) for 4 h. Total RNA was extracted from GT1-7 cells and subjected to real-time RT-PCR using primer sets specific for each gene. Values were normalized to *Gapdh* and expressed relative to the control. Values represent mean ± S.E.M. *P* values are described in the figure when $P < 0.05$ (black: vs. control, red: vs. $ZnCl_2$ alone).

(25 μM) treatment induced the expression of *Chop* and activating transcription factor 4 (*Atf4*) mRNA (Figure 2). Moreover, Ni^{2+} treatment primed the expression of *Chop*, *Gadd34*, and *Atf4*; in particular, the relative expression of *Chop* was most significantly increased by cotreatment with Ni^{2+} and Zn^{2+}. The relative expression of *Chop* after cotreatment with Ni^{2+} and Zn^{2+} was 28.6 ± 0.3 – fold (mean ± S.E.M., $n = 3$), which was significantly increased compared with Zn^{2+} alone (2.3 ± 0.1 – fold). In contrast, other ER stress-related genes including glucose-regulated protein 78 (*Grp78*), ER degradation-enhancing α-mannosidase-like protein (*Edem*), glucose-regulated protein 94 (*GrpP94*), and protein disulfide isomerase (*Pdi*) were not increased in this experimental condition. Ni^{2+} treatment alone did not increase expression of these genes (Figure 2). Next, we used Western blotting analysis to quantify the amount of CHOP protein.

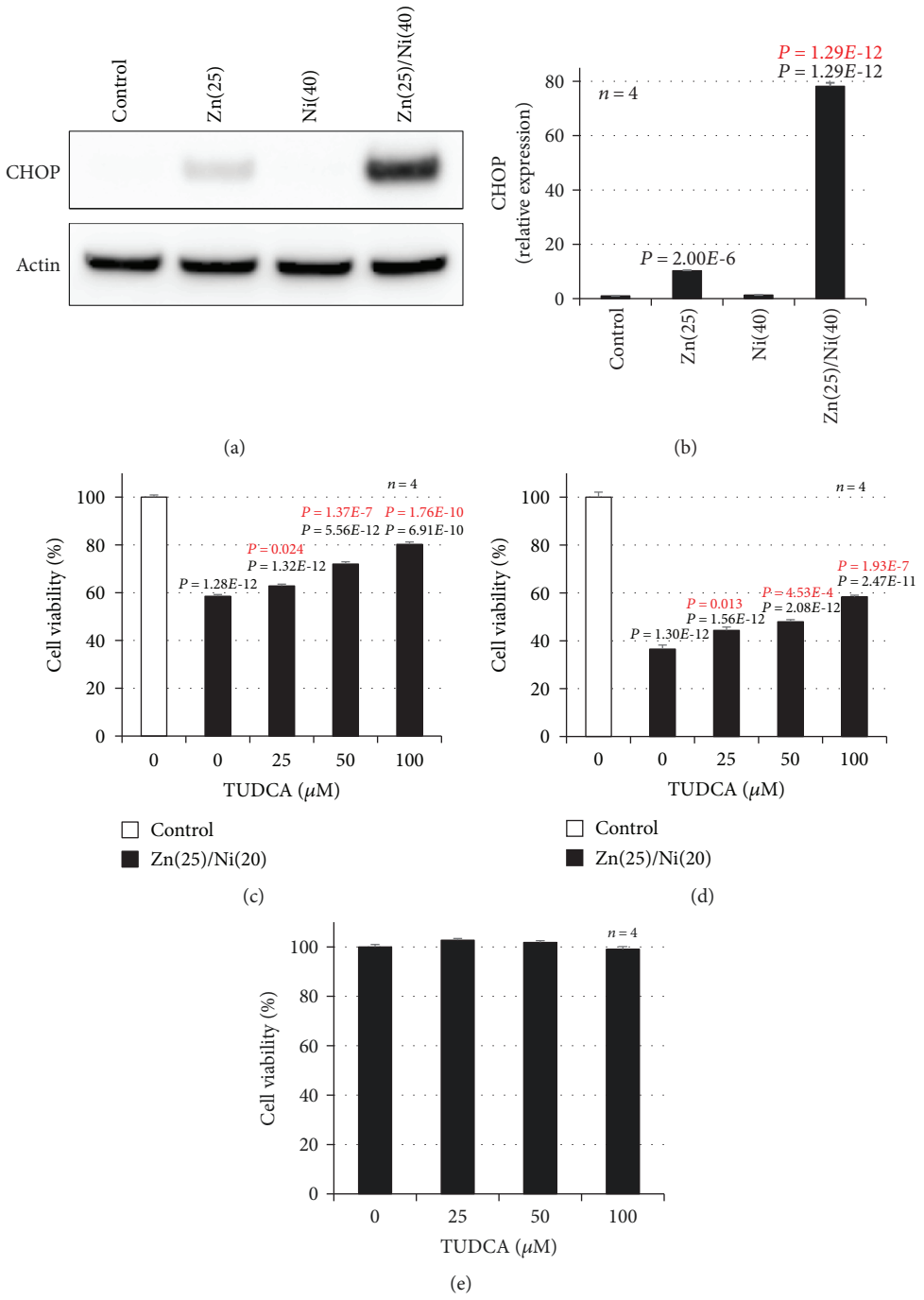

Figure 3: GT1-7 cells (6-well culture plates at a density of 7.5×10^5 cells per well) were incubated with $NiCl_2$ (Ni, 40 μM) in the absence (control) or presence of $ZnCl_2$ (Zn, 25 μM) for 7 h. Whole-cell extracts were analyzed by immunoblotting with an antibody against CHOP or actin (a). Band intensity was determined using ImageJ software (b). GT1-7 cells (96-well culture plates at a density of 3×10^4 cells per well) were pretreated with the indicated concentrations (μM) of TUDCA just before Ni^{2+}/Zn^{2+} treatment. Next, GT1-7 cells were incubated in the absence (control) or presence of $NiCl_2$ (20 or 40 μM) and $ZnCl_2$ (25 μM) for 24 h (c, d). GT1-7 cells (96-well culture plates at a density of 3×10^4 cells per well) were treated with the indicated concentrations of TUDCA for 24 h (e). Cell viability was determined using CellTiter-Glo® 2.0 (c–e). Values represent mean ± S.E.M. P values are described in the figure when $P < 0.05$: (black: control, red: vs. $ZnCl_2$ alone (b)) or (black: vs. control, red: vs. Zn(25)/Ni(20 or 40) (c, d)).

As shown in Figure 3(a), we found significantly increased amounts of CHOP protein after cotreatment with Ni^{2+} and Zn^{2+} (78.2 ± 1.3 – fold), compared with Zn^{2+} alone (10.3 ± 0.2 – fold). Ni^{2+} treatment alone did not increase the expression of CHOP protein (Figure 3(b)). Furthermore, we examined whether the ER stress inhibitor, TUDCA, attenuates Ni^{2+}/Zn^{2+}-induced neurotoxicity. As shown in Figures 3(c) and 3(d), TUDCA significantly attenuated Ni^{2+}/Zn^{2+}-induced neurotoxicity in GT1-7 cells in a dose-dependent manner. For example, the viability of cells

exposed to Ni^{2+}/Zn^{2+} (20 μM/25 μM) or Ni^{2+}/Zn^{2+} plus TUDCA (100 μM) was 58.5% ± 0.7% or 80.3% ± 1.0% (mean ± S.E.M., $n = 4$), respectively. Treatment with TUDCA alone did not affect the viability of GT1-7 cells (Figure 3(e)). These results suggest that Ni^{2+} enhanced Zn^{2+}-induced neurotoxicity by priming the ER stress response.

3.3. Activation of Oxidative Stress by Cotreatment with $NiCl_2$ and $ZnCl_2$. We next examined the involvement of oxidative stress on Ni^{2+}/Zn^{2+}-induced neurotoxicity or the ER stress response. As shown in Supplementary Figure S1A, cotreatment with Ni^{2+} and Zn^{2+} induced ROS production. In contrast, Ni^{2+} or Zn^{2+} treatment did not always induce ROS production. Moreover, Ni^{2+}/Zn^{2+} treatment induced the expression of oxidative stress-related genes, as indicated by increases in *hypoxia-inducible factor* (*Hif*)*1α*, *nuclear factor-erythroid 2-related factor 2* (*Nrf2*), *heme oxygenase 1* (*Ho1*), and *glutathione S-transferase m1* (*Gstm1*) mRNA levels. In contrast, Ni^{2+} or Zn^{2+} treatment did not increase expression of these genes (Supplementary Figure S1B). Thus, we examined the effect of N-acetylcysteine, an antioxidative compound, on Ni^{2+}/Zn^{2+}-induced neurotoxicity. As shown in Supplementary Figure S1C, N-acetylcysteine significantly attenuated Ni^{2+}/Zn^{2+}-induced neurotoxicity in GT1-7 cells in a dose-dependent manner. The viability of cells exposed to Ni^{2+}/Zn^{2+} (40 μM/25 μM) or Ni^{2+}/Zn^{2+} plus N-acetylcysteine (250 μM) was 20.8% ± 6.5% or 71.5% ± 1.7% (mean ± S.E.M., $n = 4$), respectively (Supplementary Figure S1C). Treatment with only N-acetylcysteine did not affect the viability of GT1-7 cells (Supplementary Figure S1D). Furthermore, N-acetylcysteine (250 μM) reduced the amount of CHOP protein induced by Ni^{2+}/Zn^{2+} (40 μM/25 μM) treatment (Supplementary Figure S1E and S1F). These results suggested that Ni^{2+}/Zn^{2+}-induced ER stress responses were mediated by upregulating ROS production.

3.4. Effect of Carnosine on Cu^{2+}/Zn^{2+}-Induced Neurotoxicity and the ER Stress Response. Carnosine (β-alanyl-L-histidine) is a small dipeptide with numerous activities, including antioxidant effects, proton buffering capacity, and inhibitory effects on protein carbonylation [24, 25]. Although we found previously that carnosine protected against Zn^{2+}-induced neurotoxicity [10], we have not studied the effect of carnosine on neuronal cell death induced by cotreatment with Zn^{2+} and other metals. Thus, we examined the effect of carnosine on Ni^{2+}/Zn^{2+}-induced neurotoxicity and the ER stress response in GT1-7 cells. The concentration of the chosen carnosine was according to a previous report [10]. As shown in Figures 4(a) and 4(b), cotreatment of GT1-7 cells with $NiCl_2$ (20 or 40 μM) and $ZnCl_2$ (25 μM) induced neurotoxicity with cell viabilities of 48.5% ± 0.7% and 25.5% ± 0.9% (mean ± S.E.M., $n = 4$) of the control, respectively. In contrast, carnosine significantly attenuated Ni^{2+}/Zn^{2+}-induced neurotoxicity in GT1-7 cells in a dose-dependent manner. The viability of cells exposed to Ni^{2+}/Zn^{2+} (20 μM/25 μM) plus carnosine (1, 2, and 4 mM) was 55.2% ± 0.7%, 61.6% ± 2.3%, and 70.0% ± 3.3% (mean ± S.E.M., $n = 4$), respectively, (Figure 4(a)). The viability of cells exposed to Ni^{2+}/Zn^{2+} (40 μM/25 μM) plus carnosine (1, 2, and 4 mM) was 32.0% ± 4.9%, 39.9% ± 2.2%, and 51.1% ± 1.1% (mean ± S.E.M., $n = 4$), respectively, (Figure 4(b)). Treatment with carnosine alone did not affect the viability of GT1-7 cells (Figure 4(c)). Next, we examined the effect of carnosine on Ni^{2+}/Zn^{2+}-induced ER stress responses. As shown in Figure 5, cotreatment of GT1-7 cells with Ni^2 and Zn^{2+} increased the expression of *Chop*, *Gadd34*, and *Atf4*. In contrast, carnosine treatment significantly decreased the expression of these genes in a dose-dependent manner (Figure 5). Furthermore, the amount of CHOP protein observed after cotreatment with Ni^{2+} and Zn^{2+} was reduced by carnosine treatment (Figures 6(a) and 6(b)). These results suggest that carnosine significantly attenuated Ni^2 and Zn^{2+}-induced neuronal cell death by decreasing the ER stress response. Moreover, carnosine may decrease not just neuronal cell death induced by Zn^{2+} alone but also neuronal cell death induced by Zn^{2+} and other metals.

4. Discussion

Zn is the second most abundant trace metal and has essential roles in many physiological functions such as the immune system, cell cycle, DNA replication, and protein synthesis. Moreover, Zn is a well-known cofactor for over 300 enzymes and metalloproteins [1]. Deprivation of Zn in humans causes atrophy, learning disorders, delayed physical development, taste and olfaction disorders, and immune system diseases [2, 3]. Thus, Zn supplementation reportedly exerts therapeutic effects against various diseases such as cirrhosis, ulcerative colitis, and asthma [26–28]. In the brain, Zn^{2+} accumulates in the synaptic vesicles of excitatory synapses and is released during neuronal excitation [29, 30]. Although Zn has essential roles in the brain and neuroprotective roles in normal neuronal function, excessively high concentrations of Zn are neurotoxic [6–8]. Although the amount of Zn^{2+} released from synaptic vesicles still needs confirmation, several studies estimate the concentration of Zn^{2+} in the synaptic cleft to be 1–100 μM [31–34]. Therefore, Zn^{2+} may act on neuronal cells at the concentration used in this study (25 μM). Ni, a component of enzymes such as urease and hydrogenase, is a heavy metal widely used in industrial applications [35]. A previous study showed that nickel concentration in the brain is estimated to be 0.34–1.11 μmol/kg tissue [36]. Compared with this report, we consider that the nickel concentration used in our study is slightly higher. In contrast, environmental and occupational exposure to Ni has been reported to result in an increased nickel concentration within the body [37]. Cempel and Janicka reported that oral administration of Ni increases the amount of Ni in the rat brain by approximately 7-fold [38]. Moreover, intranasal instillation of Ni reportedly reached the brain of rats via olfactory neurons [39]. Therefore, we believe that the enhanced activity of Zn^{2+} induced by Ni^{2+} in this study may also occur in the brain.

The ER stress response is important in the pathogenesis of several diseases, such as cancer, acute lung injury, and neurological disorders [40, 41]. ER stress induces the unfolded protein response, which can be distinguished by three ER stress sensors: protein kinase R-like ER kinase (PERK),

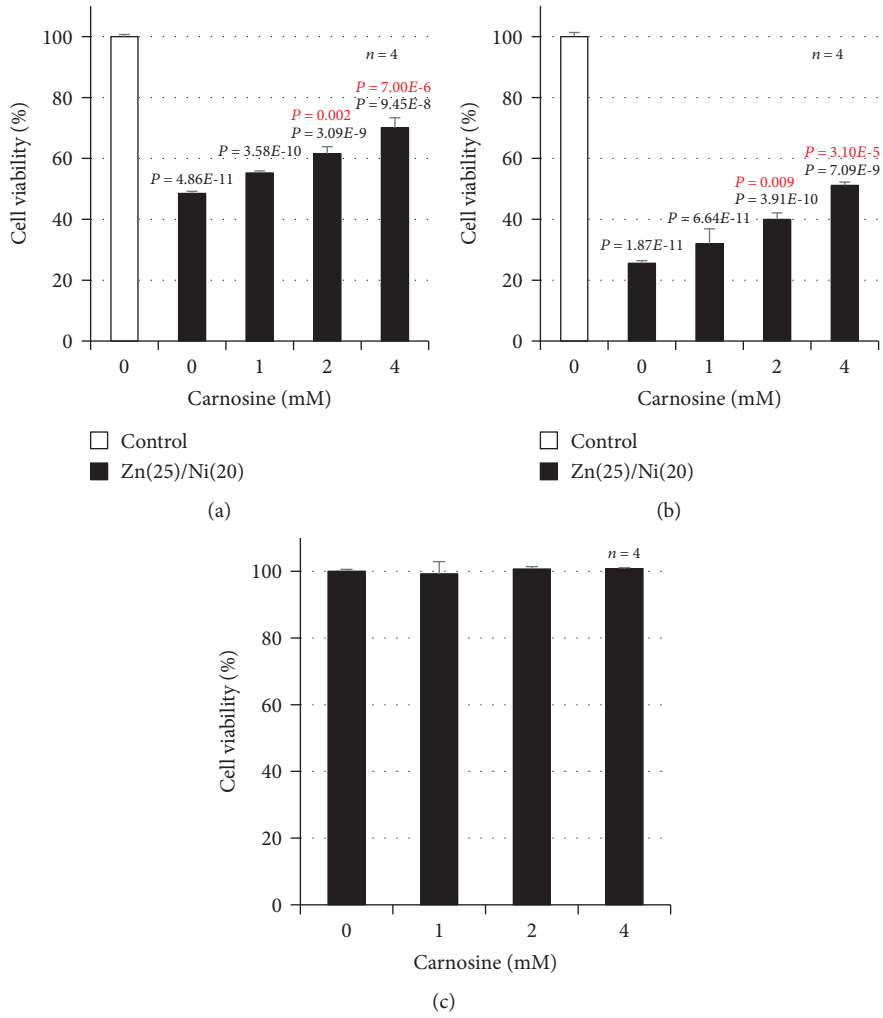

Figure 4: GT1-7 cells (96-well culture plates at a density of 3×10^4 cells per well) were pretreated with the indicated concentrations (mM) of carnosine just before Ni^{2+}/Zn^{2+} treatment. Next, GT1-7 cells were incubated in the absence (control) or presence of $NiCl_2$ (20 or 40 μM) and $ZnCl_2$ (25 μM) for 24 h (a, b). GT1-7 cells (96-well culture plates at a density of 3×10^4 cells per well) were treated with the indicated concentrations of carnosine for 24 h (c). Cell viability was determined using CellTiter-Glo® 2.0. Values represent mean ± S.E.M. P values are described in the figure when $P < 0.05$ (black: vs. control, red: vs. Zn(25)/Ni(20 or 40)).

inositol-requiring enzyme-1 (IRE1), and ATF6 [41]. Various signal transduction events are triggered by the activation of these sensors. For example, the α subunit of eukaryotic translation initiation factor 2 (eIF2) is phosphorylated by PERK, which affects the translation of ATF4 (a member of the ATF subfamily of the basic leucine zipper transcription factor superfamily). ATF4 activates the transcription of CHOP and GADD34. In contrast, IRE1 is phosphorylated and interacts with the adaptor protein tumor necrosis factor receptor-associated factor-2, which promotes JNK phosphorylation [40, 41]. As shown in Figure 2, Ni^{2+} treatment activated Zn^{2+}-induced increases in the expression of *Chop*, *Gadd34*, and *Atf4*. Hence, it is likely that the PERK/eIF2α/ATF4 pathway is activated by cotreatment with Ni^{2+} and Zn^{2+}.

However, we have been unable to determine the upstream mechanism of ER stress response induction. Thus, the mechanism by which Ni^{2+} treatment enhances Zn^{2+}-induced neuronal cell death needs clarification. As shown in Supplementary Figure S1, we suggest that ROS is one upstream mechanism of the ER stress response. As one line of evidence, bisphenol A (an endocrine-disrupting chemical) induced cellular apoptosis by activating the ROS-triggered PERK/eIF2α/CHOP pathway [42]. Moreover, hydrogen peroxide reportedly induced apoptosis by activating ER stress responses in SH-SY5Y cells [43]. Furthermore, luteolin-induced ER stress response (p-PERK/p-eIF2α/ATF4/CHOP/caspase-12 pathway) was reversed in glioblastoma cells by treatment with the antioxidant N-acetylcysteine [44]. In contrast, nickel chloride exposure induced behavioral disorders, altered neuronal microarchitecture, and induced neuronal cell death by upregulating intracellular ROS [20, 45]. Considering our results and these reports, we predict that Ni^{2+} treatment enhances Zn^{2+}-induced ER stress responses by upregulating ROS production.

As shown in Figure 5, we investigated the effect of carnosine on Ni^{2+}/Zn^{2+}-induced neurotoxicity using hypothalamic neuronal GT1-7 cells. To our knowledge, this is the first evidence that carnosine decreases neuronal cell death

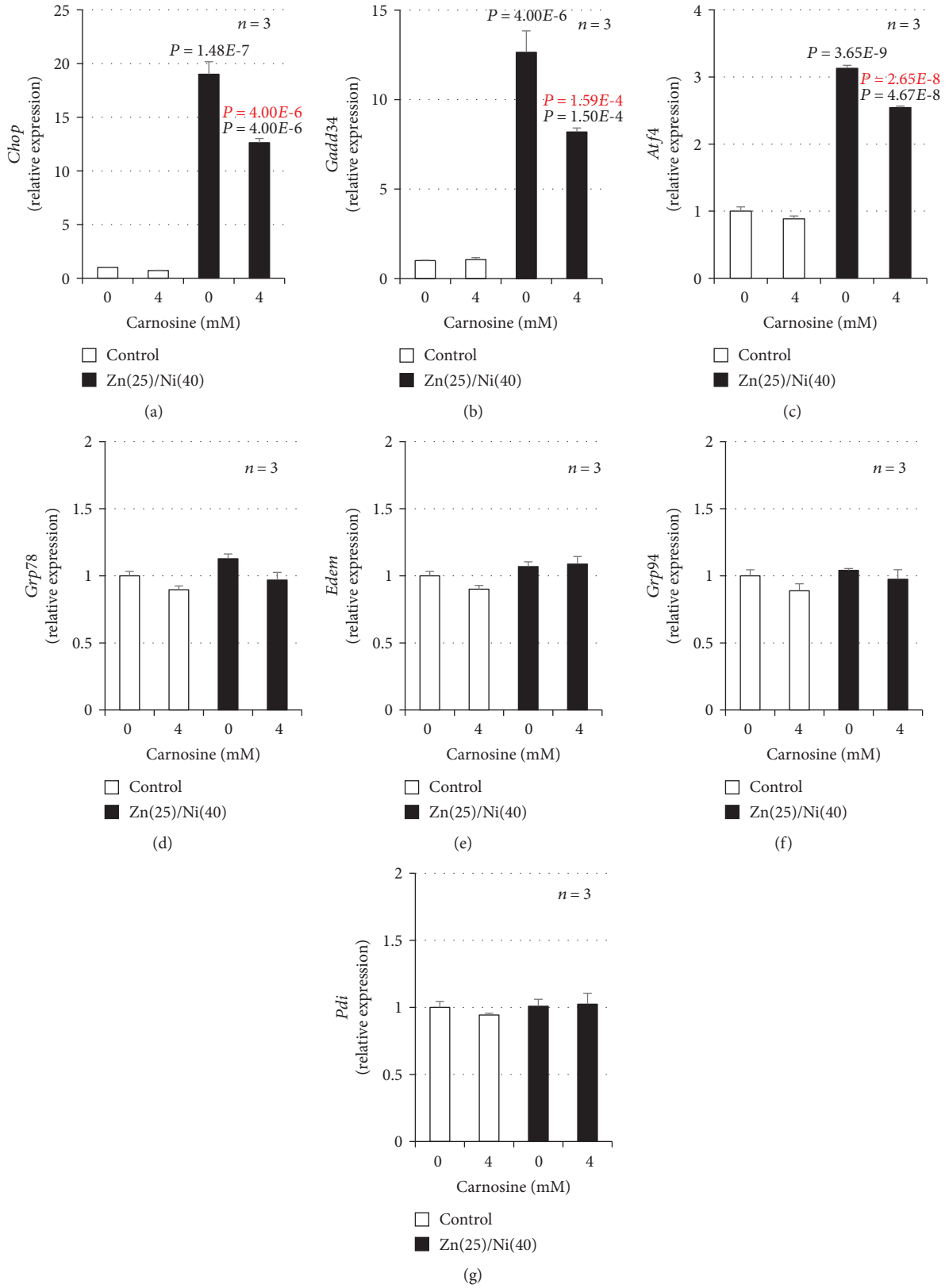

FIGURE 5: GT1-7 cells (6-well culture plates at a density of 7.5×10^5 cells per well) were pretreated with the indicated concentrations (mM) of carnosine just before Ni^{2+}/Zn^{2+} treatment. Next, GT1-7 cells were incubated in the absence (control) or presence of $NiCl_2$ (Ni, 40 μM) and $ZnCl_2$ (Zn, 25 μM) for 4 h. Total RNA was extracted and subjected to real-time RT-PCR using primer sets specific for each gene. Values were normalized to *Gapdh* and expressed relative to the control. Values represent mean ± S.E.M. *P* values are described in the figure when $P < 0.05$ (black: vs. control, red: vs. Zn(25)/Ni(40)).

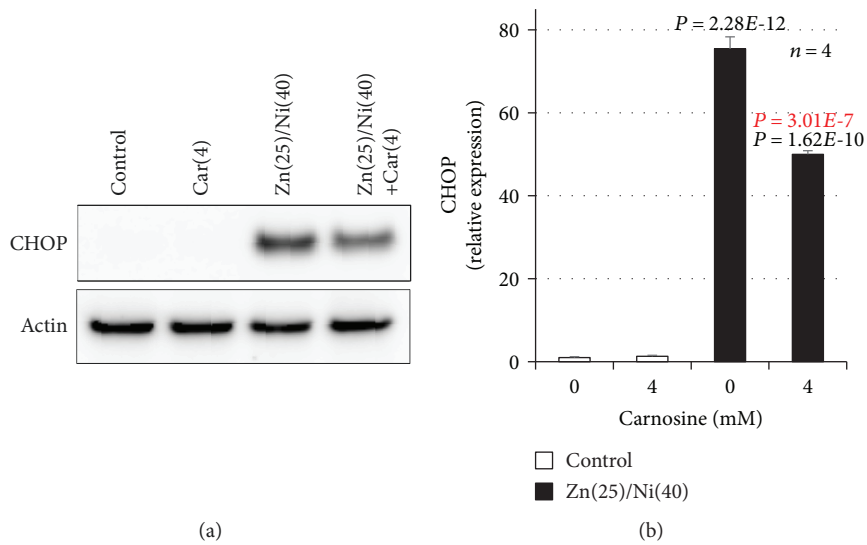

Figure 6: GT1-7 cells (6-well culture plates at a density of 7.5×10^5 cells per well) were pretreated with the indicated concentrations of carnosine just before Ni^{2+}/Zn^{2+} treatment. Next, GT1-7 cells were incubated in the absence (control) or presence of $NiCl_2$ (Ni, 40 μM) and $ZnCl_2$ (Zn, 25 μM) for 7 h. Whole-cell extracts were analyzed by immunoblotting with an antibody against CHOP or actin (a). The band intensity of CHOP was determined using ImageJ software (b). Values represent mean ± S.E.M. P values are described in the figure when $P < 0.05$ (black: vs. control, red: vs. Zn(25)/Ni(40)).

induced by the cotreatment of Zn^{2+} and other metal ions. Because Zn^{2+} and other metal ions often coexist *in vivo*, we believe that the results of this study are very important. As described above, carnosine is an endogenous dipeptide with various protective activities, such as antioxidant effects and metal ion chelation [24, 25]. Carnosine is abundant in the skeletal muscle, cerebral cortex, kidney, spleen, and plasma [25]. We previously reported that carnosine reduces Zn^{2+}-induced neuronal cell death by decreasing the ER stress response [10]. Moreover, we revealed that carnosine exerts its neuroprotective effect without metal ion chelation [10]. Notably, the antioxidant activity of carnosine has been described in many previous studies. For example, carnosine treatment activated antioxidative enzymes (Cu/Zn superoxide dismutase and glutathione peroxidase) in an experimental subarachnoid hemorrhage model [46]. Other groups showed that carnosine directly scavenges hydroxyl radicals [47, 48]. Furthermore, we reported that carnosine prevented lipopolysaccharide-induced ER stress response by suppressing LPS-dependent ROS production [23]. Considering these results, carnosine may counteract Ni and Zn-induced ER stress responses and neuronal cell death by exerting antioxidative effects. Therefore, we believe that examining the effect of other antioxidants in these models would be highly worthwhile.

The compounds 6-hydroxydopamine (6-OHDA, a neurotoxin) and rotenone (an electron transport system inhibitor), which are used to model Parkinson's disease, induce neuronal cell death and oxidative stress [49]. Several recent studies have investigated potential interactions between these compounds and trace metals on neurotoxicity. For example, Cruces-Sande et al. demonstrated that copper increases the capacity of 6-OHDA to generate oxidative stress, which may contribute to the destruction of dopaminergic neurons [50]. Another group reported that the cotreatment of iron and rotenone induced a redox imbalance (increased malondialdehyde and decreased glutathione) in the substantia nigra of rats [51]. Zn reportedly induces abnormal phosphorylation of tau by activating various phosphatases, and its phosphorylation is suggested to be involved in the development of Alzheimer's disease [9]. Therefore, we believe that it is important to examine the neurotoxicity induced both by interactions between metals and metals and by interactions between metals and causative substances of diseases, such as 6-OHDA or rotenone.

5. Conclusion

Synergistic neurotoxicity by Ni^{2+} and Zn^{2+} may cause neurological diseases such as vascular dementia, Alzheimer's disease, and Parkinson' s disease. In this study, we demonstrated that Ni^{2+} enhances Zn^{2+}-induced neurotoxicity by priming the ER stress response. Furthermore, carnosine was found to protect neuronal cells from Ni^{2+} and Zn^{2+}-dependent synergistic neurotoxicity by decreasing the ER stress response. In conclusion, compounds that decrease the ER stress response, such as carnosine, may be suitable for treating neurological diseases.

Abbreviations

ANOVA:	Analysis of variance
ATF:	Activating transcription factor
CHOP:	CCAAT-enhancer-binding protein homologous protein
Cu:	Copper
D-MEM/Ham's-F12:	Dulbecco's Modified Eagle's Medium/Ham's Nutrient Mixture F-12
EDEM:	ER degradation-enhancing α-mannosidase-like protein

eIF:	Eukaryotic translation initiation factor
ER:	Endoplasmic reticulum
Fe:	Iron
GADD34:	Growth arrest and DNA damage-inducible gene 34
Gapdh:	Glyceraldehyde-3-phosphate dehydrogenase
GRP:	Glucose-regulated protein
HRP:	Horseradish peroxidase
IRE1:	Inositol-requiring enzyme-1
LPS:	Lipopolysaccharide
Mn:	Manganese
Ni:	Nickel
6-OHDA:	6-Hydroxydopamine
PERK:	Protein kinase R-like ER kinase
PDI:	Protein disulfide isomerase
ROS:	Reactive oxygen species
Zn:	Zinc.

Data Availability

The data used to support the findings of this study are available from the corresponding author upon request.

Conflicts of Interest

The authors declare that they have no competing interests.

Authors' Contributions

K.T. and M. Kawahara were responsible for the study conception and design. K.T., M. Kasai., M.S., A.S., M. Kubota, and M. Kawahara were responsible for the acquisition, analysis, and/or interpretation of the data. K.T., M. Kasai., M.S., A.S., M. Kubota, and M. Kawahara were responsible for the drafting/revision of the work for intellectual content and context. K.T., M. Kasai., M.S., A.S., M. Kubota, and M. Kawahara gave final approval and have overall responsibility for the published work.

Acknowledgments

This research was supported by grants from The Research Foundation for Pharmaceutical Sciences and also in part by a Grant-in-Aid for Scientific Research from the Japan Society for the Promotion of Science (JSPS) (KAKENHI KIBAN (C) 18K06669). We thank the Edanz Group (www.edanzediting.com/ac) for editing a draft of this manuscript.

Supplementary Materials

Supplementary Figure S1: GT1-7 cells were incubated in the absence (control) or presence of $NiCl_2$ (Ni, 40 μM) and $ZnCl_2$ (Zn, 25 μM) for 4 h. Total RNA was extracted and subjected to real-time RT-PCR using primer sets specific for each gene. Values were normalized to Gapdh and expressed relative to the control (A). GT1-7 cells were pretreated with the indicated concentrations (μM) of N-acetylcysteine just before Ni^{2+}/Zn^{2+} treatment. Next, GT1-7 cells were incubated in the absence (control) or presence of $NiCl_2$ (40 μM) and $ZnCl_2$ (25 μM) for 24 h (B) or 7 h (D, E). GT1-7 cells were treated with the indicated concentrations of N-acetylcysteine for 24 h (C). Cell viability was determined using CellTiter-Glo® 2.0 (B, C). Whole-cell extracts were analyzed by immunoblotting with an antibody against CHOP or actin (D). The band intensity of CHOP was determined using ImageJ software (E). Values represent mean ± S.E.M. $^{*}P < 0.05$; ** or $^{\#\#}P < 0.01$ (* vs. control, $^{\#}$ vs. $ZnCl_2$ alone, Tukey's test) (A) or (* vs. control, $^{\#}$ vs. Zn(25)/Ni(20 or 40); Dunnett's test (B) or Tukey's test (E)). *(Supplementary Materials)*

References

[1] M. Hambidge, "Human zinc deficiency," *The Journal of Nutrition*, vol. 130, no. 5, pp. 1344S–1349S, 2000.

[2] A. S. Prasad, "Impact of the discovery of human zinc deficiency on health," *Journal of the American College of Nutrition*, vol. 28, no. 3, pp. 257–265, 2009.

[3] H. H. Sandstead, "Subclinical zinc deficiency impairs human brain function," *Journal of Trace Elements in Medicine and Biology*, vol. 26, no. 2-3, pp. 70–73, 2012.

[4] C. J. Frederickson, M. A. Klitenick, W. I. Manton, and J. B. Kirkpatrick, "Cytoarchitectonic distribution of zinc in the hippocampus of man and the rat," *Brain Research*, vol. 273, no. 2, pp. 335–339, 1983.

[5] J. M. Lee, M. C. Grabb, G. J. Zipfel, and D. W. Choi, "Brain tissue responses to ischemia," *Journal of Clinical Investigation*, vol. 106, no. 6, pp. 723–731, 2000.

[6] J. Y. Koh, S. W. Suh, B. J. Gwag, Y. Y. He, C. Y. Hsu, and D. W. Choi, "The role of zinc in selective neuronal death after transient global cerebral ischemia," *Science*, vol. 272, no. 5264, pp. 1013–1016, 1996.

[7] J. H. Weiss, S. L. Sensi, and J. Y. Koh, "Zn^{2+}: a novel ionic mediator of neural injury in brain disease," *Trends in Pharmacological Sciences*, vol. 21, no. 10, pp. 395–401, 2000.

[8] C. W. Shuttleworth and J. H. Weiss, "Zinc: new clues to diverse roles in brain ischemia," *Trends in Pharmacological Sciences*, vol. 32, no. 8, pp. 480–486, 2011.

[9] P. Wang and Z. Y. Wang, "Metal ions influx is a double edged sword for the pathogenesis of Alzheimer's disease," *Ageing Research Reviews*, vol. 35, pp. 265–290, 2017.

[10] D. Mizuno, K. Konoha-Mizuno, M. Mori et al., "Protective activity of carnosine and anserine against zinc-induced neurotoxicity: a possible treatment for vascular dementia," *Metallomics*, vol. 7, no. 8, pp. 1233–1239, 2015.

[11] K. I. Tanaka, M. Shimoda, V. T. G. Chuang et al., "Thioredoxin-albumin fusion protein prevents copper enhanced zinc-induced neurotoxicity via its antioxidative activity," *International Journal of Pharmaceutics*, vol. 535, no. 1-2, pp. 140–147, 2018.

[12] M. Kawahara, M. Kato-Negishi, and Y. Kuroda, "Pyruvate blocks zinc-induced neurotoxicity in immortalized hypothalamic neurons," *Cellular and molecular neurobiology*, vol. 22, no. 1, pp. 87–93, 2002.

[13] J. Sabine Becker, A. Matusch, C. Palm, D. Salber, K. A. Morton, and J. Susanne Becker, "Bioimaging of metals in brain tissue by laser ablation inductively coupled plasma mass spectrometry (LA-ICP-MS) and metallomics," *Metallomics*, vol. 2, no. 2, pp. 104–111, 2010.

[14] B. Bocca, G. Forte, F. Petrucci, O. Senofonte, N. Violante, and A. Alimonti, "Development of methods for the quantification of essential and toxic elements in human biomonitoring," *Annali-Istituto Superiore Di Sanita*, vol. 41, no. 2, pp. 165–170, 2005.

[15] N. D'Ambrosi and L. Rossi, "Copper at synapse: release, binding and modulation of neurotransmission," *Neurochemistry International*, vol. 90, pp. 36–45, 2015.

[16] C. M. Opazo, M. A. Greenough, and A. I. Bush, "Copper: from neurotransmission to neuroproteostasis," *Frontiers in Aging Neuroscience*, vol. 6, p. 143, 2014.

[17] A. Hopt, S. Korte, H. Fink et al., "Methods for studying synaptosomal copper release," *Journal of Neuroscience Methods*, vol. 128, no. 1-2, pp. 159–172, 2003.

[18] M. Aschner, "Manganese: brain transport and emerging research needs," *Environmental Health Perspectives*, vol. 108, Supplement 3, pp. 429–432, 2000.

[19] G. F. Kwakye, M. M. B. Paoliello, S. Mukhopadhyay, A. B. Bowman, and M. Aschner, "Manganese-induced parkinsonism and Parkinson's disease: shared and distinguishable features," *International Journal of Environmental Research and Public Health*, vol. 12, no. 7, pp. 7519–7540, 2015.

[20] M. D. He, S. C. Xu, Y. H. Lu et al., "L-Carnitine protects against nickel-induced neurotoxicity by maintaining mitochondrial function in neuro-2a cells," *Toxicology and Applied Pharmacology*, vol. 253, no. 1, pp. 38–44, 2011.

[21] K. I. Tanaka and M. Kawahara, "Copper enhances zinc-induced neurotoxicity and the endoplasmic reticulum stress response in a neuronal model of vascular dementia," *Frontiers in Neuroscience*, vol. 11, p. 58, 2017.

[22] K. I. Tanaka, M. Shimoda, and M. Kawahara, "Pyruvic acid prevents Cu^{2+}/Zn^{2+}-induced neurotoxicity by suppressing mitochondrial injury," *Biochemical and Biophysical Research Communications*, vol. 495, no. 1, pp. 1335–1341, 2018.

[23] K. I. Tanaka, T. Sugizaki, Y. Kanda, F. Tamura, T. Niino, and M. Kawahara, "Preventive effects of carnosine on lipopolysaccharide-induced lung injury," *Scientific Reports*, vol. 7, no. 1, article 42813, 2017.

[24] C. Sale, G. G. Artioli, B. Gualano, B. Saunders, R. M. Hobson, and R. C. Harris, "Carnosine: from exercise performance to health," *Amino Acids*, vol. 44, no. 6, pp. 1477–1491, 2013.

[25] A. A. Boldyrev, G. Aldini, and W. Derave, "Physiology and pathophysiology of carnosine," *Physiological Reviews*, vol. 93, no. 4, pp. 1803–1845, 2013.

[26] M. A. Biltagi, A. A. Baset, M. Bassiouny, M. A. Kasrawi, and M. Attia, "Omega-3 fatty acids, vitamin C and Zn supplementation in asthmatic children: a randomized self-controlled study," *Acta Paediatrica*, vol. 98, no. 4, pp. 737–742, 2009.

[27] J. Paz Matias, D. M. Costa e Silva, K. J. Climaco Cruz et al., "Effect of zinc supplementation on superoxide dismutase activity in patients with ulcerative rectocolitis," *Nutricion Hospitalaria*, vol. 31, no. 3, pp. 1434–1437, 2014.

[28] M. H. Somi, P. Rezaeifar, A. Ostad Rahimi, and B. Moshrefi, "Effects of low dose zinc supplementation on biochemical markers in non-alcoholic cirrhosis: a randomized clinical trial," *Archives of Iranian Medicine*, vol. 15, no. 8, pp. 472–476, 2012.

[29] S. Ueno, M. Tsukamoto, T. Hirano et al., "Mossy fiber Zn^{2+} spillover modulates heterosynaptic *N*-methyl-D-aspartate receptor activity in hippocampal CA3 circuits," *The Journal of Cell Biology*, vol. 158, no. 2, pp. 215–220, 2002.

[30] A. Takeda, H. Fujii, T. Minamino, and H. Tamano, "Intracellular Zn^{2+} signaling in cognition," *Journal of Neuroscience Research*, vol. 92, no. 7, pp. 819–824, 2014.

[31] A. R. Kay, "Imaging synaptic zinc: promises and perils," *Trends in Neurosciences*, vol. 29, no. 4, pp. 200–206, 2006.

[32] S. L. Sensi, L. M. T. Canzoniero, S. P. Yu et al., "Measurement of intracellular free zinc in living cortical neurons: routes of entry," *The Journal of Neuroscience*, vol. 17, no. 24, pp. 9554–9564, 1997.

[33] K. Vogt, J. Mellor, G. Tong, and R. Nicoll, "The actions of synaptically released zinc at hippocampal mossy fiber synapses," *Neuron*, vol. 26, no. 1, pp. 187–196, 2000.

[34] B. Zhang, M. Ren, F. S. Sheu, F. Watt, and A. Routtenberg, "Quantitative analysis of zinc in rat hippocampal mossy fibers by nuclear microscopy," *Neuroscience Research*, vol. 74, no. 1, pp. 17–24, 2012.

[35] R. K. Watt and P. W. Ludden, "Nickel-binding proteins," *Cellular and Molecular Life Sciences (CMLS)*, vol. 56, no. 7-8, pp. 604–625, 1999.

[36] W. N. Rezuke, J. A. Knight, and F. W. Sunderman Jr., "Reference values for nickel concentrations in human tissues and bile," *American Journal of Industrial Medicine*, vol. 11, no. 4, pp. 419–426, 1987.

[37] M. Gube, P. Brand, T. Schettgen et al., "Experimental exposure of healthy subjects with emissions from a gas metal arc welding process—part II: biomonitoring of chromium and nickel," *International Archives of Occupational and Environmental Health*, vol. 86, no. 1, pp. 31–37, 2013.

[38] M. Cempel and K. Janicka, "Distribution of nickel, zinc, and copper in rat organs after oral administration of nickel (II) chloride," *Biological Trace Element Research*, vol. 90, no. 1-3, pp. 215–226, 2002.

[39] J. Henriksson, J. Tallkvist, and H. Tjalve, "Uptake of nickel into the brain via olfactory neurons in rats," *Toxicology Letters*, vol. 91, no. 2, pp. 153–162, 1997.

[40] H. Y. Zhang, Z. G. Wang, X. H. Lu et al., "Endoplasmic reticulum stress: relevance and therapeutics in central nervous system diseases," *Molecular Neurobiology*, vol. 51, no. 3, pp. 1343–1352, 2015.

[41] J. Grootjans, A. Kaser, R. J. Kaufman, and R. S. Blumberg, "The unfolded protein response in immunity and inflammation," *Nature Reviews Immunology*, vol. 16, no. 8, pp. 469–484, 2016.

[42] L. Yin, Y. Dai, Z. Cui et al., "The regulation of cellular apoptosis by the ROS-triggered PERK/EIF2α/chop pathway plays a vital role in bisphenol A-induced male reproductive toxicity," *Toxicology and Applied Pharmacology*, vol. 314, pp. 98–108, 2017.

[43] J. Ye, Y. Han, X. Chen et al., "L-Carnitine attenuates H_2O_2-induced neuron apoptosis via inhibition of endoplasmic reticulum stress," *Neurochemistry International*, vol. 78, pp. 86–95, 2014.

[44] Q. Wang, H. Wang, Y. Jia, H. Pan, and H. Ding, "Luteolin induces apoptosis by ROS/ER stress and mitochondrial dysfunction in gliomablastoma," *Cancer Chemotherapy and Pharmacology*, vol. 79, no. 5, pp. 1031–1041, 2017.

[45] O. M. Ijomone, S. O. Okori, O. K. Ijomone, and A. P. Ebokaiwe, "Sub-acute nickel exposure impairs behavior, alters neuronal microarchitecture, and induces oxidative stress in rats' brain," *Drug and Chemical Toxicology*, vol. 41, no. 4, pp. 377–384, 2018.

[46] Z. Y. Zhang, B. L. Sun, M. F. Yang, D. W. Li, J. Fang, and S. Zhang, "Carnosine attenuates early brain injury through its antioxidative and anti-apoptotic effects in a rat experimental subarachnoid hemorrhage model," *Cellular and Molecular Neurobiology*, vol. 35, no. 2, pp. 147–157, 2015.

[47] M. Tamba and A. Torreggiani, "Hydroxyl radical scavenging by carnosine and Cu(II)-carnosine complexes: a pulse-radiolysis and spectroscopic study," *International Journal of Radiation Biology*, vol. 75, no. 9, pp. 1177–1188, 1999.

[48] M. A. Babizhayev, M. C. Seguin, J. Gueyne, R. P. Evstigneeva, E. A. Ageyeva, and G. A. Zheltukhina, "L-Carnosine (β-alanyl-L-histidine) and carcinine (β-alanylhistamine) act as natural antioxidants with hydroxyl-radical-scavenging and lipid-peroxidase activities," *Biochemical Journal*, vol. 304, no. 2, pp. 509–516, 1994.

[49] J. Bove and C. Perier, "Neurotoxin-based models of Parkinson's disease," *Neuroscience*, vol. 211, pp. 51–76, 2012.

[50] A. Cruces-Sande, E. Mendez-Alvarez, and R. Soto-Otero, "Copper increases the ability of 6-hydroxydopamine to generate oxidative stress and the ability of ascorbate and glutathione to potentiate this effect: potential implications in Parkinson's disease," *Journal of Neurochemistry*, vol. 141, no. 5, pp. 738–749, 2017.

[51] L. Yu, X. Wang, H. Chen, Z. Yan, M. Wang, and Y. Li, "Neurochemical and behavior deficits in rats with iron and rotenone co-treatment: role of redox imbalance and neuroprotection by biochanin A," *Frontiers in Neuroscience*, vol. 11, p. 657, 2017.

Hindawi
Oxidative Medicine and Cellular Longevity
Volume 2019, Article ID 1712323, 9 pages
https://doi.org/10.1155/2019/1712323

Research Article

Aberrations in Oxidative Stress Markers in Amyotrophic Lateral Sclerosis: A Systematic Review and Meta-Analysis

Zihao Wang, Zhile Bai, Xiaoyan Qin, and Yong Cheng

Key Laboratory of Ethnomedicine for Ministry of Education, Center on Translational Neuroscience, College of Life and Environmental Sciences, Minzu University of China, Beijing 100081, China

Correspondence should be addressed to Xiaoyan Qin; bjqinxiaoyan@muc.edu.cn and Yong Cheng; yongcheng@muc.edu.cn

Received 1 March 2019; Accepted 20 May 2019; Published 9 June 2019

Guest Editor: Giovanna Cenini

Oxidative stress has been reported to be involved in the onset and development of amyotrophic lateral sclerosis (ALS). Data from clinical studies have highlighted increased peripheral blood oxidative stress markers in patients with ALS, but results are inconsistent. Therefore, we quantitatively pooled data on levels of blood oxidative stress markers in ALS patients from the literature using a meta-analytic technique. A systematic search was performed on PubMed and Web of Science, and we included studies analyzing blood oxidative stress marker levels in patients with ALS and normal controls. We included 41 studies with 4,588 ALS patients and 6,344 control subjects, and 15 oxidative stress marker levels were subjected to random-effects meta-analysis. The results demonstrated that malondialdehyde (Hedges' g, 1.168; 95% CI, 0.812 to 1.523; $P < 0.001$), 8-hydroxyguanosine (Hedges' g, 2.194; 95% CI, 0.554 to 3.835; $P = 0.009$), and Advanced Oxidation Protein Product (Hedges' g, 0.555; 95% CI, 0.317 to 0.792; $P < 0.001$) levels were significantly increased in patients with ALS when compared with control subjects. Uric acid (Hedges' g, -0.798; 95% CI, -1.117 to -0.479; $P < 0.001$) and glutathione (Hedges' g, -1.636; 95% CI, -3.020 to -0.252; $P = 0.02$) levels were significantly reduced in ALS patients. In contrast, blood Cu, superoxide dismutase, glutathione peroxidase, ceruloplasmin, triglycerides, total cholesterol, low-density lipoprotein, high-density lipoprotein, coenzyme-Q10, and transferrin levels were not significantly different between cases and controls. Taken together, our results showed significantly increased blood levels of 8-hydroxyguanosine, malondialdehyde, and Advanced Oxidation Protein Product and decreased glutathione and uric acid levels in the peripheral blood of ALS patients. This meta-analysis helps to clarify the oxidative stress marker profile in ALS patients, supporting the hypothesis that oxidative stress is a central component underpinning ALS pathogenesis.

1. Introduction

Amyotrophic lateral sclerosis (ALS) is a devastating neurodegenerative disease caused by cell death of both upper and lower motor neurons [1]. It is known that 90-95% of cases are sporadic and the remaining 5-10% of cases are due to genetic predisposition [2]. The onset of ALS usually begins at the age of 50 years old for genetically inherited cases and at the age of 60 years old for sporadic cases, although the disease can start at any age [2]. It is estimated that two to three people out of 100,000 are affected by ALS in the United States and Europe every year [3, 4], while the incidence of the disease in the rest of the world remains largely unknown. Due to the poorly understood etiology of ALS, there is no effective treatment for the disease, and most patients survive between 2 to 4 years after diagnosis [5]. FDA has approved two drugs (riluzole and edaravone) for the treatment of ALS, and riluzole is reported to increase the life expectancy of patients by 2 to 3 months [6]. Therefore, it is critical to elucidate the etiology of ALS to facilitate the development of novel therapies for this devastating disease.

Although little is known regarding the cause of ALS, accumulating evidence suggests that increased inflammatory responses and oxidative stress alongside glial cell dysfunction play crucial roles in disease pathogenesis; this is supported by clinical studies showing infiltration of immune cells and heightened inflammatory cytokine profiles in the central nervous system of ALS patients [7, 8]. Although cytokine data

are inconsistent across studies, a meta-analysis by Chen et al. reported that granulocyte-colony stimulating factor, interleukin-2 (IL-2), IL-15, IL-17, monocyte chemotactic protein-1, macrophage inflammatory protein-1α, tumor necrosis factor-α (TNF-α), and vascular endothelial growth factor levels in the cerebrospinal fluid were significantly elevated in patients with ALS when compared with controls [9]. Another meta-analysis performed by our group including 25 studies clarified the peripheral blood inflammatory cytokine profile in ALS, which revealed elevated blood TNF-α, TNF receptor 1, IL-6, IL-1β, IL-8, and vascular endothelial growth factor levels in patients with ALS relative to control subjects [10]. In addition, a substantial number of clinical studies have analyzed oxidative stress markers in ALS and demonstrated that levels of prooxidative stress markers, malondialdehyde (MDA) and 8-hydroxyguanosine (8-OHdG) were increased in the peripheral blood of ALS patients [11, 12]. In contrast, decreased antioxidant glutathione and uric acid levels were observed in ALS patients [13, 14]. However, other studies have reported unaltered levels of antioxidants in patients with ALS compared to controls [15, 16]. Due to the heterogeneity of the clinical data on oxidative stress markers, the profile of oxidative stress markers in ALS patients remains unclear.

To better understand the etiology of ALS and potentially use oxidative stress markers for the diagnosis and prognosis of ALS patients, we reviewed PubMed and Web of Science systematically and pooled the data from the included studies to clarify the oxidative stress marker profile in patients with ALS.

2. Materials and Methods

This systematic review and meta-analysis was performed according to the instructions that are recommended by the PRISMA statement (Preferred Reporting Items for Systematic Reviews and Meta-Analysis) [17].

2.1. Literature Search. Two independent investigators manually reviewed English-language articles on PubMed and Web of Science from May 2018 to September 2018. The search terms for the systematic review were the following: (oxidative stress or catalase or hydroxyguanosine or malondialdehyde or uric acid or ceruloplasmin or glutathione or transferrin or low density lipoprotein or copper or cholesterol) and amyotrophic lateral sclerosis. We included original articles that reported peripheral blood levels of oxidative stress markers in ALS patients and control subjects.

2.2. Data Extraction. We extracted sample size, mean oxidative stress marker concentrations, P values, and standard deviation (s.d.) as the primary outcomes for this meta-analysis. We also extracted additional data on age, gender (proportion of males), publication year, sampling source, disease duration, and diagnosis of potential moderator analyses. The demographic and clinical variables of the included studies in this meta-analysis are presented in Supplementary Table (available here).

2.3. Statistical Analysis. The Comprehensive Meta-Analysis Version 2 software (Biostat, Englewood, NJ, USA) was used to pool the oxidative stress marker data on ALS patients. The sample size, mean oxidative stress marker concentration, and s.d. were primarily used to generate the effective size (ES). Sample size and P values were used to generate ES if oxidative stress marker concentration data were not available. An ES was calculated as the standardized mean difference in oxidative stress marker concentrations between cases and controls and then converted to Hedge's g which provides ES adjustment for sample size [18]. The 95% confidence interval (95% CI) was used to estimate the statistical significance of the pooled ES. We performed random-effects meta-analysis for this study because we estimated that the true ES would be affected by between-study and within-study variations [19]. We also performed sensitivity analysis by removing one study at a time to evaluate whether the statistical significance between cases and controls for oxidative stress marker concentrations was influenced by a single study.

The statistical difference of between-study heterogeneity was evaluated using the Cochran Q test [20], whereby statistical significance was set at P value < 0.1. The impact of between-study heterogeneity was evaluated by the I^2 index, and I^2 of 0.25, 0.50, and 0.75 suggested small, medium, and high levels of heterogeneity, respectively. We then used unrestricted maximum-likelihood random-effects metaregressions of ESs to analyze whether age, gender, or publication year had moderating effects on the outcomes of the meta-analysis. The publication bias for the included studies in this meta-analysis was determined by Egger's test [21], which assesses the degree of funnel plot asymmetry. The statistical significance of this meta-analysis was set at P value < 0.05 unless stated otherwise.

3. Results

Our initial search with the keywords produced 2,120 records from PubMed and 2,162 records from Web of Science. After screening the titles and abstracts of the records, 146 articles were selected for full-text scrutiny. Of the 146 studies, 105 studies were excluded due to the following reasons: no necessary data ($n = 77$); without a control group ($n = 8$); oxidative stress markers were analyzed in less than two studies ($n = 7$); studies were single case reports ($n = 4$); studies were review articles ($n = 5$); or data overlapped with other studies ($n = 4$). A final total of 41 articles with 4,588 ALS patients and 6,344 controls were included in this meta-analysis [11–16, 22–56] (for the flowchart, see Figure 1).

3.1. Main Associations of Blood Oxidative Stress Markers with ALS. Results from the meta-analysis showed that blood MDA (Hedges' g, 1.168; 95% CI, 0.812 to 1.523; $P < 0.001$), 8-OhDG (Hedges' g, 2.194; 95% CI, 0.554 to 3.835; $P = 0.009$), and Advanced Oxidation Protein Product (AOPP, Hedges' g, 0.555; 95% CI, 0.317 to 0.792; $P < 0.001$) levels were significantly elevated in patients with ALS when compared with controls, whereas blood uric acid (Hedges' g, -0.798; 95% CI, -1.117 to -0.479; $P < 0.001$) and glutathione

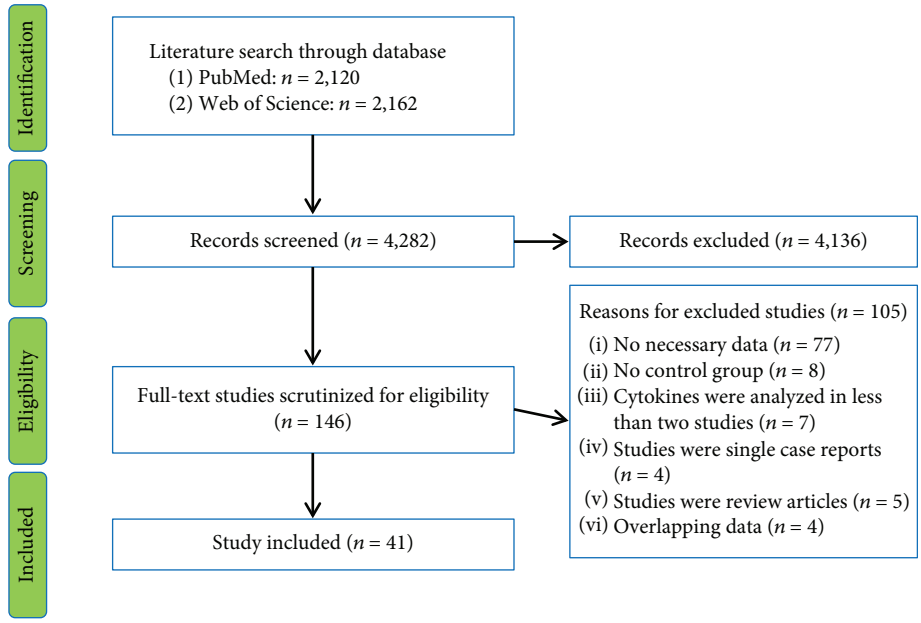

Figure 1: PRISMA flowchart of the literature search.

(Hedges' g, -1.636; 95% CI, -3.020 to -0.252; $P = 0.02$) levels were significantly decreased in ALS patients (Figures 2 and 3 and Table 1). In addition, we did not observe significant differences between ALS patients and controls for blood Cu, superoxide dismutase (SOD), glutathione peroxidase, coenzyme-Q10 (Co-Q10), ceruloplasmin, total cholesterol, triglycerides, high-density lipoprotein (HDL), low-density lipoprotein (LDL), and transferrin levels (Table 1).

3.2. Investigation of Heterogeneity. For the fifteen oxidative stress markers analyzed in the meta-analysis, AOPP and ceruloplasmin did not show between-study heterogeneity. MDA showed small levels of between-study heterogeneity, Co-Q10 showed moderate levels of between-study heterogeneity, and high levels of heterogeneity among studies were found for the other eleven markers (Table 1).

We next explored whether potential moderators accounted for the heterogeneity for the ALS-associated five oxidative stress markers. Given that blood MDA and AOPP showed low levels of between-study heterogeneity, and due to the limited number of studies with small size analyzing 8-OHdG and glutathione levels, we performed metaregression and subgroup analyses on uric acid. As shown in the Supplementary Table, the information on disease duration of ALS patients was limited. We therefore conducted metaregression analyses according to age, gender, and publication year. Metaregression analyses suggested that publication year, gender, and age did not significantly affect the results of the meta-analysis ($P > 0.05$ in all analyses).

Next, we performed subgroup analyses based on the sampling source. Uric acid levels were reduced both in the serum (Hedges' $g = -0.810$, 95%CI = −1.190 to − 0.431, $P < 0.001$) and the plasma (Hedges' $g = -0.764$, 95%CI = −1.380 to − 0.148, $P = 0.015$) of ALS patients when compared with those of the controls. However, between-study heterogeneity was increased for the serum studies ($Q = 53.542$; df = 4; $I^2 = 92.529$; $P < 0.001$) but reduced for the plasma studies ($Q = 2.478$; df = 1; $I^2 = 59.643$; $P = 0.115$).

Furthermore, we performed sensitivity analysis and showed that the significant association between blood uric acid and ALS was not influenced by any individual study.

Inspection of funnel plots visually indicated no publication bias for studies analyzing uric acid or MDA levels in ALS patients (Figure 4); these were confirmed by the Egger test (Table 1, $P > 0.1$). However, the funnel plot suggested there may be publication bias for studies analyzing glutathione levels in ALS patients (Figure 4). Further, the Egger test suggested a trend for publication bias for glutathione (Table 1, $P = 0.061$). To analyze the effect of potential publication bias, we used the classic fail-safe N[18] to compute the number of missing studies (with mean effect of zero) that would require to bring the P value above 0.05 for glutathione, and the analysis showed that 30 studies would need to be added to generate a nonsignificant association between glutathione and ALS, suggesting that potential publication bias is unlikely to significantly affect the positive outcome of the present study. Due to the limited number of studies, we were unable to perform publication bias analysis for 8-OHdG and AOPP.

4. Discussion

This meta-analysis included 41 studies with 4,588 ALS patients and 6,344 control individuals analyzing 15 oxidative stress markers from the blood. The results suggest that MDA (the important end product for lipid peroxidation), 8-OhdG (a marker for DNA damage), and AOPP were significantly elevated in the blood of ALS patients when compared with control individuals. In addition, we found that the levels of antioxidant glutathione and uric acid were significantly

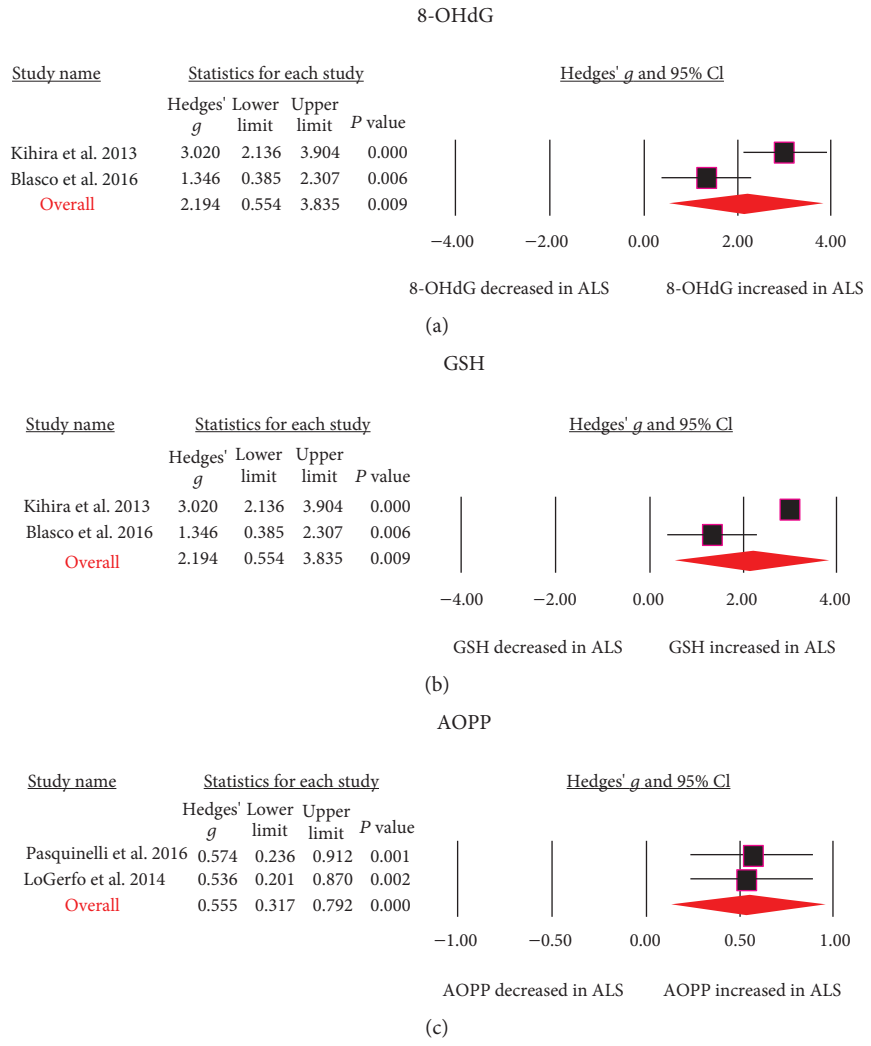

Figure 2: Studies of blood 8-OHdG, GSH, and AOPP in amyotrophic lateral sclerosis. Forest plot displaying random-effects meta-analysis results of the association between 8-OHdG (a), GSH (b), AOPP (c), and amyotrophic lateral sclerosis. GSH: glutathione; AOPP: Advanced Oxidation Protein Product; 8-OHdG: 8-hydroxyguanosine.

downregulated in patients with ALS. However, other oxidative stress markers including Cu, SOD, glutathione peroxidase, ceruloplasmin, triglycerides, total cholesterol, LDL, HDL, Co-Q10, and transferrin were not significantly associated with ALS. For the five dysregulated oxidative stress markers in ALS patients, the results associated with ESs of 8-OHdG, MDA, and GSH were large, and the ESs were medium to large for AOPP and uric acid. Sensitivity analysis indicated that no individual study influenced the significantly decreased blood uric acid levels in ALS patients, and no publication bias risks were observed for studies analyzing uric acid and MDA concentrations as determined by funnel plots and the Egger test, indicating the robustness of the results from our present study.

Although our study is the first to use a meta-analytic technique to clarify the oxidative stress marker profile in patients with ALS, it is unclear whether oxidative stress has causal effect for ALS onset and/or development. However, the important role of oxidative stress in the pathogenesis of ALS is supported by the fact that the mutations in the gene encoding the cytosolic antioxidant enzyme-SOD1 cause ALS [57]. In addition, mutant SOD1 transgenic mice exhibited age-dependent motor neuron degeneration accompanied by the biochemical changes in the nerve cells [58]. Moreover, it has been reported that uric acid levels were negatively correlated with the disease progression in ALS patients [44]. Collectively, these previous findings and our pooled clinical data of the dysfunction between the oxidation and antioxidant systems in ALS patients support the hypothesis that oxidative stress is central in the pathogenesis of ALS.

Our analyses further showed that most of the oxidative stress markers had high levels of heterogeneity among studies. However, for the five oxidative stress markers that were dysregulated in the patients with ALS, AOPP did not show between-study heterogeneity and MDA showed small levels of heterogeneity, suggesting the reproducibility of these results. In addition, we conducted subgroup and metaregression analyses to address moderators that may explain heterogeneity for uric acid. The results indicated that gender, age, and publication year did not contribute to the between-

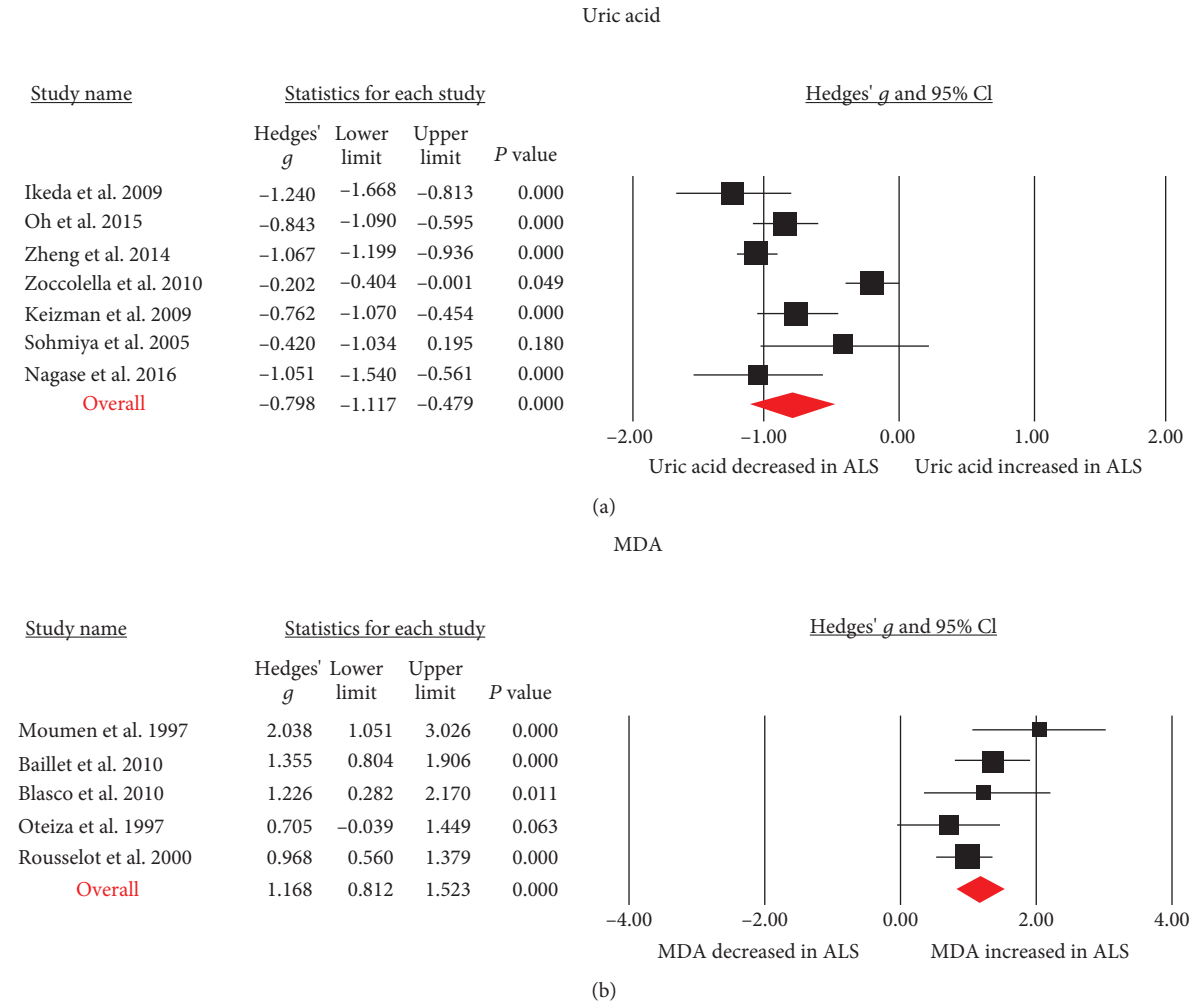

Figure 3: Studies of blood uric acid and MDA in amyotrophic lateral sclerosis. Forest plot displaying random-effects meta-analysis results of the association between uric acid (a), MDA (b), and amyotrophic lateral sclerosis. MDA: malondialdehyde.

study heterogeneity. Although subgroup analyses based on sampling source revealed that between-study heterogeneity was reduced in plasma studies analyzing uric acid levels, the lower heterogeneity is likely due to the low power of the test for heterogeneity used in meta-analyses with smaller numbers of studies. Other clinical variables including medication status and disease duration may also contribute to between-study heterogeneity. However, most of the studies included in the meta-analysis did not provide this information, thus preventing us from performing subgroup or metaregression analyses to assess whether these factors contributed to between-study heterogeneity. Indeed, a study reported that lithium and valproate cotreatment increased the survival of patients with ALS and the treatment also significantly increased blood glutathione levels in these patients [24].

The second limitation of this study is how much the alterations in oxidative stress markers in the peripheral blood reflect changes in the central nervous system. However, Djordjevic et al. reported that patients with ALS had significantly increased cerebrospinal fluid AOPP levels relative to control subjects [59]. Moreover, Murata et al. demonstrated that ALS patients had higher CSF 8-OHdG concentrations than control subjects [60]. These results support the "peripheral as a window to the brain" hypothesis. Further studies are necessary to translate these findings into practical clinical use. The third limitation of this study is that some oxidative stress markers analyzed in this study such as glutathione peroxidase had a limited number of studies with small sample sizes; therefore, it is difficult to determine significant associations between these markers and ALS. In addition, several other important oxidative stress markers such as catalase were not analyzed in the meta-analysis due to the lack of clinical studies on these markers. Future studies should clarify the role of oxidative stress in the onset and development of ALS.

In addition to prooxidative stress imbalance observed in ALS, a large number of studies have measured oxidative stress markers in other neurodegenerative diseases including Alzheimer's disease [61] and Parkinson's disease [62]. Due to the heterogeneous etiologies of these diseases, it is not surprising that results are inconsistent across studies comparing oxidative stress marker levels between patients with Alzheimer's disease or Parkinson's disease and controls. To address the inconsistent clinical data, Schrag et al. performed

Table 1: Summary of comparative outcomes for measurements of blood oxidative stress marker levels.

Cytokine	No. of studies	No. with ALS/controls	Main effect	Heterogeneity						Publication bias	
			Hedges' g (95% CI)	z score	P value	Q statistic	df	P value	I^2 statistic	Egger intercept	P value
Uric acid	7	961/1185	-0.798 (-1.117 to -0.479)	-4.906	<0.001	56.034	6	<0.001	89.292	0.910	0.750
8-OHdG	2	18/61	2.194 (0.554 to 3.835)	2.622	0.009	6.315	1	0.012	84.165	NA	NA
MDA	5	123/120	1.168 (0.812 to 1.523)	6.441	<0.001	5.793	4	0.215	30.950	1.61721	0.38172
GSH	4	71/78	-1.636 (-3.020 to -0.252)	-2.318	0.020	36.112	3	<0.001	91.692	-7.014	0.061
AOPP	2	147/133	0.555 (0.317 to 0.792)	4.571	<0.001	0.025	1	0.875	0.000	NA	NA
Ceruloplasmin	3	46/46	-0.052 (-0.475 to 0.372)	-0.239	0.811	2.168	2	0.338	7.742	2.538	0.403
Cu	10	361/471	0.014 (-0.337 to 0.366)	0.080	0.937	39.670	9	<0.001	77.313	0.09686	0.94797
Glutathione peroxidase	4	91/110	-0.679 (-1.732 to 0.373)	-1.265	0.206	29.687	3	<0.001	89.895	-4.92304	0.30857
Total cholesterol	13	2161/3870	0.144 (-0.095 to 0.383)	1.184	0.236	160.185	12	<0.001	92.509	1.50578	0.44161
HDL	9	2024/3722	-0.198 (-0.625 to 0.228)	-0.912	0.362	345.128	8	<0.001	97.682	2.99958	0.54140
LDL	9	2024/3722	0.121 (-0.283 to 0.524)	0.587	0.557	307.948	8	<0.001	97.402	2.74193	0.55440
SOD	5	96/184	-0.203 (-0.904 to 0.497)	-0.569	0.569	22.703	4	<0.001	82.381	9.11205	0.01197
Co-Q10	4	95/128	0.040 (-0.468 to 0.548)	0.156	0.876	9.953	3	0.019	69.858	-2.10679	0.75503
Transferrin	5	954/592	0.244 (-0.219 to 0.707)	1.032	0.302	50.330	4	<0.001	92.052	5.24433	0.09393
Triglyceride	8	1743/1633	-0.154 (-0.622 to 0.314)	-0.645	0.519	265.560	7	<0.001	97.364	4.85477	0.32384

Abbreviations: df: degrees of freedom; ALS: amyotrophic lateral sclerosis; 8-OHdG: 8-hydroxyguanosine; MDA: malondialdehyde; SOD: superoxide dismutase; AOPP: Advanced Oxidation Protein Product; LDL: low-density lipoprotein; HDL: high-density lipoprotein; Co-Q10: coenzyme-Q10; NA: not available.

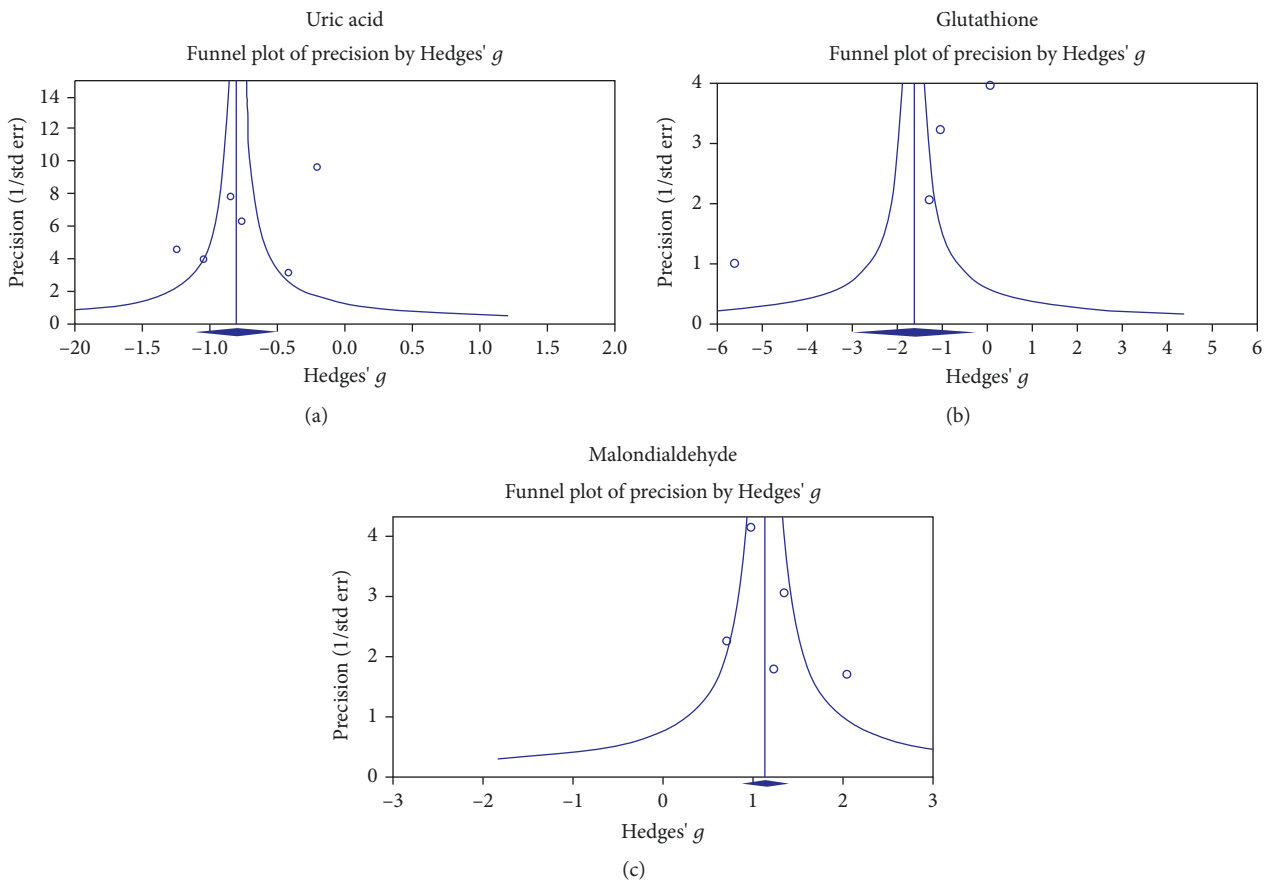

Figure 4: Funnel plots examining publication bias in studies comparing blood uric acid (a), GSH (b), and MDA (c) levels between cases and controls. GSH: glutathione; MDA: malondialdehyde.

a meta-analysis and reported that patients with Alzheimer's disease were accompanied by reduced uric acid levels and increased MDA levels in the peripheral blood [63]. In addition, a systematic review and meta-analysis performed by Wei et al. showed that blood 8-OHdG and MDA levels were elevated in Parkinson's disease patients, whereas uric acid and glutathione levels were downregulated in these patients [64]. The dysregulated profiles of oxidative stress markers in Parkinson's disease and Alzheimer's disease were similar to the findings from our meta-analysis on profiles of oxidative stress markers in ALS, suggesting a common pathway that confers vulnerability to the development of these neurodegenerative diseases.

In conclusion, the findings from the present study revealed increased 8-OhdG, MDA, and AOPP levels and reduced uric acid and glutathione levels in the peripheral blood of ALS patients. Our results clarify the oxidative stress marker profile in the blood of ALS patients and strengthens the clinical evidence that prooxidative imbalances contribute to ALS pathophysiology.

Data Availability

The data used to support the findings of this study are included within the article.

Conflicts of Interest

The authors declare that they have no conflict of interest.

Acknowledgments

This study was supported by the National Science Foundation of China (81703492), the Beijing Natural Science Foundation (7182092), the Minzu University Research Fund (2018CXTD03), and the MUC 111 project.

Supplementary Materials

Supplementary Table: characteristics of included studies measuring peripheral blood oxidative stress marker levels. *(Supplementary Materials)*

References

[1] W. Huynh, N. G. Simon, J. Grosskreutz, M. R. Turner, S. Vucic, and M. C. Kiernan, "Assessment of the upper motor neuron in amyotrophic lateral sclerosis," *Clinical Neurophysiology*, vol. 127, no. 7, pp. 2643–2660, 2016.

[2] M. C. Kiernan, S. Vucic, B. C. Cheah et al., "Amyotrophic lateral sclerosis," *The Lancet*, vol. 377, no. 9769, pp. 942–955, 2011.

[3] O. Hardiman, A. Al-Chalabi, C. Brayne et al., "The changing picture of amyotrophic lateral sclerosis: lessons from European registers," *Journal of Neurology, Neurosurgery & Psychiatry*, vol. 88, no. 7, pp. 557–563, 2017.

[4] P. Mehta, V. Antao, W. Kaye et al., "Prevalence of amyotrophic lateral sclerosis-United States, 2010-2011," *Morbidity and Mortality Weekly Report Supplements*, vol. 63, no. 7, pp. 1–14, 2014.

[5] J. D. Rothstein, "Current hypotheses for the underlying biology of amyotrophic lateral sclerosis," *Annals of Neurology*, vol. 65, Supplement 1, pp. S3–S9, 2009.

[6] R. G. Miller, J. D. Mitchell, and D. H. Moore, "Riluzole for amyotrophic lateral sclerosis (ALS)/motor neuron disease (MND)," *Cochrane Database of Systematic Reviews*, vol. 3, 2012.

[7] H. R. Martinez, C. E. Escamilla-Ocanas, C. R. Camara-Lemarroy, M. T. Gonzalez-Garza, J. Moreno-Cuevas, and M. A. Garcia Sarreon, "Increased cerebrospinal fluid levels of cytokines monocyte chemoattractant protein-1 (MCP-1) and macrophage inflammatory protein-1β (MIP-1β) in patients with amyotrophic lateral sclerosis," *Neurologia*, vol. 32, 2017.

[8] W. Zhao, D. R. Beers, and S. H. Appel, "Immune-mediated mechanisms in the pathoprogression of amyotrophic lateral sclerosis," *Journal of Neuroimmune Pharmacology*, vol. 8, no. 4, pp. 888–899, 2013.

[9] X. Chen, Y. Hu, Z. Cao, Q. Liu, and Y. Cheng, "Cerebrospinal fluid inflammatory cytokine aberrations in Alzheimer's disease, Parkinson's disease and amyotrophic lateral sclerosis: a systematic review and meta-analysis," *Frontiers in Immunology*, vol. 9, article 2122, 2018.

[10] Y. Hu, C. Cao, X. Y. Qin et al., "Increased peripheral blood inflammatory cytokine levels in amyotrophic lateral sclerosis: a meta-analysis study," *Scientific Reports*, vol. 7, no. 1, p. 9094, 2017.

[11] H. Blasco, G. Garcon, F. Patin et al., "Panel of oxidative stress and inflammatory biomarkers in ALS: a pilot study," *Canadian Journal of Neurological Sciences / Journal Canadien des Sciences Neurologiques*, vol. 44, no. 1, pp. 90–95, 2017.

[12] R. Moumen, A. Nouvelot, D. Duval, B. Lechevaliera, and F. Viadera, "Plasma superoxide dismutase and glutathione peroxidase activity in sporadic amyotrophic lateral sclerosis," *Journal of the Neurological Sciences*, vol. 151, no. 1, pp. 35–39, 1997.

[13] J. Ehrhart, A. J. Smith, N. Kuzmin-Nichols et al., "Humoral factors in ALS patients during disease progression," *Journal of Neuroinflammation*, vol. 12, no. 1, p. 127, 2015.

[14] K. Ikeda, K. Kawabe, and Y. Iwasaki, "Do serum uric acid levels reflect oxidative stress in the progression of ALS?," *Journal of the Neurological Sciences*, vol. 287, no. 1-2, p. 294, 2009.

[15] A. Baillet, V. Chanteperdrix, C. Trocme, P. Casez, C. Garrel, and G. Besson, "The role of oxidative stress in amyotrophic lateral sclerosis and Parkinson's disease," *Neurochemical Research*, vol. 35, no. 10, pp. 1530–1537, 2010.

[16] M. Sohmiya, M. Tanaka, Y. Suzuki, Y. Tanino, K. Okamoto, and Y. Yamamoto, "An increase of oxidized coenzyme Q-10 occurs in the plasma of sporadic ALS patients," *Journal of the Neurological Sciences*, vol. 228, no. 1, pp. 49–53, 2005.

[17] D. Moher, A. Liberati, J. Tetzlaff, D. G. Altman, and The PRISMA Group, "Preferred reporting items for systematic reviews and meta-analyses: the PRISMA statement," *PLoS Medicine*, vol. 6, no. 7, article e1000097, 2009.

[18] X. Y. Qin, S. P. Zhang, C. Cao, Y. P. Loh, and Y. Cheng, "Aberrations in peripheral inflammatory cytokine levels in Parkinson disease: a systematic review and meta-analysis," *JAMA Neurology*, vol. 73, no. 11, pp. 1316–1324, 2016.

[19] Y. Du, H. T. Wu, X. Y. Qin et al., "Postmortem brain, cerebrospinal fluid, and blood neurotrophic factor levels in Alzheimer's disease: a systematic review and meta-analysis," *Journal of Molecular Neuroscience*, vol. 65, no. 3, pp. 289–300, 2018.

[20] X. Y. Qin, J. C. Feng, C. Cao, H. T. Wu, Y. P. Loh, and Y. Cheng, "Association of peripheral blood levels of brain-derived neurotrophic factor with autism spectrum disorder in children: a systematic review and meta-analysis," *JAMA Pediatrics*, vol. 170, no. 11, pp. 1079–1086, 2016.

[21] X. Y. Qin, H. T. Wu, C. Cao, Y. P. Loh, and Y. Cheng, "A meta-analysis of peripheral blood nerve growth factor levels in patients with schizophrenia," *Molecular Psychiatry*, vol. 22, no. 9, pp. 1306–1312, 2017.

[22] R. M. Ahmed, E. Highton-Williamson, J. Caga et al., "Lipid metabolism and survival across the frontotemporal dementia-amyotrophic lateral sclerosis spectrum: relationships to eating behavior and cognition," *Journal of Alzheimer's Disease*, vol. 61, no. 2, pp. 773–783, 2018.

[23] A. N. A. B. Barros, M. E. T. Dourado, L. F. C. Pedrosa, and L. Leite-Lais, "Association of copper status with lipid profile and functional status in patients with amyotrophic lateral sclerosis," *Journal of Nutrition and Metabolism*, vol. 2018, Article ID 5678698, 7 pages, 2018.

[24] M. C. Boll, L. Bayliss, S. Vargas-Canas et al., "Clinical and biological changes under treatment with lithium carbonate and valproic acid in sporadic amyotrophic lateral sclerosis," *Journal of the Neurological Sciences*, vol. 340, no. 1-2, pp. 103–108, 2014.

[25] D. Bonnefont-Rousselot, L. Lacomblez, M. C. Jaudon et al., "Blood oxidative stress in amyotrophic lateral sclerosis," *Journal of the Neurological Sciences*, vol. 178, no. 1, pp. 57–62, 2000.

[26] A. Chio, A. Calvo, A. Ilardi et al., "Lower serum lipid levels are related to respiratory impairment in patients with ALS," *Neurology*, vol. 73, no. 20, pp. 1681–1685, 2009.

[27] A. Conti, S. Iannaccone, B. Sferrazza et al., "Differential expression of ceruloplasmin isoforms in the cerebrospinal fluid of amyotrophic lateral sclerosis patients," *Proteomics - Clinical Applications*, vol. 2, no. 12, pp. 1628–1637, 2008.

[28] S. De Benedetti, G. Lucchini, C. Del Bò et al., "Blood trace metals in a sporadic amyotrophic lateral sclerosis geographical cluster," *BioMetals*, vol. 30, no. 3, pp. 355–365, 2017.

[29] J. B. Delaye, F. Patin, E. Piver et al., "Low IDL-B and high LDL-1 subfraction levels in serum of ALS patients," *Journal of the Neurological Sciences*, vol. 380, pp. 124–127, 2017.

[30] L. Dupuis, P. Corcia, A. Fergani et al., "Dyslipidemia is a protective factor in amyotrophic lateral sclerosis," *Neurology*, vol. 70, no. 13, pp. 1004–1009, 2008.

[31] R. Huang, X. Guo, X. Chen et al., "The serum lipid profiles of amyotrophic lateral sclerosis patients: a study from south-west China and a meta-analysis," *Amyotrophic Lateral Sclerosis and Frontotemporal Degeneration*, vol. 16, no. 5-6, pp. 359–365, 2015.

[32] Y. Ihara, K. Nobukuni, H. Takata, and T. Hayabara, "Oxidative stress and metal content in blood and cerebrospinal fluid of amyotrophic lateral sclerosis patients with and without a Cu, Zn-superoxide dismutase mutation," *Neurological Research*, vol. 27, no. 1, pp. 105–108, 2005.

[33] K. Ikeda, T. Hirayama, T. Takazawa, K. Kawabe, and Y. Iwasaki, "Relationships between disease progression and serum levels of lipid, urate, creatinine and ferritin in Japanese patients with amyotrophic lateral sclerosis: a cross-sectional study," *Internal Medicine*, vol. 51, no. 12, pp. 1501–1508, 2012.

[34] G. D. Kanias and E. Kapaki, "Trace elements, age, and sex in amyotrophic lateral sclerosis disease," *Biological Trace Element Research*, vol. 56, no. 2, pp. 187–201, 1997.

[35] D. Keizman, M. Ish-Shalom, S. Berliner et al., "Low uric acid levels in serum of patients with ALS: further evidence for oxidative stress?," *Journal of the Neurological Sciences*, vol. 285, no. 1-2, pp. 95–99, 2009.

[36] T. Kihira, K. Okamoto, S. Yoshida et al., "Environmental characteristics and oxidative stress of inhabitants and patients with amyotrophic lateral sclerosis in a high-incidence area on the Kii Peninsula, Japan," *Internal Medicine*, vol. 52, no. 13, pp. 1479–1486, 2013.

[37] S. M. Kim, M. Y. Noh, H. Kim et al., "25-Hydroxycholesterol is involved in the pathogenesis of amyotrophic lateral sclerosis," *Oncotarget*, vol. 8, no. 7, pp. 11855–11867, 2017.

[38] A. LoGerfo, L. Chico, L. Borgia et al., "Lack of association between nuclear factor erythroid-derived 2-like 2 promoter gene polymorphisms and oxidative stress biomarkers in amyotrophic lateral sclerosis patients," *Oxidative Medicine and Cellular Longevity*, vol. 2014, Article ID 432626, 9 pages, 2014.

[39] R. M. Mitchell, Z. Simmons, J. L. Beard, H. E. Stephens, and J. R. Connor, "Plasma biomarkers associated with ALS and their relationship to iron homeostasis," *Muscle & Nerve*, vol. 42, no. 1, pp. 95–103, 2010.

[40] K. Mokuno, K. Kiyosawa, H. Honda et al., "Elevated serum levels of manganese superoxide dismutase in polymyositis and dermatomyositis," *Neurology*, vol. 46, no. 5, pp. 1445–1447, 1996.

[41] J. A. Molina, F. de Bustos, F. J. Jiménez-Jiménez et al., "Serum levels of coenzyme Q_{10} in patients with amyotrophic lateral sclerosis," *Journal of Neural Transmission*, vol. 107, no. 8-9, pp. 1021–1026, 2000.

[42] Y. Nadjar, P. Gordon, P. Corcia et al., "Elevated serum ferritin is associated with reduced survival in amyotrophic lateral sclerosis," *PLoS One*, vol. 7, no. 9, article e45034, 2012.

[43] M. Nagase, Y. Yamamoto, Y. Miyazaki, and H. Yoshino, "Increased oxidative stress in patients with amyotrophic lateral sclerosis and the effect of edaravone administration," *Redox Report*, vol. 21, no. 3, pp. 104–112, 2016.

[44] S. I. Oh, S. Baek, J. S. Park, L. Piao, K. W. Oh, and S. H. Kim, "Prognostic role of serum levels of uric acid in amyotrophic lateral sclerosis," *Journal of Clinical Neurology*, vol. 11, no. 4, pp. 376–382, 2015.

[45] P. I. Oteiza, O. D. Uchitel, F. Carrasquedo, A. L. Dubrovski, J. C. Roma, and C. G. Fraga, "Evaluation of antioxidants, protein, and lipid oxidation products in blood from sporadic amyotrophic lateral sclerosis patients," *Neurochemical Research*, vol. 22, no. 4, pp. 535–539, 1997.

[46] A. Pasquinelli, L. Chico, L. Pasquali et al., "Gly482Ser PGC-1α gene polymorphism and exercise-related oxidative stress in amyotrophic lateral sclerosis patients," *Frontiers in Cellular Neuroscience*, vol. 10, p. 102, 2016.

[47] T. L. Peters, J. D. Beard, D. M. Umbach et al., "Blood levels of trace metals and amyotrophic lateral sclerosis," *NeuroToxicology*, vol. 54, pp. 119–126, 2016.

[48] A. Radunović, H. T. Delves, W. Robberecht et al., "Copper and zinc levels in familial amyotrophic lateral sclerosis patients with CuZnSOD gene mutations," *Annals of Neurology*, vol. 42, no. 1, pp. 130-131, 1997.

[49] N. A. Sutedja, Y. T. van der Schouw, K. Fischer et al., "Beneficial vascular risk profile is associated with amyotrophic lateral sclerosis," *Journal of Neurology, Neurosurgery & Psychiatry*, vol. 82, no. 6, pp. 638–642, 2011.

[50] G. Torsdottir, J. Kristinsson, G. Gudmundsson, J. Snaedal, and T. Johannesson, "Copper, ceruloplasmin and superoxide dismutase (SOD) in amyotrophic lateral sclerosis," *Pharmacology and Toxicology*, vol. 87, no. 3, pp. 126–130, 2000.

[51] C. Veyrat-Durebex, P. Corcia, A. Mucha et al., "Iron metabolism disturbance in a French cohort of ALS patients," *BioMed Research International*, vol. 2014, Article ID 485723, 6 pages, 2014.

[52] A. Wuolikainen, J. Acimovic, A. Lovgren-Sandblom, P. Parini, P. M. Andersen, and I. Bjorkhem, "Cholesterol, oxysterol, triglyceride, and coenzyme Q homeostasis in ALS. Evidence against the hypothesis that elevated 27-hydroxycholesterol is a pathogenic factor," *PLoS One*, vol. 9, no. 11, article e113619, 2014.

[53] J. W. Yang, S. M. Kim, H. J. Kim et al., "Hypolipidemia in patients with amyotrophic lateral sclerosis: a possible gender difference?," *Journal of Clinical Neurology*, vol. 9, no. 2, pp. 125–129, 2013.

[54] Y. Zheng, L. Gao, D. Wang, and D. Zang, "Elevated levels of ferritin in the cerebrospinal fluid of amyotrophic lateral sclerosis patients," *Acta Neurologica Scandinavica*, vol. 136, no. 2, pp. 145–150, 2017.

[55] Z. Zheng, X. Guo, Q. Wei et al., "Serum uric acid level is associated with the prevalence but not with survival of amyotrophic lateral sclerosis in a Chinese population," *Metabolic Brain Disease*, vol. 29, no. 3, pp. 771–775, 2014.

[56] S. Zoccolella, I. L. Simone, R. Capozzo et al., "An exploratory study of serum urate levels in patients with amyotrophic lateral sclerosis," *Journal of Neurology*, vol. 258, no. 2, pp. 238–243, 2011.

[57] E. D'Amico, P. Factor-Litvak, R. M. Santella, and H. Mitsumoto, "Clinical perspective on oxidative stress in sporadic amyotrophic lateral sclerosis," *Free Radical Biology and Medicine*, vol. 65, pp. 509–527, 2013.

[58] F. Bozzo, A. Mirra, and M. T. Carrì, "Oxidative stress and mitochondrial damage in the pathogenesis of ALS: New perspectives," *Neuroscience Letters*, vol. 636, pp. 3–8, 2017.

[59] G. Djordjevic, S. Ljubisavljevic, S. Sretenovic, G. Kocic, I. Stojanovic, and S. Stojanovic, "The cerebrospinal fluid values of advanced oxidation protein products and total thiol content in patients with amyotrophic lateral sclerosis," *Clinical Neurology and Neurosurgery*, vol. 163, pp. 33–38, 2017.

[60] T. Murata, C. Ohtsuka, and Y. Terayama, "Increased mitochondrial oxidative damage and oxidative DNA damage contributes to the neurodegenerative process in sporadic amyotrophic lateral sclerosis," *Free Radical Research*, vol. 42, no. 3, pp. 221–225, 2008.

[61] Z. Pu, W. Xu, Y. Lin, J. He, and M. Huang, "Oxidative stress markers and metal ions are correlated with cognitive function in Alzheimer's disease," *American Journal of Alzheimer's Disease & Other Dementias®*, vol. 32, no. 6, pp. 353–359, 2017.

[62] A. Bolner, R. Micciolo, O. Bosello, and G. P. Nordera, "A panel of oxidative stress markers in Parkinson's disease," *Clinical Laboratory*, vol. 62, no. 1-2, pp. 105–112, 2016.

[63] M. Schrag, C. Mueller, M. Zabel et al., "Oxidative stress in blood in Alzheimer's disease and mild cognitive impairment: a meta-analysis," *Neurobiology of Disease*, vol. 59, pp. 100–110, 2013.

[64] Z. Wei, X. Li, X. Li, Q. Liu, and Y. Cheng, "Oxidative stress in Parkinson's disease: a systematic review and meta-analysis," *Frontiers in Molecular Neuroscience*, vol. 11, p. 236, 2018.

Hindawi
Oxidative Medicine and Cellular Longevity
Volume 2019, Article ID 2105607, 18 pages
https://doi.org/10.1155/2019/2105607

Review Article

Oxidative Stress in Neurodegenerative Diseases: From a Mitochondrial Point of View

Giovanna Cenini,[1] **Ana Lloret**,[2] **and Roberta Cascella**[3]

[1]*Institut für Biochemie und Molekularbiologie, University of Bonn, 53115 Bonn, Germany*
[2]*Department of Physiology, Faculty of Medicine, University of Valencia, Avda, Blasco Ibañez, 17, 46010 Valencia, Spain*
[3]*Department of Experimental and Clinical Biomedical Sciences, Section of Biochemistry, University of Florence, 50134 Florence, Italy*

Correspondence should be addressed to Roberta Cascella; roberta.cascella@unifi.it

Received 4 October 2018; Accepted 15 April 2019; Published 9 May 2019

Academic Editor: Anthony R. White

Age is the main risk factor for a number of human diseases, including neurodegenerative disorders such as Alzheimer's disease, Parkinson's disease, and amyotrophic lateral sclerosis, which increasing numbers of elderly individuals suffer. These pathological conditions are characterized by progressive loss of neuron cells, compromised motor or cognitive functions, and accumulation of abnormally aggregated proteins. Mitochondrial dysfunction is one of the main features of the aging process, particularly in organs requiring a high-energy source such as the heart, muscles, brain, or liver. Neurons rely almost exclusively on the mitochondria, which produce the energy required for most of the cellular processes, including synaptic plasticity and neurotransmitter synthesis. The brain is particularly vulnerable to oxidative stress and damage, because of its high oxygen consumption, low antioxidant defenses, and high content of polyunsaturated fats very prone to be oxidized. Thus, it is not surprising the importance of protecting systems, including antioxidant defenses, to maintain neuronal integrity and survival. Here, we review the role of mitochondrial oxidative stress in the aging process, with a specific focus on neurodegenerative diseases. Understanding the molecular mechanisms involving mitochondria and oxidative stress in the aging and neurodegeneration may help to identify new strategies for improving the health and extending lifespan.

1. Introduction

Aging is the primary risk factor for a number of human diseases, as well as neurodegenerative disorders [1], which increasing numbers of elderly individuals suffer. These pathological conditions, including Alzheimer's disease (AD), Parkinson's disease (PD), Huntington's disease (HD), amyotrophic lateral sclerosis (ALS), and spinocerebellar ataxia (SCA), are characterized by progressive loss of neuron cells, compromised motor or cognitive functions, and accumulation of abnormally aggregated proteins [2, 3]. A growing body of evidence highlights bioenergetic impairments as well as alterations in the reduction-oxidation (redox) homeostasis in the brain with the increasing of the age. The brain is composed by highly differentiated cells that populate different anatomical regions and requires about 20% of body basal oxygen for its functions [4]. Thus, it is not surprising that alterations in brain energy metabolisms lead to neurodegeneration.

Cellular energy is mainly produced via oxidative phosphorylation taking place within mitochondria, which are crucial organelles for numerous cellular processes, such as energy metabolism, calcium homeostasis, lipid biosynthesis, and apoptosis [5, 6]. Glucose oxidation is the most relevant source of energy in the brain, because of its high rate of ATP generation needed to maintain neuronal energy demands [4]. Thus, neurons rely almost exclusively on the mitochondria, which produce the energy required for most of the cellular processes, including synaptic plasticity and neurotransmitter synthesis [7]. Furthermore, given the central role of mitochondria in energy metabolism and in the regulation of the redox homeostasis, the study of age-related mitochondrial disorders is becoming nowadays of growing interest. Here, we review the role of mitochondria

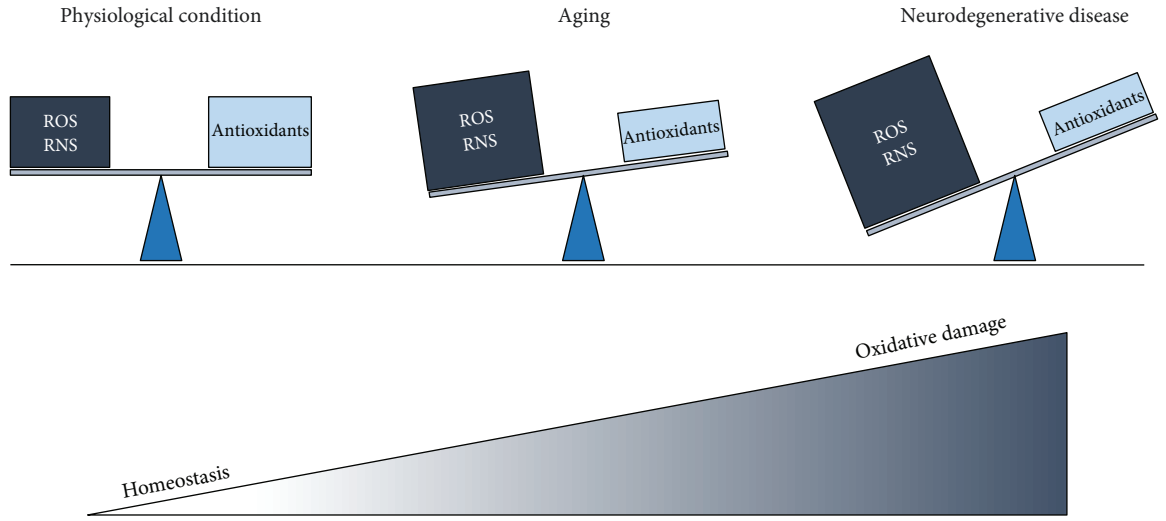

Figure 1: Schematic representation of oxidative stress in health, aging, and neurodegenerative diseases. In healthy conditions, the oxidant levels mainly produced in mitochondria are kept under control due to efficient mechanisms of defense that counterbalance the excessive production of oxidants and keep the homeostasis. However during the aging, the oxidant levels increase, while the antioxidant efficiency decreases generating an imbalance that leads to a noxious condition called oxidative stress and consequently to an oxidative damage of the main biomolecules such as proteins, lipids, nucleic acids, and carbohydrates. The overall picture intensifies in neurodegenerative conditions such as Alzheimer's disease, Parkinson's disease, and amyotrophic lateral sclerosis.

in the aging process, with a specific focus on mitochondrial oxidative stress in neurodegenerative diseases.

2. What Is the Oxidative Stress?

Reactive oxygen species (ROS) are normally produced in the cell of living organisms as a result of normal cellular metabolism and are fundamental in the maintenance of cellular homeostasis. In physiological conditions, low to moderate concentrations of ROS are involved in processes such as immune response, inflammation, synaptic plasticity, learning, and memory [8]. However, the excess of ROS production can be harmful, producing adverse oxidative modifications to cell components including mitochondrial structures as the first targets of ROS-induced damage [9]. Nevertheless, the human body is equipped with a variety of antioxidants that serve to counterbalance the effect of oxidants, including superoxide dismutase (SOD) and the glutathione (GSH) system [10]. When an imbalance between free radical production and detoxification occurs, ROS production may overwhelm antioxidant defenses, leading to the generation of a noxious condition called oxidative stress and overall to the impairment of the cellular functions. This phenomenon is observed in many pathological cases involving mitochondrial dysfunction, as well as in aging [11] (Figure 1). The brain is particularly vulnerable to oxidative stress and damage, because of its high oxygen consumption, low antioxidants defenses, and high content of polyunsaturated fats very prone to be oxidized [12].

Biological molecules such as proteins, lipids, nucleic acids, and carbohydrates are generally prone to oxidation, leading to a consistent oxidative damage of the biomolecules like change of their structures and consequently to their functions. The resulting oxidative modifications of the biomolecules are quite stable and they could be used as markers of oxidative and nitrosative stress. For example, the main products of protein oxidation are protein carbonyls and nitrated proteins [13]. Protein carbonyls derive by the direct oxidation of certain amino acids by peptide backbone scission or by Michael addition reaction with products of lipid peroxidation (e.g., HNE) or by glycoxidation reactions [14]. Detoxification of protein carbonyls happens through enzyme such as aldehyde dehydrogenase (ALDH) or by reduction of the carbonyl group to the corresponding alcohol group by carbonyl reductase (CR) [15]. Protein nitration happens in particular at tyrosine level (3-nitrotyrosine: 3-NT) through the action of reactive nitrogen species (RNS) such as peroxynitrite and nitro dioxide [16].

Another characteristic process of oxidative stress that affects lipids and leads to the formation of the relative markers is the lipid peroxidation. More in specific, lipid peroxidation derives from the damage of cellular membranes by ROS that generates a heterogeneous group of relatively stable end-products such as malondialdehyde (MDA), 4-hydroxy-2-nonenal (HNE), acrolein, and isoprostanes [17]. MDA, HNE, and acrolein are able to bind proteins and DNA leading to the alteration of conformation and function [18].

Carbohydrates are also affected by ROS. Indeed, reducing sugars plays a pivotal role in modifying proteins through the formation of advance glycation end-products (AGEs) in a nonenzymatic reaction called glycation [19]. AGEs are involved in the progress of some diseases such as diabetes mellitus, cardiac dysfunction, and neurodegenerative diseases [20].

Between all the free radicals, the hydroxy radical ($OH^{\cdot}$) is the most toxic because of its high reactivity and limitation on its diffusion from their site of the formation. $OH^{\cdot}$ has been found to damage biological molecules including nucleic acid [21]. 8-Hydroxyguanosine (8-OHG) and 8-hydroxy-2′-deoxyguanosine (8-OHdG) are the most abundant among

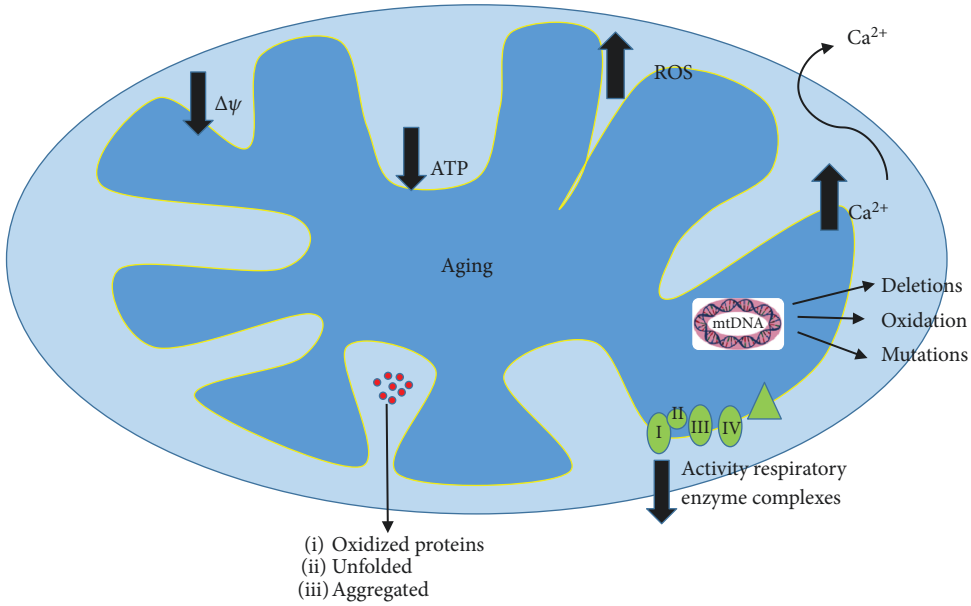

Figure 2: Rendition of the central role of mitochondrial deficiencies in aging. The ROS production in aged mitochondria is increased, the membrane potential appeared lower, ATP synthesis is reduced, the activity of respiratory enzyme complexes is declined, and oxidized proteins accumulate causing protein aggregation. Mitochondrial DNA (mtDNA) is also oxidized and deletions and mutations have found.

the oxidized bases, and they can be used as markers of RNA and DNA oxidation [22]. The involvement of nucleic acid oxidation in neurodegenerative diseases might cause not only the reduction of protein level but also translation errors *in vivo* with alteration of protein structure and function [23].

In the course of the evolution, the organisms have developed several mechanisms of protection against the noxious effects of ROS and RNS in such a way that the whole amount of prooxidants is under control, and the negative consequences are limited. The antioxidant molecules are divided into two groups: enzymatic and nonenzymatic compounds. The enzymatic group includes superoxide dismutase (SOD), catalase (CAT), glutathione peroxidase (GPx), and glutathione reductase (GR). SOD is one of the first protective mechanisms against ROS and catalyzes the conversion of $O2^{-}$ $^{\cdot}$ to H_2O_2 and O_2 [24]. The generated H_2O_2 is converted to water and O_2 by CAT. The nonenzymatic group involves glutathione (GSH), the most abundant antioxidant in most of the brain cells, thioredoxin (Trx), vitamins A, E, and C, and selenium. GSH reacts with ROS generating glutathione disulfide (GSSG) and enters a cycle together with GPx and GR. Vitamin E (also called α-tocopherol) is a lipophilic molecule acting against the lipid peroxidation [25]. Vitamin C (also called ascorbic acid) is one of the most important water-soluble antioxidants. Selenium is a crucial cofactor for the enzymes GPx and thioredoxin reductase (TrxR) and essential trace elements. All together they act and balance the levels of ROS and RNS to avoid the onset and the propagation of harmful effect in the nearby tissues.

3. Mitochondrial Damage in Aging

Aging is a degenerative physiological process induced by the accumulation of cellular lesions leading progressively to organ dysfunction and death. Although our knowledge of the aging process remains far from being complete, understanding the basis of human aging is one of the great biomedical goals. The best known and most long-standing hypothesis to explain aging is the "free radical theory of aging" proposed by Harman and coworkers [26], which postulates that aging and age-associated degenerative diseases are the result of free radical attacks on cells and tissues. This theory was later extended by Miquel and coworkers [27] who focused on mitochondria as the main source of ROS in aging cells. In this relevant work, the authors explained how mitochondrial disorganization might be an important aspect of the age-related changes of postmitotic cells such as neurons and muscle cells. This view was based on electron microscopic and biochemical studies on insects and mammals. Finally, they offered a hypothesis on intrinsic mitochondrial senescence and its possible relation to age-related changes in other cell organelles. The theory is known nowadays as "the mitochondrial theory of aging." Since this early publication, experimental evidences of the implication of mitochondria in aging have increased.

In addition to the energy generation through oxidative phosphorylation, mitochondria play an essential role in cell metabolic homeostasis, signaling, differentiation, and senescence [28]. Mitochondrial dysfunction is one of the main features of the aging process [29] (Figure 2), particularly in organs requiring a high-energy source such as the heart, muscles, brain, or liver. Although a large amount of data support the role of mitochondrial ROS production in aging, it has also recently been demonstrated the involvement of the mitochondrial permeability transition in the mechanisms of aging [30]. Indeed, the mitochondrial membrane potential appeared originally lower in old animals, and cellular peroxide levels were higher in cells from old animals with respect

to the young ones [31]. The age-associated decrease in mitochondrial membrane potential correlated with reduced ATP synthesis in tissues of old animals [32] and also in human fibroblasts from elderly subjects [33]. The mitochondrial permeability transition is due to a nonspecific pore called the mitochondrial permeability transition pore (mPTP) occurring when mitochondria become overloaded with calcium. Indeed, it is well known that aging alters cytosolic calcium pick-up and the sensitivity of the mPTP to calcium enhanced under oxidative stress conditions [34].

Using isolated mitochondria, in the past few decades, many studies revealed that the activity of respiratory enzyme complexes in the electron chain transport gradually declines with age in the liver, skin fibroblasts, brain, and skeletal muscle of humans [32, 33, 35, 36] (Figure 2). Moreover, mitochondrial morphology changed with age. Electron microscopic studies showed that mitochondrial disorganization accumulates with age in a variety of cells and tissues [26]. Although mitochondria are very dynamic organelles and can remodel their structure through fusion and fission [37], abnormalities in the process have been related to senescence in mammalian cells [38].

Age-associated oxidative damage to mtDNA was shown to correlate with mitochondrial GSH oxidation in the liver, kidney, and brain of rats and mice [39]. mtDNA deletions were also found to correlate with the level of oxidized guanosines in mtDNA [40]. Furthermore, mtDNA increasingly accumulated mutations with age in a variety of human tissues, which include point mutations [41], large-scale deletions [42], and also tandem duplications [43] (Figure 2). On the other hand, mitochondrial rRNAs were oxidized and degraded under oxidative stress conditions [44]. Oxidized proteins also accumulate progressively during aging, and an important consequence is the unfolding phenomenon that causes protein aggregation [45] (Figure 2). Many respiratory enzymes are known to be the targets of oxidation, such as complex I and ATPase [46] (Figure 2). Finally, lipid peroxidation is particularly important in the inner mitochondrial membrane due to the high content of cardiolipin [47]. In fact, oxidative stress was found to decrease cardiolipin levels more than other lipids and this decline appeared directly related to the decrease of cytochrome oxidase activity [47].

Interestingly, a switch from glycolysis to respiratory metabolism in yeast has been found to increase ROS production, activate the antioxidant response, and increase NADPH production, causing lifespan extension and hormesis response [48].

Mitochondrial dysfunction has also been related to another aging-related process, the telomere shortening [49]. PGC-1a/b are the principal regulators of mitochondrial biogenesis and function and establish the connection between telomere shortening and mitochondria malfunction [50]. When DNA is damaged, p53 levels increase and PGC1a/b are inhibited consequently leading to mitochondrial dysfunction [49, 50]. PGC-1a was also found to decrease its activity inducing loss of SIRT1 activity and mitochondrial dysfunction, particularly in the muscle [51]. Interestingly, the overexpression of PGC-1a can improve aging muscle and plays a significant role in longevity [52]. On the other hand, DNA damage can also activate AKT and mTORC1, resulting in PGC-1b-dependent mitochondrial biogenesis and ROS generation [53].

4. Mitochondrial Oxidative Stress and Its Role in Neurodegenerative Diseases

As already described above, mitochondria are key multifunctional organelles that play multiple important functions in the cell. They are essential not only in energy production but also in thermogenesis, calcium homeostasis, generating and maintaining key cellular metabolites, and redox signaling [5]. Neurons are postmitotic highly differentiated cells with a lifespan similar to that of the whole organism [54]. These excitable cells are more sensitive to the accumulation of oxidative damages compared to dividing cells and are more prone to accumulating defective mitochondria during aging [54, 55]. Thus, it is not surprising the importance of protecting systems, including antioxidant defenses, to maintain neuronal integrity and survival.

All the neurodegenerative disorders share several common features, such as the accumulation of abnormally aggregated proteins and the involvement of oxidative damage and mitochondrial dysfunction. Many of the genes associated with PD or ALS are linked to mitochondria. In addition, all aggregated misfolded proteins (β-amyloid, tau, and α-synuclein) are known to inhibit mitochondrial function and induce oxidative stress [56]. Therefore, the identification of common mechanisms underlying neurodegenerative diseases, including mitochondrial dysfunction, will increase our understanding of the essential requirements for neuronal survival that can inform future neuroprotective therapies.

5. Alzheimer's Disease

Alzheimer's disease (AD) is the most prevalent neurodegenerative disorder affecting the aged population, which is characterized by progressive deterioration of behavior, cognition, and functionality [57]. Although the pathophysiology is extremely complex and heterogeneous, the main hallmarks of AD are the senile plaques composed by extracellular deposition of amyloid beta (Aβ) peptide and the presence of intracellular tau neurofibrillary tangles (NFT) [57]. The aberrant protein aggregation results in multifactorial neuronal dysfunction affecting synaptic signaling, mitochondrial function, neuroinflammation, and neuronal loss [58, 59]. In particular, Aβ plaques were found to deplete Ca^{2+} ions storage in the endoplasmic reticulum (ER), resulting in cytosolic Ca^{2+} overload, which causes a reduction in endogenous GSH levels and ROS accumulation [60]. ROS-induced oxidative stress is one of the main important factors in the pathogenesis of AD as ROS overproduction is thought to play a critical role in the accumulation and deposition of Aβ peptides in AD [61].

The relationship between mitochondria and AD pathology is not so direct compared to other neurodegenerative disorders, although the role of oxidative stress and mitochondrial dysfunction is shown in different AD models

[62]. Thus, a reduction in complex IV activity has been demonstrated in mitochondria from the hippocampus and platelets of AD patients and in AD cybrid cells [63, 64]. Aggregation of Aβ peptides leads to oxidative stress, mitochondrial dysfunction, and energy failure prior to the development of plaque pathology [65] and can reduce mitochondrial respiration in neurons and astrocytes via the inhibition of complexes I and IV, thus causing ROS production [66]. The important role of mitochondrial ROS has been also confirmed by the results obtained with the antioxidant MitoQ, which can prevent cognitive decline, Aβ peptide accumulation, microglia inflammation, and synaptic loss in a transgenic mouse model of AD [67] and can extend lifespan and improve health in a transgenic *Caenorhabditis elegans* model of AD [68]. In addition, the inhibition of oxidative stress as a result of a polyunsaturated fatty acid diet improved cognition and memory in mice [69], rats [70], and protected worms from the paralysis by extending their lifespan [71].

It has been reported that the H_2O_2 production from synaptic mitochondria was more than fivefold higher than that from nonsynaptic mitochondria [72]. This fact indicates that neurons are more susceptible to oxidative damage than glial cells. Furthermore, isolated mitochondria from neurons incubated with Aβ peptides caused a fivefold increase in the rate of H_2O_2 production [73]. Moreover, Aβ peptides increased the aggregation of mitochondria isolated from neurons and caused cytochrome C release from mitochondria, both proapoptotic signals [73]. Studies performed in AD patients showed reduced cytochrome oxidase activity in platelets of AD subjects when compared to controls [74], and this mitochondrial defect was also demonstrated in the brain of AD patients [75]. Mitochondria from platelets of AD patients have been found depolarized, smaller on average, and less able to buffer calcium, showing lower ATP levels and an increase of oxidative stress, stress signaling, and apoptosis, with respect to controls [7]. Subjects with mild cognitive impairment also revealed mitochondrial deficiencies [76]. Fisar et al. have recently shown that both insufficiency in substrates entering into the oxidative phosphorylation system and functional disturbances in the electron transport system complex are responsible for the decrease in respiration observed in intact platelets of AD patients [77]. A very early decrease in mitochondrial complex activity has also been found in the entorhinal cortex of AD patients, but not in the frontal cortex [78].

Recently, it has been suggested that an imbalance in nuclear and mitochondrial genome-encoded oxidative phosphorylation transcripts may drive a negative feedback loop reducing mitochondrial translation and compromising oxidative phosphorylation efficiency, leading to ROS production [79]. Indeed, a deficiency of the mitochondrial oxidative phosphorylation system can impact directly on mitochondrial function and result in several disease phenotypes [80].

It has recently been shown that cells from late-onset AD patients exhibited an impaired mitochondrial metabolic potential and an abnormal redox potential, associated with reduced nicotinamide adenine dinucleotide metabolism and altered citric acid cycle activity [81]. Moreover, AD fibroblasts presented a significant reduction in mitochondrial length, changes in the expression of proteins that control mitochondrial fusion, and dysfunction of mitochondrial bioenergetics [82]. Martín-Maestro et al. also showed that multiple genes that control mitochondrial homeostasis, including fission and fusion, are downregulated in Alzheimer's patients. These defects lead to strong accumulation of aged mitochondria in AD fibroblasts [83]. Accordingly, the analysis from AD patients of genes involved in autophagy and mitophagy demonstrated a downregulation, indicating that the recycling mechanism of these aged mitochondria might be impaired [83].

AD pathogenesis has also been linked to voltage-dependent anion channel 1 (VDAC1) [84], which is expressed in the mitochondrial outer membrane and regulates the main metabolic and energetic functions of the cell, including Ca^{2+} homeostasis, oxidative stress, and mitochondrion-mediated apoptosis. Indeed, VDAC1 levels were found to increase in the AD brains and its inhibition has been proposed as the target of a novel strategy for diminishing cell death [84].

Mitochondria are highly abundant in synapsis cause of their on-site energy provision and calcium modulation [85]. Via TOM import machinery [86] and/or by local production by γ-secretase [87], Aβ peptides accumulate inside the synaptic mitochondria [88]. Then, it probably interacts with the mitochondrial heme group [73] and/or with mitochondrial matrix proteins such as amyloid-binding alcohol dehydrogenase (ABAD) [188] and blocks the electronic transport thereby compromising ATP production [89] and synaptic function [64]. A recent study performed in isolated mammalian mitochondria showed that Aβ peptides impaired mitochondrial import of nuclear-encoded precursor proteins due to a coaggregation process [90].

It has been showed from different laboratories that oxidative and nitrosative stress markers were substantially increased in AD, encouraging the idea about the crucial role of these two pathways in the progression of the disease. In several postmortem cortex areas not only from sporadic and familiar AD patients but also from patients affected by mild cognitive impairment (MCI), the levels of protein carbonyls were substantially increased compared to age-matched control subjects [91, 92]. In addition, the levels of carbonyl reductase (CR) were also found to increase in the AD brains, suggesting that the brain tries to counteract protein oxidation [15]. About markers of nitrosative stress in AD, proteomic approaches have identified a large number of proteins which are nitrated in the MCI and AD brains [93, 94]. These proteins are involved in several cellular functions such as energy metabolism, structural maintenance, pH regulation, and antioxidant.

Lipid peroxidation seems to play a particular role not only in aging but also in the pathogenesis of AD [95] and its products could be used as markers for AD identification since early stages (MCI). Indeed, in CSF and the brains from AD and MCI subjects, it has been found elevated levels of lipid peroxidation products such as HNE, malondialdehyde (MDA), acrolein, $F_{(2)}$-isoprostane, $F_{(4)}$-isoprostane, and neuroprostane [96, 97], have been found elevated, while MDA

levels was also found high in plasma and serum from AD patients [98] and colocalized with neurofibrillary tangles and senile plaques [99]. The decrease of the detoxification system efficiency in MCI and AD caused the accumulation of HNE protein adducts in neuronal cells [100]. Also in the blood, a significant increase of HNE levels has been found in AD patients compared to healthy subjects [101]. Acrolein has been reported to react with DNA bases leading to the formation of acrolein-deoxyguanosine in the AD brain [102].

Several papers published in the early nineties suggested an important role of glycation in the formation of neurofibrillary tangles and senile plaques [103, 104]. Like many other markers of oxidative stress, AGEs were also found to increase in CSF of AD patients, as well as their receptor levels in microglia cells of the AD brains [104]. While the picture in the brain is clear, the results about AGEs and soluble RAGE levels obtained in the blood from AD patients are controversial [105].

A considerable amount of evidences supports the early involvement of nucleic acids and oxidation in the cascade of neurodegeneration. DNA and RNA damage is a feature of the AD brain as well as of peripheral tissue [106]. mtDNA of cortical neurons in AD patients was found deleted with respect to age-matched controls [107]. Later, sporadic mutations in the mtDNA control regions in AD patients were also identified [108]. Interestingly, 8-OHdG levels in the mtDNA of the cerebral cortex and cerebellum from AD patients were threefold higher than in age-matched controls [109]. RNA oxidation was observed in the postmortem brains of early and latest stages of AD [110], a presymptomatic case with familial AD mutation [111], and Down syndrome with AD pathology [112], suggesting that mRNA is highly sensitive to oxidative damage. Fivefold increase in oxidized RNA was also observed in CSF of AD cases [113]. All this data suggests that nucleic acid oxidation may be considered an early event in the progression of AD.

The antioxidant levels in AD were found to change not only in the brain but also in peripheral tissues. Most of the studies have found an overall decrease in antioxidant amount and activity in the blood of AD patients since the early phases, suggesting that the physiological equilibrium between ROS/RNS production and antioxidant is altered and consequently the amount of antioxidant available is strongly compromised. In particular, SOD levels, but not the activity [114], were found to be elevated in the hippocampus and amygdala of AD patients [115], while a decrease in SOD, GPx, and CAT levels was found in the frontal and temporal cortex [116]. Nevertheless, CAT activity was found to increase in AD erythrocytes [117], suggesting an independence of the redox status between the periphery and the brain.

GSH was also found to decrease in the MCI and AD brain and erythrocytes [114, 118]. Another recent study showed higher GSH levels in the anterior and posterior cingulated from MCI patients [119]. In addition to GSH, the enzymes involved in its metabolism were also analyzed. In particular, glutathione-S-transferase (GST), a sensitive target of oxidative and nitrosative stress, was found to be carbonylated in *C. elegans* expressing Aβ42 [120] and in canine model of aging [121]. GST was also found to be nitrated in inferior parietal lobe (IPL) from MCI patients [122] and significantly elevated in the AD hippocampus, causing a decrease of its activity [118]. Since GSTs catalyze the conjugation of HNE to glutathione (GSH), the decline of its activity consequently leads to the compromise of detoxification process of HNE [123] and an accumulation of HNE-modified proteins. All these studies suggest that an alteration of GSH metabolism at the early stages of the disease could be an early marker for the detection of AD.

Another family of antioxidants particularly affected by oxidative and nitrosative stress is peroxiredoxins (Prxs), which reduces H_2O_2 [124] and presents a redox-regulated chaperone activity [125]. Prx2 oxidation was found Aβ42 dependent in SAMP8 mice [126]. However, Prx2 expression was found to increase in the AD brains [127] and Prx6 is oxidatively modified in the MCI brains [122], suggesting the presence of a compensatory mechanism.

Vitamins E and C were also found to decrease in plasma from MCI and mild AD and in CSF from AD patients [128–130]. In line with these results, another study showed a positive correlation between plasma vitamin E levels and the risk to develop AD in an advanced age [131].

Selenium levels were also affected in AD plasma with an association to the cognitive decline [132]. Nevertheless, the plasma levels of selenium seem to be independent from those of the brain [133]. The levels of seleno-containing enzyme Trx1 were also found to increase in the AD brains [134], in particular in glial cells, but not in neurons [135]. On the contrary, the long cleavage product of Trx1, Trx80, was drastically reduced in the brains and CSF from AD and MCI patients and it could be used to distinguish the stable MCI from the MCI that evolve later to AD [136].

6. Parkinson's Disease

Parkinson's disease (PD) is the second most prevalent neurodegenerative disorder, after AD, which is characterized by the progressive degeneration of the dopaminergic neurons located in the substantia nigra (SN) pars compacta [137]. The main neuropathological hallmark of PD is the presence of intracellular inclusions known as Lewy bodies (LBs) and neurites (LNs) [138], predominantly composed by misfolded and aggregated forms of the presynaptic protein α-synuclein [139].

The implication of mitochondrial dysfunction in the pathology of PD has been shown for a long time [140, 141]. The aging-related mitochondrial decline and the increasing mtDNA damage/mutations are also been associated with the increased risk for PD [142]. Indeed, it has been reported that mtDNA can impair the capacity of the organelle quality control mechanisms and thereby amplify the initial insult through a progressively increase of metabolic dysfunction and oxidative stress [143]. In particular, in some models of PD, it has been shown that environmental xenobiotics were extremely toxic and caused mitochondrial dysfunction in dopaminergic neurons leading to parkinsonian phenotypes [144].

Furthermore, the protein α-synuclein associated with PD pathogenesis is known to target the mitochondria and to decrease their function [140–142, 145, 146]. Notably, a decline of complex I activity and elevated intracellular ROS have been reported in the SN of the postmortem brain of PD patients [140, 147]. The implication of the mitochondria in PD is also supported by the presence of PD-related genes such as PINK1, PARK2 (Parkin), DJ-1, and LRRK2 which regulate mitochondrial and ROS homeostasis [148–151]. PINK1 deficiency results in impaired respiration with inhibition of complex I, and mutations in PINK1 gene cause a recessive form of PD [152, 153]. Abnormal ROS production in the mitochondria of PINK1 knockout neurons has been found to inhibit the mitochondrial Na^{2+}/Ca^{2+} exchanger or glucose transporter and to be prevented by antioxidants [152, 154]. Mitochondrial ROS play an important role not only in the pathology of PINK1 (mutation or deficiency) but also in the physiology of PINK1/Parkin-related mitophagy, by the induction of mitochondrial recruitment of Parkin [155]. In addition, it has recently been reported that mitochondrial ROS production in familial and sporadic forms of PD caused DNA damage and activated the PARP enzyme-associated DNA repair mechanism [156].

Although monomeric α-synuclein is a physiological regulator of synaptic transduction and mitochondrial bioenergetics [157], the oligomeric species appeared toxic for cells [62, 158], inhibited mitochondrial complex I [159], and induced mitochondrial depolarization [160]. In addition, oligomeric α-synuclein caused ROS production [158] independently of the known enzymatic pathways that affected mitochondrial function and induced lipid peroxidation [161]. The role of α-synuclein in mitophagy, mitochondrial fission/fusion, and protein trafficking to this organelle has also been shown [162]. Neurodegenerative impairments were also found in α-synuclein transgenic mice through the activation of mPTP [163]. The opening of mPTP appeared to be induced by oligomeric α-synuclein with respect to the monomeric protein, due to their ability to induce calcium signal in a structure-specific manner [164] and to produce ROS in the presence of free metal ions [165].

In addition to the mitochondrial dysfunction and ROS production, PD is characterized by an overall increase of end-product markers of oxidative and nitrosative stress that reflects an extensive damage on the biomolecules. This strongly suggests that these three processes are interconnected and create a cascade of events promoting a neurodegenerative condition like PD. The SN from the postmortem brains showed increased protein carbonyl levels at high molecular weight compared to the control brains or other brain regions [165]. The levels of protein nitration were also found to increase in the PD brains [166]. A recent study showed increased α-synuclein nitration levels in the brain from individuals with synucleinopathy, suggesting a direct link between nitrosative damage and the progression of neurodegenerative synucleinopathies [167]. Interestingly, an *in vitro* study showed the nitration of mitochondrial complex I that might trigger overtime a cascade of deleterious events enhancing the overall oxidative damage in PD [168]. The postmortem brains of PD patients showed increased levels of lipid peroxidation markers and oxidized proteins [169]. In particular, HNE adducts were identified in dopaminergic cells of SN, CSF, and plasma from PD patients [170, 171] and significant differences were found in plasma of PD subjects treated with L-dopa therapy [171]. Moreover, MDA levels were found to be high and attached to α-synuclein in the SN and frontal cortex of PD cases [172] supporting the idea that lipid peroxidation might precede and contribute to α-synuclein aggregation. In PD plasma, MDA levels were also found to be increased and inversely related to the age of patients [173]. Glycation also showed a strong immunoreactivity in the SN and locus coeruleus of PD patients [174], suggesting its involvement in the chemical cross-linking, proteolytic resistance, and aggregation process. Overall, the levels of glycated proteins were significantly higher in the cerebral cortex of PD patients compared to age-matched controls [175]. Since in PD the catabolic pathway activity of the most glycation agents is lower [176], the AGE concentration rises up leading to the death of dopaminergic neurons. About DNA and RNA oxidation, the levels of 8-OHdG and 8-OHG were also found to be increased in different brain regions, including SN, in serum and CFS [177, 178].

The antioxidant status of PD was found significantly modified compared to age-matched healthy subjects, as well as in AD. In particular, SOD levels, but not the activity, were found to increase in the SN and basal ganglia from PD patients [179]. In contrast, the levels of other antioxidant enzymes such as CAT, GPx, and GR did not change in PD compared to the age-matched healthy subject [179]. GSH levels were found to decrease only in the SN [180]. Interestingly, blood GSH/GSSG ratio was found to increase when the patients stopped to take PD medication such as dopamine receptor agonist suggesting how the medication could strongly influence the peripheral redox status [181].

Anyway, studies in the animal models of PD showed different outcomes compared to the human sample analysis with a degree of controversy [182, 183] probably due to the temporal length of the experimental observation time.

7. Amyotrophic Lateral Sclerosis

Amyotrophic lateral sclerosis (ALS) is a neurodegenerative disease characterized by progressive loss of motor neurons in the anterior horn of the spinal cord, leading to muscle weakness, wasting, and spasticity [184]. ALS is classified as either familial or sporadic depending on whether there is a clearly defined, inherited genetic element. The onset of sporadic (sALS) is unknown, and thus, the identification of causal genes and environmental factors remains elusive. Mutations in the first ALS gene superoxide dismutase 1 (SOD1) were found in 1993 to segregate in several fALS pedigrees [185] and subsequently in a small number of unrelated sALS cases [186]. Fifteen years later, TAR DNA binding protein 43 (TDP-43) is found to be an important constituent of protein aggregates frequently observed in postmortem material of ALS patients [187]. Although it is not yet clear how such aggregates trigger neurodegeneration in ALS, mutations in the TDP-43 gene were reported in 3% of fALS and 1-5% of patients with sALS, suggesting that TDP-43 aggregates have a

central role in triggering ALS [188, 189]. The number of ALS genes increases and it appears that the mutant proteins encoded are involved in a variety of critical processes, including mitochondria function.

The link of mitochondria to ALS has been defined by the mutations in SOD1 gene since they were found in 20% of the fALS [190]. SOD1 is an ubiquitous enzyme with several functions, including scavenger of excessive superoxide radical ($O_2^{-\cdot}$) into oxygen, modulation of cellular respiration, energy metabolism, and posttranslational modification [191]. Several SOD1 mutations were shown to affect the folding of the protein, and it is believed that the ensuing toxic gain of function might be caused by the accumulation of misfolded proteins inside the intermembrane space of mitochondria [192] with generation of free radicals that eventually lead to cell injury and death [193, 194]. Even if this may not be the main triggering mechanism, it is nonetheless recognized that mitochondrial dysfunction is central to SOD1 pathogenesis [195]. Although SOD dysfunction leads to a loss of antioxidant capability, evidences have shown that the silencing of SOD1 in mice does not lead to neurodegenerative conditions [196]. In contrast, it has recently been reported that mutant SOD1 can disturb the amino acid biosynthesis of cells in a yeast model and mediate cellular destruction, accounting for the neural degeneration in ALS [197]. In addition, the reduction of the mitochondrial ROS in neurons of a double UCP-SOD1 transgenic mouse model did not recover mitochondrial function and accelerated the progression of the disease [198]. The activity of SOD was also found to reduce in red blood cells from ALS patients [199], while SOD1 activity in the CSF showed conflicting results [200, 201].

Mitochondrial oxidative damage has also been demonstrated in patients affected by sALS [202] and in a transgenic mouse model expressing a fALS-linked mutant Cu/Zn SOD1 [203]. The spinal cord and motor cortex showed increased levels of protein carbonyls, nitrosative stress, and NOS [204, 205] suggesting selectivity about protein oxidation and nitration in ALS. Mutations of other genes associated with ALS, such as TDP-43, FUS/TLS, and p62, were also found to increase mitochondrial ROS and oxidative stress [206, 207]. In addition, exogenous-added TDP-43 aggregates were found to accumulate in the cytosol of neuronal cells causing intracellular ROS production [208].

Modifications in HNE-bound proteins have been detected in ventral horn motor neurons [209], and high free HNE levels were found high in CSF and serum of ALS patients [210, 211] suggesting a diffusion of HNE from the brain to the periphery. Proteomic analysis on the spinal cord of an ALS mouse model and in CSF [212] revealed an increase in lipid peroxidation, which was also found to increase the levels of MDA-protein adducts in the lumbar spinal and cervical cord before the onset of clinical motor signs in a murine model of ALS [213]. Despite acrolein-protein adducts were not detectable in the spinal cord of ALS patients, free MDA detection has been also confirmed in ALS subjects [205].

Glycation was first detected in the spinal cord and brain samples of both sALS and fALS [214, 215] as well as in SOD1 transgenic mice. Surprisingly, the levels of soluble RAGE were found lower in serum of ALS patients with respect to control subjects [216]. From a mechanistical point of view, *in vitro* glycation affected negatively the structure and the activity of SOD1 [217]. The roles of mRNA and DNA oxidation were showed for the first time in a mouse model of ALS, suggesting the presence of an early event before the degeneration of the motor neurons and appearance of all the symptoms. ALS patients presented an increase of nuclear 8-OHdG in the motor cortex and 10-fold higher in the spinal cord tissue [205], as well as in plasma, urine, and CSF, compared to healthy people [218].

In addition to SOD1, other antioxidants showed changes in level and activity in peripheral tissues or CFS. Anyway, the modification of GSH, GPx, and GR activities appears fluctuating in the analyzed samples, suggesting a grade of variability [219], together with the variability of the pathogenic mechanisms that both lead to a fluctuation in the antioxidant profiles of ALS patients [220]. In some studies, the levels and the activities of these enzymes were found to decrease in erythrocytes [221] and in the motor cortex [222] from ALS patients. However, in another study, the GSSG/GSH ratio was found to decrease [223], and the GPx level and the GR activity were enhanced in erythrocytes, serum, and CSF [201, 224, 225]. Moreover, other studies showed that GR activity in red blood cells from ALS patients did not change, whereas CAT levels and activity were diminished [201, 224]. In addition, plasma levels of nonenzymatic antioxidants were inconsistent, with some studies showing elevated levels [226] and other with no change [227] proving again the grade of variability of the disease.

8. Mitochondrial Dynamics and Neurodegeneration

Mitochondria are organelles with high mobility inside the cells. They can change size, morphology, and position and can also suffer fission and fusion. Fission is the process to obtain two or more daughter mitochondria from the division of a single. Fusion is the opposite: the union of two or more mitochondria to form a unique structure [228] (Figure 3). Fission and fusion are normal processes that occur continuously in many cell types. Fission is facilitated by Drp1, a protein with GTPase activity which in the mitochondrial outer membrane forms chains promoting the mitochondrial division. The chain is stabilized by MiD49 and MiD51 proteins that previously form a complex with Mff and Fis1 (Figure 3). Fusion is mediated by OPA-1 which controls the mitochondrial inner membrane fusion and by Mfn1 and Mfn2 which control the mitochondrial outer membrane fusion [229] (Figure 3).

Mitochondrial dynamics were found to be impaired in neurodegeneration. In particular, the AD brains showed abnormal expression of mitochondrial fusion and fission proteins [230], but the results are controversial. Indeed, Wang et al. reported that levels of Opa1, Drp1, Mfn1, and Mfn2 are significantly decreased, whereas the levels of Fis1 increased in the hippocampus of AD patients [231]. However, another study found increased levels of Fis1 and Drp1 and decreased levels of Mfn1, Mfn2, and Opa1 in the AD

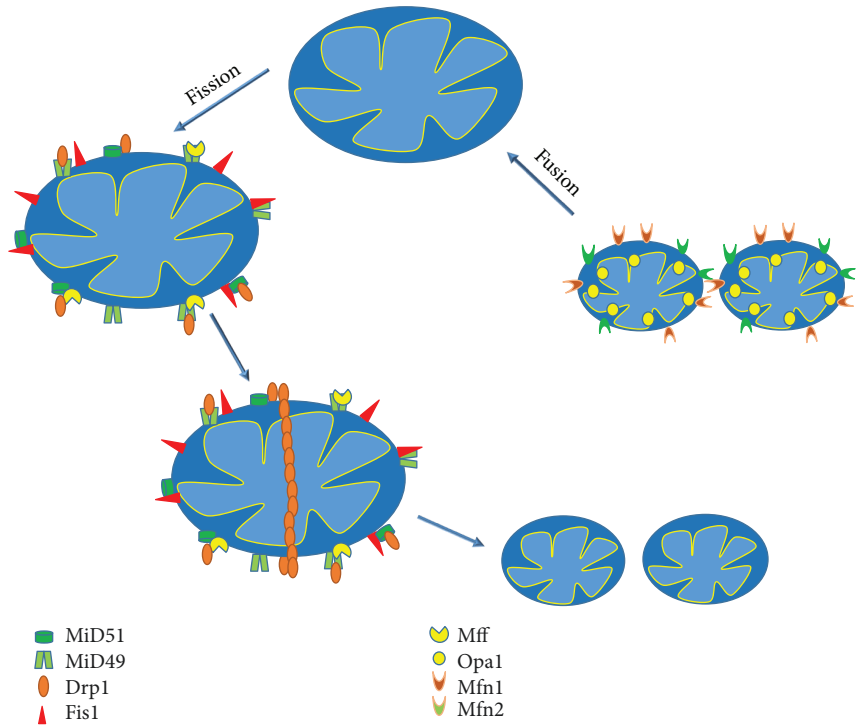

Figure 3: Schematic representation of mitochondrial dynamics. Drp1 in mitochondrial outer membrane forms chains promoting fission. The chain is stabilized by MiD49-Mff/Fis1 and MiD51-Mff/Fis1 complexes. Fusion is mediated by OPA-1 in the mitochondrial inner membrane and by Mfn1 and Mfn2 in the mitochondrial outer membrane. Drp1: dynamin-related protein-1; Fis1: mitochondrial fission protein 1; Mff: mitochondrial fission factor; MiD49: mitochondrial dynamics proteins of 49 kDa; MiD51: mitochondrial dynamic proteins of 51 kDa; OPA-1: optic atrophy 1; Mfn1: mitofusins 1; Mfn2: mitofusins 2.

frontal cortex [232]. Moreover, the knock-in mouse Drp1+/- crossed with a mouse model of AD exhibited improved mitochondrial function [233].

Mitochondrial fission and fusion were also found to be altered in PD patients, with increased levels of p-Drp1 in white cells [234]. Moreover, α-synuclein induced the inhibition of mitochondrial fusion [235] by interacting with outer membrane lipids. Experiments performed in Drosophila showed that Parkin and PINK1 regulate mitochondrial dynamics in a Drp1-depending manner [236]. Both proteins are implicated in mitophagy [237] and also in mitochondrial distribution in axons [238]. DJ-1, another important PD-related protein, also regulates mitochondrial fission as consequence of a race in ROS production and its effects can be reversed by overexpression of Parkin and PINK1 [239]. Moreover, LRRK2 was also found to change Drp1 leading to mitochondrial fragmentation [240].

Lastly, mitochondrial dynamics were also altered in ALS. Indeed, an increase in mitochondrial fission is due to excessive Drp1 levels in the ALS models [241]. Moreover, changes in the levels of Fis1, Mfn1, OPA1, and Drp1 preceded motoneuron loss and symptom onset in SOD1 mutant [242]. Mitochondrial fragmentation was also found to increase both in mutant TDP-43 and FUS, and the expression of mitochondrial fission and fusion regulators appeared modified [243, 244]. Moreover, the inactivation of Drp1 or Mfn2 prevented the deficits in mitochondrial trafficking in motoneurons of mutant SOD1 or TDP-43 [243, 245].

Taking into account that mitochondrial fission and fusion proteins regulate the assembly of respiratory complexes, the direct involvement of mitochondrial fission and fusion dynamics in mitochondrial bioenergetics could be central [246]. Therefore, it is reasonable to point out that altered mitochondrial fission and fusion is probably a mechanism leading to mitochondrial dysfunction in neurodegeneration.

9. Conclusion

Neurodegenerative diseases are becoming increasingly prevalent in our aged populations, thus representing a primary health problem especially for this age group [4, 247]. Tremendous efforts have been already made to identify neuropathological, biochemical, and genetic biomarkers of the diseases for a diagnosis at earlier stages.

In the past thirty years, an extensive research has been performed to understand the role of mitochondria and oxidative stress not only in physiological aging, but also in neurodegenerative diseases. The whole outcome clearly affirms that both processes get impaired during aging and are established features significantly involved in the progress, if not the onset, of neurodegenerative disorders. In this moment, it is still not clear if mitochondrial dysfunction and oxidative stress could be used as markers for an early detection of aging dysfunctions or be a valid therapeutic target. However, a better knowledge of the mechanism involving mitochondria and oxidative stress in the aging process and neurodegeneration may elicit new strategies for improving the quality of life of

the elderly and it would have a positive impact on the entire modern society.

Conflicts of Interest

The authors declare that there is no conflict of interests regarding the publication of this paper.

Authors' Contributions

Giovanna Cenini and Ana Lloret have contributed equally to the manuscript.

References

[1] T. Niccoli and L. Partridge, "Ageing as a risk factor for disease," *Current Biology*, vol. 22, no. 17, pp. R741–R752, 2012.

[2] Alzheimer's Association, "2016 Alzheimer's disease facts and figures," *Alzheimer's & Dementia*, vol. 12, no. 4, pp. 459–509, 2016.

[3] P. Ibáñez, A. M. Bonnet, B. Débarges et al., "Causal relation between α-synuclein locus duplication as a cause of familial Parkinson's disease," *The Lancet*, vol. 364, no. 9440, pp. 1169–1171, 2004.

[4] P. Schönfeld and G. Reiser, "Why does brain metabolism not favor burning of fatty acids to provide energy? - Reflections on disadvantages of the use of free fatty acids as fuel for brain," *Journal of Cerebral Blood Flow & Metabolism*, vol. 33, no. 10, pp. 1493–1499, 2013.

[5] E. F. Smith, P. J. Shaw, and K. J. de Vos, "The role of mitochondria in amyotrophic lateral sclerosis," *Neuroscience Letters*, 2017.

[6] B. G. Hill, G. A. Benavides, J. R. Lancaster et al., "Integration of cellular bioenergetics with mitochondrial quality control and autophagy," *Biological Chemistry*, vol. 393, no. 12, pp. 1485–1512, 2012.

[7] M. P. Mattson, M. Gleichmann, and A. Cheng, "Mitochondria in neuroplasticity and neurological disorders," *Neuron*, vol. 60, no. 5, pp. 748–766, 2008.

[8] K. T. Kishida and E. Klann, "Sources and targets of reactive oxygen species in synaptic plasticity and memory," *Antioxidants & Redox Signaling*, vol. 9, no. 2, pp. 233–244, 2007.

[9] A. C. Rego and C. R. Oliveira, "Mitochondrial dysfunction and reactive oxygen species in excitotoxicity and apoptosis: implications for the pathogenesis of neurodegenerative diseases," *Neurochemical Research*, vol. 28, no. 10, pp. 1563–1574, 2003.

[10] H. P. Indo, H. C. Yen, I. Nakanishi et al., "A mitochondrial superoxide theory for oxidative stress diseases and aging," *Journal of Clinical Biochemistry and Nutrition*, vol. 56, no. 1, pp. 1–7, 2015.

[11] A. Grimm, K. Friedland, and A. Eckert, "Mitochondrial dysfunction: the missing link between aging and sporadic Alzheimer's disease," *Biogerontology*, vol. 17, no. 2, pp. 281–296, 2016.

[12] J. N. Cobley, M. L. Fiorello, and D. M. Bailey, "13 reasons why the brain is susceptible to oxidative stress," *Redox Biology*, vol. 15, pp. 490–503, 2018.

[13] R. T. Dean, S. Fu, R. Stocker, and M. J. Davies, "Biochemistry and pathology of radical-mediated protein oxidation," *Biochemical Journal*, vol. 324, no. 1, pp. 1–18, 1997.

[14] D. A. Butterfield and E. R. Stadtman, "Chapter 7 Protein oxidation processes in aging brain," *Advances in Cell Aging and Gerontology*, vol. 2, pp. 161–191, 1997.

[15] B. Balcz, L. Kirchner, N. Cairns, M. Fountoulakis, and G. Lubec, "Increased brain protein levels of carbonyl reductase and alcohol dehydrogenase in Down syndrome and Alzheimer's disease," in *Protein Expression in Down Syndrome Brain*, G. Lubec, Ed., vol. 61, pp. 193–201, Springer, Vienna, 2001.

[16] S. Bartesaghi and R. Radi, "Fundamentals on the biochemistry of peroxynitrite and protein tyrosine nitration," *Redox Biology*, vol. 14, pp. 618–625, 2018.

[17] T. T. Reed, "Lipid peroxidation and neurodegenerative disease," *Free Radical Biology and Medicine*, vol. 51, no. 7, pp. 1302–1319, 2011.

[18] A. Winczura, D. Zdżalik, and B. Tudek, "Damage of DNA and proteins by major lipid peroxidation products in genome stability," *Free Radical Research*, vol. 46, no. 4, pp. 442–459, 2012.

[19] G. Vistoli, D. de Maddis, A. Cipak, N. Zarkovic, M. Carini, and G. Aldini, "Advanced glycoxidation and lipoxidation end products (AGEs and ALEs): an overview of their mechanisms of formation," *Free Radical Research*, vol. 47, Supplement 1, pp. 3–27, 2013.

[20] N. Ahmed, "Advanced glycation endproducts—role in pathology of diabetic complications," *Diabetes Research and Clinical Practice*, vol. 67, no. 1, pp. 3–21, 2005.

[21] M. S. Cooke, M. D. Evans, M. Dizdaroglu, and J. Lunec, "Oxidative DNA damage: mechanisms, mutation, and disease," *The FASEB Journal*, vol. 17, no. 10, pp. 1195–1214, 2003.

[22] H. J. Helbock, K. B. Beckman, and B. N. Ames, "8-Hydroxydeoxyguanosine and 8-hydroxyguanine as biomarkers of oxidative DNA damage," *Methods in Enzymology*, vol. 300, pp. 156–166, 1999.

[23] S. Dukan, A. Farewell, M. Ballesteros, F. Taddei, M. Radman, and T. Nystrom, "Protein oxidation in response to increased transcriptional or translational errors," *Proceedings of the National Academy of Sciences of the United States of America*, vol. 97, no. 11, pp. 5746–5749, 2000.

[24] H. Rodriguez-Rocha, A. Garcia-Garcia, C. Pickett et al., "Compartmentalized oxidative stress in dopaminergic cell death induced by pesticides and complex I inhibitors: distinct roles of superoxide anion and superoxide dismutases," *Free Radical Biology and Medicine*, vol. 61, pp. 370–383, 2013.

[25] R. Brigelius-Flohé and M. G. Traber, "Vitamin E: function and metabolism," *The FASEB Journal*, vol. 13, no. 10, pp. 1145–1155, 1999.

[26] D. Harman, "Aging: a theory based on free radical and radiation chemistry," *Journal of Gerontology*, vol. 11, no. 3, pp. 298–300, 1956.

[27] J. Miquel, A. C. Economos, J. Fleming, and J. E. Johnson Jr, "Mitochondrial role in cell aging," *Experimental Gerontology*, vol. 15, no. 6, pp. 575–591, 1980.

[28] T. E. S. Kauppila, J. H. K. Kauppila, and N. G. Larsson, "Mammalian mitochondria and aging: an update," *Cell Metabolism*, vol. 25, no. 1, pp. 57–71, 2017.

[29] C. López-Otín, M. A. Blasco, L. Partridge, M. Serrano, and G. Kroemer, "The hallmarks of aging," *Cell*, vol. 153, no. 6, pp. 1194–1217, 2013.

[30] B. A. I. Payne and P. F. Chinnery, "Mitochondrial dysfunction in aging: much progress but many unresolved questions," *Biochimica et Biophysica Acta (BBA) - Bioenergetics*, vol. 1847, no. 11, pp. 1347–1353, 2015.

[31] J. Sastre, F. V. Pallardó, R. Plá et al., "Aging of the liver: age-associated mitochondrial damage in intact hepatocytes," *Hepatology*, vol. 24, no. 5, pp. 1199–1205, 1996.

[32] T. M. Hagen, D. L. Yowe, J. C. Bartholomew et al., "Mitochondrial decay in hepatocytes from old rats: membrane potential declines, heterogeneity and oxidants increase," *Proceedings of the National Academy of Sciences of the United States of America*, vol. 94, no. 7, pp. 3064–3069, 1997.

[33] M. Greco, G. Villani, F. Mazzucchelli, N. Bresolin, S. Papa, and G. Attardi, "Marked aging-related decline in efficiency of oxidative phosphorylation in human skin fibroblasts," *The FASEB Journal*, vol. 17, no. 12, pp. 1706–1708, 2003.

[34] A. P. Halestrap and A. P. Richardson, "The mitochondrial permeability transition: a current perspective on its identity and role in ischaemia/reperfusion injury," *Journal of Molecular and Cellular Cardiology*, vol. 78, pp. 129–141, 2015.

[35] J. Ojaimi, C. L. Masters, K. Opeskin, P. McKelvie, and E. Byrne, "Mitochondrial respiratory chain activity in the human brain as a function of age," *Mechanisms of Ageing and Development*, vol. 111, no. 1, pp. 39–47, 1999.

[36] I. Trounce, E. Byrne, and S. Marzuki, "Decline in skeletal muscle mitochondrial respiratory chain function: possible factor in ageing," *The Lancet*, vol. 333, no. 8639, pp. 637–4639, 1989.

[37] H. Chen and D. C. Chan, "Mitochondrial dynamics–fusion, fission, movement, and mitophagy–in neurodegenerative diseases," *Human Molecular Genetics*, vol. 18, no. R2, pp. R169–R176, 2009.

[38] S. Lee, S. Y. Jeong, W. C. Lim et al., "Mitochondrial fission and fusion mediators, hFis1 and OPA1, modulate cellular senescence," *Journal of Biological Chemistry*, vol. 282, no. 31, pp. 22977–22983, 2007.

[39] J. G. de la Asuncion, A. Millan, R. Pla et al., "Mitochondrial glutathione oxidation correlates with age-associated oxidative damage to mitochondrial DNA," *The FASEB Journal*, vol. 10, no. 2, pp. 333–338, 1996.

[40] M. Hayakawa, K. Hattori, S. Sugiyama, and T. Ozawa, "Age-associated oxygen damage and mutations in mitochondrial DNA in human hearts," *Biochemical and Biophysical Research Communications*, vol. 189, no. 2, pp. 979–985, 1992.

[41] Y. Michikawa, F. Mazzucchelli, N. Bresolin, G. Scarlato, and G. Attardi, "Aging-dependent large accumulation of point mutations in the human mtDNA control region for replication," *Science*, vol. 286, no. 5440, pp. 774–779, 1999.

[42] H. C. Lee, C. Y. Pang, H. S. Hsu, and Y. H. Wei, "Differential accumulations of 4,977 bp deletion in mitochondrial DNA of various tissues in human ageing," *Biochimica et Biophysica Acta (BBA) - Molecular Basis of Disease*, vol. 1226, no. 1, pp. 37–43, 1994.

[43] Y. H. Wei, C. Y. Pang, B. J. You, and H. C. Lee, "Tandem duplications and large-scale deletions of mitochondrial DNA are early molecular events of human aging process," *Annals of the New York Academy of Sciences*, vol. 786, no. 1, pp. 82–101, 1996.

[44] D. R. Crawford, Y. Wang, G. P. Schools, J. Kochheiser, and K. J. A. Davies, "Down-regulation of mammalian mitochondrial RNAs during oxidative stress," *Free Radical Biology and Medicine*, vol. 22, no. 3, pp. 551–559, 1997.

[45] S. Reeg and T. Grune, "Protein oxidation in aging: does it play a role in aging progression?," *Antioxidants & Redox Signaling*, vol. 23, no. 3, pp. 239–255, 2015.

[46] G. Lippe, M. Comelli, D. Mazzilis, F. D. Sala, and I. Mavelli, "The inactivation of mitochondrial F_1 ATPase by H_2O_2 is mediated by iron ions not tightly bound in the protein," *Biochemical and Biophysical Research Communications*, vol. 181, no. 2, pp. 764–770, 1991.

[47] G. Paradies, F. M. Ruggiero, G. Petrosillo, and E. Quagliariello, "Age-dependent decline in the cytochrome *c* oxidase activity in rat heart mitochondria: role of cardiolipin," *FEBS Letters*, vol. 406, no. 1-2, pp. 136–138, 1997.

[48] M. Musa, M. Perić, P. Bou Dib et al., "Heat-induced longevity in budding yeast requires respiratory metabolism and glutathione recycling," *Aging*, vol. 10, no. 9, pp. 2407–2427, 2018.

[49] E. Sahin, S. Colla, M. Liesa et al., "Telomere dysfunction induces metabolic and mitochondrial compromise," *Nature*, vol. 470, no. 7334, pp. 359–365, 2011.

[50] A. Dabrowska, J. L. Venero, R. Iwasawa et al., "PGC-1α controls mitochondrial biogenesis and dynamics in lead-induced neurotoxicity," *Aging*, vol. 7, no. 9, pp. 629–643, 2015.

[51] E. F. Fang, M. Scheibye-Knudsen, L. E. Brace et al., "Defective mitophagy in XPA via PARP-1 hyperactivation and NAD^+/SIRT1 reduction," *Cell*, vol. 157, no. 4, pp. 882–896, 2014.

[52] S. Garcia, N. Nissanka, E. A. Mareco et al., "Overexpression of PGC-1α in aging muscle enhances a subset of young-like molecular patterns," *Aging Cell*, vol. 17, no. 2, article e12707, 2018.

[53] C. Correia-Melo, F. D. M. Marques, R. Anderson et al., "Mitochondria are required for pro-ageing features of the senescent phenotype," *The EMBO Journal*, vol. 35, no. 7, pp. 724–742, 2016.

[54] A. Terman, T. Kurz, M. Navratil, E. A. Arriaga, and U. T. Brunk, "Mitochondrial turnover and aging of long-lived postmitotic cells: the mitochondrial–lysosomal axis theory of aging," *Antioxidants & Redox Signaling*, vol. 12, no. 4, pp. 503–535, 2010.

[55] A. Kowald and T. B. L. Kirkwood, "Accumulation of defective mitochondria through delayed degradation of damaged organelles and its possible role in the ageing of post-mitotic and dividing cells," *Journal of Theoretical Biology*, vol. 202, no. 2, pp. 145–160, 2000.

[56] A. Y. Abramov, A. V. Berezhnov, E. I. Fedotova, V. P. Zinchenko, and L. P. Dolgacheva, "Interaction of misfolded proteins and mitochondria in neurodegenerative disorders," *Biochemical Society Transactions*, vol. 45, no. 4, pp. 1025–1033, 2017.

[57] H. W. Querfurth and F. M. LaFerla, "Alzheimer's disease," *New England Journal of Medicine*, vol. 362, no. 4, pp. 329–344, 2010.

[58] D. J. Selkoe and J. Hardy, "The amyloid hypothesis of Alzheimer's disease at 25 years," *EMBO Molecular Medicine*, vol. 8, no. 6, pp. 595–608, 2016.

[59] B. De Strooper and E. Karran, "The cellular phase of Alzheimer's disease," *Cell*, vol. 164, no. 4, pp. 603–615, 2016.

[60] E. Ferreiro, C. R. Oliveira, and C. M. F. Pereira, "The release of calcium from the endoplasmic reticulum induced by amyloid-beta and prion peptides activates the mitochondrial

apoptotic pathway," *Neurobiology of Disease*, vol. 30, no. 3, pp. 331–342, 2008.

[61] D. J. Bonda, X. Wang, G. Perry et al., "Oxidative stress in Alzheimer disease: a possibility for prevention," *Neuropharmacology*, vol. 59, no. 4-5, pp. 290–294, 2010.

[62] P. R. Angelova and A. Y. Abramov, "Alpha-synuclein and beta-amyloid – different targets, same players: calcium, free radicals and mitochondria in the mechanism of neurodegeneration," *Biochemical and Biophysical Research Communications*, vol. 483, no. 4, pp. 1110–1115, 2017.

[63] J. P. Sheehan, R. H. Swerdlow, S. W. Miller et al., "Calcium homeostasis and reactive oxygen species production in cells transformed by mitochondria from individuals with sporadic Alzheimer's disease," *The Journal of Neuroscience*, vol. 17, no. 12, pp. 4612–4622, 1997.

[64] H. Du, L. Guo, S. Yan, A. A. Sosunov, G. M. McKhann, and S. ShiDu Yan, "Early deficits in synaptic mitochondria in an Alzheimer's disease mouse model," *Proceedings of the National Academy of Sciences of the United States of America*, vol. 107, no. 43, pp. 18670–18675, 2010.

[65] C. Caspersen, N. Wang, J. Yao et al., "Mitochondrial Aβ: a potential focal point for neuronal metabolic dysfunction in Alzheimer's disease," *The FASEB Journal*, vol. 19, no. 14, pp. 2040-2041, 2005.

[66] C. S. Casley, L. Canevari, J. M. Land, J. B. Clark, and M. A. Sharpe, "β-amyloid inhibits integrated mitochondrial respiration and key enzyme activities," *Journal of Neurochemistry*, vol. 80, no. 1, pp. 91–100, 2002.

[67] "The mitochondria-targeted antioxidant MitoQ prevents loss of spatial memory retention and early neuropathology in a transgenic mouse model of Alzheimer's disease," *Journal of Neurochemistry*, vol. 31, no. 44, pp. 15703–15715, 2011.

[68] L. F. Ng, J. Gruber, I. K. Cheah et al., "The mitochondria-targeted antioxidant MitoQ extends lifespan and improves healthspan of a transgenic Caenorhabditis elegans model of Alzheimer disease," *Free Radical Biology and Medicine*, vol. 71, pp. 390–401, 2014.

[69] A. Elharram, N. M. Czegledy, M. Golod et al., "Deuterium-reinforced polyunsaturated fatty acids improve cognition in a mouse model of sporadic Alzheimer's disease," *The FEBS Journal*, vol. 284, no. 23, pp. 4083–4095, 2017.

[70] M. Zampagni, D. Wright, R. Cascella et al., "Novel *S*-acyl glutathione derivatives prevent amyloid oxidative stress and cholinergic dysfunction in Alzheimer disease models," *Free Radical Biology and Medicine*, vol. 52, no. 8, pp. 1362–1371, 2012.

[71] R. Cascella, E. Evangelisti, M. Zampagni et al., "*S*-linolenoyl glutathione intake extends life-span and stress resistance via Sir-2.1 upregulation in *Caenorhabditis elegans*," *Free Radical Biology and Medicine*, vol. 73, pp. 127–135, 2014.

[72] J. Viña, A. Lloret, S. L. Vallés et al., "Mitochondrial oxidant signalling in Alzheimer's disease," *Journal of Alzheimer's Disease*, vol. 11, no. 2, pp. 175–181, 2007.

[73] A. Lloret, M. C. Badía, N. J. Mora et al., "Gender and age-dependent differences in the mitochondrial apoptogenic pathway in Alzheimer's disease," *Free Radical Biology and Medicine*, vol. 44, no. 12, pp. 2019–2025, 2008.

[74] W. D. Parker Jr, C. M. Filley, and J. K. Parks, "Cytochrome oxidase deficiency in Alzheimer's disease," *Neurology*, vol. 40, no. 8, pp. 1302-1303, 1990.

[75] I. Maurer, S. Zierz, and H. J. Möller, "A selective defect of cytochrome c oxidase is present in brain of Alzheimer disease patients," *Neurobiology of Aging*, vol. 21, no. 3, pp. 455–462, 2000.

[76] D. F. Silva, J. E. Selfridge, J. Lu et al., "Bioenergetic flux, mitochondrial mass and mitochondrial morphology dynamics in AD and MCI cybrid cell lines," *Human Molecular Genetics*, vol. 22, no. 19, pp. 3931–3946, 2013.

[77] Z. Fisar, J. Hroudová, H. Hansíková et al., "Mitochondrial respiration in the platelets of patients with Alzheimer's disease," *Current Alzheimer Research*, vol. 13, no. 8, pp. 930–941, 2016.

[78] M. Armand-Ugon, B. Ansoleaga, S. Berjaoui, and I. Ferrer, "Reduced mitochondrial activity is early and steady in the entorhinal cortex but it is mainly unmodified in the frontal cortex in Alzheimer's disease," *Current Alzheimer Research*, vol. 14, no. 12, pp. 1327–1334, 2017.

[79] K. Lunnon, A. Keohane, R. Pidsley et al., "Mitochondrial genes are altered in blood early in Alzheimer's disease," *Neurobiology of Aging*, vol. 53, pp. 36–47, 2017.

[80] J. Smeitink, L. van den Heuvel, and S. DiMauro, "The genetics and pathology of oxidative phosphorylation," *Nature Reviews Genetics*, vol. 2, no. 5, pp. 342–352, 2001.

[81] K. C. Sonntag, W. I. Ryu, K. M. Amirault et al., "Late-onset Alzheimer's disease is associated with inherent changes in bioenergetics profiles," *Scientific Reports*, vol. 7, no. 1, article 14038, 2017.

[82] M. J. Pérez, D. P. Ponce, C. Osorio-Fuentealba, M. I. Behrens, and R. A. Quintanilla, "Mitochondrial bioenergetics is altered in fibroblasts from patients with sporadic Alzheimer's disease," *Frontiers in Neuroscience*, vol. 11, p. 553, 2017.

[83] P. Martín-Maestro, R. Gargini, E. García, G. Perry, J. Avila, and V. García-Escudero, "Slower dynamics and aged mitochondria in sporadic Alzheimer's disease," *Oxidative Medicine and Cellular Longevity*, vol. 2017, Article ID 9302761, 14 pages, 2017.

[84] V. Shoshan-Barmatz, E. Nahon-Crystal, A. Shteinfer-Kuzmine, and R. Gupta, "VDAC1, mitochondrial dysfunction, and Alzheimer's disease," *Pharmacological Research*, vol. 131, pp. 87–101, 2018.

[85] G. David and E. F. Barrett, "Mitochondrial Ca^{2+} uptake prevents desynchronization of quantal release and minimizes depletion during repetitive stimulation of mouse motor nerve terminals," *The Journal of Physiology*, vol. 548, no. 2, pp. 425–438, 2003.

[86] C. A. Hansson Petersen, N. Alikhani, H. Behbahani et al., "The amyloid β-peptide is imported into mitochondria via the TOM import machinery and localized to mitochondrial cristae," *Proceedings of the National Academy of Sciences of the United States of America*, vol. 105, no. 35, pp. 13145–13150, 2008.

[87] P. F. Pavlov, B. Wiehager, J. Sakai et al., "Mitochondrial γ-secretase participates in the metabolism of mitochondria-associated amyloid precursor protein," *The FASEB Journal*, vol. 25, no. 1, pp. 78–88, 2011.

[88] M. Manczak, T. S. Anekonda, E. Henson, B. S. Park, J. Quinn, and P. H. Reddy, "Mitochondria are a direct site of Aβ accumulation in Alzheimer's disease neurons: implications for free radical generation and oxidative damage in disease progression," *Human Molecular Genetics*, vol. 15, no. 9, pp. 1437–1449, 2006.

[89] C. Zhang, R. A. Rissman, and J. Feng, "Characterization of ATP alternations in an Alzheimer's disease transgenic mouse model," *Journal of Alzheimer's Disease*, vol. 44, no. 2, pp. 375–378, 2015.

[90] G. Cenini, C. Rüb, M. Bruderek, and W. Voos, "Amyloid β-peptides interfere with mitochondrial preprotein import competence by a coaggregation process," *Molecular Biology of the Cell*, vol. 27, no. 21, pp. 3257–3272, 2016.

[91] N. Bogdanovic, M. Zilmer, K. Zilmer, A. Rehema, and E. Karelson, "The Swedish APP670/671 Alzheimer's disease mutation: the first evidence for strikingly increased oxidative injury in the temporal inferior cortex," *Dementia and Geriatric Cognitive Disorders*, vol. 12, no. 6, pp. 364–370, 2001.

[92] R. Sultana, M. Perluigi, S. F. Newman et al., "Redox proteomic analysis of carbonylated brain proteins in mild cognitive impairment and early Alzheimer's disease," *Antioxidants & Redox Signaling*, vol. 12, no. 3, pp. 327–336, 2010.

[93] R. Sultana, H. F. Poon, J. Cai et al., "Identification of nitrated proteins in Alzheimer's disease brain using a redox proteomics approach," *Neurobiology of Disease*, vol. 22, no. 1, pp. 76–87, 2006.

[94] D. A. Butterfield, T. T. Reed, M. Perluigi et al., "Elevated levels of 3-nitrotyrosine in brain from subjects with amnestic mild cognitive impairment: implications for the role of nitration in the progression of Alzheimer's disease," *Brain Research*, vol. 1148, pp. 243–248, 2007.

[95] D. A. Butterfield, M. L. Bader Lange, and R. Sultana, "Involvements of the lipid peroxidation product, HNE, in the pathogenesis and progression of Alzheimer's disease," *Biochimica et Biophysica Acta (BBA) - Molecular and Cell Biology of Lipids*, vol. 1801, no. 8, pp. 924–929, 2010.

[96] W. R. Markesbery, R. J. Kryscio, M. A. Lovell, and J. D. Morrow, "Lipid peroxidation is an early event in the brain in amnestic mild cognitive impairment," *Annals of Neurology*, vol. 58, no. 5, pp. 730–735, 2005.

[97] T. J. Montine, J. Quinn, J. Kaye, and J. D. Morrow, "F_2-isoprostanes as biomarkers of late-onset Alzheimer's disease," *Journal of Molecular Neuroscience*, vol. 33, no. 1, pp. 114–119, 2007.

[98] M. Padurariu, A. Ciobica, L. Hritcu, B. Stoica, W. Bild, and C. Stefanescu, "Changes of some oxidative stress markers in the serum of patients with mild cognitive impairment and Alzheimer's disease," *Neuroscience Letters*, vol. 469, no. 1, pp. 6–10, 2010.

[99] R. Dei, A. Takeda, H. Niwa et al., "Lipid peroxidation and advanced glycation end products in the brain in normal aging and in Alzheimer's disease," *Acta Neuropathologica*, vol. 104, no. 2, pp. 113–122, 2002.

[100] R. Sultana and D. A. Butterfield, "Oxidatively modified GST and MRP1 in Alzheimer's disease brain: implications for accumulation of reactive lipid peroxidation products," *Neurochemical Research*, vol. 29, no. 12, pp. 2215–2220, 2004.

[101] M. L. Selley, D. R. Close, and S. E. Stern, "The effect of increased concentrations of homocysteine on the concentration of *(E)*-4-hydroxy-2-nonenal in the plasma and cerebrospinal fluid of patients with Alzheimer's disease," *Neurobiology of Aging*, vol. 23, no. 3, pp. 383–388, 2002.

[102] X. Liu, M. A. Lovell, and B. C. Lynn, "Development of a method for quantification of acrolein-deoxyguanosine adducts in DNA using isotope dilution-capillary LC/MS/MS and its application to human brain tissue," *Analytical Chemistry*, vol. 77, no. 18, pp. 5982–5989, 2005.

[103] M. D. Ledesma, P. Bonay, C. Colaço, and J. Avila, "Analysis of microtubule-associated protein tau glycation in paired helical filaments," *Journal of Biological Chemistry*, vol. 269, no. 34, pp. 21614–21619, 1994.

[104] M. Takeuchi, T. Sato, J. I. Takino et al., "Diagnostic utility of serum or cerebrospinal fluid levels of toxic advanced glycation end-products (TAGE) in early detection of Alzheimer's disease," *Medical Hypotheses*, vol. 69, no. 6, pp. 1358–1366, 2007.

[105] A. Hernanz, M. De la Fuente, M. Navarro, and A. Frank, "Plasma aminothiol compounds, but not serum tumor necrosis factor receptor II and soluble receptor for advanced glycation end products, are related to the cognitive impairment in Alzheimer's disease and mild cognitive impairment patients," *Neuroimmunomodulation*, vol. 14, no. 3-4, pp. 163–167, 2007.

[106] J. Wang, S. Xiong, C. Xie, W. R. Markesbery, and M. A. Lovell, "Increased oxidative damage in nuclear and mitochondrial DNA in Alzheimer's disease," *Journal of Neurochemistry*, vol. 93, no. 4, pp. 953–962, 2005.

[107] M. Corral-Debrinski, T. Horton, M. T. Lott et al., "Marked changes in mitochondrial DNA deletion levels in Alzheimer brains," *Genomics*, vol. 23, no. 2, pp. 471–476, 1994.

[108] P. E. Coskun, M. F. Beal, and D. C. Wallace, "Alzheimer's brains harbor somatic mtDNA control-region mutations that suppress mitochondrial transcription and replication," *Proceedings of the National Academy of Sciences of the United States of America*, vol. 101, no. 29, pp. 10726–10731, 2004.

[109] P. Mecocci, U. MacGarvey, and M. F. Beal, "Oxidative damage to mitochondrial DNA is increased in Alzheimer's disease," *Annals of Neurology*, vol. 36, no. 5, pp. 747–751, 1994.

[110] M. A. Lovell and W. R. Markesbery, "Oxidatively modified RNA in mild cognitive impairment," *Neurobiology of Disease*, vol. 29, no. 2, pp. 169–175, 2008.

[111] A. Nunomura, S. Chiba, C. F. Lippa et al., "Neuronal RNA oxidation is a prominent feature of familial Alzheimer's disease," *Neurobiology of Disease*, vol. 17, no. 1, pp. 108–113, 2004.

[112] A. Nunomura, G. Perry, M. A. Pappolla et al., "Neuronal oxidative stress precedes amyloid-β deposition in Down syndrome," *Journal of Neuropathology & Experimental Neurology*, vol. 59, no. 11, pp. 1011–1017, 2000.

[113] T. Abe, H. Tohgi, C. Isobe, T. Murata, and C. Sato, "Remarkable increase in the concentration of 8-hydroxyguanosine in cerebrospinal fluid from patients with Alzheimer's disease," *Journal of Neuroscience Research*, vol. 70, no. 3, pp. 447–450, 2002.

[114] R. Sultana, M. Piroddi, F. Galli, and D. A. Butterfield, "Protein levels and activity of some antioxidant enzymes in hippocampus of subjects with amnestic mild cognitive impairment," *Neurochemical Research*, vol. 33, no. 12, pp. 2540–2546, 2008.

[115] C. A. Massaad, "Neuronal and vascular oxidative stress in Alzheimers disease," *Current Neuropharmacology*, vol. 9, no. 4, pp. 662–673, 2011.

[116] D. L. Marcus, C. Thomas, C. Rodriguez et al., "Increased peroxidation and reduced antioxidant enzyme activity in Alzheimer's disease," *Experimental Neurology*, vol. 150, no. 1, pp. 40–44, 1998.

[117] M. C. Puertas, J. M. Martínez-Martos, M. P. Cobo, M. P. Carrera, M. D. Mayas, and M. J. Ramírez-Expósito, "Plasma oxidative stress parameters in men and women with early stage Alzheimer type dementia," *Experimental Gerontology*, vol. 47, no. 8, pp. 625–630, 2012.

[118] M. A. Lovell, C. Xie, and W. R. Markesbery, "Decreased glutathione transferase activity in brain and ventricular fluid in Alzheimer's disease," *Neurology*, vol. 51, no. 6, pp. 1562–1566, 1998.

[119] S. L. Duffy, J. Lagopoulos, I. B. Hickie et al., "Glutathione relates to neuropsychological functioning in mild cognitive impairment," *Alzheimer's & Dementia*, vol. 10, no. 1, pp. 67–75, 2014.

[120] D. Boyd-Kimball, H. F. Poon, B. C. Lynn et al., "Proteomic identification of proteins specifically oxidized in *Caenorhabditis elegans* expressing human Aβ(1–42): Implications for Alzheimer's disease," *Neurobiology of Aging*, vol. 27, no. 9, pp. 1239–1249, 2006.

[121] W. O. Opii, G. Joshi, E. Head et al., "Proteomic identification of brain proteins in the canine model of human aging following a long-term treatment with antioxidants and a program of behavioral enrichment: relevance to Alzheimer's disease," *Neurobiology of Aging*, vol. 29, no. 1, pp. 51–70, 2008.

[122] R. Sultana, T. Reed, M. Perluigi, R. Coccia, W. M. Pierce, and D. A. Butterfield, "Proteomic identification of nitrated brain proteins in amnestic mild cognitive impairment: a regional study," *Journal of Cellular and Molecular Medicine*, vol. 11, no. 4, pp. 839–851, 2007.

[123] W. Łuczaj, A. Gęgotek, and E. Skrzydlewska, "Antioxidants and HNE in redox homeostasis," *Free Radical Biology and Medicine*, vol. 111, pp. 87–101, 2017.

[124] Z. A. Wood, E. Schröder, J. Robin Harris, and L. B. Poole, "Structure, mechanism and regulation of peroxiredoxins," *Trends in Biochemical Sciences*, vol. 28, no. 1, pp. 32–40, 2003.

[125] M. E. Conway and C. Lee, "The redox switch that regulates molecular chaperones," *Biomolecular Concepts*, vol. 6, no. 4, pp. 269–284, 2015.

[126] H. F. Poon, S. A. Farr, W. A. Banks et al., "Proteomic identification of less oxidized brain proteins in aged senescence-accelerated mice following administration of antisense oligonucleotide directed at the Aβ region of amyloid precursor protein," *Molecular Brain Research*, vol. 138, no. 1, pp. 8–16, 2005.

[127] S. H. Kim, M. Fountoulakis, N. Cairns, and G. Lubec, "Protein levels of human peroxiredoxin subtypes in brains of patients with Alzheimer's disease and Down syndrome," *Journal of Neural Transmission. Supplementa*, vol. 61, pp. 223–235, 2001.

[128] F. Mangialasche, W. Xu, M. Kivipelto et al., "Tocopherols and tocotrienols plasma levels are associated with cognitive impairment," *Neurobiology of Aging*, vol. 33, no. 10, pp. 2282–2290, 2012.

[129] F. J. Jiménez-Jiménez, F. de Bustos, J. A. Molina et al., "Cerebrospinal fluid levels of alpha-tocopherol (vitamin E) in Alzheimer's disease," *Journal of Neural Transmission*, vol. 104, no. 6-7, pp. 703–710, 1997.

[130] P. Rinaldi, M. C. Polidori, A. Metastasio et al., "Plasma antioxidants are similarly depleted in mild cognitive impairment and in Alzheimer's disease," *Neurobiology of Aging*, vol. 24, no. 7, pp. 915–919, 2003.

[131] F. Mangialasche, M. Kivipelto, P. Mecocci et al., "High plasma levels of vitamin E forms and reduced Alzheimer's disease risk in advanced age," *Journal of Alzheimer's Disease*, vol. 20, no. 4, pp. 1029–1037, 2010.

[132] N. T. Akbaraly, I. Hininger-Favier, I. Carrière et al., "Plasma selenium over time and cognitive decline in the elderly," *Epidemiology*, vol. 18, no. 1, pp. 52–58, 2007.

[133] U. Schweizer, F. Streckfuß, P. Pelt et al., "Hepatically derived selenoprotein P is a key factor for kidney but not for brain selenium supply," *Biochemical Journal*, vol. 386, no. 2, pp. 221–226, 2005.

[134] V. Calabrese, R. Sultana, G. Scapagnini et al., "Nitrosative stress, cellular stress response, and thiol homeostasis in patients with Alzheimer's disease," *Antioxidants & Redox Signaling*, vol. 8, no. 11-12, pp. 1975–1986, 2006.

[135] S. Akterin, R. F. Cowburn, A. Miranda-Vizuete et al., "Involvement of glutaredoxin-1 and thioredoxin-1 in β-amyloid toxicity and Alzheimer's disease," *Cell Death & Differentiation*, vol. 13, no. 9, pp. 1454–1465, 2006.

[136] F. Gil-Bea, S. Akterin, T. Persson et al., "Thioredoxin-80 is a product of alpha-secretase cleavage that inhibits amyloid-beta aggregation and is decreased in Alzheimer's disease brain," *EMBO Molecular Medicine*, vol. 4, no. 10, pp. 1097–1111, 2012.

[137] L. M. Bekris, I. F. Mata, and C. P. Zabetian, "The genetics of Parkinson disease," *Journal of Geriatric Psychiatry and Neurology*, vol. 23, no. 4, pp. 228–242, 2010.

[138] L. S. Forno, "Neuropathology of Parkinson's Disease," *Journal of Neuropathology and Experimental Neurology*, vol. 55, no. 3, pp. 259–272, 1996.

[139] M. G. Spillantini, R. A. Crowther, R. Jakes, M. Hasegawa, and M. Goedert, "α-Synuclein in filamentous inclusions of Lewy bodies from Parkinson's disease and dementia with Lewy bodies," *Proceedings of the National Academy of Sciences of the United States of America*, vol. 95, no. 11, pp. 6469–6473, 1998.

[140] A. H. V. Schapira, J. M. Cooper, D. Dexter, P. Jenner, J. B. Clark, and C. D. Marsden, "Mitochondrial complex I deficiency in Parkinson's disease," *The Lancet*, vol. 333, no. 8649, article 1269, 1989.

[141] W. D. Parker Jr and R. H. Swerdlow, "Mitochondrial dysfunction in idiopathic Parkinson disease," *The American Journal of Human Genetics*, vol. 62, no. 4, pp. 758–762, 1998.

[142] A. H. V. Schapira and M. Gegg, "Mitochondrial contribution to Parkinson's disease pathogenesis," *Parkinson's Disease*, vol. 2011, article 159160, 7 pages, 2011.

[143] M. P. Murphy, "How mitochondria produce reactive oxygen species," *Biochemical Journal*, vol. 417, no. 1, pp. 1–13, 2009.

[144] M. I. Ekstrand, M. Terzioglu, D. Galter et al., "Progressive parkinsonism in mice with respiratory-chain-deficient dopamine neurons," *Proceedings of the National Academy of Sciences of the United States of America*, vol. 104, no. 4, pp. 1325–1330, 2007.

[145] H. Elkon, J. Don, E. Melamed, I. Ziv, A. Shirvan, and D. Offen, "Mutant and wild-type α-synuclein interact with mitochondrial cytochrome C oxidase," *Journal of Molecular Neuroscience*, vol. 18, no. 3, pp. 229–238, 2002.

[146] L. Devi, V. Raghavendran, B. M. Prabhu, N. G. Avadhani, and H. K. Anandatheerthavarada, "Mitochondrial import and accumulation of α-synuclein impair complex I in human dopaminergic neuronal cultures and Parkinson disease

brain," *Journal of Biological Chemistry*, vol. 283, no. 14, pp. 9089–9100, 2008.

[147] W. D. Parker Jr, J. K. Parks, and R. H. Swerdlow, "Complex I Deficiency in Parkinson's disease frontal cortex," *Brain Research*, vol. 1189, pp. 215–218, 2008.

[148] E. M. Valente, P. M. Abou-Sleiman, V. Caputo et al., "Hereditary early-onset Parkinson's disease caused by mutations in *PINK1*," *Science*, vol. 304, no. 5674, pp. 1158–1160, 2004.

[149] W. C. Nichols, N. Pankratz, D. Hernandez et al., "Genetic screening for a single common *LRRK2* mutation in familial Parkinson's disease," *The Lancet*, vol. 365, no. 9457, pp. 410–412, 2005.

[150] V. Bonifati, P. Rizzu, M. van Baren et al., "Mutations in the *DJ-1* gene associated with autosomal recessive early-onset parkinsonism," *Science*, vol. 299, no. 5604, pp. 256–259, 2002.

[151] W. P. Gilks, P. M. Abou-Sleiman, S. Gandhi et al., "A common *LRRK2* mutation in idiopathic Parkinson's disease," *The Lancet*, vol. 365, no. 9457, pp. 415-416, 2005.

[152] S. Gandhi, A. Wood-Kaczmar, Z. Yao et al., "PINK1-associated Parkinson's disease is caused by neuronal vulnerability to calcium-induced cell death," *Molecular Cell*, vol. 33, no. 5, pp. 627–638, 2009.

[153] C. Piccoli, A. Sardanelli, R. Scrima et al., "Mitochondrial respiratory dysfunction in familiar parkinsonism associated with PINK1 mutation," *Neurochemical Research*, vol. 33, no. 12, pp. 2565–2574, 2008.

[154] M. Kostic, M. H. R. Ludtmann, H. Bading et al., "PKA phosphorylation of NCLX reverses mitochondrial calcium overload and depolarization, promoting survival of PINK1-deficient dopaminergic neurons," *Cell Reports*, vol. 13, no. 2, pp. 376–386, 2015.

[155] B. Xiao, J. Y. Goh, L. Xiao, H. Xian, K. L. Lim, and Y. C. Liou, "Reactive oxygen species trigger Parkin/PINK1 pathway–dependent mitophagy by inducing mitochondrial recruitment of Parkin," *Journal of Biological Chemistry*, vol. 292, no. 40, pp. 16697–16708, 2017.

[156] M. Delgado-Camprubi, N. Esteras, M. P. M. Soutar, H. Plun-Favreau, and A. Y. Abramov, "Deficiency of Parkinson's disease-related gene *Fbxo7* is associated with impaired mitochondrial metabolism by PARP activation," *Cell Death and Differentiation*, vol. 24, no. 1, pp. 120–131, 2017.

[157] J. Burré, S. Vivona, J. Diao, M. Sharma, A. T. Brunger, and T. C. Südhof, "Properties of native brain α-synuclein," *Nature*, vol. 498, no. 7453, pp. E4–E6, 2013.

[158] G. Fusco, S. W. Chen, P. T. F. Williamson et al., "Structural basis of membrane disruption and cellular toxicity by α-synuclein oligomers," *Science*, vol. 358, no. 6369, pp. 1440–1443, 2017.

[159] E. S. Luth, I. G. Stavrovskaya, T. Bartels, B. S. Kristal, and D. J. Selkoe, "Soluble, Prefibrillar α-Synuclein Oligomers Promote Complex I-dependent, Ca^{2+}-induced Mitochondrial Dysfunction," *Journal of Biological Chemistry*, vol. 289, no. 31, pp. 21490–21507, 2014.

[160] K. Banerjee, M. Sinha, C. L. L. Pham et al., "α-Synuclein induced membrane depolarization and loss of phosphorylation capacity of isolated rat brain mitochondria: Implications in Parkinson's disease," *FEBS Letters*, vol. 584, no. 8, pp. 1571–1576, 2010.

[161] P. R. Angelova, M. H. Horrocks, D. Klenerman, S. Gandhi, A. Y. Abramov, and M. S. Shchepinov, "Lipid peroxidation is essential for α-synuclein-induced cell death," *Journal of Neurochemistry*, vol. 133, no. 4, pp. 582–589, 2015.

[162] S. Mullin and A. Schapira, "α-Synuclein and Mitochondrial Dysfunction in Parkinson's Disease," *Molecular Neurobiology*, vol. 47, no. 2, pp. 587–597, 2013.

[163] L. J. Martin, S. Semenkow, A. Hanaford, and M. Wong, "The mitochondrial permeability transition pore regulates Parkinson's disease development in mutant α-synuclein transgenic mice," *Neurobiology of Aging*, vol. 35, no. 5, pp. 1132–1152, 2014.

[164] P. R. Angelova, M. H. R. Ludtmann, M. H. Horrocks et al., "Ca^{2+} is a key factor in α-synuclein-induced neurotoxicity," *Journal of Cell Science*, vol. 129, no. 9, pp. 1792–1801, 2016.

[165] E. Floor and M. G. Wetzel, "Increased protein oxidation in human substantia nigra pars compacta in comparison with basal ganglia and prefrontal cortex measured with an improved dinitrophenylhydrazine assay," *Journal of Neurochemistry*, vol. 70, no. 1, pp. 268–275, 1998.

[166] S. R. Danielson and J. K. Andersen, "Oxidative and nitrative protein modifications in Parkinson's disease," *Free Radical Biology and Medicine*, vol. 44, no. 10, pp. 1787–1794, 2008.

[167] R. Burai, N. Ait-Bouziad, A. Chiki, and H. A. Lashuel, "Elucidating the role of site-specific nitration of α-synuclein in the pathogenesis of Parkinson's disease via protein semisynthesis and mutagenesis," *Journal of the American Chemical Society*, vol. 137, no. 15, pp. 5041–5052, 2015.

[168] S. J. Chinta and J. K. Andersen, "Nitrosylation and nitration of mitochondrial complex I in Parkinson's disease," *Free Radical Research*, vol. 45, no. 1, pp. 53–58, 2011.

[169] M. F. Beal, "Oxidatively modified proteins in aging and disease," *Free Radical Biology and Medicine*, vol. 32, no. 9, pp. 797–803, 2002.

[170] A. Yoritaka, N. Hattori, K. Uchida, M. Tanaka, E. R. Stadtman, and Y. Mizuno, "Immunohistochemical detection of 4-hydroxynonenal protein adducts in Parkinson disease," *Proceedings of the National Academy of Sciences of the United States of America*, vol. 93, no. 7, pp. 2696–2701, 1996.

[171] M. L. Selley, "(E)-4-hydroxy-2-nonenal may be involved in the pathogenesis of Parkinson's disease," *Free Radical Biology and Medicine*, vol. 25, no. 2, pp. 169–174, 1998.

[172] E. Dalfo and I. Ferrer, "Early α-synuclein lipoxidation in neocortex in Lewy body diseases," *Neurobiology of Aging*, vol. 29, no. 3, pp. 408–417, 2008.

[173] C. M. Chen, J. L. Liu, Y. R. Wu et al., "Increased oxidative damage in peripheral blood correlates with severity of Parkinson's disease," *Neurobiology of Disease*, vol. 33, no. 3, pp. 429–435, 2009.

[174] R. Castellani, M. A. Smith, G. L. Richey, and G. Perry, "Glycoxidation and oxidative stress in Parkinson disease and diffuse Lewy body disease," *Brain Research*, vol. 737, no. 1-2, pp. 195–200, 1996.

[175] E. Dalfó, M. Portero-Otín, V. Ayala, A. Martínez, R. Pamplona, and I. Ferrer, "Evidence of oxidative stress in the neocortex in incidental Lewy body disease," *Journal of Neuropathology & Experimental Neurology*, vol. 64, no. 9, pp. 816–830, 2005.

[176] P. J. Thornalley, "Glutathione-dependent detoxification of α-oxoaldehydes by the glyoxalase system: involvement in disease mechanisms and antiproliferative activity of glyoxalase I inhibitors," *Chemico-Biological Interactions*, vol. 111-112, pp. 137–151, 1998.

[177] T. Abe, C. Isobe, T. Murata, C. Sato, and H. Tohgi, "Alteration of 8-hydroxyguanosine concentrations in the cerebrospinal fluid and serum from patients with Parkinson's disease," *Neuroscience Letters*, vol. 336, no. 2, pp. 105–108, 2003.

[178] J. Zhang, G. Perry, M. A. Smith et al., "Parkinson's disease is associated with oxidative damage to cytoplasmic DNA and RNA in substantia nigra neurons," *The American Journal of Pathology*, vol. 154, no. 5, pp. 1423–1429, 1999.

[179] R. J. Marttila, H. Lorentz, and U. K. Rinne, "Oxygen toxicity protecting enzymes in Parkinson's disease," *Journal of the Neurological Sciences*, vol. 86, no. 2-3, pp. 321–331, 1988.

[180] R. K. B. Pearce, A. Owen, S. Daniel, P. Jenner, and C. D. Marsden, "Alterations in the distribution of glutathione in the substantia nigra in Parkinson's disease," *Journal of Neural Transmission*, vol. 104, no. 6-7, pp. 661–677, 1997.

[181] M. B. Mbangata, R. V. Kartha, U. Mishra, L. D. Coles, P. J. Tuite, and J. C. Cloyd, "Oxidative stress status in patients with Parkinson's disease on and off medication," *Movement Disorders*, vol. 29, p. S143, 2014.

[182] J. Choi, H. D. Rees, S. T. Weintraub, A. I. Levey, L. S. Chin, and L. Li, "Oxidative modifications and aggregation of Cu, Zn-superoxide dismutase associated with Alzheimer and Parkinson diseases," *Journal of Biological Chemistry*, vol. 280, no. 12, pp. 11648–11655, 2005.

[183] E. Romuk, W. Szczurek, M. Oleś et al., "The evaluation of the changes in enzymatic antioxidant reserves and lipid peroxidation in chosen parts of the brain in an animal model of Parkinson disease," *Advances in Clinical and Experimental Medicine*, vol. 26, no. 6, pp. 953–959, 2017.

[184] M. C. Kiernan, S. Vucic, B. C. Cheah et al., "Amyotrophic lateral sclerosis," *The Lancet*, vol. 377, no. 9769, pp. 942–955, 2011.

[185] D. R. Rosen, T. Siddique, D. Patterson et al., "Mutations in Cu/Zn superoxide dismutase gene are associated with familial amyotrophic lateral sclerosis," *Nature*, vol. 362, no. 6415, pp. 59–62, 1993.

[186] A. C. Bowling, J. B. Schulz, R. H. Brown Jr, and M. F. Beal, "Superoxide dismutase activity, oxidative damage, and mitochondrial energy metabolism in familial and sporadic amyotrophic lateral sclerosis," *Journal of Neurochemistry*, vol. 61, no. 6, pp. 2322–2325, 1993.

[187] M. Neumann, D. M. Sampathu, L. K. Kwong et al., "Ubiquitinated TDP-43 in frontotemporal lobar degeneration and amyotrophic lateral sclerosis," *Science*, vol. 314, no. 5796, pp. 130–133, 2006.

[188] J. Sreedharan, I. P. Blair, V. B. Tripathi et al., "TDP-43 mutations in familial and sporadic amyotrophic lateral sclerosis," *Science*, vol. 319, no. 5870, pp. 1668–1672, 2008.

[189] V. M. van Deerlin, J. B. Leverenz, L. M. Bekris et al., "*TARDBP* mutations in amyotrophic lateral sclerosis with TDP-43 neuropathology: a genetic and histopathological analysis," *The Lancet Neurology*, vol. 7, no. 5, pp. 409–416, 2008.

[190] J. Gamez, M. Corbera-Bellalta, G. Nogales et al., "Mutational analysis of the Cu/Zn superoxide dismutase gene in a Catalan ALS population: should all sporadic ALS cases also be screened for *SOD1*?," *Journal of the Neurological Sciences*, vol. 247, no. 1, pp. 21–28, 2006.

[191] R. A. Saccon, R. K. A. Bunton-Stasyshyn, E. M. C. Fisher, and P. Fratta, "Is SOD1 loss of function involved in amyotrophic lateral sclerosis?," *Brain*, vol. 136, no. 8, pp. 2342–2358, 2013.

[192] S. Vucic, D. Burke, and M. C. Kiernan, "Diagnosis of motor neuron disease," in *The Motor Neuron Disease Handbook*, M. C. Kiernan, Ed., pp. 89–115, Australasian Medical Publishing Company Limited, Sydney, 2007.

[193] L. I. Bruijn, M. F. Beal, M. W. Becher et al., "Elevated free nitrotyrosine levels, but not protein-bound nitrotyrosine or hydroxyl radicals, throughout amyotrophic lateral sclerosis (ALS)-like disease implicate tyrosine nitration as an aberrant in vivo property of one familial ALS-linked superoxide dismutase 1 mutant," *Proceedings of the National Academy of Sciences of the United States of America*, vol. 94, no. 14, pp. 7606–7611, 1997.

[194] L. I. Bruijn, M. K. Houseweart, S. Kato et al., "Aggregation and motor neuron toxicity of an ALS-linked SOD1 mutant independent from wild-type SOD1," *Science*, vol. 281, no. 5384, pp. 1851–1854, 1998.

[195] F. Tafuri, D. Ronchi, F. Magri, G. P. Comi, and S. Corti, "SOD1 misplacing and mitochondrial dysfunction in amyotrophic lateral sclerosis pathogenesis," *Frontiers in Cellular Neuroscience*, vol. 9, p. 333, 2015.

[196] K. Hensley, M. Mhatre, S. Mou et al., "On the relation of oxidative stress to neuroinflammation: lessons learned from the G93A-SOD1 mouse model of amyotrophic lateral sclerosis," *Antioxidants & Redox Signaling*, vol. 8, no. 11-12, pp. 2075–2087, 2006.

[197] E. L. Bastow, A. R. Peswani, D. S. J. Tarrant et al., "New links between *SOD1* and metabolic dysfunction from a yeast model of Amyotrophic Lateral Sclerosis (ALS)," *Journal of Cell Science*, vol. 129, pp. 4118–4129, 2016.

[198] P. M. Peixoto, H. J. Kim, B. Sider, A. Starkov, T. L. Horvath, and G. Manfredi, "UCP2 overexpression worsens mitochondrial dysfunction and accelerates disease progression in a mouse model of amyotrophic lateral sclerosis," *Molecular and Cellular Neuroscience*, vol. 57, pp. 104–110, 2013.

[199] Y. Ihara, K. Nobukuni, H. Takata, and T. Hayabara, "Oxidative stress and metal content in blood and cerebrospinal fluid of amyotrophic lateral sclerosis patients with and without a Cu, Zn-superoxide dismutase mutation," *Neurological Research*, vol. 27, no. 1, pp. 105–108, 2005.

[200] M. C. Boll, M. Alcaraz-Zubeldia, S. Montes, L. Murillo-Bonilla, and C. Rios, "Raised nitrate concentration and low SOD activity in the CSF of sporadic ALS patients," *Neurochemical Research*, vol. 28, no. 5, pp. 699–703, 2003.

[201] A. Nikolić-Kokić, Z. Stević, D. Blagojević, B. Davidović, D. R. Jones, and M. B. Spasić, "Alterations in anti-oxidative defence enzymes in erythrocytes from sporadic amyotrophic lateral sclerosis (SALS) and familial ALS patients," *Clinical Chemistry and Laboratory Medicine (CCLM)*, vol. 44, no. 5, pp. 589–593, 2006.

[202] I. C. Shaw, P. S. Fitzmaurice, J. D. Mitchell, and P. G. Lynch, "Studies on cellular free radical protection mechanisms in the anterior horn from patients with amyotrophic lateral sclerosis," *Neurodegeneration*, vol. 4, no. 4, pp. 391–396, 1995.

[203] N. Shibata, "Transgenic mouse model for familial amyotrophic lateral sclerosis with superoxide dismutase-1 mutation," *Neuropathology*, vol. 21, no. 1, pp. 82–92, 2001.

[204] P. J. Shaw, P. G. Ince, G. Falkous, and D. Mantle, "Oxidative damage to protein in sporadic motor neuron disease spinal cord," *Annals of Neurology*, vol. 38, no. 4, pp. 691–695, 1995.

[205] R. J. Ferrante, S. E. Browne, L. A. Shinobu et al., "Evidence of increased oxidative damage in both sporadic and familial amyotrophic lateral sclerosis," *Journal of Neurochemistry*, vol. 69, no. 5, pp. 2064–2074, 1997.

[206] E. Onesto, C. Colombrita, V. Gumina et al., "Gene-specific mitochondria dysfunctions in human *TARDBP* and *C9ORF72* fibroblasts," *Acta Neuropathologica Communications*, vol. 4, no. 1, p. 47, 2016.

[207] F. Bartolome, N. Esteras, A. Martin-Requero et al., "Pathogenic *p62/SQSTM1* mutations impair energy metabolism through limitation of mitochondrial substrates," *Scientific Reports*, vol. 7, no. 1, article 1666, 2017.

[208] C. Capitini, S. Conti, M. Perni et al., "TDP-43 inclusion bodies formed in bacteria are structurally amorphous, non-amyloid and inherently toxic to neuroblastoma cells," *PLoS One*, vol. 9, no. 1, article e86720, 2014.

[209] W. A. Pedersen, W. Fu, J. N. Keller et al., "Protein modification by the lipid peroxidation product 4-hydroxynonenal in the spinal cords of amyotrophic lateral sclerosis patients," *Annals of Neurology*, vol. 44, no. 5, pp. 819–824, 1998.

[210] E. P. Simpson, Y. K. Henry, J. S. Henkel, R. G. Smith, and S. H. Appel, "Increased lipid peroxidation in sera of ALS patients: a potential biomarker of disease burden," *Neurology*, vol. 62, no. 10, pp. 1758–1765, 2004.

[211] R. G. Smith, Y. K. Henry, M. P. Mattson, and S. H. Appel, "Presence of 4-hydroxynonenal in cerebrospinal fluid of patients with sporadic amyotrophic lateral sclerosis," *Annals of Neurology*, vol. 44, no. 4, pp. 696–699, 1998.

[212] M. Perluigi, H. Fai Poon, K. Hensley et al., "Proteomic analysis of 4-hydroxy-2-nonenal-modified proteins in G93A-SOD1 transgenic mice-A model of familial amyotrophic lateral sclerosis," *Free Radical Biology and Medicine*, vol. 38, no. 7, pp. 960–968, 2005.

[213] E. D. Hall, P. K. Andrus, J. A. Oostveen, T. J. Fleck, and M. E. Gurney, "Relationship of oxygen radical-induced lipid peroxidative damage to disease onset and progression in a transgenic model of familial ALS," *Journal of Neuroscience Research*, vol. 53, no. 1, pp. 66–77, 1998.

[214] S. Kikuchi, K. Shinpo, A. Ogata et al., "Detection of N epsilon-(carboxymethyl)lysine (CML) and non-CML advanced glycation end-products in the anterior horn of amyotrophic lateral sclerosis spinal cord," *Amyotrophic Lateral Sclerosis*, vol. 3, no. 2, pp. 63–68, 2002.

[215] N. Shibata, A. Hirano, T. E. Hedley-Whyte et al., "Selective formation of certain advanced glycation end products in spinal cord astrocytes of humans and mice with superoxide dismutase-1 mutation," *Acta Neuropathologica*, vol. 104, no. 2, pp. 171–178, 2002.

[216] J. Ilzecka, "Serum-soluble receptor for advanced glycation end product levels in patients with amyotrophic lateral sclerosis," *Acta Neurologica Scandinavica*, vol. 120, no. 2, pp. 119–122, 2009.

[217] K. Arai, S. Maguchi, S. Fujii, H. Ishibashi, K. Oikawa, and N. Taniguchi, "Glycation and inactivation of human Cu-Zn-superoxide dismutase. Identification of the in vitro glycated sites," *Journal of Biological Chemistry*, vol. 262, no. 35, pp. 16969–16972, 1987.

[218] T. Murata, C. Ohtsuka, and Y. Terayama, "Increased mitochondrial oxidative damage and oxidative DNA damage contributes to the neurodegenerative process in sporadic amyotrophic lateral sclerosis," *Free Radical Research*, vol. 42, no. 3, pp. 221–225, 2009.

[219] S. Sussmuth, J. Brettschneider, A. Ludolph, and H. Tumani, "Biochemical markers in CSF of ALS patients," *Current Medicinal Chemistry*, vol. 15, no. 18, pp. 1788–1801, 2008.

[220] E. Cova, P. Bongioanni, C. Cereda et al., "Time course of oxidant markers and antioxidant defenses in subgroups of amyotrophic lateral sclerosis patients," *Neurochemistry International*, vol. 56, no. 5, pp. 687–693, 2010.

[221] H. Tanaka, M. Shimazawa, M. Takata et al., "ITIH4 and Gpx3 are potential biomarkers for amyotrophic lateral sclerosis," *Journal of Neurology*, vol. 260, no. 7, pp. 1782–1797, 2013.

[222] N. Weiduschat, X. Mao, J. Hupf et al., "Motor cortex glutathione deficit in ALS measured *in vivo* with the J-editing technique," *Neuroscience Letters*, vol. 570, pp. 102–107, 2014.

[223] H. Tohgi, T. Abe, K. Yamazaki, T. Murata, E. Ishizaki, and C. Isobe, "Increase in oxidized NO products and reduction in oxidized glutathione in cerebrospinal fluid from patients with sporadic form of amyotrophic lateral sclerosis," *Neuroscience Letters*, vol. 260, no. 3, pp. 204–206, 1999.

[224] D. Blagojević, M. B. Spasić, and A. M. Michelson, "Glutathione peroxidase in amyotrophic lateral sclerosis: the effects of selenium supplementation," *Journal of Environmental Pathology, Toxicology and Oncology*, vol. 17, no. 3&4, pp. 325–329, 1998.

[225] M. Kuźma, Z. Jamrozik, and A. Barańczyk-Kuźma, "Activity and expression of glutathione S-transferase pi in patients with amyotrophic lateral sclerosis," *Clinica Chimica Acta*, vol. 364, no. 1-2, pp. 217–221, 2006.

[226] A. N. Kokić, Z. Stević, S. Stojanović et al., "Biotransformation of nitric oxide in the cerebrospinal fluid of amyotrophic lateral sclerosis patients," *Redox Report*, vol. 10, no. 5, pp. 265–270, 2005.

[227] P. I. Oteiza, O. D. Uchitel, F. Carrasquedo, A. L. Dubrovski, J. C. Roma, and C. G. Fraga, "Evaluation of antioxidants, protein, and lipid oxidation products in blood from sporadic amyotrophic lateral sclerosis patients," *Neurochemical Research*, vol. 22, no. 4, pp. 535–539, 1997.

[228] I. Scott and R. J. Youle, "Mitochondrial fission and fusion," *Essays In Biochemistry*, vol. 47, pp. 85–98, 2010.

[229] J. Pinnell and K. Tieu, "Chapter eight - mitochondrial dynamics in neurodegenerative diseases," *Advances in Neurotoxicology*, vol. 1, pp. 211–246, 2017.

[230] D. H. Cho, T. Nakamura, J. Fang et al., "S-nitrosylation of Drp1 mediates β-amyloid-related mitochondrial fission and neuronal injury," *Science*, vol. 324, no. 5923, pp. 102–105, 2009.

[231] X. Wang, B. Su, H. G. Lee et al., "Impaired balance of mitochondrial fission and fusion in Alzheimer's disease," *Journal of Neuroscience*, vol. 29, no. 28, pp. 9090–9103, 2009.

[232] M. Manczak, M. J. Calkins, and P. H. Reddy, "Impaired mitochondrial dynamics and abnormal interaction of amyloid beta with mitochondrial protein Drp1 in neurons from patients with Alzheimer's disease: implications for neuronal damage," *Human Molecular Genetics*, vol. 20, no. 13, pp. 2495–2509, 2011.

[233] M. Manczak, R. Kandimalla, D. Fry, H. Sesaki, and P. H. Reddy, "Protective effects of reduced dynamin-related protein 1 against amyloid beta-induced mitochondrial dysfunction and synaptic damage in Alzheimer's disease," *Human Molecular Genetics*, vol. 25, no. 23, pp. 5148–5166, 2016.

[234] D. Santos and S. M. Cardoso, "Mitochondrial dynamics and neuronal fate in Parkinson's disease," *Mitochondrion*, vol. 12, no. 4, pp. 428–437, 2012.

[235] F. Kamp, N. Exner, A. K. Lutz et al., "Inhibition of mitochondrial fusion by α-synuclein is rescued by PINK1, Parkin and DJ-1," *The EMBO Journal*, vol. 29, no. 20, pp. 3571–3589, 2010.

[236] A. C. Poole, R. E. Thomas, L. A. Andrews, H. M. McBride, A. J. Whitworth, and L. J. Pallanck, "The PINK1/Parkin pathway regulates mitochondrial morphology," *Proceedings of the National Academy of Sciences of the United States of America*, vol. 105, no. 5, pp. 1638–1643, 2008.

[237] C. Vives-Bauza, C. Zhou, Y. Huang et al., "PINK1-dependent recruitment of Parkin to mitochondria in mitophagy," *Proceedings of the National Academy of Sciences of the United States of America*, vol. 107, no. 1, pp. 378–383, 2010.

[238] X. Wang, D. Winter, G. Ashrafi et al., "PINK1 and Parkin target Miro for phosphorylation and degradation to arrest mitochondrial motility," *Cell*, vol. 147, no. 4, pp. 893–906, 2011.

[239] I. Irrcher, H. Aleyasin, E. L. Seifert et al., "Loss of the Parkinson's disease-linked gene DJ-1 perturbs mitochondrial dynamics," *Human Molecular Genetics*, vol. 19, no. 19, pp. 3734–3746, 2010.

[240] X. Wang, M. H. Yan, H. Fujioka et al., "LRRK2 regulates mitochondrial dynamics and function through direct interaction with DLP1," *Human Molecular Genetics*, vol. 21, no. 9, pp. 1931–1944, 2012.

[241] J. Magrane, I. Hervias, M. S. Henning, M. Damiano, H. Kawamata, and G. Manfredi, "Mutant SOD1 in neuronal mitochondria causes toxicity and mitochondrial dynamics abnormalities," *Human Molecular Genetics*, vol. 18, no. 23, pp. 4552–4564, 2009.

[242] J. Gao, L. Wang, J. Liu, F. Xie, B. Su, and X. Wang, "Abnormalities of mitochondrial dynamics in neurodegenerative diseases," *Antioxidants*, vol. 6, no. 2, p. 25, 2017.

[243] W. Wang, L. Li, W. L. Lin et al., "The ALS disease-associated mutant TDP-43 impairs mitochondrial dynamics and function in motor neurons," *Human Molecular Genetics*, vol. 22, no. 23, pp. 4706–4719, 2013.

[244] J. Deng, M. Yang, Y. Chen et al., "FUS interacts with HSP60 to promote mitochondrial damage," *PLOS Genetics*, vol. 11, no. 9, article e1005357, 2015.

[245] W. Song, Y. Song, B. Kincaid, B. Bossy, and E. Bossy-Wetzel, "Mutant $SOD1^{G93A}$ triggers mitochondrial fragmentation in spinal cord motor neurons: neuroprotection by SIRT3 and PGC-1α," *Neurobiology of Disease*, vol. 51, pp. 72–81, 2013.

[246] S. Cogliati, C. Frezza, M. E. Soriano et al., "Mitochondrial cristae shape determines respiratory chain supercomplexes assembly and respiratory efficiency," *Cell*, vol. 155, no. 1, pp. 160–171, 2013.

[247] M. Hamer and Y. Chida, "Physical activity and risk of neurodegenerative disease: a systematic review of prospective evidence," *Psychological Medicine*, vol. 39, no. 1, pp. 3–11, 2009.

Hindawi
Oxidative Medicine and Cellular Longevity
Volume 2019, Article ID 1050476, 12 pages
https://doi.org/10.1155/2019/1050476

Research Article

Amyloid Peptide β1-42 Induces Integrin αIIbβ3 Activation, Platelet Adhesion, and Thrombus Formation in a NADPH Oxidase-Dependent Manner

Aisha Alsheikh Abubaker,[1] Dina Vara,[2] Caterina Visconte,[3] Ian Eggleston,[1] Mauro Torti,[3] Ilaria Canobbio,[3] and Giordano Pula[2]

[1]*Pharmacy and Pharmacology, University of Bath, UK*
[2]*Institute of Biomedical and Clinical Sciences, University of Exeter Medical School, UK*
[3]*Department of Biology and Biotechnology, University of Pavia, Italy*

Correspondence should be addressed to Giordano Pula; g.pula@exeter.ac.uk

Received 23 July 2018; Revised 5 November 2018; Accepted 13 December 2018; Published 14 March 2019

Guest Editor: Roberta Cascella

The progression of Alzheimer's dementia is associated with neurovasculature impairment, which includes inflammation, microthromboses, and reduced cerebral blood flow. Here, we investigate the effects of β amyloid peptides on the function of platelets, the cells driving haemostasis. Amyloid peptide β1-42 (Aβ1-42), Aβ1-40, and Aβ25-35 were tested in static adhesion experiments, and it was found that platelets preferentially adhere to Aβ1-42 compared to other Aβ peptides. In addition, significant platelet spreading was observed over Aβ1-42, while Aβ1-40, Aβ25-35, and the scAβ1-42 control did not seem to induce any platelet spreading, which suggested that only Aβ1-42 activates platelet signalling in our experimental conditions. Aβ1-42 also induced significant platelet adhesion and thrombus formation in whole blood under venous flow condition, while other Aβ peptides did not. The molecular mechanism of Aβ1-42 was investigated by flow cytometry, which revealed that this peptide induces a significant activation of integrin αIIbβ3, but does not induce platelet degranulation (as measured by P-selectin membrane translocation). Finally, Aβ1-42 treatment of human platelets led to detectable levels of protein kinase C (PKC) activation and tyrosine phosphorylation, which are hallmarks of platelet signalling. Interestingly, the NADPH oxidase (NOX) inhibitor VAS2870 completely abolished Aβ1-42-dependent platelet adhesion in static conditions, thrombus formation in physiological flow conditions, integrin αIIbβ3 activation, and tyrosine- and PKC-dependent platelet signalling. In summary, this study highlights the importance of NOXs in the activation of platelets in response to amyloid peptide β1-42. The molecular mechanisms described in this manuscript may play an important role in the neurovascular impairment observed in Alzheimer's patients.

1. Introduction

Alzheimer's disease (AD) is a multifactorial age-related neurodegenerative disorder representing 60-80% of dementia cases [1]. Prominent morphological hallmarks of the disease include pathological accumulation of insoluble aggregates of polymeric protein fragments known as β amyloid peptides deposited in the brain parenchyma (amyloid plaques) and within the cerebral vessel walls (cerebral amyloid angiopathy (CAA)), formation of neurofibrillary tangles within neurons (tau pathology), oxidative stress and chronic neurovascular inflammation resulting in blood hypoperfusion, and damages to the blood brain barrier (BBB) [2]. The manifestation of these pathological conditions eventually lead to neurovascular dysfunction, neuronecrosis, cognitive decline, and ultimately death [3].

Epidemiological data, postmortem pathological examination, and experimental studies on both human and animal AD brains have revealed significant correlations and shared pathophysiological mechanisms between Alzheimer's and

vascular diseases [4–9]. Common contributing causes include conditions such as hypertension, diabetes mellitus, hypercholesterolemia, apolipoprotein E (APOE) 4 polymorphism, and traumatic brain injury [10].

The potential role of platelets in Alzheimer's disease has been investigated in a number of studies. The initial work of Rosenberg et al. in 1997 highlighted possible platelet activation in AD patients due to altered APP processing [11]. His work was followed up by Sevush et al. in 1998 and by other groups later on, and it was confirmed that there is an aberrant and chronic preactivation of platelets that can eventually contribute towards atherothrombosis, CAA, and progression of AD [12]. Several studies showed a correlation between AD and platelet abnormalities, including abnormal membrane fluidity, increased β-secretase activity, and altered APP metabolism [13]; α-degranulation, P-selectin surface expression, and integrin αIIbβ3 activation [14]; platelet adhesion [15, 16]; formation of leukocyte-platelet complexes [12]; coagulation abnormalities [17–19]; and platelet adhesion and accumulation at vascular β amyloid deposition sites, where they were shown to modulate β amyloid complexation into aggregates [20].

Several authors utilised both soluble and fibril forms of β amyloid peptides as agonists and demonstrated that Aβ peptides are able to promote platelet activation, adhesion, and aggregation. For example, fibrillar Aβ1-40 was shown to induce platelet aggregation by binding to scavenger receptors CD36 and GP1bα and activating p38 MAPK/COX1 pathways. This induces the release of the potent aggregation agonist thromboxane A2 (TxA2) [21]. Donner et al. more recently showed that Aβ1-40 can bind to integrin αIIbβ3 and trigger the release of ADP and clusterin (a chaperone protein), which promoted the formation of Aβ1-40 fibrils [22]. In addition, the use of synthetic Aβ25-35, which retains the biological and toxic properties of the full length Aβ1-40 and Aβ1-42, has been shown to activate the PAR1 thrombin receptor and stimulate an intracellular signalling cascade involving Ras/Raf, PI3K, P38MAPK, and cPLA2 and TxA2 formation and release [23].

NADPH oxidases (NOXs) are the only enzyme family recognized for their sole primary function of generating reactive oxygen species (ROS), and they have been proposed as the main source of ROS in platelets during haemostasis [24]. Recently, two types of NOXs have been identified in human and mouse platelets (NOX1 and NOX2) [25], but a comprehensive understanding of their activation signalling pathways in response to β amyloid peptides remains elusive. An interesting paper published by Walsh et al. demonstrated that oligomeric and fibrillar forms of Aβ1-42 can act as a ligand for the GPVI receptor and activate platelets [26]. Since NOX1 has been shown to play a key role in signalling for the GPVI receptor [25, 27], this may suggest that Aβ1-42 acts through a NOX1-dependent activation of platelets.

Recently, we demonstrated that upon stimulation of platelets by both monomeric or fibril forms of Aβ1-42, significant intracellular superoxide anion formation can be detected using a novel flow cytometry method using the molecular probe dihydroethidium (DHE) [28]. Here, we further investigate the effects of different Aβ (Aβ1-42, Aβ1-40, Aβ25-35, and scrambled Aβ1-42 control) on platelet activation and adhesion in static and physiological flow conditions. The use of pan-NOX inhibitor VAS2870 [28] allows the assessment of the role of NOXs on platelet adhesion and activation. Our primary objective is to understand the mechanism underlining β amyloid peptide-dependent regulation of platelets, which can potentially improve our understanding of AD and facilitate the development of pharmacological tools to combat the progression of this disease.

2. Materials and Methods

2.1. Reagents. Dimethylsulfoxide (DMSO), indomethacin, prostaglandin E_1 (PGE_1), bovine serum albumin (BSA), sodium citrate solution (4% w/v), fibrinogen, thrombin from human plasma, 4% w/v paraformaldehyde, TRITC-conjugated phalloidin, 3,3′-dihexyloxacarbocyanine iodide (DiOC6), VAS2870, D-(+)-glucose monohydrate, and 4-(2-hydroxyethyl) piperazine-1-ethanesulfonic acid (HEPES) were from Sigma-Aldrich (Poole, UK). Fibrillar collagen was from Chrono-Log Corporation (Havertown, PA US). The anti-phosphotyrosine antibody (4G10) was from Upstate Biotechnology Inc. (Lake Placid, US). Anti-PKC phosphor-substrate antibody was from Cell Signaling Technology (Danvers, US). Anti-pleckstrin antibody was from Abcam (Cambridge, UK). FITC-PAC1 and PE-Cy5-CD62P (P-selectin) antibodies were from Becton Dickinson, (Wokingham, UK). Peroxidase-conjugated anti-IgG antibodies were from Bio-Rad (Hercules, US). The chemiluminescent substrate kit was from Merck Millipore (Burlington, US). Amyloid peptides were synthesized by LifeTein (New Jersey, US). The sequences of the peptides are as follows:

(i) Aβ1-40 (4.3 kDa): DAEFRHDSGYEVHHQKLVF FAEDVGSNKGAIIGLMVGGVV

(ii) Aβ1-42 (4.5 kDa): DAEFRHDSGYEVHHQKLVF-FAEDVGSNKGAII GLMVGGVVIA

(iii) Scrambled Aβ1-42: (4.5 kDa): DEFAKNIGHHDG-VAVHMYKGRQVEFIGSIALVFEDVGSAGLV

(iv) Aβ23-35 (1.0 kDa): GSNKGAIIGLM

2.2. Preparation of Washed Platelets. Human whole blood was obtained from healthy volunteers following Royal Devon and Exeter NHS Foundation Trust Code of Ethics and Research Conduct and under NRES South West – Central Bristol committee approval (Rec n. 14/SW/1089). 20–30 ml of blood were drawn in the presence of the anticoagulant sodium citrate (0.5% w/v). Platelet rich plasma (PRP) was then isolated from whole blood by centrifugation at $200 \times g$ for 20 mins. PRP was then subjected to a second centrifugation at $500 \times g$ for 10 mins in the presence of indomethacin (10 μM) and PGE_1 (40 ng/ml). Platelets were resuspended in modified Tyrode's HEPES buffer (145 mM NaCl, 2.9 mM KCl, 10 mM HEPES, 1 mM $MgCl_2$, and pH 7.3; 5 mM D-glucose was added before use).

2.3. Adhesion Assay. Round coverslips (22 mm) were placed in a clear flat-bottom 6-well plate and then coated overnight

at 4°C with 10 μM Aβ1-42, Aβ1-40, Aβ25-35, scrambled Aβ1-42, or 5 mg/ml BSA, all diluted in PBS. Excess solution was then gently removed, and the coverslips were blocked with 0.5% w/v BSA in PBS for 1 h at room temperature. Coated dishes were then washed gently with PBS. Washed platelets were resuspended at a density of 2×10^7 platelets/ml. 0.5 ml of washed platelets were incubated for 30 mins at 37°C. Nonadherent platelets were discarded, and the adherent ones were gently washed with PBS and then fixed with 4% w/v paraformaldehyde for 10 mins at RT. 0.1% v/v Triton X-100/PBS was added to permeabilize the platelets. After 5 mins, 0.1% Triton X-100/PBS was removed, and the coated coverslips were washed with PBS and then blocked with 5 mg/ml BSA in PBS for 30 mins. Fixed platelets were then stained with 10 μM TRITC-conjugated phalloidin for 1 hour at RT and then washed with PBS. Coverslips were mounted onto microscope slides using Vectashield. Evaluation of platelet adhesion and spreading was performed using a Leica LED fluorescence microscope, and digital images were acquired at 10x and 100x magnification objectives. Platelet coverage and surface area were measured using ImageJ (version 1.52e, Wayne Rasband, NIH).

2.4. Thrombus Formation Assay under Physiological Flow. Human peripheral blood was anticoagulated with sodium citrate 0.25% w/v. Platelets were fluorescently labelled by incubation with 1 μM 3,3′-dihexyloxacarbocyanine iodide (DiOC6) for 10 minutes. ibidi Vena8 Fluoro+ microchips (ibidi GmbH, Martinsried, Germany) were coated with 10 μM Aβ peptides or 0.1 mg/ml fibrillar collagen. Nonspecific binding sites were saturated with 0.1% w/v BSA. Physiological flow conditions (200–1000 sec^{-1}) were applied using an ExiGo pump (Cellix Ltd. Microfluidics Solutions, Dublin, Ireland). Images of the thrombi formed after 10 minutes of flow were obtained with an EVOS Fl microscope (Thermo Fisher Scientific, Waltham, MA, US). Platelet coverage was measured using ImageJ (version 1.52e, Wayne Rasband, NIH).

2.5. Flow Cytometry. Platelets isolated as described above were resuspended at 2×10^7 cells/ml density. After stimulation in suspension as described (5–20 μM Aβ1-42, Aβ1-40, Aβ25-35, scrambled Aβ1-42, or 0.5 unit/ml thrombin) for 10 minutes at 37°C, platelets were incubated for a further 10 minutes with PAC1 and anti-P-selectin antibodies conjugated to FITC and PE-Cy5, respectively. 1 in 10 dilution in Tyrode's buffer was used to stop the immunolabelling of the platelets. Surface fluorescence was assessed using a FACSAria III flow cytometer (BD Biosciences, San Jose, USA).

2.6. Immunoblotting. Platelet samples (0.2 ml, 1×10^9 platelets/ml) were stimulated at 37°C under stirring conditions (1,200 rpm) with Aβ1-42, Aβ1-40, and Aβ25-35 (including 1 mM $CaCl_2$) in a 490D aggregometer (Chrono-Log Corporation, Havertown, PA, US). Where indicated, the NOX inhibitor VAS2870 (10 μM) was preincubated for 10 minutes before treatments with Aβ peptides. The reaction was stopped after 3 minutes by the addition of a half volume of 3x SDS sample buffer (37.5 mM Tris, pH 8.3, 288 mM glycine, 6% SDS, 1.5% DTT, 30% glycerol, and 0.03% bromophenol blue) followed by heating the samples at 95°C for 5 minutes. Platelet proteins were separated on SDS-PAGE gels, transferred to a PVDF membrane, and analysed in immunoblotting using anti-phosphotyrosine antibody (4G10), anti-phospho-PKC substrate antibody, and anti-pleckstrin antibodies. Reactive proteins were visualized by ECL.

2.7. Statistical Analysis. Data were analysed by one-way ANOVA with Bonferroni posttest using the statistical software GraphPad Prism. Results were expressed as the mean ± standard error (SEM). Differences were considered significant at P value < 0.05.

3. Results

Initial experiments were carried out to examine the effect of amyloidogenic peptides on human platelet adhesion in static conditions by allowing platelet suspensions to rest on coverslips coated with scrambled Aβ1-42, Aβ1-42, Aβ1-40, and Aβ25-35 for 30 minutes. Adhering platelets were then fixed, permeabilized, and stained with TRITC-phalloidin. Phalloidin is a poisonous molecule extracted from the mushroom *Amanita phalloides* that binds strongly to filaments of actin (F-actin), which is a major component of the cell cytoskeleton [29]. In these experiments, phalloidin allows effective visualization of adhered platelets. Figure 1(a) shows the high number of adhered platelets to Aβ1-42. Adhesion to Aβ1-40, or Aβ25-35 is higher than control scrambled Aβ1-42 peptide, but this difference is not statistically significant. The quantification of adhered platelets from 4 independent experiments is shown in Figure 1(b). The statistical analysis (one-way ANOVA with Bonferroni posttest) shows significance ($P < 0.05$) for the increase in platelet adhesion to Aβ1-42 compared to scrambled Aβ1-42.

In order to assess platelet spreading on Aβ peptides, Figure 2(a) displays the morphological changes in adhering platelets at a higher magnification (100x). Initial adhesion is characterised by shape change from discoid into irregular or round shape and filopodia formation, while complete adhesion and signalling activation is associated with extensive platelet spreading and formation of lamellipodia. Aβ1-40 and Aβ25-35 induced only the morphological changes of the early phase of platelet adhesion, with few fine processes extending into different directions (filopodia). On the other hand, platelets adhering to Aβ1-42 show full spreading, with the formation of extensive lamellipodia and a significant increase in surface area coverage. Figure 2(b) quantifies the average surface area of the platelets confirming the effectiveness of Aβ1-42 as a substrate for signalling activation and platelet spreading, while no platelet spreading is observed for Aβ1-40 and Aβ25-35.

Since platelets demonstrated significant adhesion and spreading on Aβ1-42, we next investigated the effects of the NOX inhibitor VAS2870 on this substrate. Both platelet adhesion and spreading were strongly impaired. In Figure 3(a), we show the quantification of platelets adhering to Aβ1-42 in the presence or absence of VAS2870. Although the number of adhering platelets is not completely abated by

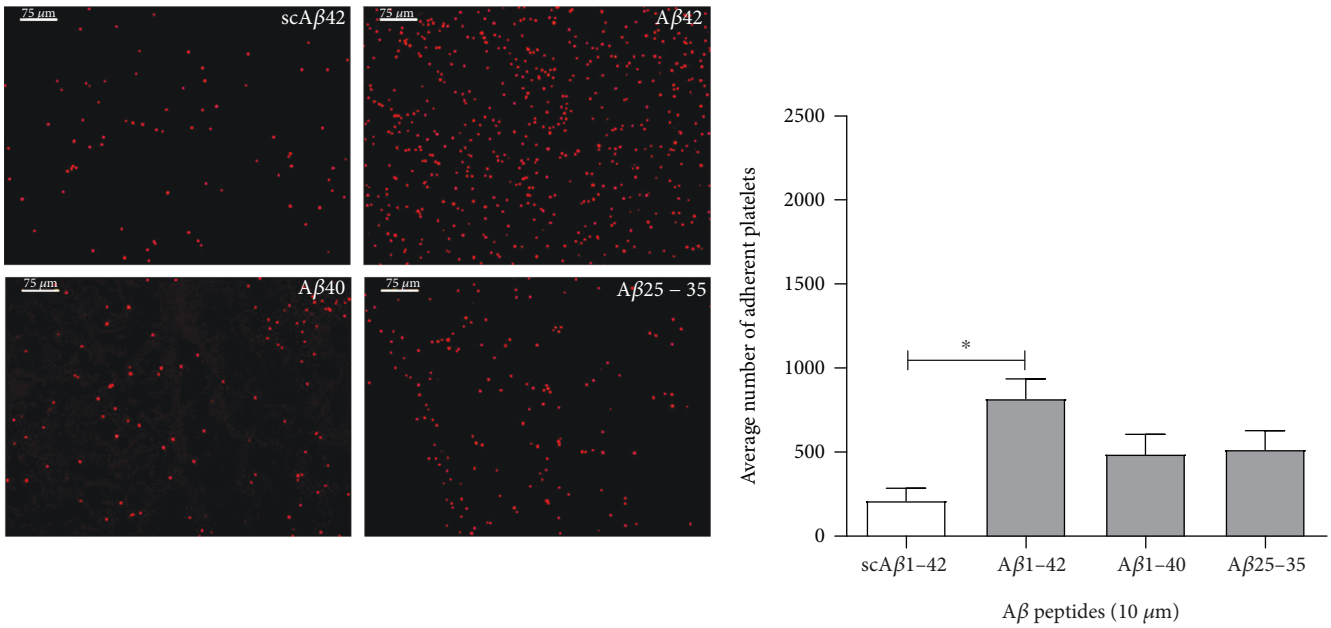

Figure 1: β amyloid peptides in static conditions support platelet adhesion. Human platelet suspensions were plated on glass coverslips coated with 10 μM scrambled Aβ1-42 (scAβ42), Aβ1-42, Aβ1-40, and Aβ25-35. The adhered platelets after 30 minutes shown in (a) were fixed, permeabilized, and stained with TRITC-conjugated phalloidin and are representative images at 10x magnification. The quantification of the adhered platelets evaluated as the mean number of platelets per optical field is shown in (b). Statistical significance for 4 independent experiments was analysed by one-way ANOVA with Bonferroni posttest ($^*P < 0.05$), with bars representing standard error of the mean (SEM).

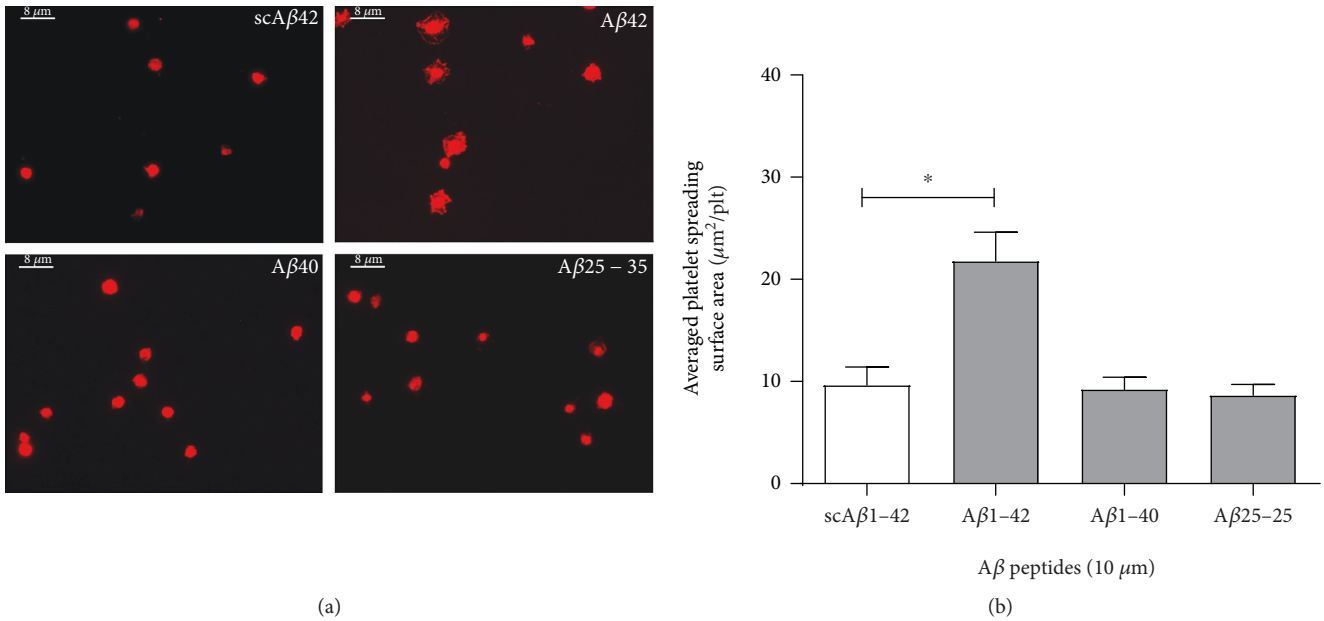

Figure 2: β amyloid peptides in static conditions support platelet spreading. Human platelet suspensions were plated on glass coverslips coated with 10 μM scrambled Aβ1-42 (scAβ42), Aβ1-42, Aβ1-40, and Aβ25-35. The adhered platelets shown in (a) were fixed, permeabilized, and stained with TRITC-conjugated phalloidin and are representative images at 100x magnification. The quantification of the mean surface area of the adhered platelets (μm^2/plt) is shown in (b). Statistical significance for 4 independent experiments was analysed by one-way ANOVA with Bonferroni posttest ($^*P < 0.05$), with bars representing standard error of the mean (SEM).

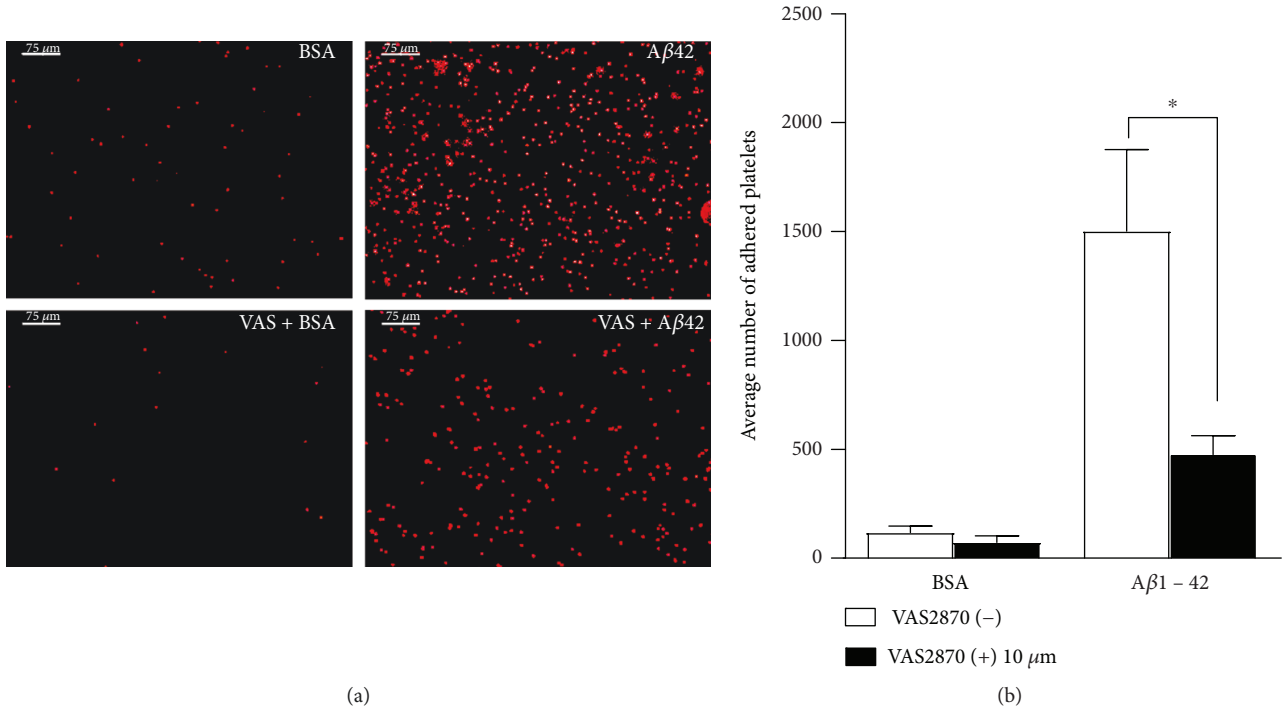

Figure 3: Effect of NOX inhibitor VAS2870 on platelet adhesion to Aβ1-42. Human platelet suspension was preincubated with NOX inhibitor VAS2870 (10 μM) for 30 mins then plated on glass coverslips coated with 10 μM Aβ1-42 and 5 mg/ml BSA in PBS. The numbers of the adhered platelets fixed, permeabilized, and stained with TRITC-conjugated phalloidin are shown in (a), and representative images at 10x magnification are displayed. The quantification of the adhered platelets evaluated as the mean number of the adhered platelets per optical field is shown (b). Statistical significance for 4 independent experiments was analysed by one-way ANOVA with Bonferroni posttest ($^*P < 0.05$), with bars representing standard error of the mean (SEM).

VAS2870, there was a statistically significant decrease in the number of adhering platelets in the presence of this inhibitor (Figure 3(b)).

When observing adhering platelets at a higher magnification (100x), VAS2870 appeared to significantly reduce the platelet spreading and the resulting surface area per platelet was lower than in the absence of the NOX inhibitor (Figure 4(a)). Statistical analysis revealed statistical significance of the effect of VAS2870 on platelet spreading (Figure 4(b)).

Next, we tested whether Aβ peptides can stimulate platelet adhesion under physiological shear. We tested both arterial (1,000 sec^{-1}) and venous shear (200 sec^{-1}) [30]. At 1,000 sec^{-1}, the tensile strength of the binding of platelets to Aβ peptides is not sufficient to guarantee effective adhesion and thrombus formation (Figures 5(a) and 5(b)). At lower shear rate corresponding to venous circulation (200 sec^{-1}), Aβ1-42 but not Aβ1-40, Aβ25-35, or scrambled Aβ1-42 induced convincing platelet adhesion and thrombus formation (Figures 5(c), 5(e) and 5(f)). Similarly to what was observed in static conditions, the inhibition of NOX with VAS2870 (10 μM) inhibited platelet adhesion (and thrombus formation) in response to Aβ1-42 (Figures 5(d) and 5(g)).

As the mechanisms leading to platelet adhesion to Aβ1-42 remain unclear, but previous work suggest a role for integrin αIIbβ3 on the adhesion to Aβ1-40 [22, 31], we tested the activation of this integrin using the antibody PAC1 by flow cytometry. These experiments suggested that only Aβ1-42 (but not Aβ1-40, Aβ2535, or scrambled Aβ1-42) induced a convincing activation of integrin αIIbβ3 (Figures 6(a)–6(g)). NOX inhibition with 10 μM VAS2870 abolished Aβ1-42-induced αIIbβ3 activation (Figure 6(d)). Interestingly, no significant translocation of P-selectin to the surface of the platelets was observed, suggesting that Aβ peptides (including Aβ1-42) cannot stimulate effective platelet degranulation on their own.

We next investigated the effect of Aβ1-42 on intracellular platelet signalling using phosphospecific immunoblotting. Both unstimulated and Aβ1-42-stimulated human platelets were treated with either DMSO (control) or VAS2870. They were then lysed, and the resulting protein extracts were separated by SDS-PAGE. Immunoblotting for phosphotyrosine and phosphorylated PKC substrates is shown in Figure 7. These antibodies are used to determine whether tyrosine phosphorylation cascades and PKC are activated by Aβ1-42 treatment, but they do not allow the identification of the targets of the phosphorylation events and function as a qualitative evidence of activation of the abovementioned signalling pathways. In these experiments, pleckstrin is used simply as a loading control. Tyrosine phosphorylation is one of the key events that occur upon platelet activation, therefore detecting tyrosine phosphorylation of platelet proteins provides a proof that Aβ1-42 induces platelet signalling activation. Figure 7(a) shows the phosphotyrosine profile of

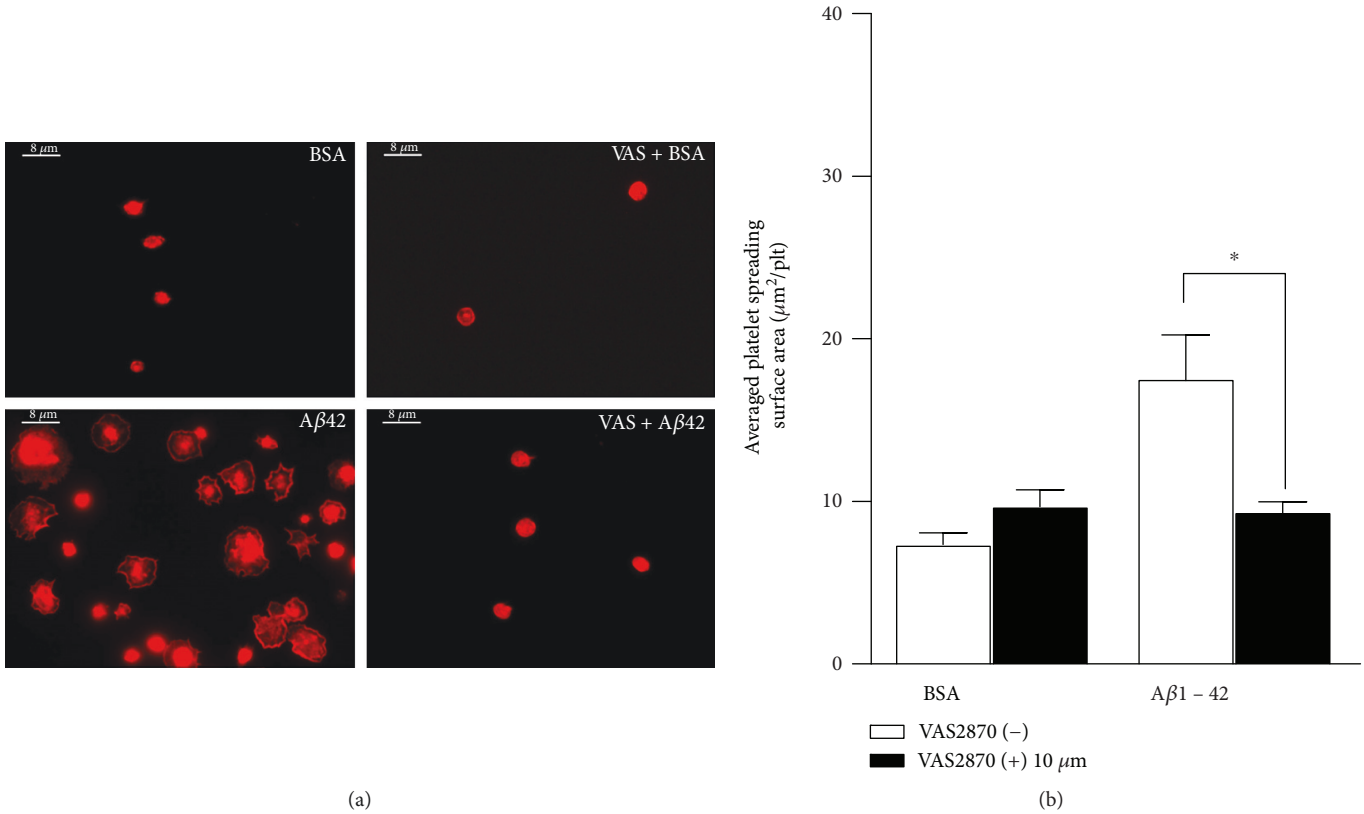

Figure 4: Effect of NOX inhibitor VAS2870 on platelet spreading on Aβ1-42. Human platelet suspension was preincubated with NOX inhibitor VAS2870 (10 μM) for 30 mins then plated on glass coverslips coated with 10 μM Aβ1-42 and 5 mg/ml BSA in PBS. The surface area of the adhered platelets fixed, permeabilized, and stained with TRITC-conjugated phalloidin is shown in (a), and representative images at 100x magnification are displayed. The quantification of the surface area of the adhered platelets (μm^2/plt) is shown in (b). Statistical significance for 4 independent experiments was analysed by one-way ANOVA with Bonferroni posttest ($^*P < 0.05$), with bars representing standard error of the mean (SEM).

resting and Aβ1-42-treated platelets in the absence or presence of VAS2870. Several bands are observed upon stimulation with Aβ1-42 (compared to DMSO-treated controls), which suggests activation of tyrosine kinase-dependent pathways and generation of tyrosine-phosphorylated protein substrates. Very significantly, the pretreatment with VAS2870 leads to the abolishment of tyrosine phosphorylation in response to Aβ1-42, which suggests that the activity of NADPH oxidases is necessary for the signalling induced by this peptide.

PKC is an essential protein kinase enzyme that is activated by diacylglycerol (DAG) and Ca^{2+} released from internal stores. The activation of PKC is a well-known intracellular event induced by platelet activation, which is usually accompanied by phosphorylation of regulatory serine/threonine residues in PKC substrate proteins [32–34]. In Figure 7(b), several bands corresponding to different substrate proteins for PKC appear more intensely upon Aβ1-42 stimulation, suggesting that PKC is activated by this peptide. PKC activation is strongly associated to platelet activation and induction of thrombus formation [34–36]. The abolishment of phospho-PKC immunostaining by VAS2870 suggests that NADPH oxidase activity is required for the Aβ1-42-dependent platelet signalling leading to PKC activation.

4. Discussion

The differential ability of the tested β amyloid peptides to induce platelet adhesive responses in static and flow conditions is extremely interesting, but it remains difficult to explain. Nonetheless, our observations are not isolated, as Aβ1-42 has been identified as the most biologically active of the amyloid peptides [37–39]. The biological activity of Aβ1-42 is associated to a marked toxicity of this peptide in several experimental systems [37–39]. One possible explanation is the marked propensity of Aβ1-42 to form fibrils compared to Aβ1-40 [40], which is due to the promotion of intermolecular interactions between amyloid monomers induced by the hydrophobic properties of the extra amino acids of Aβ1-42 compared to Aβ1-40. Recent studies have confirmed the enhanced propensity of Aβ1-42 to form fibrils compared to other Aβ peptides [41, 42]. This draws an interesting parallel with the effect of collagen on platelets. The activation of GPVI on platelets and induction of thrombus formation depends on the fibrillary structure of collagen (i.e., monomeric collagen does not induce platelet activation) [43]. Therefore, similarly to collagen, the β amyloid peptides may also need to be in a fibrillar form to bind adjacent receptors and induce effective

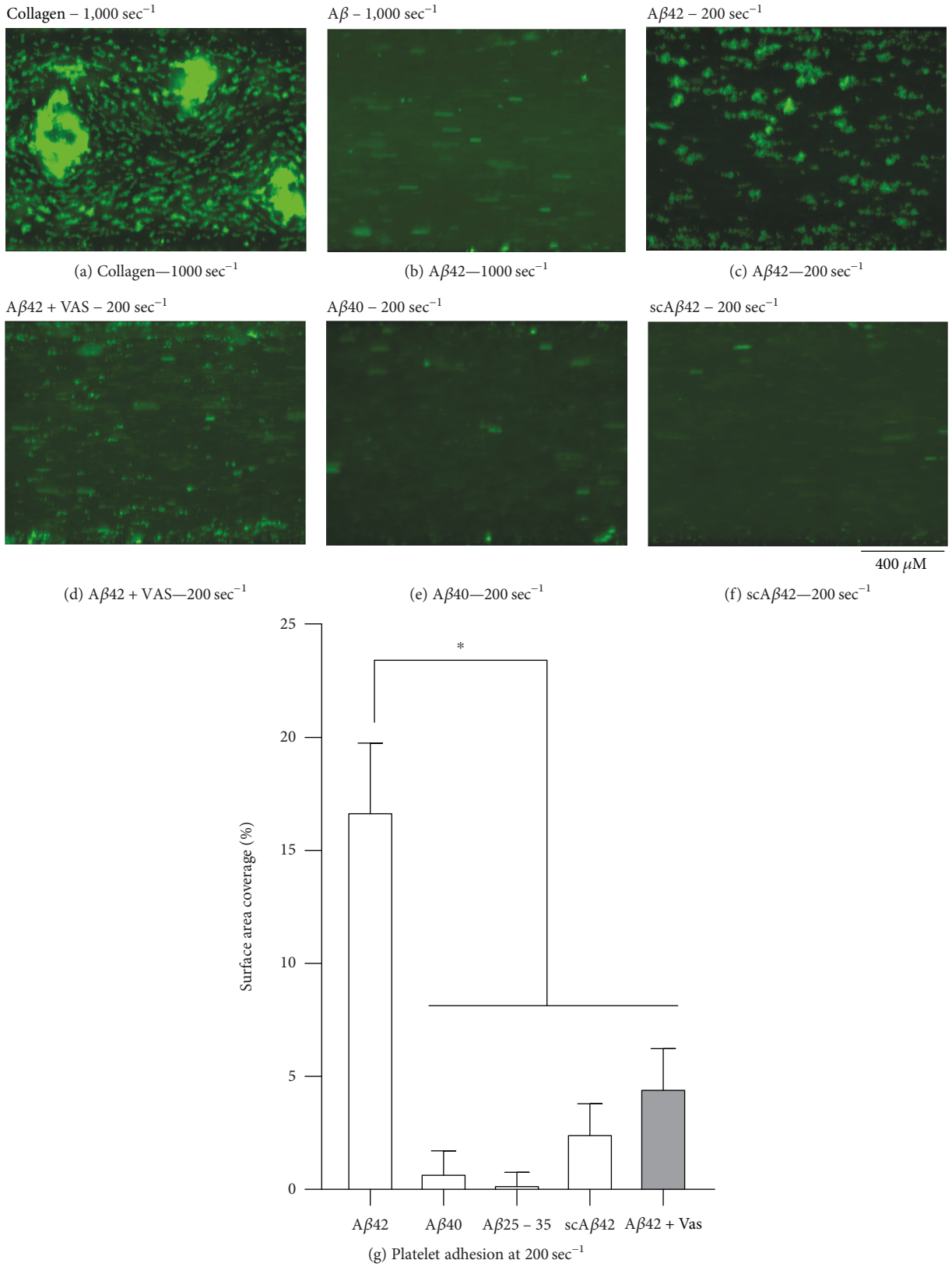

Figure 5: Adhesion of platelets to amyloid peptides under physiological shear stress. Flow biochips (ibidi Vena8 Fluoro+) were coated with 0.1 mg/ml fibrillary collagen or 10 μM scrambled Aβ1-42 (scAβ42), Aβ1-42, Aβ1-40, and Aβ25-35. Platelet adhesion was tested in human whole blood at shear rates of 1,000 sec^{-1} and 200 sec^{-1}. Where indicated, 10 μM VAS2870 was added to the blood to inhibit NOXs. Pictures shown here are representative of 3 independent experiments. Surface coverage analysis was performed using ImageJ and statistically analysed by one-way ANOVA with Bonferroni posttest ($^*P < 0.05$).

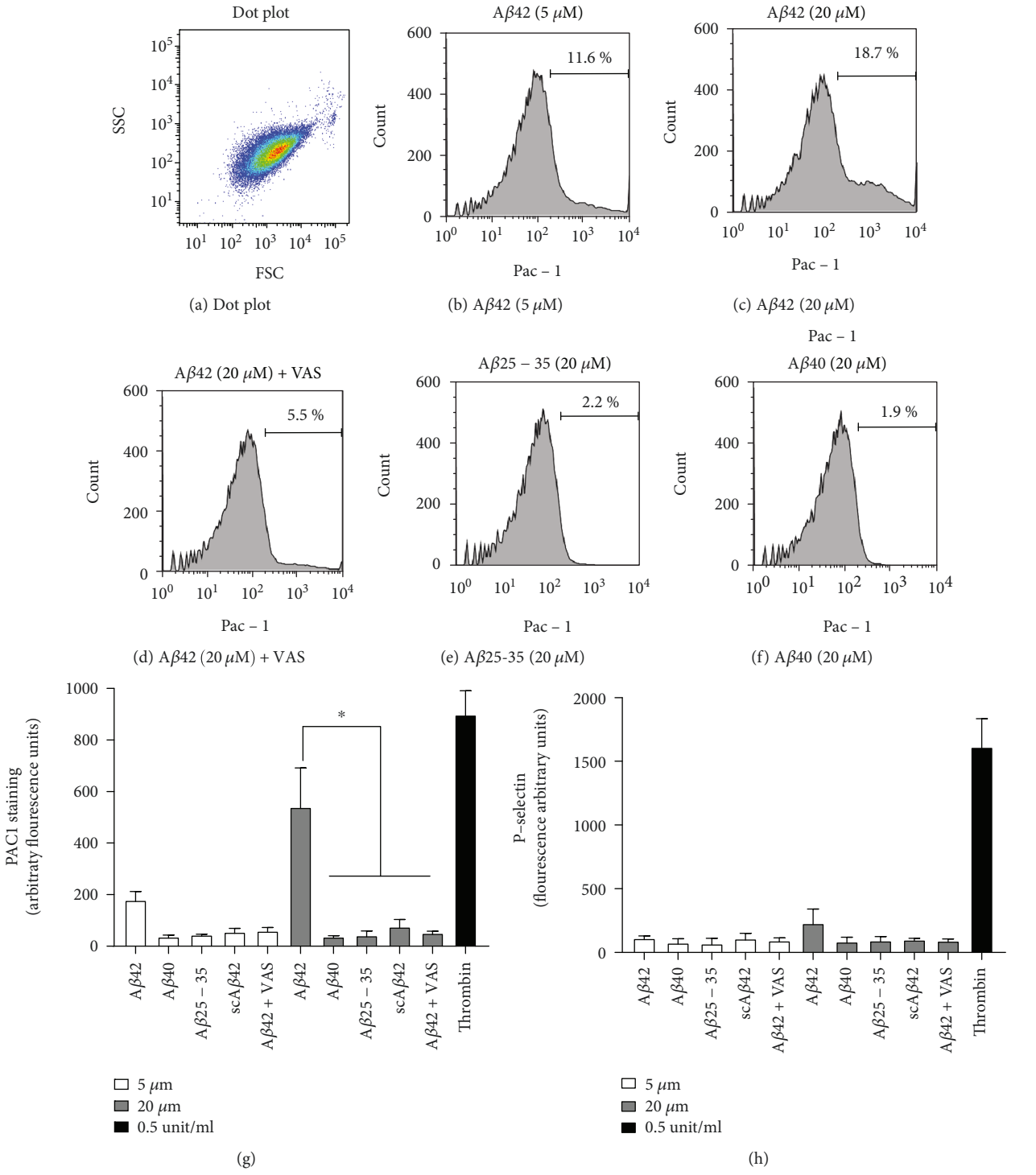

Figure 6: Activation of integrin αIIbβ3 by Aβ1-42. Washed platelets were stimulated as indicated with Aβ1-42, Aβ1-40, Aβ25-35, or scrambled Aβ1-42 or 0.5 units/ml thrombin for 10 minutes and then labelled with FITC-PAC1 (b-g) and PE-Cy5-P-selectin (h) for a further 10 minutes. A side-scattering (SSC)/forward-scattering (FSC) dot plot is shown in (a) and suggests the high purity of the platelet preparation. The histograms for the intensity of PAC1 staining in the different conditions are shown in (b-f) (representative of 3 independent experiments). Data analyses are shown in (g) and (h). Statistical analysis by one-way ANOVA with Bonferroni posttest is shown in (g) and (h) ($n = 3$, $^*P < 0.05$).

intracellular signalling in platelets. This seems to favour the hypothesis that GPVI is the receptor for β amyloid peptides on platelets, as this receptor preferentially binds substrates in a fibrillary form, which allows the contemporaneous interaction of the same fibril to different receptors (GPVI and integrin $\alpha 2\beta 1$ in the case of collagen) [44, 45].

Our static adhesion results are in partial disagreement with older studies describing the ability of Aβ25-35 and

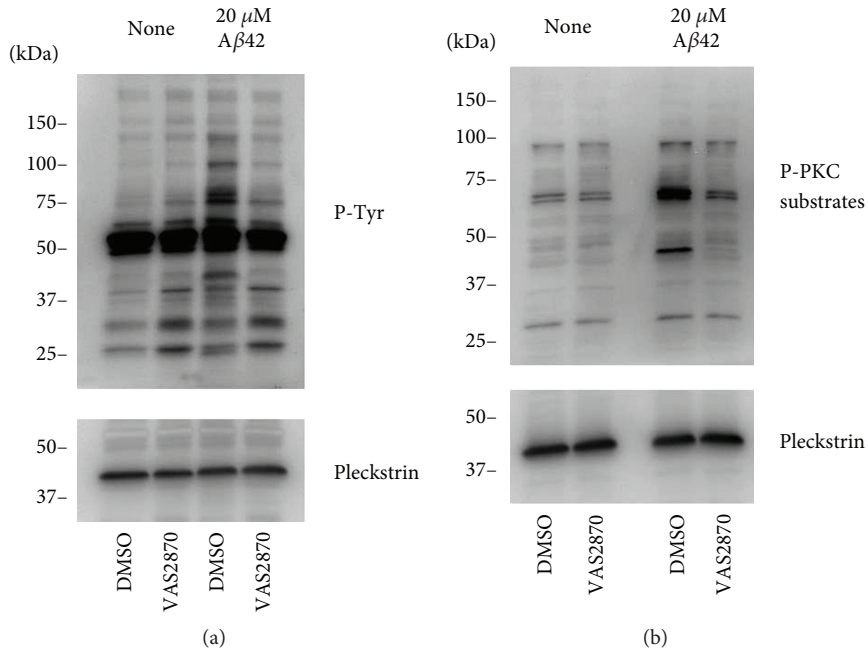

Figure 7: Aβ42-induced signalling in platelets. (a, b) Unstimulated and Aβ42-stimulated (20 μM) human platelets were treated with 10 μM DMSO or VAS2870. Total proteins were separated by SDS-PAGE as described in the Materials and Methods, and protein phosphorylation was analysed by immunoblotting with the indicated antibodies: (a) anti-p-Tyr and anti-pleckstrin antibody and (b) anti-PKC phosphosubstrate and anti-pleckstrin antibody. The figure represents blots from three independent experiments.

Aβ1-40 to promote platelet adhesion [16, 22, 31, 46]. In reality, in our experiments, Aβ1-40 and Aβ25-35 coating led to a noticeable increase in platelet adhesion (from less than 200 platelets per optical field on scrambled peptides to around 400). Possibly because of the extent of the effect of Aβ1-42 (over 800 platelets per optical field), the effect of these two peptides did not have statistically significant results. Analysis of adhering platelets at a higher magnification revealed that Aβ1-40 and Aβ25-35 did not induce extensive platelet spreading, with most platelets adhering to these substrates displaying a spherical morphology and modest filopodia formation, which is indicative of partial activation. These data are therefore suggesting some ability of Aβ25-35 and Aβ1-40 to induce platelet adhesion, but a significantly higher platelet adhesion to Aβ1-42, which is likely to induce more extensive platelet intracellular signalling and full spreading (as suggested by spreading data on Figure 3). The conditions utilised for the resuspension of the peptides and the coating of the surfaces in this and Canobbio et al.'s study of 2013 [16] are different, which is likely to affect the level of peptide fibrillation and ability to bind platelets. Further investigation of this discrepancy is necessary to fully understand how platelet binding of β amyloid peptides is regulated. As platelet adhesion under static conditions recapitulates platelet adhesion in the bloodstream, these data suggest the possibility that microthrombosis observed in the neurovasculature of AD patients is due to platelet adhesion to Aβ1-42 accumulating in the perivascular space and migrating into the bloodstream via endothelial cell transport [47].

We also tested Aβ peptides for their ability to induce thrombus formation in whole blood under physiological shear. In previous studies, it was shown that Aβ25-35 was not able to induce thrombus formation on its own [35]. This was confirmed in the present study. The ability of amyloid peptides to potentiate platelet adhesion on collagen that we showed in previous studies was not investigated in this manuscript because the Aβ1-42 peptide showed a remarkable ability to induce platelet adhesion on its own. Although Aβ1-42 has been shown to potentiate platelet adhesion to collagen and other substrates previously [14, 48], here we present the first evidence that this peptide alone is sufficient to induce thrombus formation under flow.

Integrin αIIbβ3 has been suggested as the receptor on platelets for Aβ1-40 [22, 31]. Therefore, we analysed whether this integrin is activated in the presence of Aβ peptides. Integrins are adhesion receptors characterised by two activation states (active and inactive), with only the active state able to interact and bind its substrates. The signalling leading to integrin activation is known as inside-out signalling, while the signalling triggered by the engagement of the integrin with its substrate is known as outside-in signalling [49]. With the PAC1 antibody, we were able to assess the activation of αIIbβ3, which is significant for Aβ1-42 (but not for Aβ1-40, Aβ25-35, or scrambled Aβ1-42). This is a significant finding suggesting profound differences in the biological effect of Aβ peptides, with only Aβ1-42 inducing signalling activation in platelets. This is in contrast with previous studies showing the signalling response induced by Aβ1-40 [22, 31] or Aβ25-35 [35]. This discrepancy remains difficult to explain, but the differences in the experimental conditions and the preparation of the peptide are a likely explanation. In addition, our current study cannot categorically exclude

some level of platelet activation by other Aβ peptides (as shown, e.g., in the static adhesion experiments where Aβ1-40 and Aβ25-35 induce a moderate increase compared to controls). Certainly, Aβ1-42 represents by far the most active Aβ peptide in our hands.

One important question that remains unanswered relates to the receptor responsible for the initial engagement of Aβ1-42. Integrin αIIbβ3 is the most expressed and functionally crucial adhesion receptor in platelets [50]. Its activation is the consequence of a signalling cascade known as inside-out signalling, which requires receptor-dependent activation. Therefore, although integrin αIIbβ3 is likely to participate in platelet adhesion to Aβ peptides, an alternative receptor is likely to exist. Different receptors have been suggested, including protease-activated receptor 1 [23], GPVI [27], and CD36 [21]. Our current data do not help to resolve this impasse.

The intracellular signalling involved in platelet adhesion and activation by β amyloid peptides has been studied by several groups. For example, Sonkar et al. showed that exposure to Aβ25-35 resulted in increased myosin light chain (MLC) phosphorylation and RhoA-GTP levels. This led to the conclusion that Aβ25-35 induces cellular activation via RhoA-dependent modulation of actin and cytoskeletal reorganisation [51]. Our previous investigations also showed that Aβ25-35 promoted intracellular calcium increase by entry from the extracellular environment, which led to dense granule and ADP release, and in turn to the activation of the $P2Y_{12}$ receptor, the small GTPase Rap1b, and both PI3K and MAP kinase pathways [35]. In this study, we utilised tyrosine phosphorylation and PKC-dependent phosphorylation tested by immunoblotting (Figures 7(a) and 7(b)) as markers of platelet activation and to confirm that NOX activity is crucial to trigger Aβ-dependent signalling in platelets. No further detail on the signalling cascades triggered by Aβ peptides can be drawn from this study. The activation of tyrosine phosphorylation and PKC-dependent protein phosphorylation cascades are central to platelet activation and common to most platelet agonists [52, 53]. We have shown previously the modulation of PKC activity by NOX inhibitors, possibly via dampening of GPVI receptor signalling [25]. Other investigators highlighted the link between NOX activation and PKC activity. In fact, this appears to be a bidirectional interaction, not only with different PKC isozymes showing the ability to activate NOXs (e.g., [54]) but also with NOX-dependent ROS leading to oxidation and activation of PKC enzymes [55]. The data from our current study could be explained by either direct PKC stimulation or triggering of cell signalling leading to PKC activation.

Interestingly, although the effect on αIIbβ3 by Aβ1-42 was very evident (i.e., similar to thrombin for 20 μM Aβ1-42), there was no apparent platelet degranulation, as measured by P-selectin immunostaining. This implies that differently to canonical agonists such as thrombin, collagen, or thromboxane A2, Aβ1-42 induces integrin activation without full platelet activation (i.e., partial stimulation). This may explain the poor activity of Aβ1-42 as a platelet agonist in some traditional assays, such as platelet aggregation [28].

In general, the variability in the peptides utilised (e.g., Aβ25-35, Aβ1-40, or Aβ1-42) and the focus of different studies on different receptors and signalling pathways led to apparently contradicting results. For example, an intriguing study reported the reduction of Aβ peptide-dependent platelet activation by fibrinogen [56]. Although the underlying mechanisms remain difficult to explain, this observation may be correlated to our data on Aβ peptide-dependent activation of integrin αIIbβ3 (which is the main fibrinogen receptor on platelets). The use by authors of the above study of a different Aβ peptide for their stimulations (i.e., Aβ25-35) makes any comparison of our and their studies difficult. Further studies are required to resolve these contradictions.

This study highlights the importance of NADPH oxidase activation and platelet oxidative responses in the prothrombotic responses induced by Aβ1-42, which is the β amyloid peptide accumulating in the brain of Alzheimer's and cerebral amyloid angiopathy (CAA) patients. In addition to giving us some direction in the elucidation of the molecular mechanisms underlying platelet activation by β amyloid peptides, these data suggest a potential therapeutic opportunity aiming at limiting the vascular component of Alzheimer's disease by targeting NADPH oxidase activity.

Data Availability

The manuscript does not contain data-intensive results and did not require the use of online repositories. Raw data are available on request by contacting the corresponding author.

Disclosure

The views expressed are those of the author and not necessarily those of the NHS, the NIHR, or the Department of Health.

Conflicts of Interest

The authors have no conflicts of interest.

Acknowledgments

The authors would like to thank Dr. Pia Leete at the University of Exeter Medical School for her support with cell imaging techniques. This work was funded by Alzheimer's Research UK (ARUK-PG2017A-3) and the British Heart Foundation (PG/15/40/31522). This article presents independent research funded by the above funders and supported by the National Institute for Health Research (NIHR) Exeter Clinical Research Facility.

References

[1] V. Kljajevic, "Overestimating the effects of healthy aging," *Frontiers in Aging Neuroscience*, vol. 7, p. 164, 2015.

[2] E. E. Smith and S. M. Greenberg, "β-Amyloid, blood vessels, and brain function," *Stroke*, vol. 40, no. 7, pp. 2601–2606, 2009.

[3] A. R. Nelson, M. D. Sweeney, A. P. Sagare, and B. V. Zlokovic, "Neurovascular dysfunction and neurodegeneration in dementia and Alzheimer's disease," *Biochimica et Biophysica*

Acta (BBA) - Molecular Basis of Disease, vol. 1862, no. 5, pp. 887–900, 2016.

[4] D. J. Werring, S. M. Gregoire, and L. Cipolotti, "Cerebral microbleeds and vascular cognitive impairment," *Journal of the Neurological Sciences*, vol. 299, no. 1-2, pp. 131–135, 2010.

[5] Y. Nakata-Kudo, T. Mizuno, K. Yamada et al., "Microbleeds in Alzheimer disease are more related to cerebral amyloid angiopathy than cerebrovascular disease," *Dementia and Geriatric Cognitive Disorders*, vol. 22, no. 1, pp. 8–14, 2006.

[6] M. Haglund, M. Sjobeck, and E. Englund, "Severe cerebral amyloid angiopathy characterizes an underestimated variant of vascular dementia," *Dementia and Geriatric Cognitive Disorders*, vol. 18, no. 2, pp. 132–137, 2004.

[7] C. Humpel, "Chronic mild cerebrovascular dysfunction as a cause for Alzheimer's disease?," *Experimental Gerontology*, vol. 46, no. 4, pp. 225–232, 2011.

[8] S. van Rooden, J. D. C. Goos, A. M. van Opstal et al., "Increased number of microinfarcts in Alzheimer disease at 7-T MR imaging," *Radiology*, vol. 270, no. 1, pp. 205–211, 2014.

[9] N. F. Chi, L. N. Chien, H. L. Ku, C. J. Hu, and H. Y. Chiou, "Alzheimer disease and risk of stroke: a population-based cohort study," *Neurology*, vol. 80, no. 8, pp. 705–711, 2013.

[10] J. T. O'Brien and H. S. Markus, "Vascular risk factors and Alzheimer's disease," *BMC Medicine*, vol. 12, no. 1, p. 218, 2014.

[11] R. N. Rosenberg, F. Baskin, J. A. Fosmire et al., "Altered amyloid protein processing in platelets of patients with Alzheimer disease," *Archives of Neurology*, vol. 54, no. 2, pp. 139–144, 1997.

[12] S. Sevush, W. Jy, L. L. Horstman, W. W. Mao, L. Kolodny, and Y. S. Ahn, "Platelet activation in Alzheimer disease," *Archives of Neurology*, vol. 55, no. 4, pp. 530–536, 1998.

[13] J. A. Johnston, W. W. Liu, D. T. R. Coulson et al., "Platelet beta-secretase activity is increased in Alzheimer's disease," *Neurobiology of Aging*, vol. 29, no. 5, pp. 661–668, 2008.

[14] N. S. Gowert, L. Donner, M. Chatterjee et al., "Blood platelets in the progression of Alzheimer's disease," *PLoS One*, vol. 9, no. 2, article e90523, 2014.

[15] C. I. Prodan, E. D. Ross, J. A. Stoner, L. D. Cowan, A. S. Vincent, and G. L. Dale, "Coated-platelet levels and progression from mild cognitive impairment to Alzheimer disease," *Neurology*, vol. 76, no. 3, pp. 247–252, 2011.

[16] I. Canobbio, S. Catricala, L. G. Di Pasqua et al., "Immobilized amyloid Abeta peptides support platelet adhesion and activation," *FEBS Letters*, vol. 587, no. 16, pp. 2606–2611, 2013.

[17] G. L. Suidan, P. K. Singh, S. Patel-Hett et al., "Abnormal clotting of the intrinsic/contact pathway in Alzheimer disease patients is related to cognitive ability," *Blood Advances*, vol. 2, no. 9, pp. 954–963, 2018.

[18] D. Zamolodchikov, T. Renne, and S. Strickland, "The Alzheimer's disease peptide β-amyloid promotes thrombin generation through activation of coagulation factor XII," *Journal of Thrombosis and Haemostasis*, vol. 14, no. 5, pp. 995–1007, 2016.

[19] M. Cortes-Canteli, D. Zamolodchikov, H. J. Ahn, S. Strickland, and E. H. Norris, "Fibrinogen and altered hemostasis in Alzheimer's disease," *Journal of Alzheimer's Disease*, vol. 32, no. 3, pp. 599–608, 2012.

[20] A. Jarre, N. S. Gowert, L. Donner et al., "Pre-activated blood platelets and a pro-thrombotic phenotype in APP23 mice modeling Alzheimer's disease," *Cellular Signalling*, vol. 26, no. 9, pp. 2040–2050, 2014.

[21] E. Herczenik, B. Bouma, S. J. A. Korporaal et al., "Activation of human platelets by misfolded proteins," *Arteriosclerosis, Thrombosis, and Vascular Biology*, vol. 27, no. 7, pp. 1657–1665, 2007.

[22] L. Donner, K. Falker, L. Gremer et al., "Platelets contribute to amyloid-β aggregation in cerebral vessels through integrin αIIbβ3-induced outside-in signaling and clusterin release," *Science Signaling*, vol. 9, no. 429, p. ra52, 2016.

[23] M. Y. Shen, G. Hsiao, T. H. Fong et al., "Amyloid beta peptide-activated signal pathways in human platelets," *European Journal of Pharmacology*, vol. 588, no. 2-3, pp. 259–266, 2008.

[24] T. Seno, N. Inoue, D. Gao et al., "Involvement of NADH/NADPH oxidase in human platelet ROS production," *Thrombosis Research*, vol. 103, no. 5, pp. 399–409, 2001.

[25] D. Vara, M. Campanella, and G. Pula, "The novel NOX inhibitor 2-acetylphenothiazine impairs collagen-dependent thrombus formation in a GPVI-dependent manner," *British Journal of Pharmacology*, vol. 168, no. 1, pp. 212–224, 2013.

[26] T. G. Walsh, M. C. Berndt, N. Carrim, J. Cowman, D. Kenny, and P. Metharom, "The role of Nox1 and Nox2 in GPVI-dependent platelet activation and thrombus formation," *Redox Biology*, vol. 2, pp. 178–186, 2014.

[27] O. Elaskalani, I. Khan, M. Morici et al., "Oligomeric and fibrillar amyloid beta 42 induce platelet aggregation partially through GPVI," *Platelets*, vol. 29, no. 4, pp. 415–420, 2018.

[28] A. A. Abubaker, D. Vara, I. Eggleston, I. Canobbio, and G. Pula, "A novel flow cytometry assay using dihydroethidium as redox-sensitive probe reveals NADPH oxidase-dependent generation of superoxide anion in human platelets exposed to amyloid peptide β," *Platelets*, pp. 1–9, 2017.

[29] E. Wulf, A. Deboben, F. A. Bautz, H. Faulstich, and T. Wieland, "Fluorescent phallotoxin, a tool for the visualization of cellular actin," *Proceedings of the National Academy of Sciences of the United States of America*, vol. 76, no. 9, pp. 4498–4502, 1979.

[30] M. H. Kroll, J. D. Hellums, L. V. McIntire, A. I. Schafer, and J. L. Moake, "Platelets and shear stress," *Blood*, vol. 88, no. 5, pp. 1525–1541, 1996.

[31] L. Donner, L. Gremer, T. Ziehm et al., "Relevance of N-terminal residues for amyloid-β binding to platelet integrin $\alpha_{IIb}\beta_3$, integrin outside-in signaling and amyloid-β fibril formation," *Cellular Signalling*, vol. 50, pp. 121–130, 2018.

[32] G. Pula, D. Crosby, J. Baker, and A. W. Poole, "Functional interaction of protein kinase Cα with the tyrosine kinases Syk and Src in human platelets," *The Journal of Biological Chemistry*, vol. 280, no. 8, pp. 7194–7205, 2005.

[33] G. Pula, K. Schuh, K. Nakayama, K. I. Nakayama, U. Walter, and A. W. Poole, "PKCδ regulates collagen-induced platelet aggregation through inhibition of VASP-mediated filopodia formation," *Blood*, vol. 108, no. 13, pp. 4035–4044, 2006.

[34] J. K. T. Wentworth, G. Pula, and A. W. Poole, "Vasodilator-stimulated phosphoprotein (VASP) is phosphorylated on Ser^{157} by protein kinase C-dependent and -independent mechanisms in thrombin-stimulated human platelets," *Biochemical Journal*, vol. 393, no. 2, pp. 555–564, 2006.

[35] I. Canobbio, G. F. Guidetti, B. Oliviero et al., "Amyloid β-peptide-dependent activation of human platelets: essential role for Ca^{2+} and ADP in aggregation and thrombus formation," *Biochemical Journal*, vol. 462, no. 3, pp. 513–523, 2014.

[36] S. Magwenzi, C. Woodward, K. S. Wraith et al., "Oxidized LDL activates blood platelets through CD36/NOX2-mediated inhibition of the cGMP/protein kinase G signaling cascade," *Blood*, vol. 125, no. 17, pp. 2693–2703, 2015.

[37] R. Bhatia, H. Lin, and R. Lal, "Fresh and globular amyloid β protein (1-42) induces rapid cellular degeneration: evidence for AβP channel-mediated cellular toxicity," *The FASEB Journal*, vol. 14, no. 9, pp. 1233–1243, 2000.

[38] C. G. Glabe, "Common mechanisms of amyloid oligomer pathogenesis in degenerative disease," *Neurobiology of Aging*, vol. 27, no. 4, pp. 570–575, 2006.

[39] V. Soura, M. Stewart-Parker, T. L. Williams et al., "Visualization of co-localization in Aβ42-administered neuroblastoma cells reveals lysosome damage and autophagosome accumulation related to cell death," *Biochemical Journal*, vol. 441, no. 2, pp. 579–590, 2012.

[40] J. Roche, Y. Shen, J. H. Lee, J. Ying, and A. Bax, "Monomeric $A\beta^{1-40}$ and $A\beta^{1-42}$ peptides in solution adopt very similar Ramachandran map distributions that closely resemble random coil," *Biochemistry*, vol. 55, no. 5, pp. 762–775, 2016.

[41] M. Baldassarre, C. M. Baronio, L. A. Morozova-Roche, and A. Barth, "Amyloid β-peptides 1-40 and 1-42 form oligomers with mixed β-sheets," *Chemical Science*, vol. 8, no. 12, pp. 8247–8254, 2017.

[42] N. Itoh, E. Takada, K. Okubo et al., "Not oligomers but amyloids are cytotoxic in the membrane-mediated amyloidogenesis of amyloid-β peptides," *Chembiochem*, vol. 19, no. 5, pp. 430–433, 2018.

[43] P. A. Smethurst, D. J. Onley, G. E. Jarvis et al., "Structural basis for the platelet-collagen interaction: the smallest motif within collagen that recognizes and activates platelet glycoprotein VI contains two glycine-proline-hydroxyproline triplets," *Journal of Biological Chemistry*, vol. 282, no. 2, pp. 1296–1304, 2007.

[44] R. W. Farndale, P. R. Siljander, D. J. Onley, P. Sundaresan, C. G. Knight, and M. J. Barnes, "Collagen-platelet interactions: recognition and signalling," *Biochemical Society Symposium*, vol. 70, pp. 81–94, 2003.

[45] P. R.-M. Siljander, S. Hamaia, A. R. Peachey et al., "Integrin activation state determines selectivity for novel recognition sites in fibrillar collagens," *Journal of Biological Chemistry*, vol. 279, no. 46, pp. 47763–47772, 2004.

[46] I. Canobbio, C. Visconte, B. Oliviero et al., "Increased platelet adhesion and thrombus formation in a mouse model of Alzheimer's disease," *Cellular Signalling*, vol. 28, no. 12, pp. 1863–1871, 2016.

[47] Y. X. Guo, L. Y. He, M. Zhang, F. Wang, F. Liu, and W. X. Peng, "1,25-Dihydroxyvitamin D_3 regulates expression of LRP1 and RAGE *in vitro* and *in vivo*, enhancing $A\beta_{1-40}$ brain-to-blood efflux and peripheral uptake transport," *Neuroscience*, vol. 322, pp. 28–38, 2016.

[48] C. Visconte, J. Canino, G. F. Guidetti et al., "Amyloid precursor protein is required for in vitro platelet adhesion to amyloid peptides and potentiation of thrombus formation," *Cellular Signalling*, vol. 52, pp. 95–102, 2018.

[49] P. E. Hughes and M. Pfaff, "Integrin affinity modulation," *Trends in Cell Biology*, vol. 8, no. 9, pp. 359–364, 1998.

[50] Y. Q. Ma, J. Qin, and E. F. Plow, "Platelet integrin $\alpha_{IIb}\beta_3$: activation mechanisms," *Journal of Thrombosis and Haemostasis*, vol. 5, no. 7, pp. 1345–1352, 2007.

[51] V. K. Sonkar, P. P. Kulkarni, and D. Dash, "Amyloid β peptide stimulates platelet activation through RhoA-dependent modulation of actomyosin organization," *The FASEB Journal*, vol. 28, no. 4, pp. 1819–1829, 2014.

[52] A. J. Moroi and S. P. Watson, "Impact of the PI3-kinase/Akt pathway on ITAM and hemITAM receptors: haemostasis, platelet activation and antithrombotic therapy," *Biochemical Pharmacology*, vol. 94, no. 3, pp. 186–194, 2015.

[53] M. T. Harper and A. W. Poole, "Diverse functions of protein kinase C isoforms in platelet activation and thrombus formation," *Journal of Thrombosis and Haemostasis*, vol. 8, no. 3, pp. 454–462, 2010.

[54] P. Sharma, A. T. Evans, P. J. Parker, and F. J. Evans, "NADPH-oxidase activation by protein kinase C-isotypes," *Biochemical and Biophysical Research Communications*, vol. 177, no. 3, pp. 1033–1040, 1991.

[55] D. Cosentino-Gomes, N. Rocco-Machado, and J. R. Meyer--Fernandes, "Cell signaling through protein kinase C oxidation and activation," *International Journal of Molecular Sciences*, vol. 13, no. 9, pp. 10697–10721, 2012.

[56] V. Sonkar, P. P. Kulkarni, S. N. Chaurasia et al., "Plasma fibrinogen is a natural deterrent to amyloid β-induced platelet activation," *Molecular Medicine*, vol. 22, pp. 224–232, 2016.

Hindawi
Oxidative Medicine and Cellular Longevity
Volume 2019, Article ID 4248529, 29 pages
https://doi.org/10.1155/2019/4248529

Research Article

Glycine Protects against Hypoxic-Ischemic Brain Injury by Regulating Mitochondria-Mediated Autophagy via the AMPK Pathway

Chen-chen Cai, Jiang-hu Zhu, Li-xia Ye, Yuan-yuan Dai, Ming-chu Fang, Ying-ying Hu, Shu-lin Pan, Si Chen, Pei-jun Li, Xiao-qin Fu, and Zhen-lang Lin

Department of Neonatology, The Second Affiliated Hospital and Yuying Children's Hospital of Wenzhou Medical University, Wenzhou, Zhejiang 325027, China

Correspondence should be addressed to Zhen-lang Lin; linzhenlang@hotmail.com

Received 4 July 2018; Revised 10 August 2018; Accepted 14 September 2018; Published 6 February 2019

Academic Editor: Ana Lloret

Hypoxic-ischemic encephalopathy (HIE) is detrimental to newborns and is associated with high mortality and poor prognosis. Thus, the primary aim of the present study was to determine whether glycine could (1) attenuate HIE injury in rats and hypoxic stress in PC12 cells and (2) downregulate mitochondria-mediated autophagy dependent on the adenosine monophosphate-(AMP-) activated protein kinase (AMPK) pathway. Experiments conducted using an *in vivo* HIE animal model and *in vitro* hypoxic stress to PC12 cells revealed that intense autophagy associated with mitochondrial function occurred during *in vivo* HIE injury and *in vitro* hypoxic stress. However, glycine treatment effectively attenuated mitochondria-mediated autophagy. Additionally, after identifying alterations in proteins within the AMPK pathway in rats and PC12 cells following glycine treatment, cyclosporin A (CsA) and 5-aminoimidazole-4-carboxamide-1-b-4-ribofuranoside (AICAR) were administered in these models and indicated that glycine protected against HIE and $CoCl_2$ injury by downregulating mitochondria-mediated autophagy that was dependent on the AMPK pathway. Overall, glycine attenuated hypoxic-ischemic injury in neurons via reductions in mitochondria-mediated autophagy through the AMPK pathway both *in vitro* and *in vivo*.

1. Introduction

Hypoxic-ischemic injury in the neonatal brain is associated with detrimental and lethal consequences secondary to perinatal asphyxia [1]. Neonates diagnosed with hypoxic-ischemic encephalopathy (HIE) exhibit enhanced morbidity with poor clinical outcomes, which have increased awareness of this disorder worldwide [2]. In developed countries, approximately 1–8 per 1000 live births are diagnosed with HIE, while 26 per 1000 live births suffered from this serious disease in developing countries [3]. The high cost and complicated therapeutic strategies associated with HIE typically result in difficulties maintaining adherence to treatment for patients and families. Even worse, severe cases of HIE often result in poor prognoses that include lifelong issues, like cerebral palsy, epilepsy, mental retardation, learning and cognitive disabilities, and hearing loss [4]. Thus, the development of inexpensive and effective treatment modalities is necessary to allow families to continue beneficial treatments that enhance the long-term prognoses of neonates.

It has been shown that autophagy is highly correlated with the pathogenesis of HIE, although autophagy is an important degradation process designed to protect intracellular homeostasis under conditions of hypoxic-ischemic injury [5, 6]. To a large extent, this process also degrades a significant number of abnormal proteins, injured intracellular organelles, and degraded normal proteins to influence neuronal function under conditions where fewer organelles are working [7]. In particular, the selective degradation of mitochondria is an important process in the nervous system.

Mitochondria are organelles that supply energy to the cell and play important roles in the nervous system. Suffering from the hypoxic or ischemic condition, mitochondria are sensitive and becoming swelling or mitochondrial fusion

[8]. Accumulating evidence suggests that mitochondrial dysfunction also plays a central role in a variety of nervous system diseases. For example, insults of hypoxic or ischemic conditions to neurons may result from generation of reactive oxygen species (ROS), particularly reactive oxygen-free radicals or other molecules, which act as crucial physiological components of intracellular signaling pathways [9]. However, most ROS are primarily generated by damaged mitochondria [10] that typically exhibit abnormalities in mitochondrial membrane potential (MMP). In parallel, MMP acts as an indicator of mitochondria-mediated autophagy [11]. For further investigation to study mitochondria-mediated autophagy among researches, cyclosporin A (CsA), as a traditional inhibitor, is widely used to suppress this autophagy process [12].

In addition to producing the majority of intracellular adenosine triphosphate (ATP), mitochondria are also the key factor to maintain the homeostasis within the intracellular environment. The adenosine monophosphate- (AMP-) activated protein kinase (AMPK) pathway is a key sensor of mitochondrial function and is sensitive to downward trends in ATP. Under conditions of energy imbalance or ROS generation in which AMPK signaling is disrupted, ATP levels decrease and intracellular AMP levels increase with particular subunits (α, β, and γ) of AMPK to activate the AMPK pathway. α subunit of AMPK acts as a catalytic role and regulatory β and γ subunits keep the stable condition to AMPK. Among these subunits, γ subunit contains nucleotide binding domains, while β subunit should be stimulated allosterically to activate AMPK. Furthermore, α subunit is pivotal to AMPK activation, including phosphorylation [13]. In our previous concepts, the AMPK pathway always benefits recovery and plays a vital role in the cellular environment. For example, the AMPK pathway exhibits a range of activation such that it protects neurons under conditions of hypoxic attack but does not benefit neurons under hypoxic conditions if it is overactivated [14]. In parallel, phosphorylation of AMPK did not always play a protective role to maintain the energy regeneration process. It may highly conserve autophagy kinase like Atg1, which mostly stimulates mitochondria-mediated autophagy [15]. Thus, the AMPK signaling pathway reflects the condition of mitochondrial function, such as fission or the recycling of the phospholipid membranes of mitochondria [16]. Furthermore, to figure out the relation between the AMPK pathway and mitochondria-mediated autophagy, a classical agonist of the AMPK pathway, 5-aminoimidazole-4-carboxamide-1-b-4-ribofuranoside (AICAR) [17], preserves AMPK activation *in vivo* and *in vitro*, which was confirmed in the present study.

Cobalt chloride ($CoCl_2$), as a chemical compound, is widely acknowledged as a classical stimulator to hypoxic-ischemic condition, which triggers ROS generation and transcriptional dysfunction of some genes, including hypoxia-inducible factor 1 (HIF-1) and pCNA [18]. In particular, $CoCl_2$-induced injury may destroy mitochondrial membrane potential, ATP level, and increase mitochondrial fission [19]. PC12 cell is a cell line derived from rat pheochromocytoma and its highly differentiated cell type is similar to neuronal characteristics, which is widely used as an *in vitro* model for observing neuronal pathogeneses [20]. Therefore, $CoCl_2$-treated PC12 cell, as the hypoxic model, was used in our study to observe the mitochondria insults related with autophagy.

Glycine is a common substance present in numerous biomolecules where it plays a fundamental role in cellular metabolism. Glycine also acts as a neurotransmitter or N-methyl-D-aspartate receptor coagonist, which is reported for its effectiveness among neurodegenerative diseases, like Alzheimer's disease [21]. Moreover, mitochondria oxidatively decompose glycine into CO_2, NH_4^+, NADH, and a methylene group to create methylenetetrahydrofolate, which sustains homeostasis [22]. However, the inhibition of oxidative phosphorylation and/or glycolytic energy production by glycine may protect intracellular energy production, which plays a protective role against neurological diseases, such as stroke or intracerebral hemorrhage [23]. Indeed, glycine protects against injuries mediated by hypoxia, hypoxia-reoxygenation, ROS, and chemical energy depletion [24]. Moreover, glycine has been increasingly employed as an effective therapeutic strategy for the protection of mitochondria in preclinical experiments in the liver [25] and kidney [26].

To date, few studies [27] have investigated whether glycine protects against hypoxic-ischemic injury in the brain by regulating mitochondria-mediated autophagy processes that are dependent on the AMPK pathway. Therefore, the present study is aimed at determining the role that glycine plays in neuroprotection via the regulation of mitochondria-mediated autophagy using both *in vivo* and *in vitro* models to aid future research.

2. Material and Methods

2.1. Drug and Reagents. Glycine (assay ≥ 98.5%; G5417-MSDS) and $CoCl_2 \cdot 6H_2O$ (C8661-25G) were purchased from Sigma-Aldrich (St. Louis, MO, USA). Dulbecco's modified Eagle medium (DMEM; 10569044) and fetal bovine serum (FBS; 10099141) were obtained from Gibco (Grand Island, NY, USA). 2,3,5-Triphenyltetrazolium chloride (TTC; 17779-10X10ML-F) was purchased from Sigma-Aldrich (St. Louis, MO, USA). 2′,7′-dichlorodihydrofluorescein diacetate (DCFH-DA; S0033) was purchased from Beyotime (Beijing, China). 5-Aminoimidazole-4-carboxamide-1-b-4-ribofuranoside (AICAR; A9978-25MG) was acquired from Sigma-Aldrich (St. Louis, MO, USA) and cyclosporin A (CsA; S2286) was obtained from Selleckchem (Houston, TX, USA). Cell counting kit-8 (CCK-8; CK04) was gained from Solarbio (Beijing, China). MitoSOX Red (40778ES50) was delivered from Yeasen (Shanghai, China). Tetramethylrhodamine ethyl ester perchlorate (TMRE; 87917-25MG) and Hoechst 33258 (94403-1ML) were also purchased from Sigma-Aldrich (St. Louis, MO, USA). 4,6-Diamidino-2-phenylindole (DAPI; C1002) and terminal deoxynucleotidyl transferase dUTP nick end labeling (TUNEL; C1088) were purchased from Beyotime (Shanghai, China).

Primary antibodies are as follows: mouse antihypoxia-inducible factor 1-alpha (HIF-1α, Abcam, Cambridge, MA, USA; H1alpha67), rabbit anti-Mitofusin 2 (Mfn-2, Cell Signaling Technology, Danvers, MA, USA; 9482s), mouse

anti-parkin (Abcam, Cambridge, MA, USA; ab77924), rabbit anti-PINK1 (Abcam, Cambridge, MA, USA; ab23707), rabbit anti-p62 (Cell Signaling Technology, Danvers, MA, USA; 23214), rabbit anti-LC3 B (Cell Signaling Technology, Danvers, MA, USA; 3868), rabbit anti-Bnip3 (Abcam, Cambridge, MA, USA; ab109362), rabbit anti-Thr^{172} phosphorylated $AMPK_{\alpha}$ (Cell Signaling Technology, Danvers, MA, USA; 50081), rabbit antiglyceraldehyde-3-phosphate dehydrogenase (GAPDH, Cell Signaling Technology, Danvers, MA, USA; 5174T), rabbit anti-$AMPK_{\alpha}$ (Cell Signaling Technology, Danvers, MA, USA; 5832), and rabbit anti-Ser^{2448} phosphorylated mTOR (Cell Signaling Technology, Danvers, MA, USA; 5536). Secondary antibodies are as follows: goat anti-rabbit secondary antibody (ab150077) and rabbit anti-mouse secondary antibody (ab150125) were purchased from Abcam.

2.2. Animal Care, Surgery, and Ethical Certification. Sprague-Dawley (SD) rats were provided by the Animal Center of the Chinese Academy of Sciences, placed in individual housing of Wenzhou Medical University Animal Center (ethic number: wydw2014-0058), allowed free access to water and standard feed, and maintained in specific pathogen-free conditions under a 12/12 h light cycle at $23 \pm 2^{\circ}C$ and $60 \pm 10\%$ humidity. The rats were then crossbred to generate neonate SD rats that, on postnatal day 7 (P7), underwent minor surgery. Overall, 205 healthy neonatal 4-day-old rats were used in this study. 125 4-day-old rats were randomly allocated in 5 experimental groups and 25 4-day-old rats in each experimental group, and 80 7-day-old rats used to figure out the optimum dosage of glycine at a dose-dependent manner. For searching the optimum dosage of glycine, series of dose-dependent manner tests were used to figure out the most effective and economic dosage in order to gain the best recovery [28]. Briefly, 7-day-old pups in the HIE + glycine group were pretreated with an optimum intraperitoneal (i.p.) dose of glycine, while pups in the HIE + glycine + CsA and the HIE + glycine + AICAR groups were treated with CsA (5 mg/kg) [29] and AICAR (50 mg/kg) [30] started at 4-day-old rats, respectively, for 3 days, then followed by glycine administration at 7-day-old rats. The model employed in the present study was adapted from Vannucci and Vannucci [31]. For the surgery, the 7-day-old pups were anesthetized with anhydrous ether and underwent an incision at the middle of the neck followed by unilateral ligation of the left common carotid artery. Following suturing of the incision, the pups were allowed to recover for 2 h. Then, they were placed in a confined space with an environment consisting of humidified nitrogen-oxygen mixture (92% nitrogen and 8% oxygen, 3–4 l/min) for 2 h to induce further hypoxia. Pups in the sham group were anaesthetized, and the same midline incisions were performed without ligation of the common carotid arteries, followed with saline (the same volume, i.p.) pretreatment. This is aimed at guaranteeing the same surgical stimulations in both sham and experimental animals in order to exclude unrelated variables caused by surgery itself. All pups returned to their rearing cages for subsequent experimental procedures. In the following days, the rats were given daily administration of the drugs or saline. All animal procedures and operations were performed according to the animal use and care protocol based on the *Guide for the Care and Use of Laboratory Animals* from the National Institutes of Health and Wenzhou Medical University.

2.3. Evaluation of the Infarct Areas. To measure the infarct areas alleviated by drug administrations, 7-day-old rats from each group were anesthetized and sacrificed 24 h after surgery. 2,3,5-Triphenyltetrazolium chloride (TTC, Sigma-Aldrich, St. Louis, MO, USA) was used to quantify infarct volume and figure out the optimum dosage of glycine. Each brain was frozen at $-20^{\circ}C$ for 15 min and cut into 2 mm coronal slices. Next, the brain slices were immersed in a 1% TTC solution in the dark for 30 min at $37^{\circ}C$ and incubated in 4% paraformaldehyde. Brain infarct areas were calculated using the ImageJ software (National Institutes of Health, Bethesda, MD, USA).

2.4. Measurement of Brain Water Content. To measure the dropsy status of injured hemispheres under hypoxic-ischemic condition and drug efficacy on the edema hemisphere, the 7-day-old rats were anesthetized with diethyl ether and sacrificed for brain analyses, as previously described [32]. The ipsilateral hemispheres from the sham group, HIE group, and HIE + glycine group were isolated to measure wet weight (accurate to 0.1 mg), and each hemisphere was placed in a drying oven ($100^{\circ}C$) for 48 h to measure the dry weight (accurate to 0.1 mg) again. The percentages of brain water content in the hemisphere were calculated using the following equation: $([\text{wet weight} - \text{dry weight}]/\text{wet weight}) \times 100\%$.

2.5. Histopathological Analysis. From the observation on pathological tissues, the isolated brains from each group among 7-day-old rats were collected 24 h after surgery and 14-day-old rats were gained 7 days after surgery or drug administration, perfused with phosphate-buffered saline (PBS; pH 7.4, 20 ml) followed by 4% (*w*/*v*) paraformaldehyde (20 ml). They were then embedded in paraffin and cut into coronal sections (5 μm) for histological evaluation, which showed directly about integrity of hemisphere or functional neuron quantity between the cortex and hippocampus. The paraffin-embedded brain sections were dewaxed, rehydrated, and stained with hematoxylin and eosin (HE) or Nissl solution (Solarbio, Beijing, China). The results of the histological procedures were measured using light microscopy.

2.6. Transmission Electron Microscopy. To further understand the inner autophagy process or mitochondrial status among neurons, transmission electron microscopy (TEM, H-600IV; HITACHI, Tokyo, Japan) was used to observe directly this phenomenon. The 7-day-old pups were intracardially perfused with 2.5% glutaraldehyde and 2% paraformaldehyde in cacodylate buffer (0.1 mol/l, pH 7.4), and then the brains were postfixed overnight at $4^{\circ}C$ in the same fixative. The brains were rinsed in 1% osmium tetroxide, dehydrated in an acetone series, infiltrated in Epon 812 for a longer period, and finally embedded. Next, ultrathin sections were cut with a diamond knife and stained with uranyl acetate and lead citrate. The sections were examined using TEM

and the mitochondrial forms in both the cortex and hippocampus of each group were assessed.

2.7. Hindlimb Suspension Testing. After observing pathological alterations and subcellular structures above, the further neuronal functions or improvements should also be measured. Hindlimb suspension was performed to evaluate the right hindlimb muscular strength while its ipsilateral hemisphere was damaged. Among 14-day-old rats, a hindlimb suspension test [33] was used to detect neuromuscular function in the right hindlimb. Briefly, a jar that was padded at the bottom with medical cotton balls to mitigate the consequences of falling was used and hindlimbs of the rats were placed on the edge of a tube. Behavior was scored as follows: 4, normal hindlimb separation with the tail raised; 3, hindlimbs were relatively weak and close together but not touching each other; 2, hindlimbs were often touching; 1, apparent weakness of the hindlimbs with the tail raised and limbs in a clasped position; and 0, a constant clasped condition of the hindlimbs with the tail lowered or failure to hold onto the edge for any period of time.

2.8. Berderson Behavioral Test. The Berderson behavioral test [34] was employed to assess palsy in the contralateral limbs of the 28-day-old rats. Briefly, the rats were held gently by the tail, suspended one meter above a platform, and their forelimb flexion was observed and scored as follows: 0 (normal), rats extend forelimbs toward the floor with no neurological deficits; 1, the forelimb contralateral to the injured hemisphere was often flexed in different postures including slight wrist flexion, shoulder adduction with extension at the elbow, posturing with full flexion of wrist and/or elbow, and/or adduction with severe internal rotation of the shoulder; 2, rats were placed on a large paperboard that could be gripped by the claws, gentle lateral pressure was applied behind the shoulder until the forelimbs slid several inches (which was frequently shown in each direction with their tails held), and severely dysfunctional rats exhibited consistently reduced resistance to the lateral push toward the paretic side; and 3, rats consistently circled toward the paretic side. Each neurological examination was performed in a 3–5 min period using a double-blind procedure.

2.9. Longa Assessment. After 4 weeks after model surgery, neuronal function among 28-day-old rats is ideally mature among normal adult rats. Longa scores [35] are judged at 28-day-old rats; we observed each rat walking behaviors to evaluate its ipsilateral hemisphere injury or improvement by drug administration. Scores are as follows: 0, normal function, no neurologic deficits; 1, flexion of the right front paw observed while the tail was raised, mild neurological deficit; 2, spontaneous circling to the right when walking, moderate neurological deficit; 3, body slanted to the right when walking, severe neurological deficit; and 4, not able to walk spontaneously without possible loss of consciousness. Each neurological examination was performed three times using a double-blind procedure.

2.10. Cell Cultures and Treatment. Differentiated PC12 cells were provided by the Type Culture Collection of the Chinese Academy of Sciences (Shanghai, China). The cells were cultured in DMEM (Gibco, Grand Island, NY, USA) supplemented with 10% (*vol*/*vol*) FBS (Gibco, Grand Island, NY, USA) in a humidified incubator with an atmosphere of 5% CO_2 at 37°C in 6-well plates (3 ml culture media per well) or 96-well plates (200 μl culture media per well). In the $CoCl_2$ group, the PC12 cells were only treated with $CoCl_2$, whereas the PC12 cells in the $CoCl_2$ + glycine group were pretreated with glycine (ps. 1 μM glycine: 1 ml culture media added with 1 μl 1 mM glycine, according to the dose-dependent manner) and then underwent hypoxic injury in the same manner as the $CoCl_2$ group.

In another set of experiments, PC12 cells were pretreated with CsA (1 μM, Selleckchem, Houston, TX, USA) for 24 h prior to the glycine and $CoCl_2$ treatments. To further assess the functions of the AMPK pathway using *in vitro* experiments, PC12 cells were pretreated with AICAR (0.5 mM) for 3 h prior to the operations mentioned above.

2.11. Cell Viability Assay. Cell viability was measured with the nonradioactive cell counting kit-8 (CCK-8, Solarbio) to understand PC12 cell conditions (activation or survival). PC12 cells at a density of 1×10^4 were seeded on a 96-well plate in DMEM supplemented with 10% (*vol*/*vol*) FBS and administered $CoCl_2$ or glycine in a dose- and time-dependent manner after 12 h of cultivation. Next, a culture medium supplied with the CCK-8 solution was added for an additional hour and its absorbance was measured with a microplate reader (Tecan Group Ltd., Männedorf, Switzerland) at a wavelength of 490 nm.

2.12. Measurement of Intracellular ROS Production. To analyze the ROS generation under the hypoxic-ischemic environment, PC12 cells were digested with trypsin, washed twice with PBS, and finally incubated with the ROS-specific fluorescent probe dye dichlorodihydrofluorescein diacetate (DCFH-DA; Beyotime, Shanghai, China) for 30 min at 37°C. Following incubation, the cells were collected and suspended in washing buffer, and ROS production was detected using a flow cytometer.

2.13. Detection of Mitochondrial ROS. Mitochondrial ROS level was measured using MitoSOX Red (Yeasen, Shangai, China), which was a fluorescent indicator of mitochondrial superoxide anions. Briefly, PC12 cells were washed with Hank's balanced salt solution (HBSS) and incubated in the dark with 5 μM MitoSOX Red for 20 min at 37°C. Additionally, cell nuclei were stained with 4′,6′-diamidino-2-phenylindol (DAPI, Beyotime) for 5 min at room temperature. The cells were washed with PBS and imaged using fluorescence microscopy (Olympus IX73) with excitation and emission filters of 510 and 580 nm, respectively.

2.14. Measurement of the MMP. The MMP was measured using confocal microscopy with tetramethylrhodamine ethyl ester (TMRE) staining (Sigma-Aldrich). This technique is aimed at discovering the function of mitochondria or indirectly reflecting the insults among mitochondria. Following administration of the study drugs as described above, the cells were treated with 50 nM TMRE and further incubated

for 45 min at 37°C. Additionally, nuclei of the PC12 cells were loaded with Hoechst dye to determine the position of each cell.

2.15. Terminal Deoxynucleotidyl Transferase dUTP Nick End Labeling. Terminal deoxynucleotidyl transferase dUTP nick end labeling (TUNEL; Beyotime) assays were performed following the administrations of each drug. Subsequent to TUNEL staining, the cells were stained with a DAPI solution in the dark for 5 min at room temperature to identify nuclei. This tool helped to understand the apoptosis undergoing among cellular environments. Fluorescence imaging was performed with a fluorescence microscope (Olympus IX73), and the numbers of TUNEL-positive cells are presented as the percentage of positive nuclei/total nuclei × 100%.

2.16. Immunofluorescence Analysis. For the immunofluorescence analyses, PC12 cells were washed three times with PBS and incubated with 4% paraformaldehyde at 4°C for 25 min. Next, the cells were loaded with 0.3% Triton X-100 for 15 min and incubated in 5% bovine serum albumin (BSA) at 37°C for 30 min. The primary antibody anti-Mfn-2, an indicator of further figuring out the outer membrane protein of mitochondria and indirect reflection of mitochondrial situation, was applied to the cells at 4°C for 12 h, followed by incubation with an appropriate secondary antibody at 37°C for 1 h. Additionally, the nuclei were stained with DAPI; images from each group were obtained with a fluorescence microscope (Olympus IX73) and the data were analyzed with the ImageJ software.

2.17. Monodansylcadaverine Staining. Autophagic vacuoles are frequently observed during autophagy and can be visualized by monodansylcadaverine (MDC) staining [36]. In the present study, PC12 cells were seeded in six-well plates with sterile cover slips and each group of PC12 cells was incubated with 0.05 mM MDC (Sigma-Aldrich, USA) in culture medium in the dark for 30 min at 37°C following pretreatment with a drug or an operation. After the incubation, cells were washed with PBS and analyzed with a fluorescence microscope (Olympus IX73; Olympus, Tokyo, Japan).

2.18. Western Blot Analysis. For Western blot analyses, the cells were washed with PBS, loaded with radioimmunoprecipitation assay (RIPA) buffer with the PMSF protease inhibitor, and placed upon ice for 30 min. Tissue samples from the cortex and hippocampus were isolated from the ischemic hemisphere, and proteins were extracted using a mammalian tissue extraction reagent. Additionally, the protein samples were homogenized and analyzed as previously described [37]. Briefly, equivalent amounts of protein were separated by 10% sodium dodecyl sulfate polyacrylamide gel electrophoresis (SDS-PAGE), transferred to polyvinylidene difluoride (PVDF) membranes (0.22 μm), and blocked with 5% skim milk for 2 h at room temperature. Subsequently, the membranes were incubated in the appropriate primary antibodies overnight at 4°C followed by incubation with a secondary antibody (at appropriate dilutions) for 2 h at room temperature. The membranes were quantitatively analyzed using the Image Lab software with densitometry after the addition of an enhanced chemiluminescence substrate (Bio-Rad, Hercules, CA, USA).

2.19. Statistical Analysis. All data are expressed as the mean ± standard error of the mean (SEM) and were analyzed with a one-way analysis of variance (ANOVA) test followed by Newman-Keuls tests for intergroup comparisons. P value less than 0.05 was considered to indicate statistical significance. P value < 0.01 indicated that the probability of the experimental value falling into the control distribution was lower than a P value < 0.05. P value < 0.001 indicated that the probability of the experimental value falling into the control distribution was lower than a P value < 0.01. All data were analyzed using the SPSS 17.0 software (SPSS Inc., Chicago, IL, USA).

3. Results

3.1. Glycine Attenuated Hypoxic-Ischemic Injury in the Brains of Neonatal Rats. In the present study, infarct volume was quantified in rats from the sham, HIE, and HIE + glycine groups. In the HIE rats, glycine reduced the infarct area at an optimum dose of 600 mg/kg (dose/body weight) (Figures 1(a) and 1(b)). Western blot analyses assessing expression of the transcription factor hypoxia-inducible factor 1-alpha (HIF-1α) revealed that several different doses of glycine (200–1000 mg/kg) significantly reduced the expression of HIF-1α, indicating a rescue effect of glycine (Figures 1(c) and 1(d)). Therefore, all further experiments were performed with 600 mg/kg of glycine as the treatment standard. The rat brains of the sham, HIE, and HIE + glycine (600 mg/kg) groups were collected and their wet and dry ratios were measured. In the paraformaldehyde-fixed brains of each group, edema was easily identified in the left hemisphere of HIE rats but glycine administration attenuated the affected area to a certain extent (Figure 1(e)). Staining procedures in the cortex and hippocampus of the HIE group revealed more obvious edema than the sham group. However, these injuries were alleviated in the HIE + glycine group. Nissl stainings of the cortex and hippocampus were analyzed to assess neuronal viability (Figures 1(c)–1(k)). The number of functional neurons in Nissl-stained images was assessed to determine the effectiveness of glycine for treating or protecting neurons against hypoxic-ischemic injury. TEM images intuitively revealed the extent of mitochondrial injury in tissues. The HIE group exhibited swelling symptoms of injury in mitochondria, whereas the HIE + glycine group showed relatively normal mitochondria in neurons from the cortex and hippocampus (Figure 1(l)). Furthermore, the HIE group contained the highest quantity of autophagosomes, whereas the HIE + glycine group greatly reduced the quantity which exhibited the effectiveness of glycine upon alleviating autophagy.

3.2. Glycine Protected against Hypoxic-Ischemic Injury in the Brains via Attenuation of Mitochondrial-Mediated Autophagy. Following isolation of the cortex and hippocampus tissues, proteins were extracted for Western blot analyses. The protein levels of Binp3, p62, and microtubule-associated

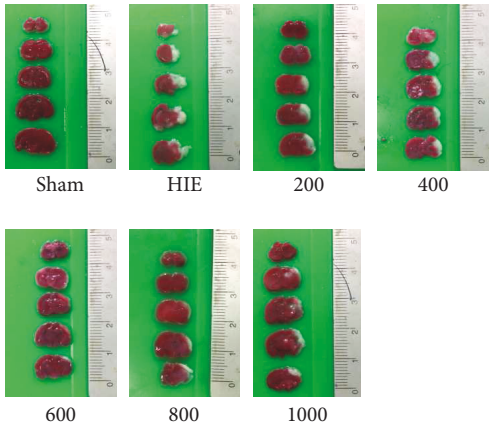

(a)

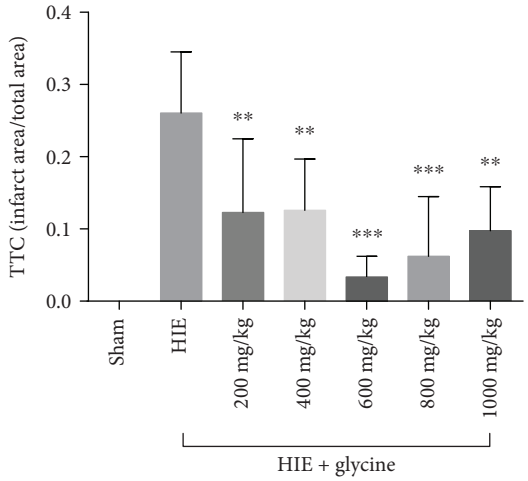

(b)

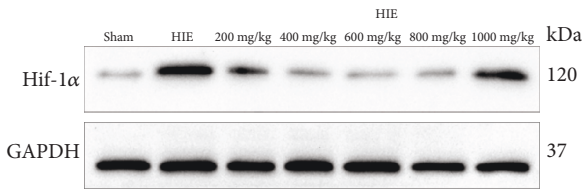

(c)

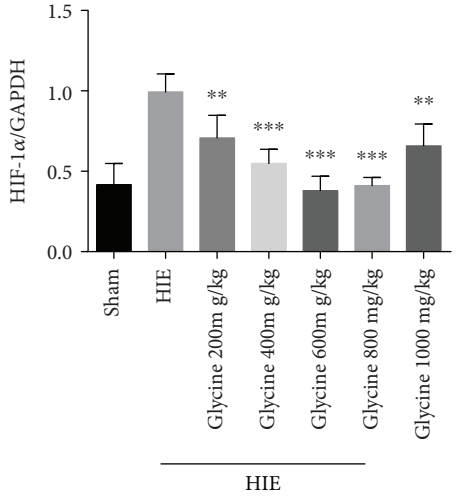

(d)

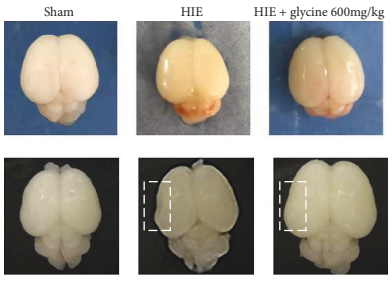

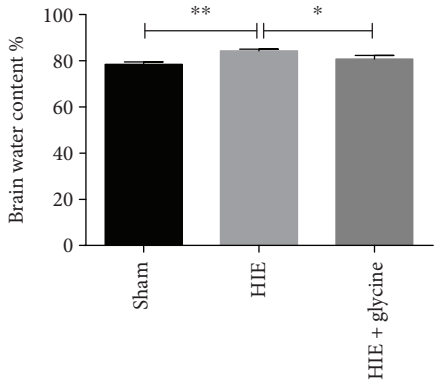

(e)

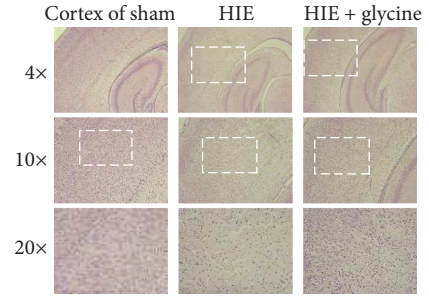

(f)

Figure 1: Continued.

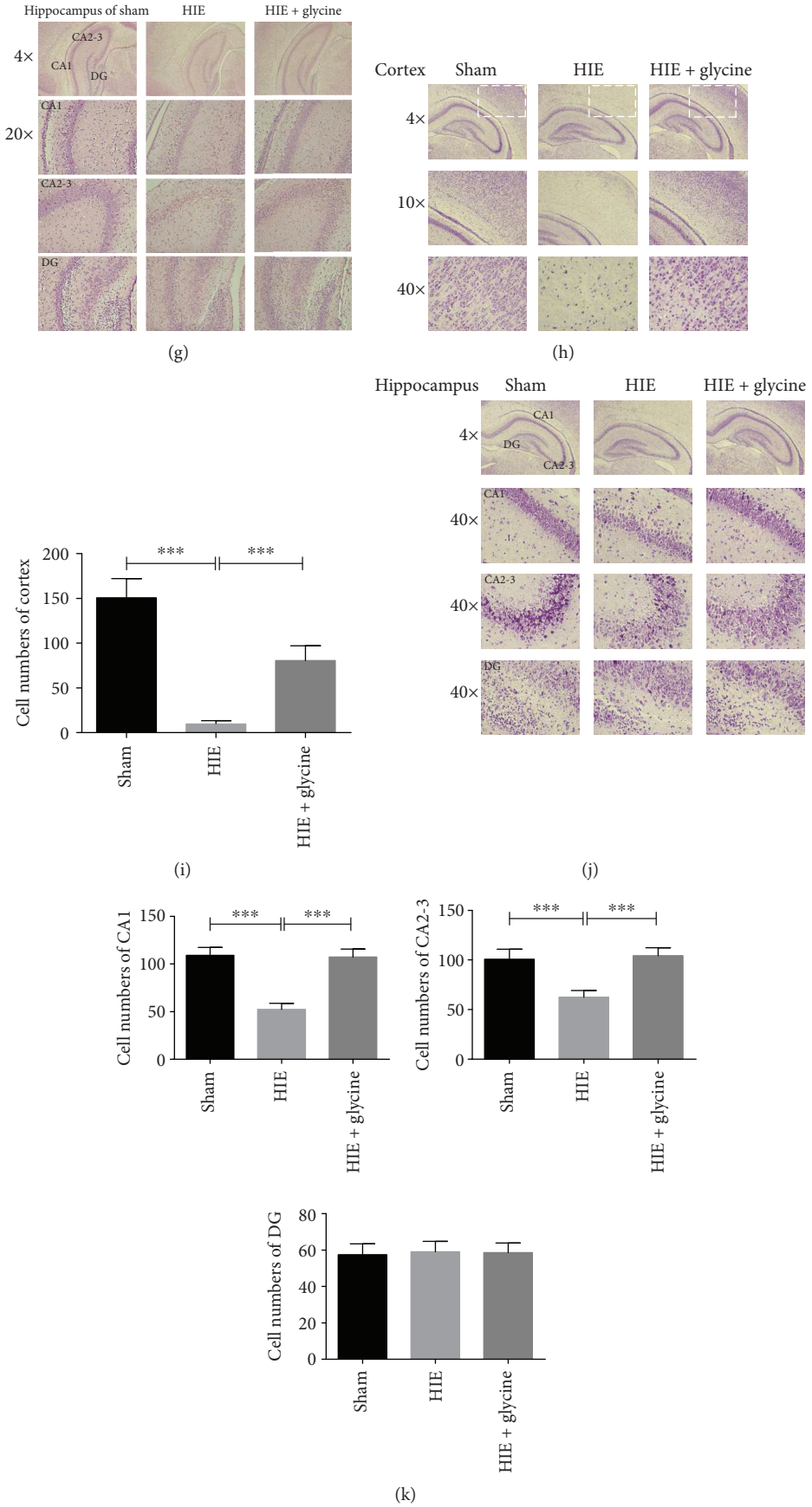

Figure 1: Continued.

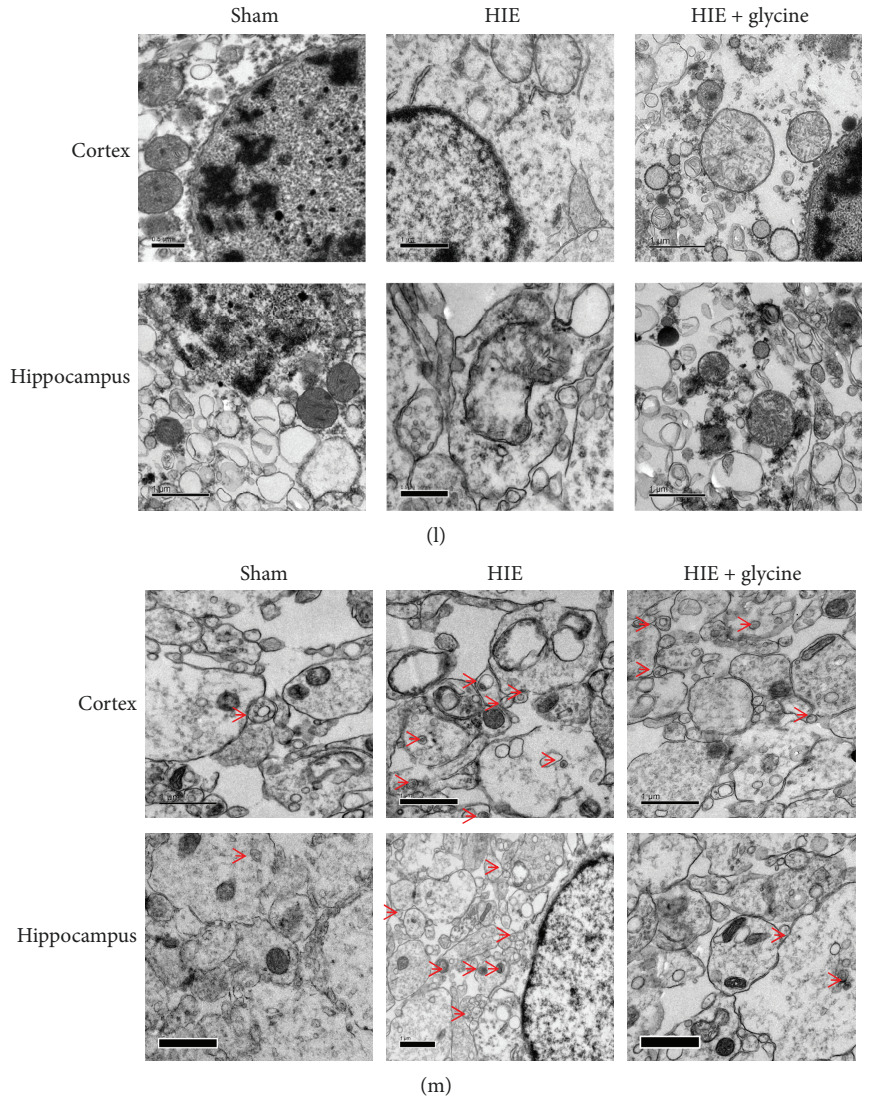

Figure 1: Glycine attenuated hypoxic-ischemic injury in the brains of neonatal rats. (a) TTC staining of sham rats, rats of HIE, and HIE rats with administration of glycine 200 mg/kg, 400 mg/kg, 600 mg/kg, 800 mg/kg, and 1000 mg/kg. (b) Calculation of infarct area shown by TTC staining (of the sham group). $^{*}P < 0.05$, $^{**}P < 0.01$, and $^{***}P < 0.001$ versus the HIE group. $n = 5$. (c) Protein expression level of HIF-1α of sham rats, rats of HIE, and HIE rats with administration of glycine 200 mg/kg, 400 mg/kg, 600 mg/kg, 800 mg/kg, and 1000 mg/kg. (d) Analyses of HIF-1α (of GAPDH). $^{*}P < 0.05$, $^{**}P < 0.01$, and $^{***}P < 0.001$ versus the HIE group. $n = 3$. (e) The brains were isolated from pups of the sham group, HIE group, and HIE with administration of the glycine group. Ratio of wet and dry is calculated in each group. $n = 5$. The brains (fixed with 4% paraformaldehyde) further showed dropsical areas and effectiveness of glycine administration. (f) HE staining of the cortex and hippocampus on the ipsilateral sides in rats of each group. (h) Nissl staining of the cortex on the ipsilateral sides in rats of each group is shown. (i) The analysis of cell number of neurons in the cortex on each group. $^{***}P < 0.001$. $n = 5$. (j) Nissl staining of the hippocampus on the ipsilateral sides in rats of each group. (k) Analysis of cell number of neurons in the hippocampus on each group. $^{***}P < 0.001$. $n = 5$. (l) Transmission electron microscope reveals status of mitochondria happened in tissues. (m) Transmission electron microscope discovers autophagosomes (red arrows) in tissues.

protein 1 light chain 3 (LC3 II/I) were assayed to determine the extent of autophagy. Additionally, Bnip3, parkin, PINK1, and Mfn2 protein levels were measured to evaluate how mitochondrial function mediated subsequent autophagy in the brain. The results indicated that protein expression in the cortex and hippocampus showed the same tendencies. The injured mitochondria exhibited dysfunction that was reflected by parkin and PINK1. Once dysfunction occurred within the mitochondria, PINK1 phosphorylated the parkin protein and both proteins accumulated on the outer membranes of mitochondria. Therefore, the expression of parkin and PINK1 was the highest among the HIE group, whereas Mfn-2 was expressed at a low level. Additionally, downstream autophagy-related proteins, such as Bnip3, parkin, PINK1, and LC3II/I, were significantly elevated in the tissues from the HIE group, whereas the HIE + glycine group showed significant improvements. Briefly, Bnip3 belongs to Bcl-2 family proteins, which acted as a sensitive factor in

hypoxic condition [38] or mitochondrial dysfunction [39]. The previous study also indicated that upregulation of Bnip3 was related with the autophagy induction [40]. The level of LC3 was an important autophagic marker, which was widely used to identify autophagy proceed. p62 protein also played a role in autophagy that selectively decreased autophagy process [41]. Alteration of the protein expressions mentioned above revealed that glycine administration improved or recovered dysfunctional mitochondria and alleviated autophagy following hypoxic-ischemic injury. Following glycine treatment, parkin and PINK1 expression levels were lower than those of the HIE group and Mfn-2 protein expression began to increase. Similarly, the autophagic process was altered by glycine treatment and enhanced the recovery of mitochondria. Compared to the HIE group, p62 protein expressed at a higher degree while Bnip3 and LC3II/I protein levels were decreased a lot following glycine treatment (Figures 2(a)–2(d)).

To determine whether mitochondria-mediated autophagy played a role in the regulation of pathogenesis in the nervous system, rat neonates were pretreated with CsA beginning at P4 through the HIE operation and then received daily doses of glycine only. The cortical and hippocampal samples of the HIE + glycine + CsA group revealed a protective effect of glycine. Compared to the HIE + glycine group, Mfn-2 and p62 protein levels were enhanced by glycine, whereas parkin, PINK1, Bnip3, and LC3 II/I levels were lower, which illustrated that the brains exposed to hypoxic-ischemic injury exhibited extensive mitochondria-mediated autophagy and glycine attenuated these insults by regulating this autophagy (Figures 2(e)–2(h)). Moreover, histopathological analyses revealed that the cortex and hippocampus structures in the HIE + glycine + CsA group exhibited the best recovery among four groups (Figures 2(i) and 2(j)). Nissl staining procedures were conducted to determine neuron status among four groups and revealed that cortical neurons in the HIE + glycine + CsA group preserved a better functional status than in the HIE and HIE + glycine groups. In the hippocampus, neurons from CA1 and CA2–3 regions also exhibited good recovery (Figures 2(k) and 2(l)).

3.3. Glycine Eliminated Mitochondria-Mediated Autophagy via Regulation of the AMPK Pathway. Proteins in the AMPK pathway, including p-AMPK$_\alpha$ and p-mammalian target of rapamycin (p-mTOR), were also assessed and showed differences among groups in the cortex or hippocampus. p-AMPK$_\alpha$ proteins were expressed at the highest level in the HIE group while p-mTOR expression decreased greatly. In the HIE + glycine group, glycine treatment alleviated the increase in p-AMPK$_\alpha$ protein expression and improved p-mTOR expression, which confirmed that glycine administration influenced the AMPK pathway *in vivo* (Figures 3(a) and 3(b)).

To examine the relationships among HIE pathogenesis, glycine, and the AMPK pathway, an agonist of the AMPK pathway, AICAR, was employed to overactivate the AMPK pathway in rats under HIE operations. In the HIE + glycine + AICAR group, p-AMPK$_\alpha$ protein expression increased, whereas p-mTOR protein expressions and other proteins associated with mitochondria-mediated autophagy exhibited poorer results than the HIE + glycine group. At the same time, parkin, PINK1, Bnip3, and LC3 II/I protein levels showed the highest degree, whereas Mfn-2 and p62 protein expressed the lowest level among four groups (Figures 3(c)–3(f)). Taken together, these results indicate that overactivation of AMPK blocked the effectiveness of glycine that downregulates the AMPK pathway and subsequently influences AMPK-regulated autophagy. In other words, compared with the HIE group, glycine administration could downregulate the AMPK pathway in the hypoxic-ischemic insult and alleviate mitochondria-mediated autophagy to gain the protection in the HIE + glycine group.

3.4. Glycine Improved Prognosis of Rats following Hypoxic-Ischemic Injury. The bodyweights of the pups were assessed at three different ages: 7, 14, and 28 days. The bodyweights did not differ significantly in each group at 7 days (before operations). However, at 14 days, the HIE + glycine group showed improvements in bodyweight, compared with the HIE and HIE + glycine + AICAR groups. The HIE + glycine + CsA group exhibited the best weight gain among five groups, whereas rats from the HIE + glycine + AICAR group showed the lowest amount of weight gain. At 28 days, the rats of the HIE + glycine + AICAR group exhibited the lowest weight and two pups died. Following long-term glycine treatment, there was no significant difference between the HIE + glycine group and the HIE + glycine + CsA group, though these two groups exhibited better weight gains than the HIE group (Figure 4(a)).

At 7 days after surgery, three neonate rats from each group were sacrificed to further investigate the protective effects of glycine. Atrophy in the left brain showed significant improvements following treatment with glycine or glycine combined with CsA (Figure 4(b)). The HIE + glycine + AICAR group exhibited serious atrophy and had the worst prognosis among five groups. HE staining revealed the efficacy of glycine, especially in the HIE + glycine + AICAR group, in that the cortex and hippocampus exhibited considerable atrophy and were difficult to recognize. However, brain tissues from the HIE + glycine group and the HIE + glycine + CsA group exhibited better recovery than the HIE and HIE + glycine + ICAR groups (Figure 4(c)).

The present study also assessed neuromuscular ability in 14-day-old pups after surgery (Table 1). Over a period of 28 days, Longa and Berderson tests (Tables 2 and 3, respectively) were performed to measure neurodeficiencies in neuromuscular behaviors. The HIE + glycine + CsA group had the best scores on the behavioral test, whereas the condition of the HIE + glycine + AICAR group did not differ significantly from the HIE group (Table 1). At 28 days of age, the Longa test revealed that the HIE + glycine and HIE + glycine + CsA groups showed better mobility compared with the HIE and HIE + glycine + AICAR groups. Additionally, based on the results above, it was evident that the HIE + glycine + AICAR group did not perform well on the Longa test (Table 2). In parallel, the rats from this group also did not perform well on the Berderson test (Table 3).

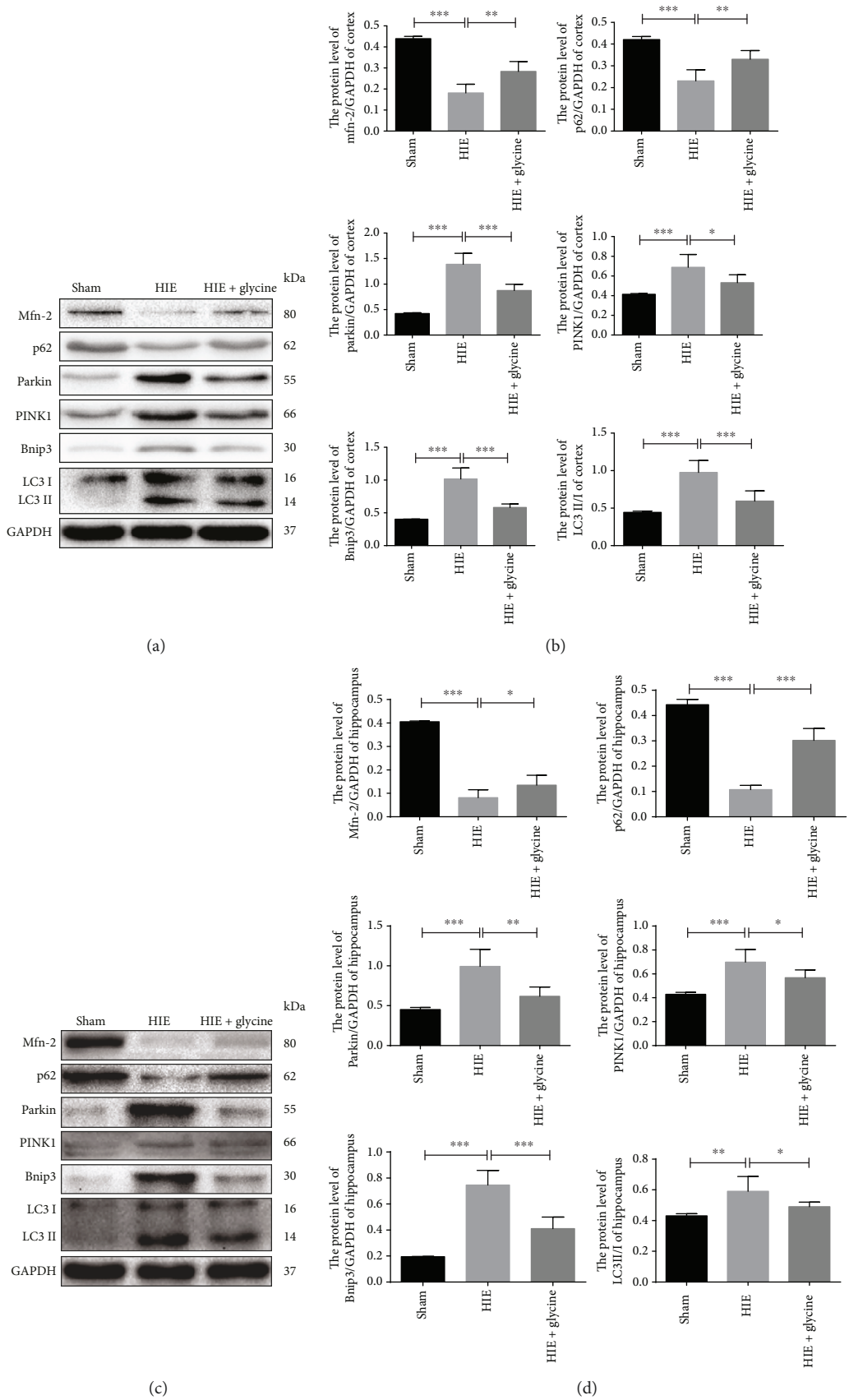

Figure 2: Continued.

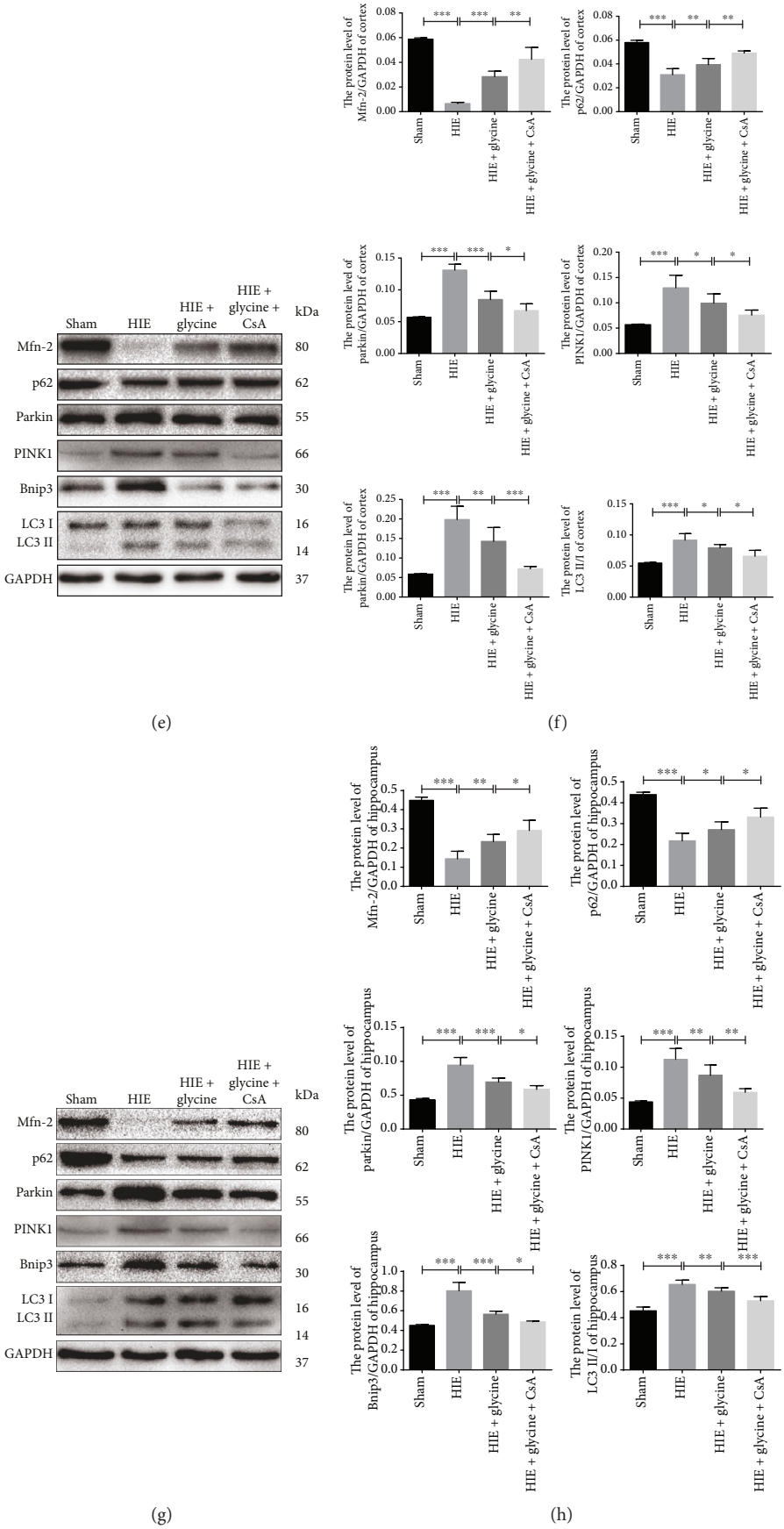

Figure 2: Continued.

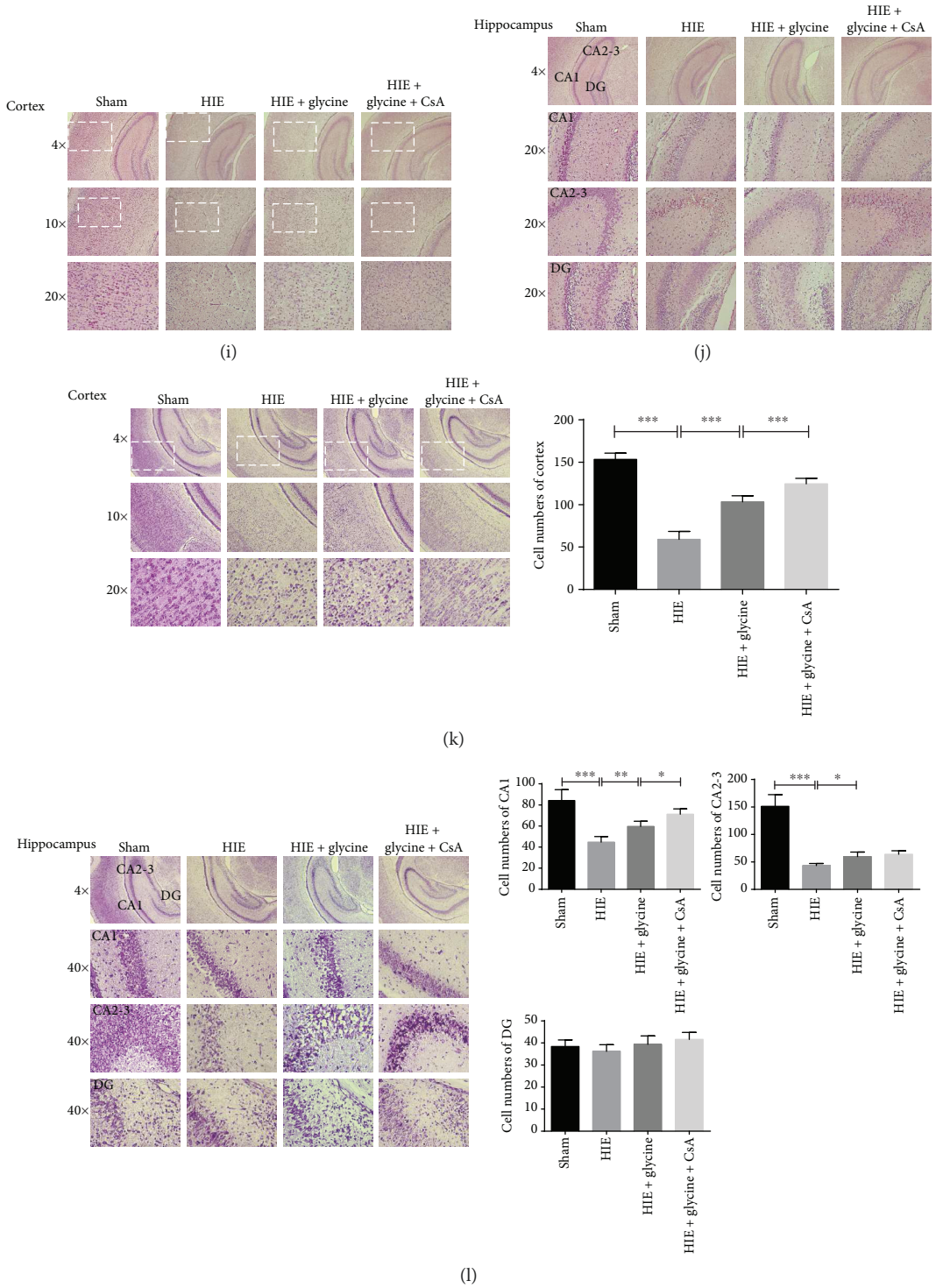

Figure 2: Glycine protected against hypoxic-ischemic injury in the brains via attenuation of mitochondrial-mediated autophagy. (a) Protein expression level of Mfn-2, p62, parkin, PINK1, Bnip3, LC3 II, and LC3 I on the cortex from ipsilateral sides of the sham group, HIE group, and HIE with administration of the glycine group (of GAPDH). (b) Analyses of Mfn-2, p62, parkin, PINK1, Bnip3, LC3 II, and LC3 I in each group. (c) Protein expression level of Mfn-2, p62, parkin, PINK1, Bnip3, LC3 II, and LC3 I on the hippocampus from ipsilateral sides of each group (of GAPDH). (e) Analyses of Mfn-2, p62, parkin, PINK1, Bnip3, LC3 II, and LC3 I in each group. (e) Protein expression level of Mfn-2, p62, parkin, PINK1, Bnip3, LC3 II, and LC3 I in each group from the cortex. (f) Analyses of Mfn-2, p62, parkin, PINK1, Bnip3, LC3 II, and LC3 I in each group. (g) Protein expression level of Mfn-2, p62, parkin, PINK1, Bnip3, LC3 II, and LC3 I in each group from the hippocampus. (h) Analyses of Mfn-2, p62, parkin, PINK1, Bnip3, LC3 II, and LC3 I in each group. (i) HE stainings of the cortex of four groups. (j) HE stainings of the hippocampus among four groups. (k) Nissl stainings in the cortex from four groups and neuron numbers were analyzed. $^{***}P < 0.001$. (l) Nissl stainings in the hippocampus from four groups and neuron numbers were analyzed. $^{*}P < 0.05$, $^{**}P < 0.01$, and $^{***}P < 0.001$. $n = 5$.

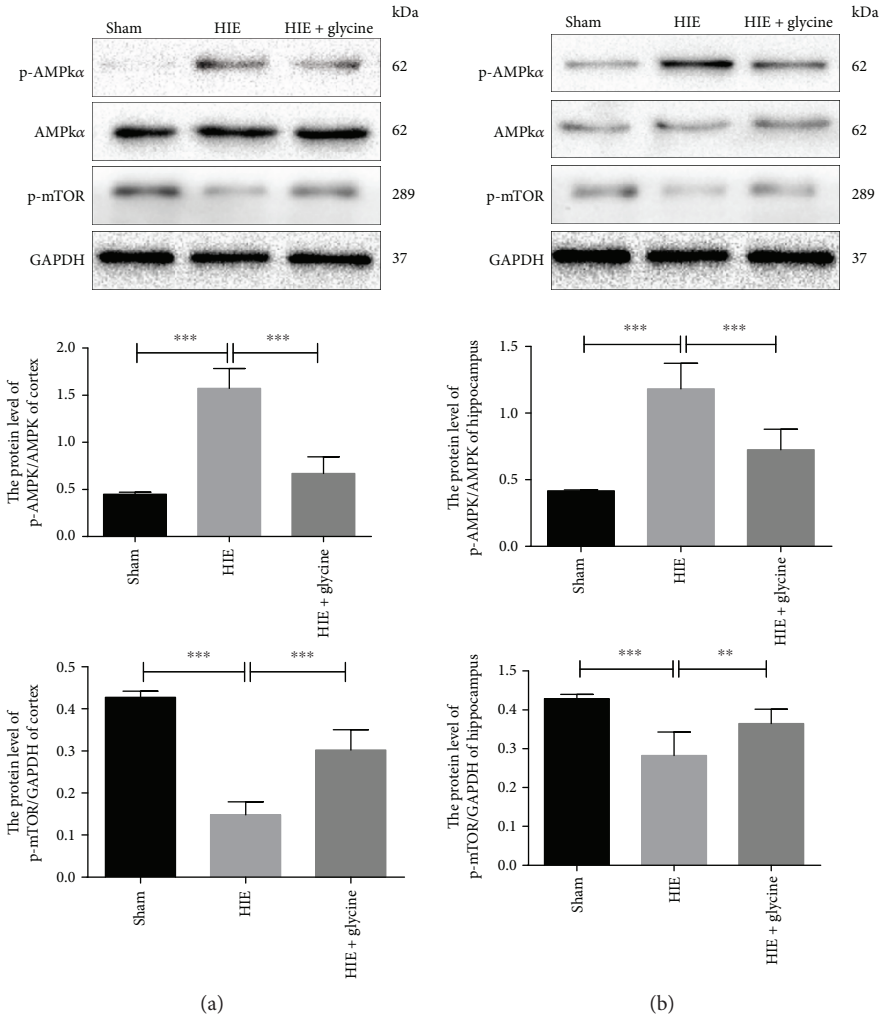

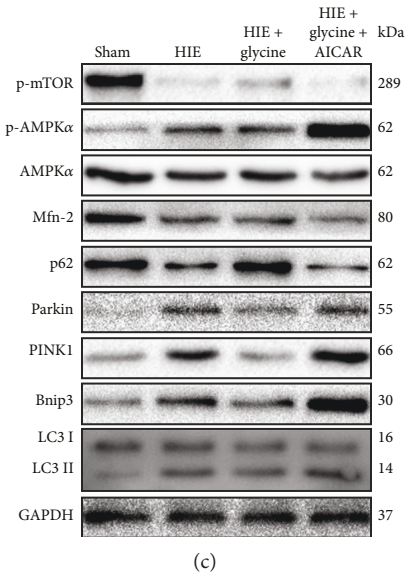

Figure 3: Continued.

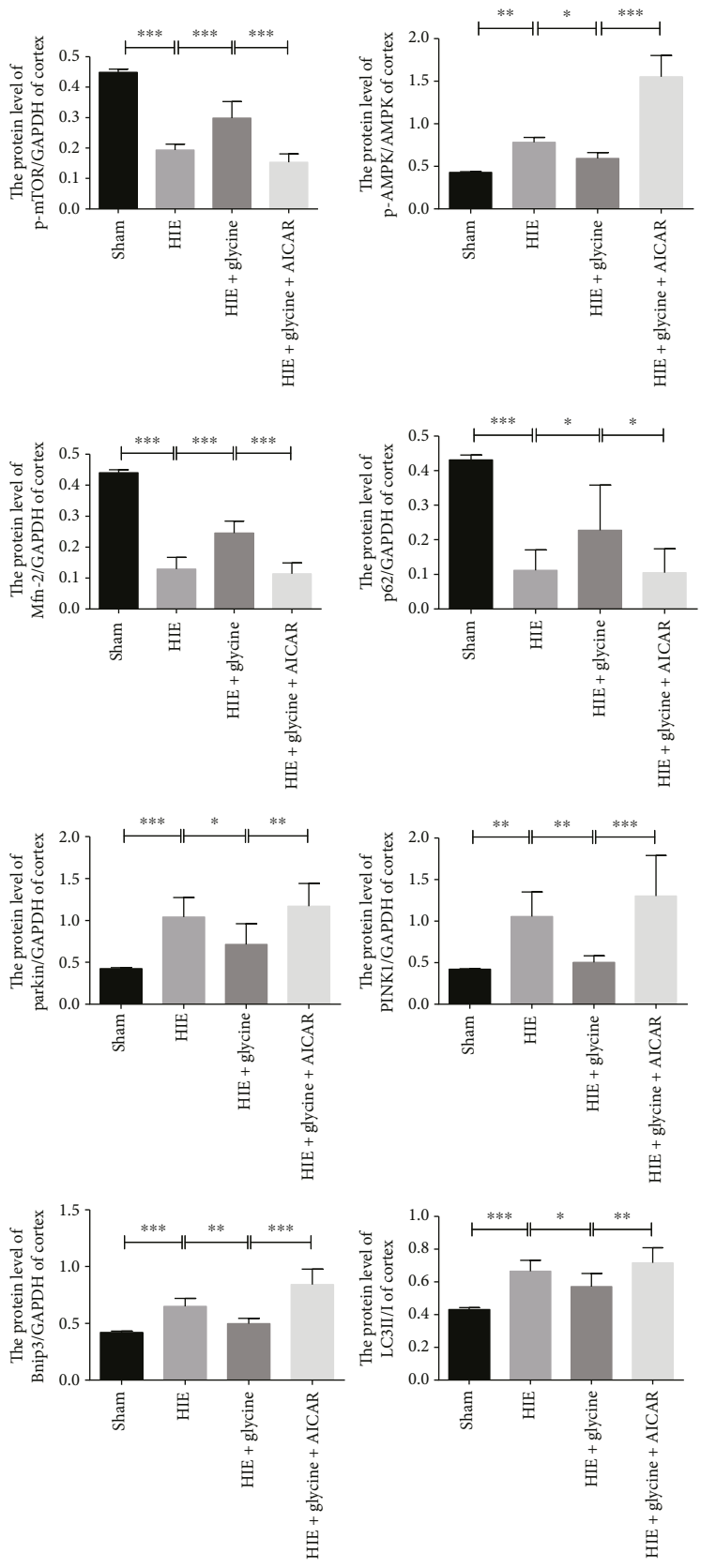

(d)

Figure 3: Continued.

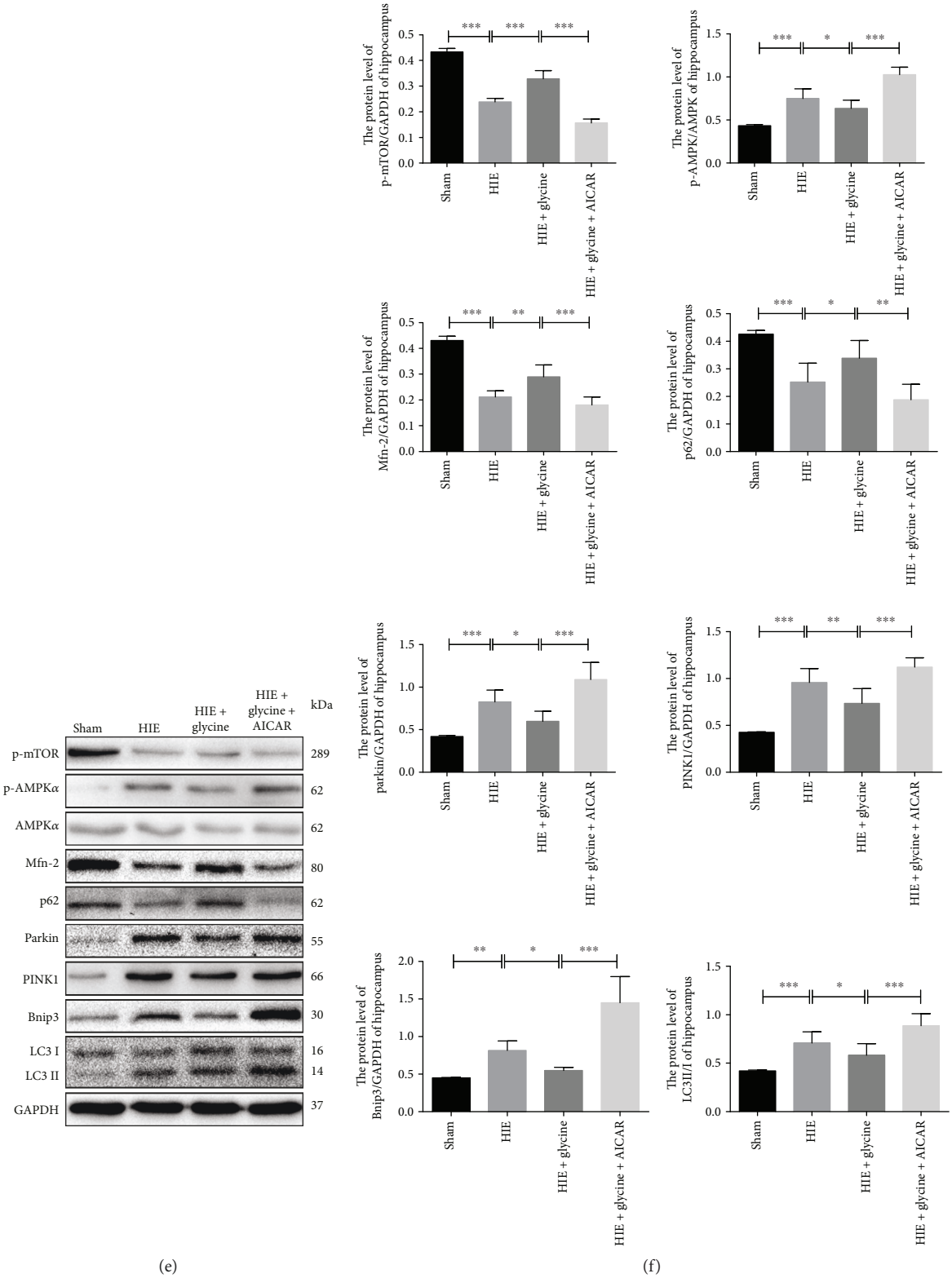

Figure 3: Glycine eliminated mitochondria-mediated autophagy via regulation of the AMPK pathway. (a) Protein expression level of p-AMPK$_\alpha$ in the cortex from ipsilateral sides of each group and analysis of p-AMPK$_\alpha$ (of AMPK$_\alpha$), p-mTOR (of GAPDH). (b) Protein expression level of p-AMPK$_\alpha$ on the hippocampus from ipsilateral sides of each group and analysis. (c) Protein expressions of p-mTOR, p-AMPK$_\alpha$, AMPK$_\alpha$, Mfn-2, p62, parkin, PINK1, Bnip3, LC3 II, and LC3 I from the cortex. (d) Analyses of protein expressions above. (e) Protein expressions of p-mTOR, p-AMPK$_\alpha$, AMPK$_\alpha$, Mfn-2, p62, parkin, PINK1, Bnip3, LC3 II, and LC3 I from the cortex. (f) Analysis of protein expressions above. $^*P < 0.05$, $^{**}P < 0.01$, and $^{***}P < 0.001$. $n = 5$.

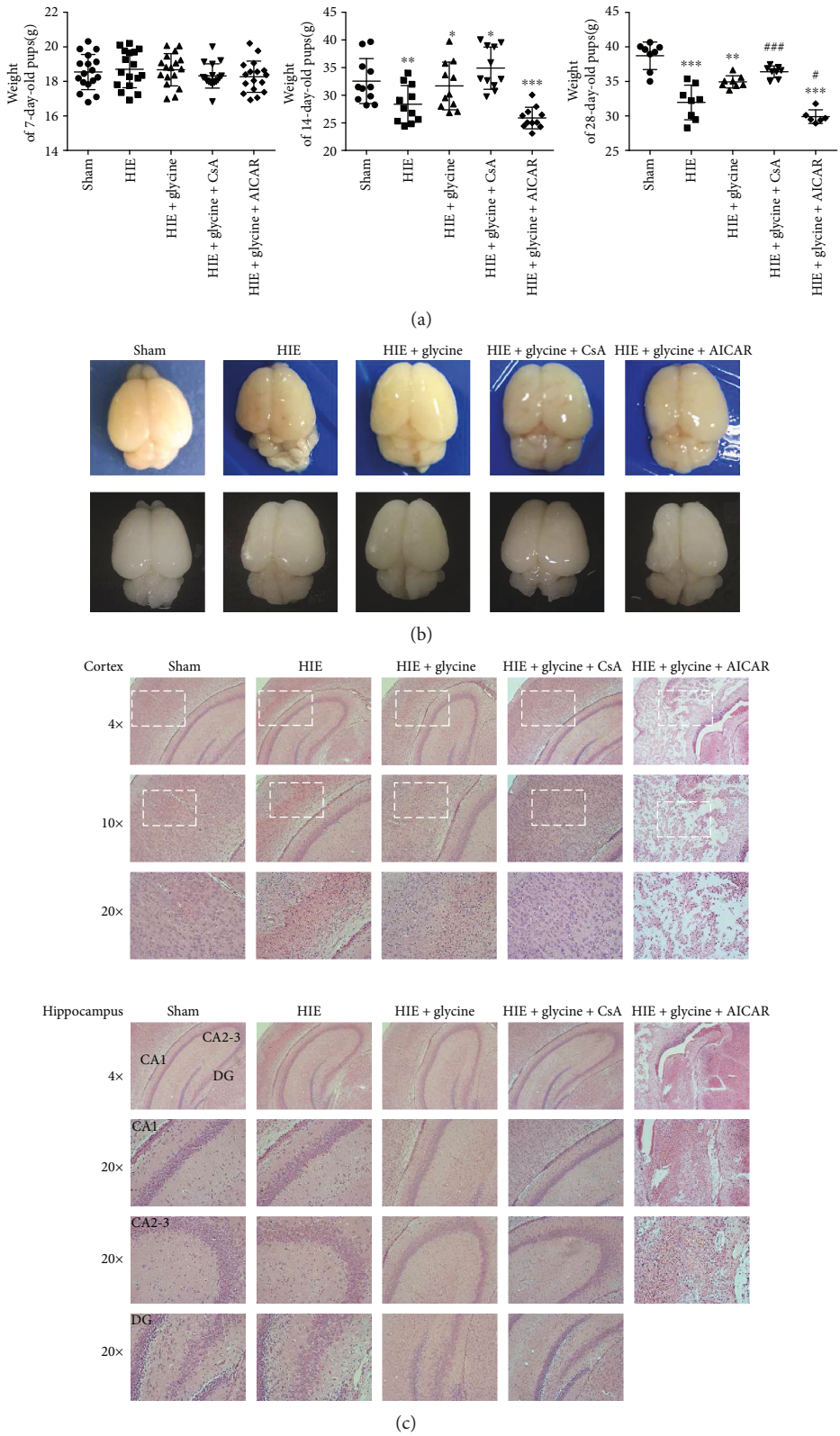

FIGURE 4: Glycine improved prognosis of rats following hypoxic-ischemic injury. (a) Weights of rats of 7 days, 14 days, and 28 days. $^{*}P < 0.05$ and $^{***}P < 0.001$. $^{\#}P < 0.05$, $^{\#\#}P < 0.01$, and $^{\#\#\#}P < 0.001$. (b) The brains isolated from 14-day-old rats of each group. Fresh brain tissue is shown at the first line and dehydrated brains tissue is shown at the second line. $n = 3$. (c) HE staining of the cortex and hippocampus from ipsilateral sides of each group. $n = 3$.

Table 1: Assessment of hindlimb suspension of 14-day-old pups.

Group	Number	Hindlimb suspension
Sham	11	4.00 ± 0.00
HIE	11	$1.24 \pm 0.11^{***}$
HIE + glycine	11	$2.15 \pm 0.12^{***,\#\#\#}$
HIE + glycine + CsA	11	$2.60 \pm 0.11^{***,\#\#\#,\&\&}$
HIE + glycine + AICAR	11	$1.30 \pm 0.11^{***,\&\&\&}$

Dates were presented as mean ± SEM from rats from each group. $^{***}P < 0.001$ versus the sham group. $^{\#\#\#}P < 0.001$ versus the HIE group. $^{\&\&}P < 0.01$ and $^{\&\&\&}P < 0.001$ versus the HIE + glycine group.

Table 2: Longa scores of 28-day-old pups.

Group	Number	Hindlimb suspension
Sham	8	0.00 ± 0.00
HIE	8	$1.75 \pm 0.14^{***}$
HIE + glycine	8	$1.00 \pm 0.13^{***,\#\#\#}$
HIE + glycine + CsA	8	$0.83 \pm 0.13^{***,\#\#\#}$
HIE + glycine + AICAR	6	$1.70 \pm 0.13^{***,\&\&\&}$

Dates were presented as mean ± SEM from rats from each group. $^{***}P < 0.001$ versus the sham group. $^{\#\#\#}P < 0.001$ versus the HIE group. $^{\&\&\&}P < 0.001$ versus the HIE + glycine group.

Table 3: Berderson assessment of 28-day-old pups.

Group	Number	Hindlimb suspension
Sham	8	0.00 ± 0.00
HIE	8	$2.08 \pm 0.15^{***}$
HIE + glycine	8	$1.45 \pm 0.10^{***,\#\#\#}$
HIE + glycine + CsA	8	$0.95 \pm 0.11^{***,\#\#\#,\&\&}$
HIE + glycine + AICAR	6	$2.04 \pm 0.14^{***,\&\&\&}$

Dates were presented as mean ± SEM from rats from each group. $^{***}P < 0.001$ versus the sham group. $^{\#\#\#}P < 0.001$ versus the HIE group. $^{\&\&}P < 0.01$ and $^{\&\&\&}P < 0.001$ versus the HIE + glycine group.

3.5. Glycine Attenuated $CoCl_2$-Induced Cytotoxicity, Cellular ROS, and Apoptosis in PC12 Cells. The initial effects of $CoCl_2$ on neurons were detected using the CCK8 method. In the present study, $CoCl_2$ (800–1000 μM) significantly inhibited cellular viability within 24 h in a dose- and time-dependent manner compared with the control group (Figure 5(a)). Moreover, the optimum dose of glycine (8–10 μM) effectively protected PC12 cells against $CoCl_2$-induced injury (800–1000 μM) in the same manner as the $CoCl_2$ group (Figure 5(b)). DCFH-DA fluorescence was used to detect the level of ROS generation in each group and revealed that glycine pretreatment decreased ROS generation and protected against $CoCl_2$-induced injury in PC12 cells (Figure 5(c)). TUNEL staining indicated that glycine also downregulated apoptosis to protect PC12 cells (Figure 5(d)).

3.6. Glycine Attenuated $CoCl_2$-Induced Mitochondrial ROS Generation, Restored the MPP, Improved Mfn-2 Protein Levels, and Alleviated Autophagy in PC12 Cells. As an indication of injured status in cells, mitochondria largely generated superoxide molecules by influencing various signaling pathways. MitoSOX, which confirmed the position of the mitochondrial matrix and detected superoxide anions in mitochondria, was used to assess oxidative stress in mitochondria of PC12 cells. Cells that underwent $CoCl_2$ injury showed a significant increase in oxidative stress in mitochondria (Figure 6(a)), but the administration of an optimum dose of glycine lowered ROS generation. Additionally, PC12 cells were loaded with TMRE to evaluate the MMP, which reflected mitochondrial function. $CoCl_2$ impaired mitochondria by decreasing the MMP, but glycine dramatically promoted the MMP (Figure 6(b)). Furthermore, Mfn-2 expression was at a low level in the $CoCl_2$ group (Figure 6(c)), but glycine upregulated the Mfn-2 protein expression. According to the results of MDC staining, which specifically identified autophagic vacuoles, showed that the $CoCl_2$ + glycine group gained the lower value of MDC immunofluorescence than the $CoCl_2$ group. This result also illustrated that glycine could downregulate autophagy (Figure 6(d)).

3.7. Glycine Protected PC12 Cells against $CoCl_2$-Induced Injury via Regulation of Mitochondria-Mediated Autophagy. The present study examined the expression of parkin, PINK1, Mfn-2, Bnip3, p62, and LC3II/I (Figures 7(a) and 7(b)) and found increased expression of parkin, PINK1, Bnip3, and LC3II/I in the $CoCl_2$ group. However, glycine pretreatment before $CoCl_2$ ($CoCl_2$ + glycine) significantly reduced such effect. At the same time, the expressions of Mfn-2 and p62 decreased following $CoCl_2$ injury, but glycine pretreatment promoted the expressions of Mfn-2 and p62. CsA, a conventional inhibitor of mitochondria-mediated autophagy, was used to determine whether glycine regulated autophagy. Following treatment with a combination of CsA and glycine, the expressions of parkin, PINK1, Bnip3, and LC3 II/I were largely inhibited, whereas the expression of Mfn-2 and p62 was increased (Figures 7(c) and 7(d)). Additionally, the administration of CsA increased cellular viability such that it was better compared with the $CoCl_2$ + glycine group (Figure 7(e)).

MDC staining revealed that the $CoCl_2$ + glycine + CsA and $CoCl_2$ + glycine groups exhibited a less degree of autophagy, particularly the $CoCl_2$ + glycine + CsA group (Figure 7(f)). TUNEL staining in PC12 cells further confirmed that glycine protected PC12 cells (Figure 7(g)). Assessments of mitochondrial function included measurements of mitochondrial ROS generation, MMP, and Mfn-2 expression (Figures 7(h)–7(j)). In all four groups, glycine significantly decreased mitochondria-mediated autophagy, especially via the parkin/ PINK1 pathway, which has been linked to mitochondria-mediated autophagy.

3.8. Glycine Protected PC12 Cells against $CoCl_2$ Injury via Regulation of AMPK-Dependent Mitochondria-Mediated Autophagy. Because AMPK is phosphorylated upon activation of the AMPK pathway, it acts an energy sensor that reflects the condition of mitochondria. Analyses of p-AMPK expression in PC12 cells revealed high levels of p-$AMPK_\alpha$ in the $CoCl_2$-treated group, but glycine pretreatment reduced the levels of p-$AMPK_\alpha$. The mTOR pathway is the

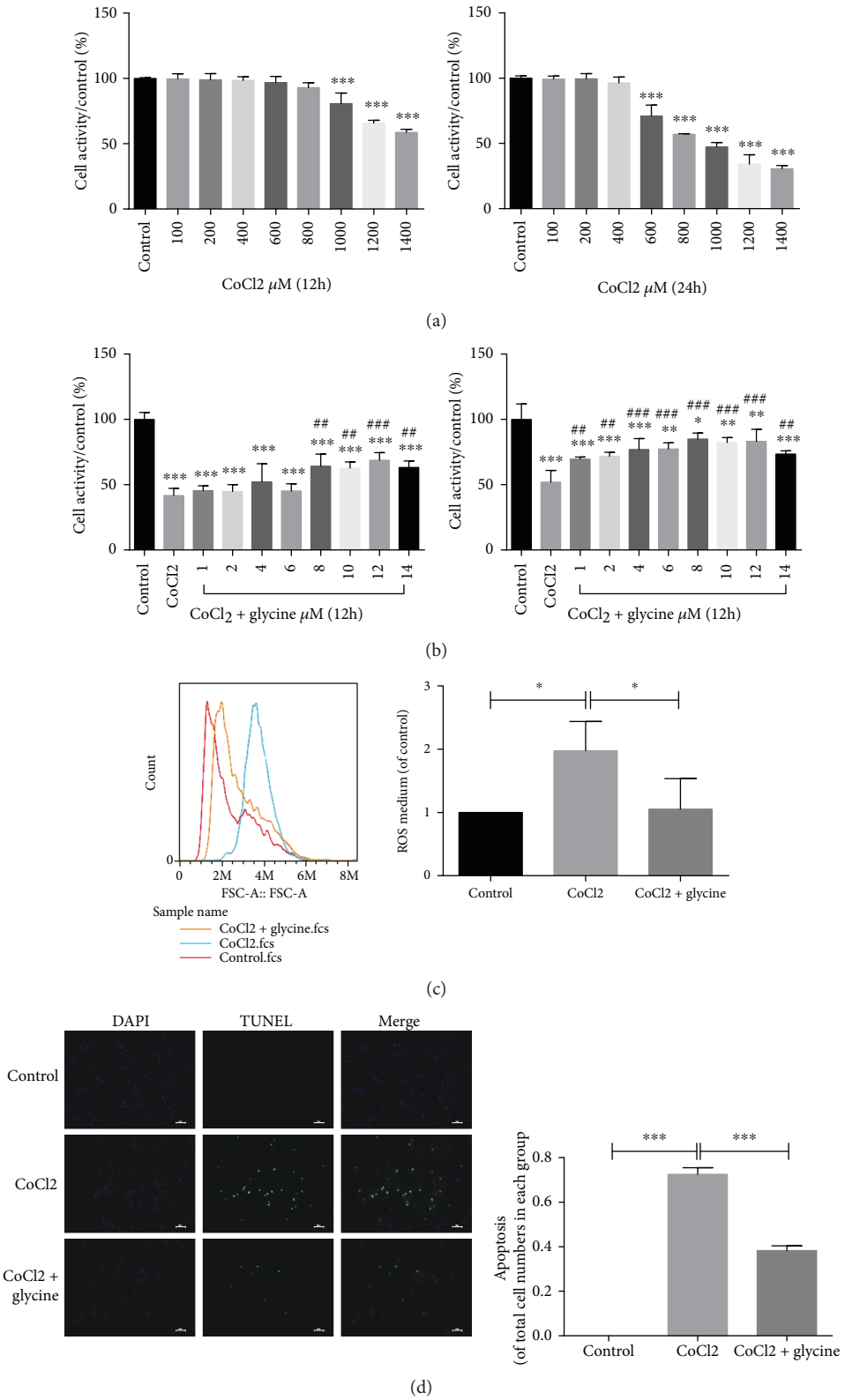

FIGURE 5: Glycine attenuated $CoCl_2$-induced cytotoxicity, cellular ROS, and apoptosis in PC12 cells. (a) PC12 cells treated with $CoCl_2$ on dose-dependent manner for 12 hours and 24 hours by CCK8. (b) PC12 cells were pretreated with different concentrations of glycine for 12 hours and 24 hours. Then, PC12 cells were treated with $CoCl_2$ (800–1000 μM) and cell viability was determined by CCK8. $^{*}P < 0.05$, $^{**}P < 0.01$, and $^{***}P < 0.001$ versus the control group. $^{\#\#}P < 0.01$ and $^{\#\#\#}P < 0.001$ versus the $CoCl_2$ group. (c) ROS generation of the control group, $CoCl_2$ group, and $CoCl_2$ + glycine group was determined by flow cytometry assay of DCFH-DA. $^{*}P < 0.05$. $n = 3$. (d) Apoptotic cells of each group were detected by TUNEL and DAPI staining. $^{***}P < 0.001$. $n = 3$.

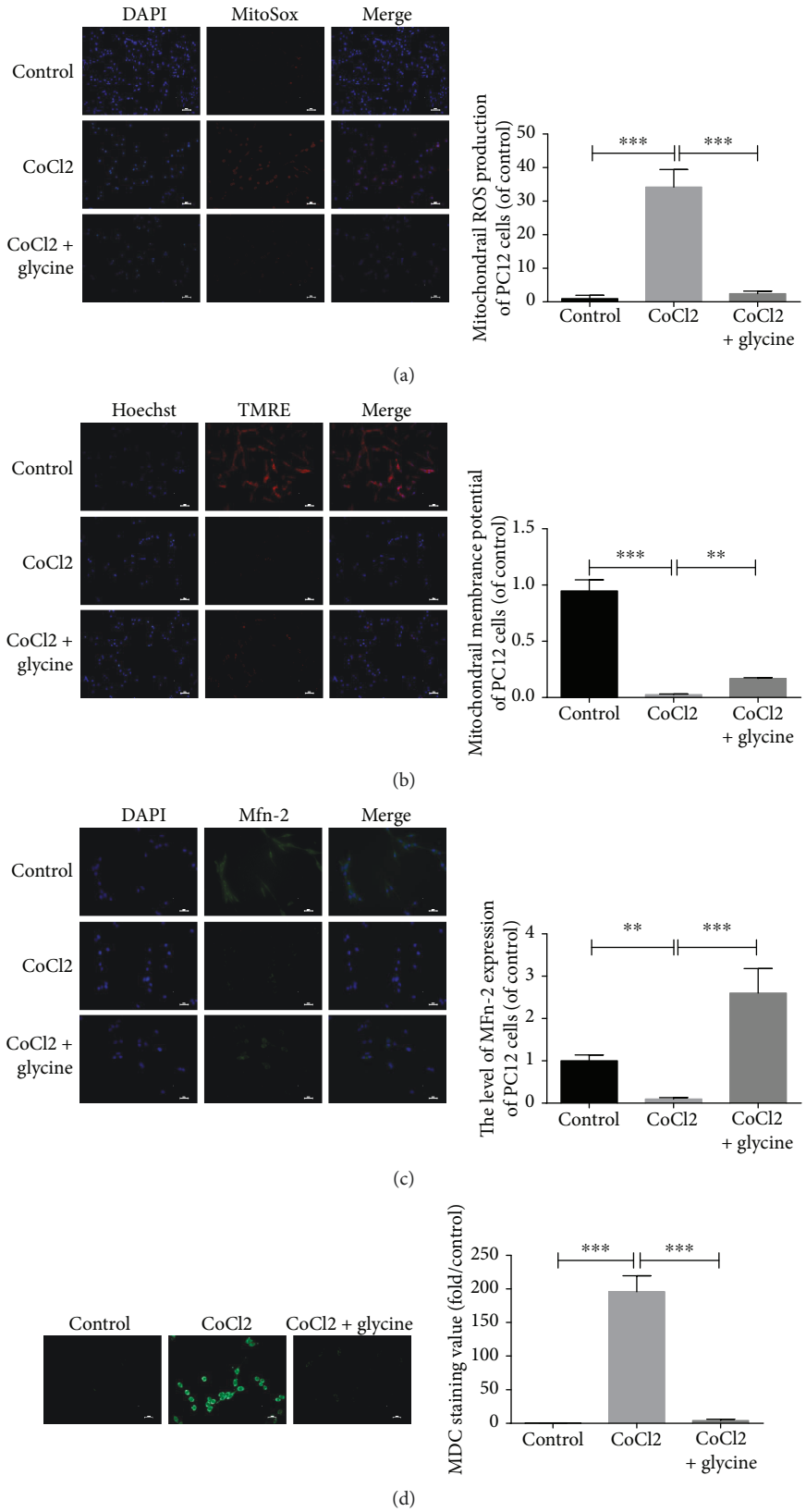

Figure 6: Glycine attenuated $CoCl_2$-induced mitochondrial ROS generation, restored the MPP, improved Mfn-2 protein levels, and alleviated autophagy in PC12 cells. (a) Mitochondrial ROS generation of each group was detected by MitoSOX and DAPI staining. (b) Mitochondrial membrane potential of each group was determined by TMRE and Hoechst staining. (c) Protein expression level of Mfn-2 from outer membrane of mitochondria was measured by immunofluorescence. (d) Autophagic vacuoles from each group were measured by MDC staining. $^{**}P < 0.01$ and $^{***}P < 0.001$. $n = 3$.

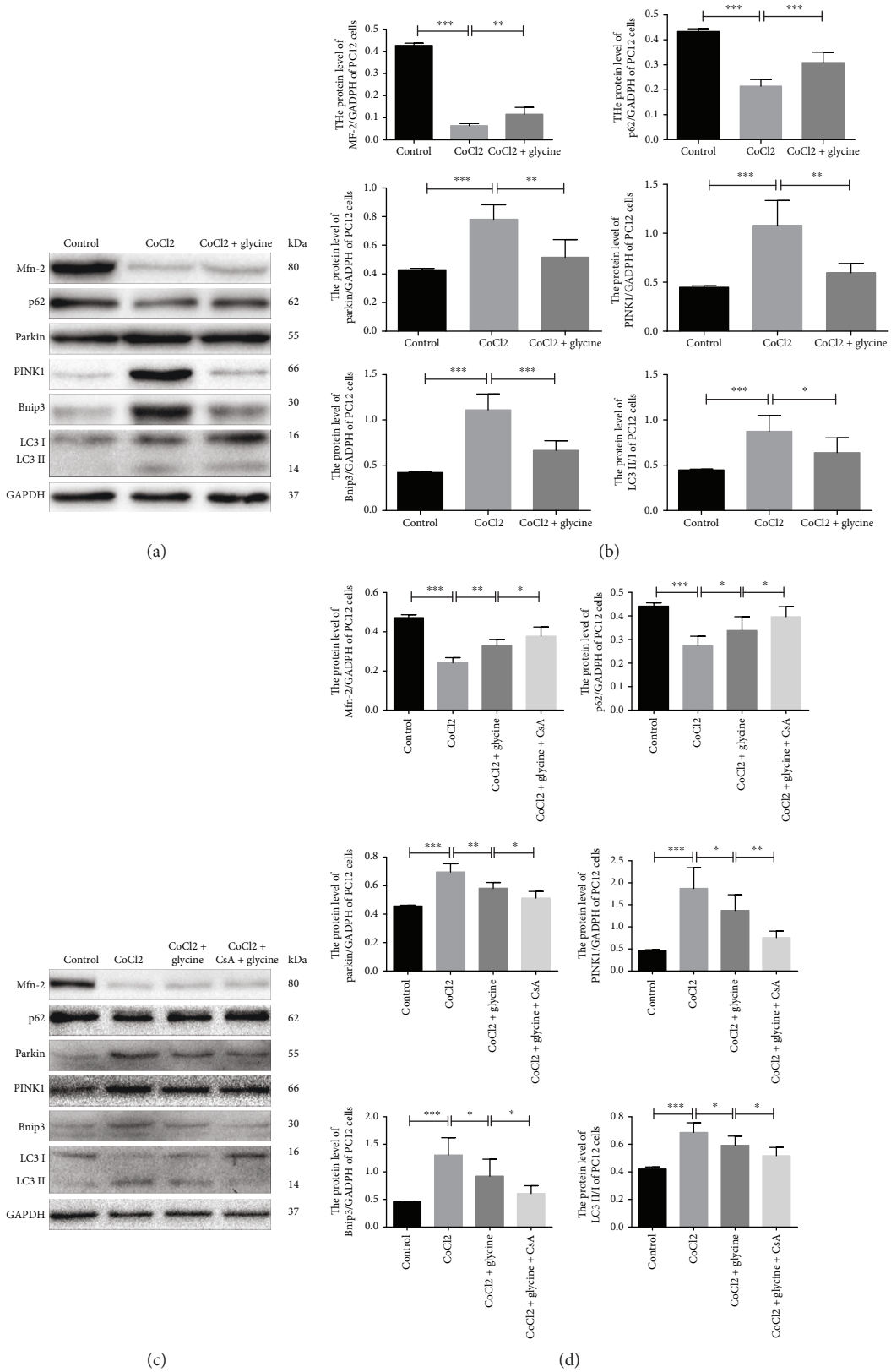

Figure 7: Continued.

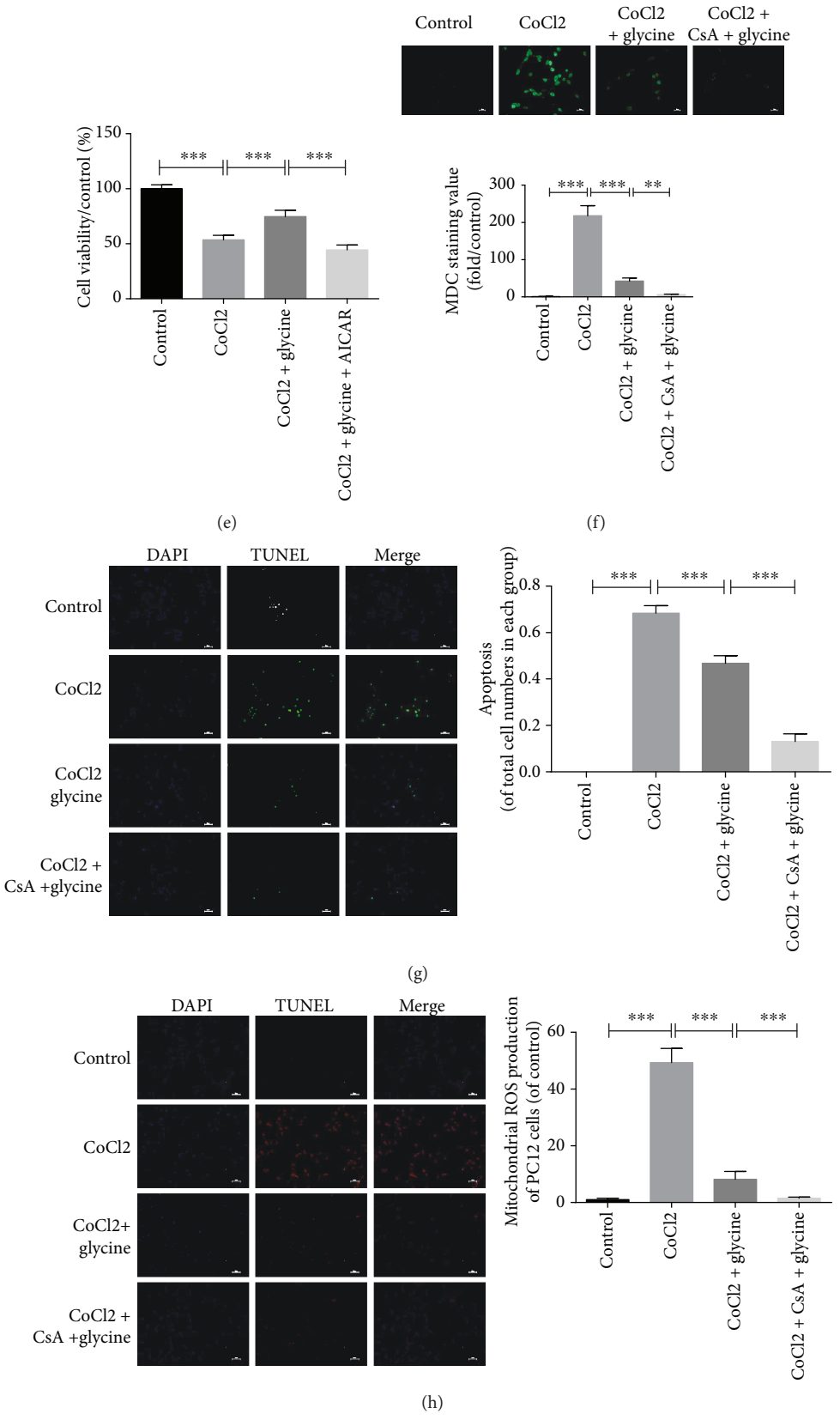

Figure 7: Continued.

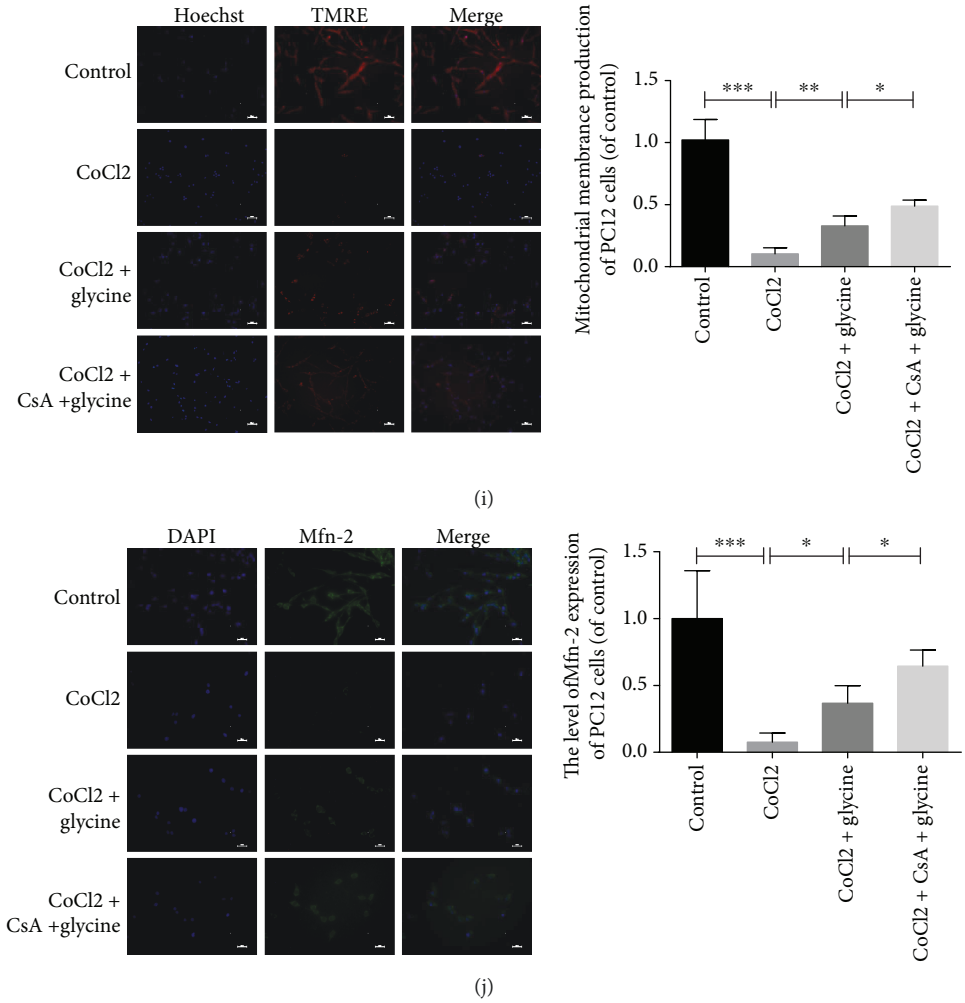

Figure 7: Glycine protected PC12 cells against $CoCl_2$-induced injury via regulation of mitochondria-mediated autophagy. (a) Protein expression level of Mfn-2, p62, parkin, PINK1, Bnip3, LC3 II, and LC3 I in PC12 cells of each group. (b) Analyses of Mfn-2, p62, parkin, PINK1, Bnip3, LC3 II, and LC3 I in each group. (c) After treatment of CsA, protein expression levels of Mfn-2, p62, parkin, PINK1, Bnip3, LC3 II, and LC3 I in PC12 cells of four groups were determined by Western blotting. (d) Analysis of all protein expressions. (e) Cell viability of four groups was detected by CCK8. (f) Apoptotic cells from each group were measured by TUNEL and DAPI staining. (g) Mitochondrial ROS generations were detected by immunofluorescence of MitoSOX and DAPI staining. (h) Mitochondrial membrane potential was detected in each group by TMRE and Hoechst staining. (i) The Mfn-2, protein of mitochondrial outer membrane, was used to measure function of mitochondria. $^{*}P < 0.05$, $^{**}P < 0.01$, and $^{***}P < 0.001$. $n = 3$.

downstream of the AMPK pathway, and assessments in the present study showed that $CoCl_2$ injury had an adverse effect on this pathway as well (Figures 8(a) and 8(b)). To determine whether the AMPK pathway modulated $CoCl_2$-induced mitochondria-mediated autophagy, AICAR, an AMPK pathway agonist was used to modulate protein expression. In the CoCl2 + glycine + AICAR group, the expressions of parkin, PINK1, Bnip3, LC3II/I, and p-AMPK$_\alpha$ were evident at a high degree while the expressions of Mfn-2, p-mTOR, and p62 were low (Figures 8(c) and 8(d)). At the same time, the group administrated CsA in combination with glycine exhibited the lowest viability (Figure 8(e)).

MDC staining revealed that the $CoCl_2$ + glycine + AICAR group had the highest intensity of autophagy of the four groups, whereas the $CoCl_2$ + glycine group exhibited attenuations in autophagy (Figure 8(f)). Moreover, TUNEL staining revealed that glycine pretreatment protected against $CoCl_2$ injury, whereas overactivation of the AMPK pathway in the $CoCl_2$ + glycine + AICAR group produced the highest number of TUNEL-positive cells (Figure 8(g)). Immunofluorescence analyses of the PC12 cells revealed that the mitochondrial function of the $CoCl_2$ + glycine + AICAR group did not show significant improvements with the $CoCl_2$ group (Figures 8(h)–8(j)). However, the $CoCl_2$ + glycine group exhibited high levels of protection against $CoCl_2$ injury. Parallel analyses confirmed the overactivation of the AMPK pathway by AICAR. This result suggests that the AMPK pathway played an important role in $CoCl_2$-induced mitochondria-mediated autophagy.

4. Discussion

The present study was the first to investigate whether glycine could protect against hypoxic-ischemic injury in the nervous

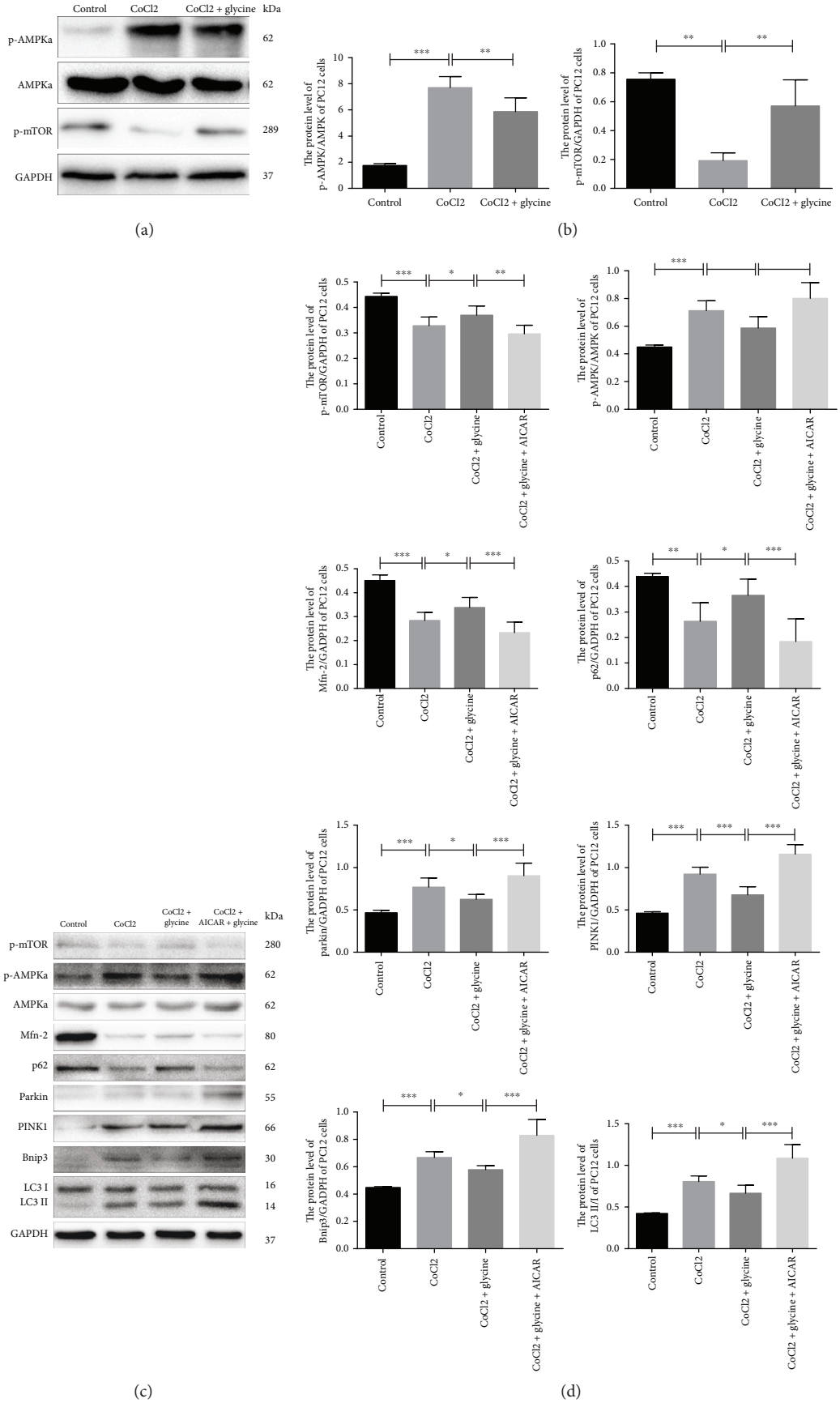

Figure 8: Continued.

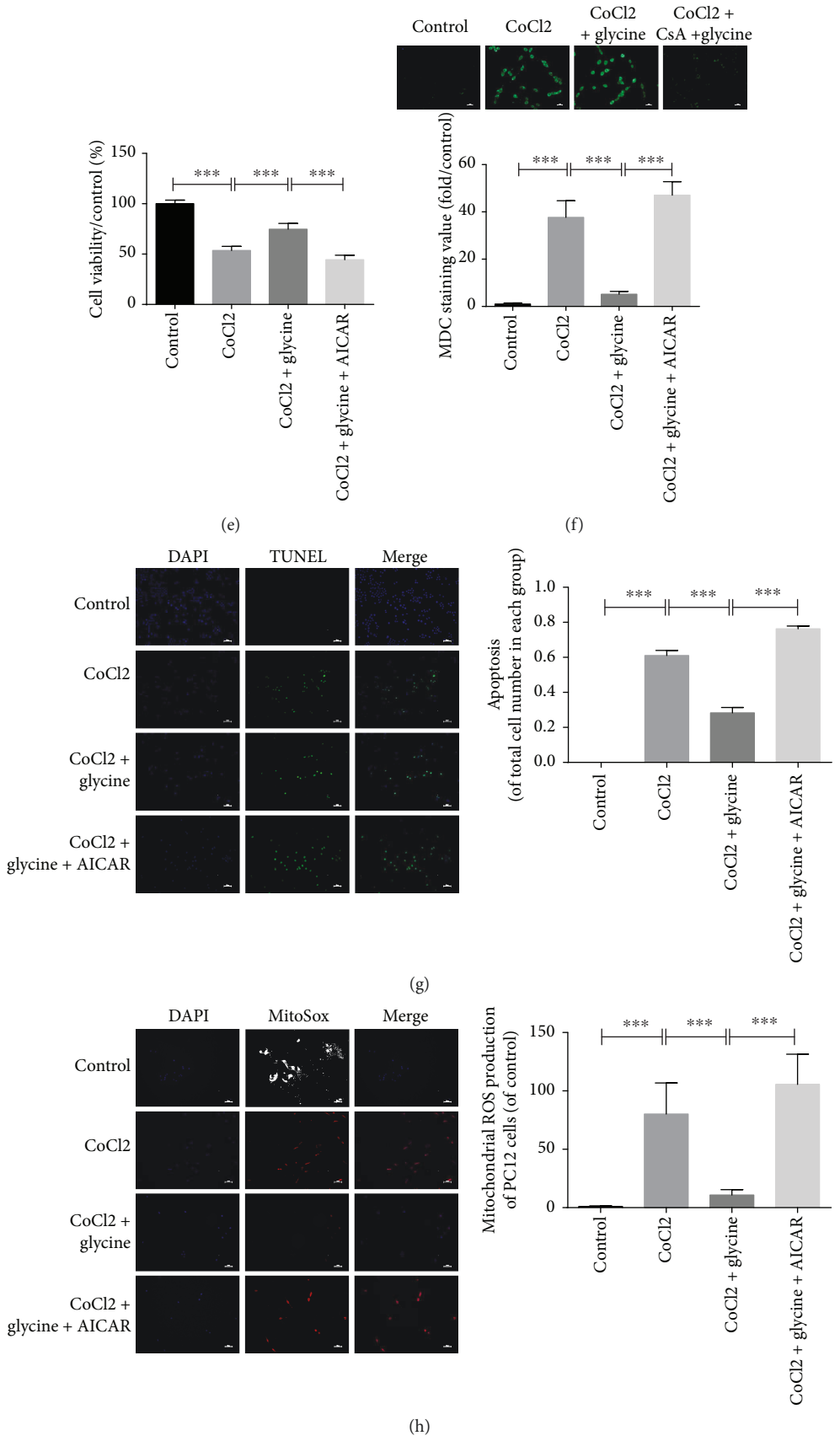

Figure 8: Continued.

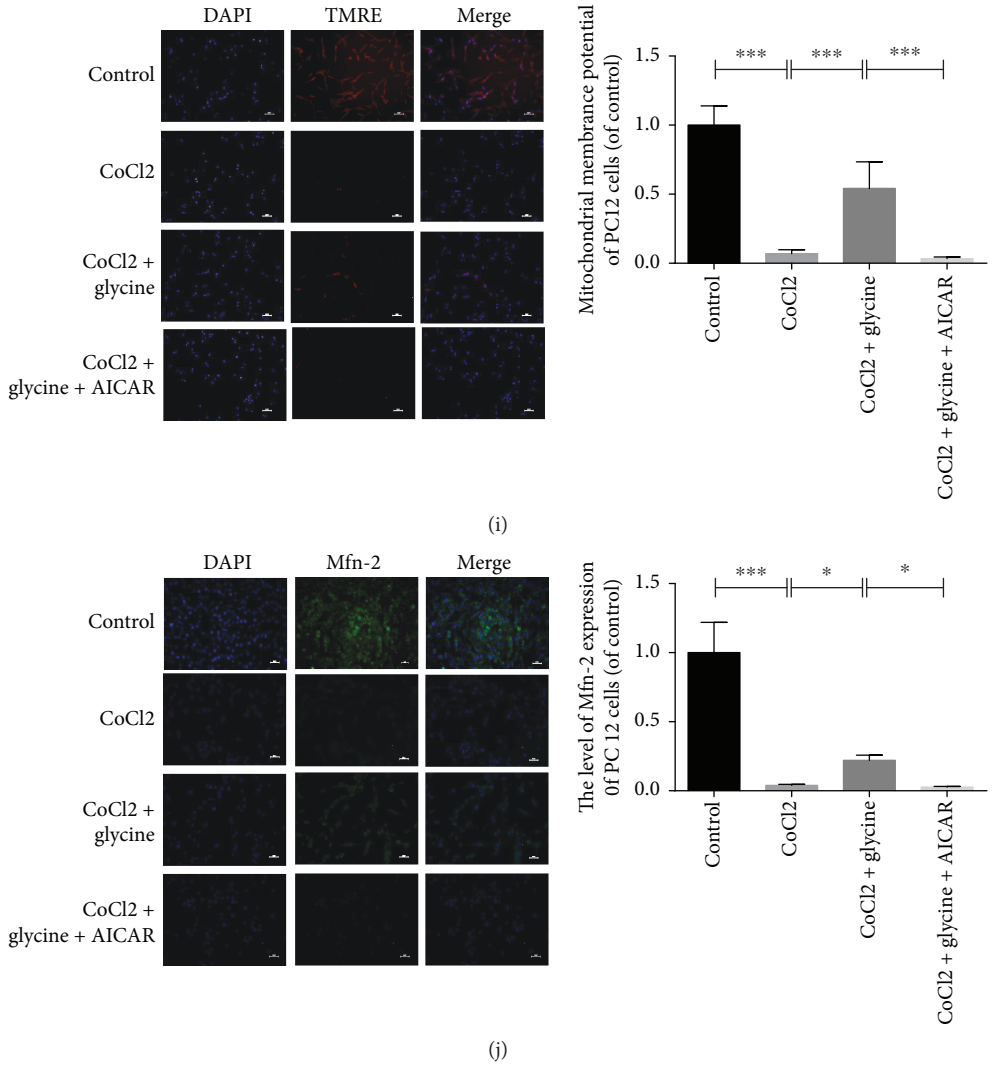

FIGURE 8: Glycine protected PC12 cells against $CoCl_2$ injury via regulation of AMPK-dependent mitochondria-mediated autophagy. (a) p-$AMPK_\alpha$ protein expression was detected by Western blotting in each group. (b) Analyses of p-$AMPK_\alpha$ protein (of $AMPK_\alpha$) and p-mTOR (of GAPDH). (c) Agonist of the AMPK pathway, CsA, was used to overactivate proteins from the AMPK pathway. Protein expressions of four groups were detected by Western blotting. (d) Analysis of all protein expressions. (e) Cell viability in four groups was also measured by CCK8. (f) Autophagic vacuoles from each group were measured by MDC staining. (g) Apoptotic cells from each group were measured by TUNEL and DAPI staining. (h) Mitochondrial ROS generations were detected by immunofluorescence of MitoSOX and DAPI staining. (i) Mitochondrial membrane potential was detected in each group by TMRE and Hoechst staining. (j) Mfn-2, protein of mitochondrial outer membrane, was used to measure function of mitochondria. $^*P < 0.05$, $^{**}P < 0.01$, and $^{***}P < 0.001$. $n = 3$.

system by regulating mitochondria-mediated autophagy via the AMPK pathway using *in vivo* and *in vitro* experiments.

Pathogeneses of HIE have been studied a lot, such as endoplasmic reticulum stress [42], inflammation among white matter [43], or neuron apoptosis [44]. In recent years, autophagy has become the new target in various systems. Without exception, a few researches illustrated the relation between HIE and autophagy. Previous studies have demonstrated that autophagy is related to a wide variety of physiological and pathological processes [45, 46]. Particularly in hypoxic-ischemic situations, autophagy plays a vital role in the metabolic regulation of different organs [47–49]. Furthermore, autophagy represents a significant mechanism by which cellular homeostasis is maintained to allow for further adjustments in HIE [50, 51]. Compared with some results about autophagy, their opinions about appropriately increasing profitable autophagy gained the protection in HIE. It is true that autophagy gains two extremes, protection and destruction [52]. An excessive degree of autophagy can be harmful to the whole cell or tissues [53, 54], which was demonstrated in the present study. Our results demonstrated that the injured side of the brain was severely hydrophobic, exhibited signs of cortical liquidation, and showed destruction of the cortex and hippocampus following HIE operations. Additionally, there was a high level of LC3 protein expression, which is a traditional indicator of autophagy in the HIE and $CoCl_2$ groups. Bnip3, which can be used to measure autophagy, was also expressed at a high level in the HIE and $CoCl_2$ groups. This is similar to the findings of previous studies showing that Bnip3 is sensitive to hypoxic-ischemic pathogenesis and may

potentially serve as a biomarker of excessive autophagy, which has been verified in other studies [55]. CsA, a conventional inhibitor of mitochondria-mediated autophagy, largely decreased the intensity of autophagy compared with the $CoCl_2$ + glycine and HIE + glycine groups. In the *in vivo* experiments, neonatal rats were pretreated with CsA to inhibit autophagy and brain samples from these animals showed good recovery when CsA was combined with daily glycine administration. Similar results were obtained from the *in vitro* experiments that revealed good cell viability and MMP. Taken together, the present findings indicate that high levels of mitochondria-mediated autophagy degraded abnormal proteins and digested organelles, particularly mitochondria but influenced normal functioning proteins and organelles, which could be catastrophic to the cellular environment and body. The present TEM results easily identified edematous mitochondria in all three groups of rats. Outer membrane protein levels were also assessed to determine mitochondrial function. The expression levels of Mfn-2 are indicative of the dysfunction or fusion of mitochondria, which, in turn, activates autophagy [56, 57]. Moreover, PINK1 phosphorylates parkin and recruits it to the mitochondria, which damage these organelles. In the HIE group and $CoCl_2$ group, the high expression levels of parkin and PINK1 indicated serious damage to the mitochondria. However, MDC staining in PC12 cells revealed that glycine treatment effectively alleviated the autophagy process compared with the $CoCl_2$ and $CoCl_2$ + glycine + AICAR groups. Therefore, novel treatments that immediately downregulate mitochondria-mediated autophagy are urgently needed to aid adjustment and recovery.

The administration of glycine is an effective treatment following hypoxic or hypoxic-ischemic injury in the liver [58], kidney [26], and various cell types [59–61]. In the present study, there were significant decreases in LC3 and Bnip3 protein levels following glycine pretreatment. At the same time, electron microscopy analyses indicated that glycine inhibited excessive autophagy. It is known that glycine protects against energy depletion by promoting the metabolism of intracellular or mitochondrial functions [24]. In the present study, glycine attenuated hypoxic-ischemic injury in the brain and improved mitochondrial function. HE and Nissl staining procedures revealed that glycine decreased the number of dying neurons and ameliorated the expression of related proteins while immunofluorescent analyses showed that outer membrane proteins in the mitochondria were altered by glycine. Taken together, these findings indicated that glycine could be an effective strategy for the promotion of mitochondrial function. Furthermore, glycine downregulated proteins related to mitochondria-mediated autophagy. Moreover, seven consecutive days of treatment with glycine resulted in a good prognosis in the behavioral test in 28-day-old rats. However, it has also been shown that glycine regulates the basic states of function in astrocytes and microglia by activating glycine receptors to promote recovery in the nervous system [62]. The present study did not verify the effectiveness of glycine in nonneuronal cell types.

AMPK is an energy-sensing center activated by stress or dysfunction in mitochondria [16, 63]. ATP deficiencies, or an increased ratio of AMP to ATP, usually originate from dysfunction of mitochondria. Under the hypoxic-ischemic insult, the mitochondria are sensitive (observing mitochondrial status), generating ROS and making chaos in energy supply. Subsequently, activation of the AMPK pathway (activated by α subunit in the ATP/AMP disorder) modulates mitochondrial function under conditions of stress, hypoxia, and/or ischemia [64]. In this process, extensive phosphorylation of AMPK also maintains autophagy kinase, which mostly induces mitochondria-mediated autophagy. Analyzing autophagy protein expressions among animal and cell models, we will help to directly understand the condition of mitochondria-mediated autophagy *in vivo* and *in vitro*.

Previous studies have demonstrated that mTOR protein expression is inhibited by activation of AMPK and that mTORC2 [65], as part of mTOR, plays a role to participate in the autophagy process [66]. Under hypoxic attack and other unfavorable conditions, AMPK activation inhibits the mTOR signaling pathway. In the present study, there were high levels of phosphorylation of AMPK expressed but low levels of p-mTOR following the HIE group or $CoCl_2$ injury.

One previous study reported that the suppression of AMPK activity had no harmful effects on the basic functions of mitochondria and good recovery of cellular metabolism was evident on following treatment [67]. However, the role of the AMPK pathway is complex and may vary under conditions. Within a specific range, AMPK plays a protective role; however, overactivation of the AMPK pathway can worsen intracellular status, especially in neurons exposed to a hypoxic environment [14]. To further understand the relationship of glycine with the AMPK pathway, AICAR, an agonist of AMPK, was administrated to measure autophagic proteins. Glycine treatment inhibited AICAR-induced activation of the AMPK pathway and downregulated autophagy. Of the three groups in the present study, p-AMPK expression levels were highest following HIE or $CoCl_2$ injury. However, the administration of AICAR in combination with glycine demonstrated the activation of AMPK proteins, ROS degeneration, and worsened mitochondrial function, which then enhanced autophagy. Detailed molecular mechanisms underlying inactivation of the AMPK pathway by glycine still require further investigation. However, previous studies have suggested several possibilities [68]. For example, fatty acid oxidation increases and glucose oxidation suppressed following AMPK activation [69, 70]. However, glycine pretreatment may attenuate fatty acid oxidation and adjust glucose oxidation to normal levels, which would aid in recovery of the whole neuron and its functions. AICAR, as an agonist of the AMPK pathway, revealed that activation of the AMPK pathway had detrimental effects. Rats that received daily treatments of AICAR and glycine did not show good recovery in terms of protection or further treatment. Similarly, PC12 cells pretreated with AICAR and glycine exhibited poor recovery following overactivation of the AMPK pathway.

There are several limitations of the present study that should be noted when interpreting the results. HIE models typically use knockout rats to assess the manner in which

glycine ameliorates HIE injury. Moreover, primary neurons can be collected and analyzed to assess the effects of glycine but evaluation of various cell types would strengthen the present results. Finally, it remains to be elucidated whether glycine regulates fatty acid oxidation.

In summary, the present data provide the first evidence that glycine attenuated hypoxic-ischemic injury in neurons or the nervous system by decreasing mitochondria-mediated autophagy through regulating the AMPK pathway using both in vitro and in vivo experiments. Since the pathogeneses of HIE are currently too complex to develop accurate and effective therapy, glycine may serve as a more inexpensive and effective alternative to other medicines. Additionally, identifying the optimum dosage of glycine for improved prognosis will be important.

Data Availability

The data used to support the findings of this study are available from the corresponding author upon request.

Conflicts of Interest

The authors declare that they have no conflict of interest.

Authors' Contributions

Cai CC drafted the article and designed the study mainly. Zhu JH helped to design experiments and write part of the article. Ye LX and Dai YY helped to design figures and contribute to analyze part of the data. Fang MC, Hu YY, and Pan SL contributed to design figures and helped to analyze related data. Chen S, Li PJ, and Fu XQ designed tables and helped to analyze related data. Lin ZL contributed to critical revision of the manuscript. They approved the final version and agreed to be accountable for the study.

Acknowledgments

This study was funded by the National Natural Science Foundation of China (grant numbers 81701489 and 81771624), the Beijing Medical and Health Foundation (grant number B17137), and the Wenzhou Science and Technology Bureau (grant number Y20160020).

Supplementary Materials

Supplementary Figure 1. The dosage of glycine pretreatment has no effect on normal cortex status of neonatal rats. (A) Protein expressions were examined for evaluating mitochondria-mediated autophagy extent between the sham and sham + glycine groups. (B) Analyses of all protein expressions. $n = 5$. Supplementary Figure 2. The dosage of glycine pretreatment has no effect on normal hippocampus status of neonatal rats. (A) Protein expressions were examined for evaluating mitochondria-mediated autophagy extent between the sham and sham + glycine groups. (B) Analyses of all protein expressions. $n = 5$. Supplementary Figure 3. The dosage of glycine administration has no influence on normal status of PC12 cells. (A) Protein expressions were examined for evaluating mitochondria-mediated autophagy extent between control and control + glycine groups. (B) Analyses of all protein expressions. $n = 3$. (C) Cell viability between two groups. $n = 5$. *(Supplementary Materials)*

References

[1] L. Lehtonen, A. Gimeno, A. Parra-Llorca, and M. Vento, "Early neonatal death: a challenge worldwide," *Seminars in Fetal & Neonatal Medicine*, vol. 22, no. 3, pp. 153–160, 2017.

[2] Á. Sánchez-Illana, A. Núñez-Ramiro, M. Cernada et al., "Evolution of energy related metabolites in plasma from newborns with hypoxic-ischemic encephalopathy during hypothermia treatment," *Scientific Reports*, vol. 7, no. 1, article 17039, 2017.

[3] M. Douglas-Escobar and M. D. Weiss, "Hypoxic-ischemic encephalopathy: a review for the clinician," *JAMA Pediatrics*, vol. 169, no. 4, pp. 397–403, 2015.

[4] A. J. du Plessis and J. J. Volpe, "Perinatal brain injury in the preterm and term newborn," *Current Opinion in Neurology*, vol. 15, no. 2, pp. 151–157, 2002.

[5] Q. Lu, V. A. Harris, S. Kumar, H. M. Mansour, and S. M. Black, "Autophagy in neonatal hypoxia ischemic brain is associated with oxidative stress," *Redox Biology*, vol. 6, pp. 516–523, 2015.

[6] S. Carloni, M. C. Albertini, L. Galluzzi, G. Buonocore, F. Proietti, and W. Balduini, "Increased autophagy reduces endoplasmic reticulum stress after neonatal hypoxia-ischemia: role of protein synthesis and autophagic pathways," *Experimental Neurology*, vol. 255, pp. 103–112, 2014.

[7] N. Mizushima, B. Levine, A. M. Cuervo, and D. J. Klionsky, "Autophagy fights disease through cellular self-digestion," *Nature*, vol. 451, no. 7182, pp. 1069–1075, 2008.

[8] Q. Han, G. Li, M. S. M. Ip et al., "Haemin attenuates intermittent hypoxia-induced cardiac injury via inhibiting mitochondrial fission," *Journal of Cellular and Molecular Medicine*, vol. 22, no. 5, pp. 2717–2726, 2018.

[9] J. Gao, Y. Deng, C. Yin et al., "Icariside II, a novel phosphodiesterase 5 inhibitor, protects against H2O2-induced PC12 cells death by inhibiting mitochondria-mediated autophagy," *Journal of Cellular and Molecular Medicine*, vol. 21, no. 2, pp. 375–386, 2017.

[10] J. Huang, G. Y. Lam, and J. H. Brumell, "Autophagy signaling through reactive oxygen species," *Antioxidants & Redox Signaling*, vol. 14, no. 11, pp. 2215–2231, 2011.

[11] S. Rodriguez-Enriquez, L. He, and J. J. Lemasters, "Role of mitochondrial permeability transition pores in mitochondrial autophagy," *The International Journal of Biochemistry & Cell Biology*, vol. 36, no. 12, pp. 2463–2472, 2004.

[12] C. Zhang, X. Yu, J. Gao et al., "PINK1/parkin-mediated mitophagy was activated against 1,4-benzoquinone-induced apoptosis in HL-60 cells," *Toxicology in Vitro*, vol. 50, pp. 217–224, 2018.

[13] A. S. Kim, E. J. Miller, T. M. Wright et al., "A small molecule AMPK activator protects the heart against ischemia-reperfusion injury," *Journal of Molecular and Cellular Cardiology*, vol. 51, no. 1, pp. 24–32, 2011.

[14] X. Zhang, R. Gao, J. Li et al., "A pharmacological activator of AMP-activated protein kinase protects hypoxic neurons in a concentration-dependent manner," *Neurochemical Research*, vol. 35, no. 8, pp. 1281–1289, 2010.

[15] J. Kim, M. Kundu, B. Viollet, and K. L. Guan, "AMPK and mTOR regulate autophagy through direct phosphorylation of Ulk1," *Nature Cell Biology*, vol. 13, no. 2, pp. 132–141, 2011.

[16] E. Q. Toyama, S. Herzig, J. Courchet et al., "AMP-activated protein kinase mediates mitochondrial fission in response to energy stress," *Science*, vol. 351, no. 6270, pp. 275–281, 2016.

[17] C. Cerveró, N. Montull, O. Tarabal, L. Piedrafita, J. E. Esquerda, and J. Calderó, "Chronic treatment with the AMPK agonist AICAR prevents skeletal muscle pathology but fails to improve clinical outcome in a mouse model of severe spinal muscular atrophy," *Neurotherapeutics*, vol. 13, no. 1, pp. 198–216, 2016.

[18] G. Wang, T. K. Hazra, S. Mitra, H. M. Lee, and E. W. Englander, "Mitochondrial DNA damage and a hypoxic response are induced by CoCl(2) in rat neuronal PC12 cells," *Nucleic Acids Research*, vol. 28, no. 10, pp. 2135–2140, 2000.

[19] Y. He, X. Gan, L. Zhang et al., "$CoCl_2$ induces apoptosis via a ROS-dependent pathway and Drp1-mediated mitochondria fission in periodontal ligament stem cells," *American Journal of Physiology-Cell Physiology*, vol. 315, no. 3, pp. C389–C397, 2018.

[20] J. A. Roth, L. Feng, J. Walowitz, and R. W. Browne, "Manganese-induced rat pheochromocytoma (PC12) cell death is independent of caspase activation," *Journal of Neuroscience Research*, vol. 61, no. 2, pp. 162–171, 2000.

[21] V. Moschetti, M. Desch, S. Goetz et al., "Safety, tolerability and pharmacokinetics of oral BI 425809, a glycine transporter 1 inhibitor, in healthy male volunteers: a partially randomised, single-blind, placebo-controlled, first-in-human study," *European Journal of Drug Metabolism and Pharmacokinetics*, vol. 43, no. 2, pp. 239–249, 2018.

[22] A. S. Tibbetts and D. R. Appling, "Compartmentalization of mammalian folate-mediated one-carbon metabolism," *Annual Review of Nutrition*, vol. 30, no. 1, pp. 57–81, 2010.

[23] D. Zhao, J. Chen, Y. Zhang et al., "Glycine confers neuroprotection through PTEN/AKT signal pathway in experimental intracerebral hemorrhage," *Biochemical and Biophysical Research Communications*, vol. 501, no. 1, pp. 85–91, 2018.

[24] F. Petrat, K. Boengler, R. Schulz, and H. de Groot, "Glycine, a simple physiological compound protecting by yet puzzling mechanism(s) against ischaemia-reperfusion injury: current knowledge," *British Journal of Pharmacology*, vol. 165, no. 7, pp. 2059–2072, 2012.

[25] R. Heidari, V. Ghanbarinejad, H. Mohammadi et al., "Mitochondria protection as a mechanism underlying the hepatoprotective effects of glycine in cholestatic mice," *Biomedicine & Pharmacotherapy*, vol. 97, pp. 1086–1095, 2018.

[26] L. Jiang, X. Qin, X. Zhong et al., "Glycine-induced cytoprotection is mediated by ERK1/2 and AKT in renal cells with ATP depletion," *European Journal of Cell Biology*, vol. 90, no. 4, pp. 333–341, 2011.

[27] A. Roldan, J. Figueras-Aloy, R. Deulofeu, and R. Jimenez, "Glycine and other neurotransmitter amino acids in cerebrospinal fluid in perinatal asphyxia and neonatal hypoxic-ischaemic encephalopathy," *Acta Paediatrica*, vol. 88, no. 10, pp. 1137–1141, 1999.

[28] H. Mori, K. Momosaki, J. Kido et al., "Amelioration by glycine of brain damage in neonatal rat brain following hypoxia-ischemia," *Pediatrics International*, vol. 59, no. 3, pp. 321–327, 2017.

[29] S.-g. Qiao, Y. Sun, B. Sun et al., "Sevoflurane postconditioning protects against myocardial ischemia/reperfusion injury by restoring autophagic flux via an NO-dependent mechanism," *Acta Pharmacologica Sinica*, pp. 1–11, 2018.

[30] M. Dulovic, M. Jovanovic, M. Xilouri et al., "The protective role of AMP-activated protein kinase in alpha-synuclein neurotoxicity in vitro," *Neurobiology of Disease*, vol. 63, pp. 1–11, 2014.

[31] R. C. Vannucci and S. J. Vannucci, "Perinatal hypoxic-ischemic brain damage: evolution of an animal model," *Developmental Neuroscience*, vol. 27, no. 2–4, pp. 81–86, 2005.

[32] W. Zhang, H. Zhang, H. Mu et al., "Omega-3 polyunsaturated fatty acids mitigate blood-brain barrier disruption after hypoxic-ischemic brain injury," *Neurobiology of Disease*, vol. 91, pp. 37–46, 2016.

[33] D. N. Feather-Schussler and T. S. Ferguson, "A battery of motor tests in a neonatal mouse model of cerebral palsy," *Journal of Visualized Experiments*, no. 117, 2016.

[34] Y. Yang, X. J. Zhang, J. Yin, and L. T. Li, "Brain damage related to hemorrhagic transformation following cerebral ischemia and the role of K_{ATP} channels," *Brain Research*, vol. 1241, pp. 168–175, 2008.

[35] S. Liang, Y. Lin, B. Lin et al., "Resting-state functional magnetic resonance imaging analysis of brain functional activity in rats with ischemic stroke treated by electro-acupuncture," *Journal of Stroke and Cerebrovascular Diseases*, vol. 26, no. 9, pp. 1953–1959, 2017.

[36] S. J. Cho, S. M. Yun, C. Jo et al., "SUMO1 promotes Aβ production via the modulation of autophagy," *Autophagy*, vol. 11, no. 1, pp. 100–112, 2015.

[37] T. Mahmood and P. C. Yang, "Western blot: technique, theory, and trouble shooting," *North American Journal of Medical Sciences*, vol. 4, no. 9, pp. 429–434, 2012.

[38] L. A. Kubasiak, O. M. Hernandez, N. H. Bishopric, and K. A. Webster, "Hypoxia and acidosis activate cardiac myocyte death through the Bcl-2 family protein BNIP3," *Proceedings of the National Academy of Sciences of the United States of America*, vol. 99, no. 20, pp. 12825–12830, 2002.

[39] K. M. Regula, K. Ens, and L. A. Kirshenbaum, "Inducible expression of BNIP3 provokes mitochondrial defects and hypoxia-mediated cell death of ventricular myocytes," *Circulation Research*, vol. 91, no. 3, pp. 226–231, 2002.

[40] S. Daido, T. Kanzawa, A. Yamamoto, H. Takeuchi, Y. Kondo, and S. Kondo, "Pivotal role of the cell death factor BNIP3 in ceramide-induced autophagic cell death in malignant glioma cells," *Cancer Research*, vol. 64, no. 12, pp. 4286–4293, 2004.

[41] A. Bresciani, M. C. Spiezia, R. Boggio et al., "Quantifying autophagy using novel LC3B and p62 TR-FRET assays," *PLoS One*, vol. 13, no. 3, article e0194423, 2018.

[42] S. Liu, D. Xin, L. Wang et al., "Therapeutic effects of L-cysteine in newborn mice subjected to hypoxia-ischemia brain injury via the CBS/H_2S system: role of oxidative stress and endoplasmic reticulum stress," *Redox Biology*, vol. 13, pp. 528–540, 2017.

[43] L. R. Shiow, G. Favrais, L. Schirmer et al., "Reactive astrocyte COX2-PGE2 production inhibits oligodendrocyte maturation in neonatal white matter injury," *Glia*, vol. 65, no. 12, pp. 2024–2037, 2017.

[44] X. H. Ge, L. Shao, and G. J. Zhu, "Oxymatrine attenuates brain hypoxic-ischemic injury from apoptosis and oxidative stress: role of p-Akt/GSK3β/HO-1/Nrf-2 signaling pathway," *Metabolic Brain Disease*, vol. 33, no. 6, pp. 1869–1875, 2018.

[45] X. Wu, H. Won, and D. C. Rubinsztein, "Autophagy and mammalian development," *Biochemical Society Transactions*, vol. 41, no. 6, pp. 1489–1494, 2013.

[46] I. Dikic, T. Johansen, and V. Kirkin, "Selective autophagy in cancer development and therapy," *Cancer Research*, vol. 70, no. 9, pp. 3431–3434, 2010.

[47] Y. Romero, M. Bueno, R. Ramirez et al., "mTORC1 activation decreases autophagy in aging and idiopathic pulmonary fibrosis and contributes to apoptosis resistance in IPF fibroblasts," *Aging cell*, vol. 15, no. 6, pp. 1103–1112, 2016.

[48] A. K. Au, Y. Chen, L. du et al., "Ischemia-induced autophagy contributes to neurodegeneration in cerebellar Purkinje cells in the developing rat brain and in primary cortical neurons in vitro," *Biochimica et Biophysica Acta (BBA) - Molecular Basis of Disease*, vol. 1852, no. 9, pp. 1902–1911, 2015.

[49] H. Choi, C. Merceron, L. Mangiavini et al., "Hypoxia promotes noncanonical autophagy in nucleus pulposus cells independent of MTOR and HIF1A signaling," *Autophagy*, vol. 12, no. 9, pp. 1631–1646, 2016.

[50] L. Ye, Z. Feng, D. Doycheva et al., "CpG-ODN exerts a neuroprotective effect via the TLR9/pAMPK signaling pathway by activation of autophagy in a neonatal HIE rat model," *Experimental Neurology*, vol. 301, Part A, pp. 70–80, 2018.

[51] D. C. Rubinsztein, J. E. Gestwicki, L. O. Murphy, and D. J. Klionsky, "Potential therapeutic applications of autophagy," *Nature Reviews Drug Discovery*, vol. 6, no. 4, pp. 304–312, 2007.

[52] Z. Zheng, L. Zhang, Y. Qu et al., "Mesenchymal stem cells protect against hypoxia-ischemia brain damage by enhancing autophagy through brain derived neurotrophic factor/mammalin target of rapamycin signaling pathway," *Stem Cells*, vol. 36, no. 7, pp. 1109–1121, 2018.

[53] A. Melk, A. Baisantry, and R. Schmitt, "The yin and yang of autophagy in acute kidney injury," *Autophagy*, vol. 12, no. 3, pp. 596-597, 2016.

[54] J. Zhou, Y. Fan, J. Zhong et al., "TAK1 mediates excessive autophagy via p38 and ERK in cisplatin-induced acute kidney injury," *Journal of Cellular and Molecular Medicine*, vol. 22, no. 5, pp. 2908–2921, 2018.

[55] A. Hamacher-Brady, N. R. Brady, S. E. Logue et al., "Response to myocardial ischemia/reperfusion injury involves Bnip3 and autophagy," *Cell Death and Differentiation*, vol. 14, no. 1, pp. 146–157, 2006.

[56] A. Nardin, E. Schrepfer, and E. Ziviani, "Counteracting PINK/parkin deficiency in the activation of mitophagy: a potential therapeutic intervention for Parkinson's disease," *Current Neuropharmacology*, vol. 14, no. 3, pp. 250–259, 2016.

[57] G. Amadoro, V. Corsetti, F. Florenzano et al., "Morphological and bioenergetic demands underlying the mitophagy in post-mitotic neurons: the pink–parkin pathway," *Frontiers in aging neuroscience*, vol. 6, 2014.

[58] N. Dehne, T. Li, F. Petrat, U. Rauen, and H. de Groot, "Critical O2 and NO concentrations in NO-induced cell death in a rat liver sinusoidal endothelial cell line," *Biological Chemistry*, vol. 385, no. 3-4, pp. 341–349, 2004.

[59] K. Zhang, J. M. Weinberg, M. A. Venkatachalam, and Z. Dong, "Glycine protection of PC-12 cells against injury by ATP-depletion," *Neurochemical Research*, vol. 28, no. 6, pp. 893–901, 2003.

[60] P. Zhao, H. Qian, and Y. Xia, "GABA and glycine are protective to mature but toxic to immature rat cortical neurons under hypoxia," *The European Journal of Neuroscience*, vol. 22, no. 2, pp. 289–300, 2005.

[61] F. U. Amin, S. A. Shah, and M. O. Kim, "Glycine inhibits ethanol-induced oxidative stress, neuroinflammation and apoptotic neurodegeneration in postnatal rat brain," *Neurochemistry International*, vol. 96, pp. 1–12, 2016.

[62] J. van den Eynden, S. S. Ali, N. Horwood et al., "Glycine and glycine receptor signalling in non-neuronal cells," *Frontiers in Molecular Neuroscience*, vol. 2, p. 9, 2009.

[63] M. Frederich and J. A. Balschi, "The relationship between AMP-activated protein kinase activity and AMP concentration in the isolated perfused rat heart," *The Journal of Biological Chemistry*, vol. 277, no. 3, pp. 1928–1932, 2002.

[64] D. Qi and L. H. Young, "AMPK: energy sensor and survival mechanism in the ischemic heart," *Trends in Endocrinology and Metabolism*, vol. 26, no. 8, pp. 422–429, 2015.

[65] N. Gurusamy, I. Lekli, S. Mukherjee et al., "Cardioprotection by resveratrol: a novel mechanism via autophagy involving the mTORC2 pathway," *Cardiovascular Research*, vol. 86, no. 1, pp. 103–112, 2010.

[66] J. M. Rodríguez-Vargas, M. J. Ruiz-Magaña, C. Ruiz-Ruiz et al., "ROS-induced DNA damage and PARP-1 are required for optimal induction of starvation-induced autophagy," *Cell Research*, vol. 22, no. 7, pp. 1181–1198, 2012.

[67] R. R. Russell III, J. Li, D. L. Coven et al., "AMP-activated protein kinase mediates ischemic glucose uptake and prevents postischemic cardiac dysfunction, apoptosis, and injury," *Journal of Clinical Investigation*, vol. 114, no. 4, pp. 495–503, 2004.

[68] S. Jager, C. Handschin, J. St.-Pierre, and B. M. Spiegelman, "AMP-activated protein kinase (AMPK) action in skeletal muscle via direct phosphorylation of PGC-1α," *Proceedings of the National Academy of Sciences of the United States of America*, vol. 104, no. 29, pp. 12017–12022, 2007.

[69] M. M. Mihaylova and R. J. Shaw, "The AMPK signalling pathway coordinates cell growth, autophagy and metabolism," *Nature Cell Biology*, vol. 13, no. 9, pp. 1016–1023, 2011.

[70] T. A. Hopkins, J. R. B. Dyck, and G. D. Lopaschuk, "AMP-activated protein kinase regulation of fatty acid oxidation in the ischaemic heart," *Biochemical Society Transactions*, vol. 31, no. 1, pp. 207–212, 2003.

Hindawi
Oxidative Medicine and Cellular Longevity
Volume 2018, Article ID 1427412, 8 pages
https://doi.org/10.1155/2018/1427412

Research Article

Effects of Low-Frequency Electromagnetic Field on Oxidative Stress in Selected Structures of the Central Nervous System

Jan Budziosz[1], **Agata Stanek**[2], **Aleksander Sieroń**[2], **Joanna Witkoś**[1], **Armand Cholewka**[3] and **Karolina Sieroń**[1]

[1]*School of Health Sciences in Katowice, Department of Physical Medicine, Chair of Physiotherapy, Medical University of Silesia, Medyków Street 12, 40-752 Katowice, Poland*
[2]*School of Medicine with the Division of Dentistry in Zabrze, Department of Internal Medicine, Angiology and Physical Medicine, Medical University of Silesia, Batorego Street 15, 41-902 Bytom, Poland*
[3]*Department of Medical Physics, Chełkowski Institute of Physics, University of Silesia, 4 Uniwersytecka Street, 40-007 Katowice, Poland*

Correspondence should be addressed to Agata Stanek; astanek@tlen.pl

Received 1 September 2018; Revised 7 November 2018; Accepted 14 November 2018; Published 13 December 2018

Academic Editor: Ana Lloret

Objective.The aim of the study was to evaluate the effects of a 28-day exposure to a 50 Hz electromagnetic field of 10 kV/m on the oxidative stress in selected rat central nervous system (CNS) structures. *Material and Methods*. Twenty male Wistar rats served as experimental subjects. Ten rats were exposed to an electromagnetic field with a frequency of 50 Hz, intensity of 10 kV/m, and magnetic induction of 4.3 pT for 22 hours a day. The control group of ten rats was subject to sham exposure. Homogenates of the frontal cortex, hippocampus, brainstem, hypothalamus, striatum, and cerebellum were evaluated for selected parameters of oxidative stress. *Results*. Following the four-week exposure to a low-frequency electromagnetic field, the mean malondialdehyde levels and total oxidant status of CNS structures did not differ significantly between the experimental and control groups. However, the activities of antioxidant enzymes in brain structure homogenates were decreased except for frontal cortex catalase, glutathione peroxidase, and hippocampal glutathione reductase. The low-frequency electromagnetic field had no effect on the nonenzymatic antioxidant system of the examined brain structures except for the frontal cortex. *Conclusion*. The four-week exposure of male rats to a low-frequency electromagnetic field did not affect oxidative stress in the investigated brain structures.

1. Introduction

An electromagnetic field (EMF) occurs naturally in our environment. It is generated by geological structures in the Earth's crust, and all devices powered with alternating currents. Multihour use of such devices, including medical apparatus, results in a prolonged exposure to a low-frequency EMF (≤50 Hz). This may lead to disturbances in homeostasis and consequent disruption of the prooxidative-antioxidative balance within the central nervous system (CNS) of people permanently working in close proximity to devices generating electromagnetic fields [1].

In the last decade, the effects of a low-frequency electromagnetic field (LFEMF) on the human body have been referred to as electromagnetic sensitivity syndrome commonly associated with the rapid development of wireless technologies [2, 3]. The molecular mechanisms of nonthermal and nonionizing effects at low field intensities remain to be elucidated. Nevertheless, the number of research studies on this issue continues to grow [4–6]. A wide range of health problems associated with exposure to computer monitors, mobile phones, and other EMF-generating appliances has been reported. The most common symptoms include fatigue, irritation, headache, dryness of the skin and mucous membranes, sleep disturbance, and hormonal imbalance as well as cardiac and neural effects [7, 8]. Exposure to an EMF has also been linked with allergic reactions confirmed by a marked increase in the number of mast cells [9]. Numerous

epidemiological studies have confirmed a significant increase in the risk of brain tumours [10, 11], parotid gland tumours [12], malignant melanoma [13], and lymphomas [14].

Several researchers have emphasised that exposure to the EMF might also cause increased reactive oxygen species (ROS) production and lead to oxidative stress [2, 15]. ROS have been implicated in the pathogenesis of neurodegenerative diseases including Alzheimer's disease, multiple sclerosis, or amyotrophic lateral sclerosis [16, 17]. It has also been found that oxidative stress might be involved in the development of Parkinson's disease [18, 19] and in the pathogenesis of mental disorders [20, 21]. Despite differences in the clinical features of neurodegenerative diseases, it has been suggested that they share common mechanisms such as dysregulation of iron metabolism, protein aggregation, oxidative stress, inflammatory processes, and mitochondrial dysfunction. However, all these phenomena have so far been studied separately without considering possible interactions or an option that they might occur as cascading events. Nevertheless, oxidative stress has been mentioned as the primary cause of neural cell damage [22].

The effect of the LFEMF on the prooxidative-antioxidative balance in CNS structures is yet to be extensively studied. Furthermore, only whole brain homogenates from experimental animals were evaluated. No assessment was carried out regarding particular brain structures, markers of oxidative stress, or activity of enzymatic and nonenzymatic antioxidant systems. Such incomplete analysis severely hinders the interpretation of results.

Therefore, the aim of this study was to evaluate the effects of a 28-day exposure to a 50 Hz electromagnetic field of 10 kV/m on the oxidative stress in selected CNS structures (frontal cortex, hippocampus, brainstem, hypothalamus, striatum, and cerebellum) of male rats.

2. Material and Methods

2.1. Animals. The study was performed with the approval no. 65/2008 of the Bioethical Committee for Animal Experimentation of the Medical University of Silesia in Katowice, Poland. All animals received humane care in compliance with the 8th edition of the *Guide for the Care and Use of Laboratory Animals* published by the National Institute of Health [23].

Twenty male Wistar rats aged 10 weeks and weighing approximately 280 grams served as the experimental subjects. The animals were bred at the Institute of Experimental Medicine, Medical University of Silesia in Katowice Ligota, Poland. During the experiment, the rats were kept under optimal environmental conditions, i.e., at a temperature of 21°C and constant humidity, maintaining their 24-hour circadian rhythm. They were housed 10 per cage in plastic cages and fed with standard laboratory pellet food (Labofed B) and water at libitum.

2.2. Experimental Model. The rats were randomly divided into four groups, consisting of 10 animals each. Group A was exposed daily to an electromagnetic field with a frequency of 50 Hz, intensity of 10 kV/m, and magnetic induction of 4.3 pT. Exposure duration was 22 hours per day (with a break between 08 : 00 and 10 : 00). During the exposure, the animals remained in a plastic cage positioned between two electrodes placed 50 centimeters apart. The plastic cage did not impede the electromagnetic field and allowed the free movement of the rats. One electrode received a potential of 5 kV from a high-voltage transformer. The cage housing the rats was placed on the ground electrode. The control group of ten rats (group C) were subject to sham exposure (22 hours a day). Rats from group M were exposed for 28 successive days to an electromagnetic field with a frequency of 900 MHz generated by a mobile phone. Rats from group A + M were exposed, for 28 successive days, simultaneously to both a 50 Hz electromagnetic field and a radio-frequency electromagnetic field generated by a mobile phone. The physical parameters and duration of exposure were identical to those described for group A and group M.

In this manuscript, we have only presented the findings from group A and the control group.

Following the cycle of a 28-day exposure to an electromagnetic field and sham exposure, the rats were fasted for 24 hours and euthanized and the brains were removed. The dissection of brain structures was carried out by a person experienced in rat dissection. After decapitation and opening the skull, the brain was removed and the following structures were dissected: frontal cortex, striatum, hippocampus, hypothalamus, and cerebellum. For identifying brain structures, sections were systematically compared with images from the adult rat brain atlas [24]. The sampled tissues were frozen in solid carbon dioxide (dry ice), weighed, and kept deep-frozen at -70°C.

2.3. Preparation of Brain Tissue Homogenates. On the day of laboratory determinations, the tissues were homogenized for 3 minutes at 50 revolutions per minute using the Glas-Col Tissue Homogenizing System at a room temperature of 21°C. The tissues were homogenized in physiological buffered saline. The following were then determined in the obtained 5% tissue homogenates: total oxidant status (TOS), malondialdehyde (MDA), superoxide dismutase (SOD) and its isoenzymes (copper-zinc dismutase (SOD-CuZn), manganese dismutase (SOD-Mn)), catalase (CAT), glutathione peroxidase (GPx), glutathione reductase (GR), glutathione S-transferase (GST), and total antioxidant capacity (TAC).

2.4. Biochemical Analysis

2.4.1. Oxidative Stress Marker Analysis

(1) Determination of Prooxidative Status Parameters: Lipid Peroxidation Products and Total Oxidative Status. The intensity of lipid peroxidation in the brain homogenates was measured spectrofluorimetrically as thiobarbituric acid-reactive substances (TBARS) according to Ohkawa et al. [25]. The TBARS concentrations were expressed as malondialdehyde (MDA) equivalents in μmol/g protein. The inter- and intra-assay coefficients of variations (CV) were 2.2% and 8.4%, respectively.

The total oxidant status (TOS) was determined with the method described by Erel [26] and expressed in μmol/g protein. The inter- and intra-assay coefficients of variations (CV) were 2.1% and 6.3%, respectively.

(2) Determination of the Activity of Antioxidant Enzymes. The superoxide dismutase (SOD-E.C.1.15.1.1) activity in brain homogenates was assayed using the Oyanagui method [27]. Enzymatic activity was expressed in nitrite unit (NU) in each mg of hemoglobin (Hb) or ml of blood plasma. One nitrite unit (1 NU) means a 50% inhibition of nitrite ion production by SOD in this method. SOD isoenzymes (SOD-Mn and SOD-CuZn) were measured using potassium cyanide as the inhibitor of the SOD-ZnCu isoenzyme. The inter- and intra-assay coefficients of variations (CV) were 2.8% and 5.4%, respectively.

Catalase (CAT-E.C.1.11.1.6.) activity was determined with the peroxide-purpald method developed by Johansson and Håkan Borg [28]. The method is based on the reaction of catalase with methanol in the presence of an optimal concentration of hydrogen peroxide. The obtained formaldehyde is measured spectrophotometrically at 550 nm with Purpald as a chromogen. The enzymatic activity of catalase was expressed in IU/g of protein. The inter- and intra-assay coefficients of variations (CV) were 2.6% and 6.1%, respectively.

The activity of brain homogenates' glutathione peroxidase (GPx-E.C.1.11.1.9.) was assayed using Paglia and Valentine's kinetic method [29], with t-butyl peroxide as a substrate and expressed as micromoles of NADPH oxidized per minute and normalised to one gram of protein [IU/g protein]. The inter- and intra-assay coefficients of variations (CV) were 3.3% and 7.4%, respectively.

The glutathione reductase activity (GR-E.C.1.6.4.2) in brain homogenates was assayed using Richterich's kinetic method [30], expressed as micromoles of NADPH utilized per minute, and normalised to one gram of protein [IU/g protein]. The inter- and intra-assay coefficients of variations (CV) were 2.2% and 5.7%, respectively.

The activity of glutathione S-transferase (GST-E.C.2.5.1.18) was determined with the kinetic method of Habig and Jakoby [31], expressed as micromoles of thioether formed per minute and normalised to one gram of protein [IU/g protein]. The inter- and intra-assay coefficients of variations (CV) were 3.4% and 7.3%, respectively.

(3) Determination of Nonenzymatic Antioxidant Status. Total antioxidant capacity (TAC) concentration in brain structure homogenates was determined with the method of Erel [32] based on oxidized ABTS (green in colour) decolorisation by antioxidants present in the sample and calibrated using Trolox and expressed in mmol/g protein. The inter- and intra-assay coefficients of variations (CV) were 1.1% and 3.8%, respectively.

2.5. Statistical Analysis. The obtained results were presented as the mean ± standard deviation (M ± SD) and analyzed using Statistica 7.1 PL software. All parameters of the group exposed to the electromagnetic field were compared to sham-exposed animals (control group). The Shapiro-Wilk test was used to test for normality of the distribution of particular variables. Intergroup differences were examined using a single-factor parametric ANOVA for quantitative variables. Additionally, the relationships identified by the ANOVA were verified using the NIR post hoc test for the particular groups. The level of statistical significance ($p < 0.05$) was used in all analyses.

3. Results

3.1. Oxidative Stress Parameters in the Frontal Cortex. In the frontal cortex homogenates from rats exposed to the LFEMF (group A), the mean activities of SOD, SOD-Mn, GPx, GST, and TOS were significantly lower, while the mean CAT activity was higher compared to the control rats (group C). However, the mean concentrations of MDA and TOS as well as the mean activities of SOD-CuZn and GR in rats exposed to the LFEMF did not differ significantly in comparison to the control group (Table 1).

3.2. Oxidative Stress Parameters in the Hippocampus. In the hippocampus homogenates from rats exposed to the low-frequency electromagnetic field, the mean activity of GR was significantly higher, while GST activity was significantly lower in comparison to the control group. However, no significant differences were observed between the mean MDA, TOS, and TAC concentrations as well as the mean SOD, SOD-Mn, SOD-CuZn, CAT, and GPx activities in rats exposed to the low-frequency electromagnetic field compared to the control group (Table 2).

3.3. Oxidative Stress Parameters in the Brainstem. In the brainstem homogenates from rats exposed to the LFEMF, the mean activities of SOD, SOD-Mn, SOD-CuZn, GR, and GST were significantly lower in comparison to those of the control rats. However, the mean MDA, TOS, and TAC concentrations as well as the mean CAT and GPx activities did not differ significantly in rats exposed to the LFEMF in comparison to the control group (Table 3).

3.4. Oxidative Stress Parameters in the Hypothalamus. In the hypothalamus homogenates from rats exposed to the LFEMF, the mean activity of GST homogenates was significantly higher compared to the control group. However, the mean MDA, TOS, and TAC concentrations as well as the mean SOD, SOD-Mn, SOD-CuZn, CAT, GPx, and GR activities in the hypothalamus homogenates from rats exposed to the LFEMF did not differ significantly in comparison to the sham-exposed rats (Table 4).

3.5. Oxidative Stress Parameters in the Striatum. In the striatum homogenates from rats exposed to the LFEMF, the mean activity of GST homogenates was significantly lower in comparison to the control group. The GST activity was the only parameter whose values differed significantly between the studied groups. However, the mean MDA, TOS, and TAC concentrations as well as the mean SOD, SOD-Mn, SOD-CuZn, CAT, GPx, and GR activities in the striatum homogenates from rats exposed to the LFEMF did not differ significantly in comparison to the sham-exposed rats (Table 5).

Table 1: Concentrations of oxidative stress biomarkers: malondialdehyde (MDA) and total oxidant status (TOS); activity of antioxidant enzymes: superoxide dismutase (SOD) and isoenzymes (SOD-Mn, SOD-CuZn), catalase (CAT), glutathione peroxidase (GPx), glutathione reductase (GR), and glutathione S-transferase (GST); and concentration of nonenzymatic antioxidants—total antioxidant capacity (TAC) in the frontal cortex homogenates from rats exposed to low-frequency electromagnetic field (group A) and sham-exposed rats (control group) (group C) with results of ANOVA for all examined groups (A, C, M, and A + M) and post hoc NIR test for two selected groups: A and C.

Parameter	Group A M ± SD	Group C M ± SD	ANOVA results F; p value	p value of NIR test
MDA concentration (μmol/g protein)	1.12 ± 0.09	1.04 ± 0.16	9.68; **<0.001**	0.538
TOS concentration (μmol/g protein)	2.17 ± 0.35	2.10 ± 0.39	0.6; 0.622	0.623
SOD activity (NU/mg protein)	49.38 ± 5.85	56.80 ± 3.25	13.02; **<0.001**	**<0.001**
SOD-Mn activity (NU/mg protein)	29.75 ± 3.12	35.05 ± 2.53	13.02; **<0.001**	**<0.001**
SOD-CuZn activity (NU/mg protein)	19.63 ± 4.45	21.75 ± 2.19	2.82; 0.040	0.219
CAT activity (IU/g protein)	6.16 ± 0.92	3.48 ± 1.05	17.66; **<0.001**	**<0.001**
GPx activity (IU/g protein)	0.59 ± 0.09	0.77 ± 0.13	3.87; 0.017	**<0.01**
GR activity (IU/g protein)	18.96 ± 1.98	19.91 ± 1.28	14.81; **<0.001**	0.097
GST activity (IU/g protein)	2.03 ± 0.21	2.99 ± 0.21	47.03; **<0.001**	**<0.01**
TAC concentration (mmol/g protein)	0.06 ± 0.00	0.07 ± 0.01	3.34; **0.031**	**<0.01**

Table 2: Concentrations of oxidative stress biomarkers: malondialdehyde (MDA) and total oxidant status (TOS); activity of antioxidant enzymes: superoxide dismutase (SOD) and isoenzymes (SOD-Mn, SOD-CuZn), catalase (CAT), glutathione peroxidase (GPx), glutathione reductase (GR), and glutathione S-transferase (GST); and concentration of nonenzymatic antioxidants—total antioxidant capacity (TAC) in the hippocampus homogenates from rats exposed to low-frequency electromagnetic field (group A) and sham-exposed rats (control group) (group C) with results of ANOVA for all examined groups (A, C, M, and A + M) and post hoc NIR test for two selected groups: A and C.

Parameter	Group A M ± SD	Group C M ± SD	ANOVA results F; p value	p value of NIR test
MDA concentration (μmol/g protein)	1.79 ± 0.48	1.56 ± 0.34	1.86; 0.156	0.294
TOS concentration (μmol/g protein)	2.68 ± 0.43	2.36 ± 0.23	1.50; 0.232	0.081
SOD activity (NU/mg protein)	70.73 ± 9.09	65.78 ± 6.63	8.78; **0.035**	1.000
SOD-Mn activity (NU/mg protein)	38.75 ± 3.87	37.05 ± 3.02	13.66; **<0.001**	0.278
SOD-CuZn activity (NU/mg protein)	31.98 ± 6.64	28.73 ± 6.37	1.06; 0.379	0.212
CAT activity (IU/g protein)	5.02 ± 0.78	5.79 ± 0.76	14.40; **<0.001**	0.084
GPx activity (IU/g protein)	0.45 ± 0.19	0.47 ± 0.13	0.20; 0.898	0.848
GR activity (IU/g protein)	30.56 ± 3.34	26.97 ± 2.19	11.56; **<0.001**	**<0.01**
GST activity (IU/g protein)	3.92 ± 0.37	4.57 ± 0.28	6.96; **<0.001**	**<0.01**
TAC concentration (mmol/g protein)	0.10 ± 0.01	0.09 ± 0.01	0.38; 0.765	0.612

3.6. Oxidative Stress Parameters in the Cerebellum. In the cerebellum homogenates from rats exposed to the LFEMF, only the mean activity of GST homogenates was significantly lower in comparison to the control group. However, the mean MDA, TOS, and TAC concentrations as well as the mean SOD, SOD-Mn, SOD-CuZn, CAT, GPx, and GR activities in the group of rats exposed to the LFEMF did not differ significantly in comparison to the sham-exposed rats (Table 6).

4. Discussion

It has been found that the electromagnetic field may disrupt the prooxidative-antioxidative balance through increased ROS production, impaired ROS elimination, or the combined effect of both processes [33, 34]. Hence, the evaluation of oxidative stress severity must comprise the determination of oxidative stress markers as well as the activity of the enzymatic and nonenzymatic antioxidant systems simultaneously [35, 36].

Our study on the effects of a 4-week exposure of male rats to the LFEMF did not reveal any statistically significant differences in the mean MDA and TOS concentrations in CNS structures between the rats exposed to the LFEMF and sham-exposed animals. Hence, chronic exposure to the low-frequency electromagnetic field does not seem to have resulted in increased lipid peroxidation and ROS generation in the rat brain.

In the frontal cortex of rats exposed to the LFEMF, the mean activities of SOD and SOD-Mn homogenates were lower by 13.1% and 15.1%, respectively, compared to the control group. In addition, the mean activities of SOD, SOD-Mn, and SOD-CuZn in the brainstem of rats exposed to the LFEMF were lower by 16.5%, 15.9%, and 17.1%,

Table 3: Concentrations of oxidative stress biomarkers: malondialdehyde (MDA) and total oxidant status (TOS); activity of antioxidant enzymes: superoxide dismutase (SOD) and isoenzymes (SOD-Mn, SOD-CuZn), catalase (CAT), glutathione peroxidase (GPx), glutathione reductase (GR), and glutathione S-transferase (GST); and concentration of nonenzymatic antioxidants—total antioxidant capacity (TAC) in the brainstem homogenates from rats exposed to low-frequency electromagnetic field (group A) and sham-exposed rats (control group) (group C) with results of ANOVA for all examined groups (A, C, M, and A + M) and post hoc NIR test for two selected groups: A and C.

Parameter	Group A M ± SD	Group C M ± SD	ANOVA results F; p value	p value of NIR test
MDA concentration (μmol/g protein)	1.93 ± 0.46	2.60 ± 0.38	3.12; **0.020**	0.568
TOS concentration (μmol/g protein)	4.04 ± 1.25	3.19 ± 1.36	1.14; 0.349	0.217
SOD activity (NU/mg protein)	120.63 ± 5.58	144.45 ± 9.87	16.81; **<0.001**	**<0.001**
SOD-Mn activity (NU/mg protein)	63.79 ± 4.43	75.84 ± 6.37	14.76; **<0.001**	**<0.01**
SOD-CuZn activity (NU/mg protein)	56.84 ± 4.05	68.61 ± 8.48	17.26; **<0.001**	**<0.01**
CAT activity (IU/g protein)	11.64 ± 1.40	12.81 ± 1.10	14.26; **<0.01**	0.932
GPx activity (IU/g protein)	1.14 ± 0.31	1.38 ± 0.17	1.72; 0.181	0.103
GR activity (IU/g protein)	21.68 ± 1.55	28.95 ± 1.24	38.32; **<0.001**	**<0.001**
GST activity (IU/g protein)	3.77 ± 0.25	5.52 ± 0.54	34.71; **<0.001**	**<0.001**
TAC concentration (mmol/g protein)	0.12 ± 0.02	0.11 ± 0.04	0.57; 0.636	0.304

Table 4: Concentrations of oxidative stress biomarkers: malondialdehyde (MDA) and total oxidant status (TOS); activity of antioxidant enzymes: superoxide dismutase (SOD) and isoenzymes (SOD-Mn, SOD-CuZn), catalase (CAT), glutathione peroxidase (GPx), glutathione reductase (GR), and glutathione S-transferase (GST); and concentration of nonenzymatic antioxidants—total antioxidant capacity (TAC) in the hypothalamus homogenates from rats exposed to low-frequency electromagnetic field (group A) and sham-exposed rats (control group) (group C) with results of ANOVA for all examined groups (A, C, M, and A + M) and post hoc NIR test for two selected groups: A and C.

Parameter	Group A M ± SD	Group C M ± SD	ANOVA results F; p value	p value of NIR test
MDA concentration (μmol/g protein)	1.03 ± 0.15	0.76 ± 0.13	11.76; <**0.001**	0.079
TOS concentration (μmol/g protein)	2.85 ± 0.51	2.68 ± 0.35	1.37; 0.268	0.535
SOD activity (NU/mg protein)	72.00 ± 12.56	82.99 ± 7.58	1.40; 0.260	0.064
SOD-Mn activity (NU/mg protein)	48.53 ± 5.67	52.41 ± 4.11	0.73; 0.543	0.263
SOD-CuZn activity (NU/mg protein)	23.46 ± 9.42	30.59 ± 3.76	6.48; **0.029**	0.119
CAT activity (IU/g protein)	9.11 ± 2.78	8.80 ± 1.73	0.28; 0.841	0.800
GPx activity (IU/g protein)	0.47 ± 0.44	0.43 ± 0.30	0.54; 0.660	0.862
GR activity (IU/g protein)	23.91 ± 3.14	24.05 ± 2.22	2.69; **0.046**	0.921
GST activity (IU/g protein)	4.86 ± 0.94	6.33 ± 0.49	11.18; **<0.001**	**<0.001**
TAC concentration (mmol/g protein)	0.09 ± 0.01	0.10 ± 0.01	1.03; 0.393	0.652

respectively, in comparison to the control group. However, the mean SOD activity in the hippocampus, hypothalamus, striatum, and cerebellum in rats exposed to the LFEMF did not differ significantly in comparison to the control group. The mean CAT activity in the rats exposed to the LFEMF was only significantly higher by 77% in the frontal cortex compared to the control group. No significant differences in the mean CAT activity were found between the rats exposed to the LFEMF and the control group with respect to the examined remaining brain structures. In addition, the GPx activity in rats exposed to the LFEMF was lower by 23.6% than that of the control rats, but again, only in the frontal cortex. In the remaining examined brain structures, the GPx activity in rats exposed to the LFEMF did not differ significantly when compared to the control group. The mean GR activity in the rats exposed to the LFEMF was higher by 13.3% in the hippocampus, while in the brainstem its activity was lower by 25.1% in comparison to the control group. No significant differences in GR activity were found between the rats exposed to the LFEMF and the control group with respect to the remaining investigated brain structures. GST activity in rats exposed to the LFEMF was significantly lower in all investigated brain structures: in the frontal cortex by 32%, in the hippocampus by 14.2%, in the brainstem by 31.7%, in the hypothalamus by 23.2%, in the striatum by 11.5%, and in the cerebellum by 18.2% compared to the control group. Similarly, in our study, the mean TAC concentrations in the rats exposed to the LFEMF were lower by 13.4% in comparison to the control group, but only in the frontal cortex. No significant differences in TAC concentrations

Table 5: Concentrations of oxidative stress biomarkers: malondialdehyde (MDA) and total oxidant status (TOS); activity of antioxidant enzymes: superoxide dismutase (SOD) and isoenzymes (SOD-Mn, SOD-CuZn), catalase (CAT), glutathione peroxidase (GPx), glutathione reductase (GR), and glutathione S-transferase (GST); and concentration of nonenzymatic antioxidants—total antioxidant capacity (TAC) in the striatum homogenates from rats exposed to low-frequency electromagnetic field (group A) and sham-exposed rats (control group) (group C) with results of ANOVA for all examined groups (A, C, M, and A + M) and post hoc NIR test for two selected groups: A and C.

Parameter	Group A M ± SD	Group C M ± SD	ANOVA results F; p value	p value of NIR test
MDA concentration (μmol/g protein)	1.02 ± 0.12	1.12 ± 0.26	1.86; 0.156	0.278
TOS concentration (μmol/g protein)	1.64 ± 0.99	1.75 ± 0.86	14.70; **<0.01**	1.000
SOD activity (NU/mg protein)	64.35 ± 15.38	64.16 ± 8.73	16.16; 0.201	1.000
SOD-Mn activity (NU/mg protein)	32.49 ± 3.87	32.78 ± 2.31	4.60; **<0.01**	0.487
SOD-CuZn activity (NU/mg protein)	31.86 ± 13.15	31.39 ± 8.29	1.13; 0.350	0.908
CAT activity (IU/g protein)	4.73 ± 2.12	3.79 ± 1.20	55.86;**<0.001**	0.277
GPx activity (IU/g protein)	1.15 ± 0.22	1.25 ± 0.15	6.16; **<0.01**	0.238
GR activity (IU/g protein)	25.92 ± 3.56	25.55 ± 2.76	21.42; **<0.001**	1.000
GST activity (IU/g protein)	2.93 ± 0.34	3.32 ± 0.19	6.63; **<0.01**	**<0.01**
TAC concentration (mmol/g protein)	0.08 ± 0.01	0.08 ± 0.01	0.36; 0.783	0.347

Table 6: Concentrations of oxidative stress biomarkers: malondialdehyde (MDA) and total oxidant status (TOS); activity of antioxidant enzymes: superoxide dismutase (SOD) and isoenzymes (SOD-Mn, SOD-CuZn), catalase (CAT), glutathione peroxidase (GPx), glutathione reductase (GR), and glutathione S-transferase (GST); and concentration of nonenzymatic antioxidants—total antioxidant capacity (TAC) in the cerebellum homogenates from rats exposed to low-frequency electromagnetic field (group A) and sham-exposed rats (control group) (group C) with results of ANOVA for all examined groups (A, C, M, and A + M) and post hoc NIR test for two selected groups: A and C.

Parameter	Group A M ± SD	Group C M ± SD	ANOVA results F; p value	p value of NIR test
MDA concentration (μmol/g protein)	3.30 ± 1.269	2.76 ± 0.79	13.73; **<0.001**	0.292
TOS concentration (μmol/g protein)	4.14 ± 0.58	4.40 ± 0.76	14.82; **<0.01**	1.000
SOD activity (NU/mg protein)	99.80 ± 16.56	94.77 ± 4.84	21.23; **<0.01**	1.000
SOD-Mn activity (NU/mg protein)	97.71 ± 14.55	92.05 ± 4.12	20.89; **<0.001**	1.000
SOD-CuZn activity (NU/mg protein)	2.28 ± 2.17	2.71 ± 1.21	17.86; **<0.001**	1.000
CAT activity (IU/g protein)	12.38 ± 3.42	9.74 ± 2.96	4.07; **0.014**	0.129
GPx activity (IU/g protein)	1.88 ± 0.23	1.79 ± 0.23	13.01; **<0.01**	1.000
GR activity (IU/g protein)	19.08 ± 3.36	18.93 ± 1.11	15.62; **<0.01**	1.000
GST activity (IU/g protein)	2.93 ± 0.42	3.58 ± 0.53	18.39; **<0.001**	**<0.01**
TAC concentration (mmol/g protein)	0.07 ± 0.06	0.13 ± 0.01	20.32; **<0.001**	1.000

were found between the rats exposed to the LFEMF and the control group with respect to the remaining investigated brain structures.

Different responses of oxidative stress parameters in brain structures under investigation might have been caused by the different impact of the LFEMF on these structures as well as differences in their functions.

There are only a few reports available on the effects of the LFEMF on prooxidative-antioxidative balance within the central nervous system, but it should be noted that, due to a high level of aerobic metabolism, large amounts of unsaturated fatty acids, and lower antioxidant activity, neurons are particularly vulnerable to disturbances in the prooxidative-antioxidative balance [37, 38].

The available results of researches are not unequivocal, which might be due to the differences in the physical parameters of applied electromagnetic fields and different methodologies of exposure. Jelenković et al. [39] are the only investigators who have evaluated the effects of exposure to the LFEMF on several brain structures in rats. However, the nonenzymatic antioxidant system was not assessed, and hence, no ultimate conclusions can be drawn regarding the prooxidative-antioxidative balance. Also, the rats were exposed to the LFEMF (50 Hz, 0.5 mT) for 7 days only. Nevertheless, the production of superoxide anion radical and MDA concentrations increased in all CNS-investigated structures. A significant increase in nitric oxide production was found in the frontal cortex and hypothalamus, while higher SOD activity was only observed in the hypothalamus.

Akdag et al. [40] examined brain homogenates of rats exposed to a 100 or 500 μT electromagnetic field for 2 hours a day for 10 months. The CAT activity decreased in both

exposure groups. The TAC concentration was lower in the 500 μT group compared to the 100 μT and sham-exposed groups, while MDA, TOS concentration, and oxidative stress index were higher.

Lee et al. [41] observed a significant increase in chemiluminescence and SOD activity in brain homogenates of mice after a 3-hour exposure to a 60 Hz electromagnetic field.

Falone et al. [42] showed that continuous 10-day exposure to a 50 Hz, 0.1 mT EMF significantly affected the antioxidative capacity of the female rat brain, the effect being age-dependent. The activity of antioxidant enzymes increased in young and decreased in old animals. This observation was supported by the results of Rageh et al. [43], who exposed 10-day-old rats to a continuous 50 Hz, 0.5 mT electromagnetic field for 30 days. They found that EMF exposure resulted in higher MDA concentration and SOD activity and increased the rate of oxidative damage to cellular DNA. It should be emphasized though that the above study was performed using juvenile rats whose CNS had not been fully developed yet.

Physical factors of limited intensity might also have some beneficial effects in the form of adaptive process stimulation. Ciejka et al. [44] observed that a longer exposure to a 7 mT, 40 Hz electromagnetic field apparently resulted in the adaptation to experimental conditions. An analysis of brain homogenates of adult rats after a 60-minute daily exposure to the electromagnetic field over a period of 10 days revealed a significant increase in the sulfhydryl group and protein concentration, while a 30-minute daily exposure caused a significant increase in lipid peroxidation.

The exposure of our experimental rats to a 50 Hz EMF lasted for four weeks. Since human exposure to the EMF is typically long-term, we did not aim to examine the effects of short-term exposure. The issue is challenging and requires further studies.

5. Conclusions

Summing up, it can be concluded that a four-week exposure of male rats to the low-frequency electromagnetic field does not affect oxidative stress in the studied brain structures.

Data Availability

All data are included in the tables in the article.

Conflicts of Interest

The authors declare that there is no conflict of interests regarding the publication of this paper.

Acknowledgments

This study was supported by the grant no N N511351737 from the Ministry of Science and Higher Education.

References

[1] X. Zhang, K. Yarema, and A. Xu, *Biological Effects of Static Magnetic Fields*, Springer Nature, Singapore, 2017.

[2] I. Yakymenko, O. Tsybulin, E. Sidorik, D. Henshel, O. Kyrylenko, and S. Kyrylenko, "Oxidative mechanisms of biological activity of low-intensity radiofrequency radiation," *Electromagnetic Biology and Medicine*, vol. 35, no. 2, pp. 186–202, 2016.

[3] H. Wang and X. Zhang, "Magnetic fields and reactive oxygen species," *International Journal of Molecular Sciences*, vol. 18, no. 10, p. 2175, 2017.

[4] B. Yokus, D. U. Cakir, M. Z. Akdag, C. Sert, and N. Mete, "Oxidative DNA damage in rats exposed to extremely low frequency electro magnetic fields," *Free Radical Research*, vol. 39, no. 3, pp. 317–323, 2005.

[5] S. Chater, H. Abdelmelek, T. Douki et al., "Exposure to static magnetic field of pregnant rats induces hepatic GSH elevation but not oxidative DNA damage in liver and kidney," *Archives of Medical Research*, vol. 37, no. 8, pp. 941–946, 2006.

[6] M. Lupke, J. Rollwitz, and M. Simkó, "Cell activating capacity of 50 Hz magnetic fields to release reactive oxygen intermediates in human umbilical cord blood-derived monocytes and in mono mac 6 cells," *Free Radical Research*, vol. 38, no. 9, pp. 985–993, 2004.

[7] K. Buchner and H. Eger, "Changes of clinically important neurotransmitters under the influence of modulated RF fields—a long-term study under real-life conditions," *Umwelt-Medizin-Gesellschaft*, vol. 24, no. 1, pp. 44–57, 2011.

[8] R. Santini, P. Santini, J. M. Danze, P. le Ruz, and M. Seigne, "Symptoms experienced by people in vicinity of base station: i/incidences of distance and sex," *Pathologie Biologie*, vol. 50, no. 6, pp. 369–373, 2002.

[9] O. Johansson, "Electrohypersensitivity: state-of-the-art of a functional impairment," *Electromagnetic Biology and Medicine*, vol. 25, no. 4, pp. 245–258, 2006.

[10] The INTERPHONE Study Group, "Brain tumour risk in relation to mobile telephone use: results of the INTERPHONE international case–control study," *International Journal of Epidemiology*, vol. 39, no. 3, pp. 675–694, 2010.

[11] L. Hardell and M. Carlberg, "Mobile phones, cordless phones and the risk for brain tumours," *International Journal of Oncology*, vol. 35, no. 1, pp. 5–17, 2009.

[12] S. Sadetzki, A. Chetrit, A. Jarus-Hakak et al., "Cellular phone use and risk of benign and malignant parotid gland tumors - a nationwide case-control study," *American Journal of Epidemiology*, vol. 167, no. 4, pp. 457–467, 2008.

[13] L. Hardell, M. Carlberg, K. Hansson Mild, and M. Eriksson, "Case-control study on the use of mobile and cordless phones and the risk for malignant melanoma in the head and neck region," *Pathophysiology*, vol. 18, no. 4, pp. 325–333, 2011.

[14] N. A. Bonekamp, A. Völkl, H. D. Fahimi, and M. Schrader, "Reactive oxygen species and peroxisomes: struggling for balance," *BioFactors*, vol. 35, no. 4, pp. 346–355, 2009.

[15] B. Poniedziałek, P. Rzymski, J. Karczewski, F. Jaroszyk, and K. Wiktorowicz, "Reactive oxygen species (ROS) production in human peripheral blood neutrophils exposed *in vitro* to static magnetic field," *Electromagnetic Biology and Medicine*, vol. 32, no. 4, pp. 560–568, 2013.

[16] M. Koch, J. Mostert, A. Arutjunyan et al., "Peripheral blood leukocyte NO production and oxidative stress in multiple sclerosis," *Multiple Sclerosis Journal*, vol. 14, no. 2, pp. 159–165, 2008.

[17] E. Granot and R. Kohen, "Oxidative stress in childhood—in health and disease states," *Clinical Nutrition*, vol. 23, no. 1, pp. 3–11, 2004.

[18] S. Manoharan, G. J. Guillemin, R. S. Abiramasundari, M. M. Essa, M. Akbar, and M. D. Akbar, "The role of reactive oxygen species in the pathogenesis of Alzheimer's disease, Parkinson's disease, and Huntington's disease: a mini review," *Oxidative Medicine and Cellular Longevity*, vol. 2016, Article ID 8590578, 15 pages, 2016.

[19] J. Blesa, I. Trigo-Damas, A. Quiroga-Varela, and V. R. Jackson-Lewis, "Oxidative stress and Parkinson's disease," *Frontiers in Neuroanatomy*, vol. 9, p. 91, 2015.

[20] S. P. Mahadik and S. Mukherjee, "Free radical pathology and antioxidant defense in schizophrenia: a review," *Schizophrenia Research*, vol. 19, no. 1, pp. 1–17, 1996.

[21] A. Huss, T. Koeman, H. Kromhout, and R. Vermeulen, "Extremely low frequency magnetic field exposure and Parkinson's disease—a systematic review and meta-analysis of the data," *International Journal of Environmental Research and Public Health*, vol. 12, no. 7, pp. 7348–7356, 2015.

[22] R. Tarawneh and J. E. Galvin, "Potential future neuroprotective therapies for neurodegenerative disorders and stroke," *Clinics in Geriatric Medicine*, vol. 26, no. 1, pp. 125–147, 2010.

[23] "National Research Council (US) Committee for the update of the guide for the care and use of laboratory animals," in *Guide for the Care and Use of Laboratory Animals*, National Academies Press (US), Washington (DC), 8th edition edition, 2011, http://www.ncbi.nlm.nih.gov/books/NBK54050/.

[24] G. Paxinos and C. Watson, *The Rat Brain in Stereotaxic Coordinates*, Academic Press, San Diego, CA, 6th Edn edition, 2007.

[25] H. Ohkawa, N. Ohishi, and K. Yagi, "Assay for lipid peroxides in animal tissues by thiobarbituric acid reaction," *Annals of Clinical Biochemistry*, vol. 95, no. 2, pp. 351–358, 1979.

[26] O. Erel, "A new automated colorimetric method for measuring total oxidant status," *Clinical Biochemistry*, vol. 38, no. 12, pp. 1103–1111, 2005.

[27] Y. Ōyanagui, "Reevaluation of assay methods and establishment of kit for superoxide dismutase activity," *Analytical Biochemistry*, vol. 142, no. 2, pp. 290–296, 1984.

[28] L. H. Johansson and L. A. Håkan Borg, "A spectrophotometric method for determination of catalase activity in small tissue samples," *Annals of Clinical Biochemistry*, vol. 174, no. 1, pp. 331–336, 1988.

[29] D. Paglia and W. Valentine, "Studies on the quantitative and qualitative characterization of erythrocyte glutathione peroxidase," *Journal of Laboratory and Clinical Medicine*, vol. 70, no. 1, pp. 158–169, 1967.

[30] R. Richterich, *Clinical Chemistry: Theory and Practice*, Academic Press, New York, 1969.

[31] W. H. Habig and W. B. Jakoby, "[51] Assays for differentiation of glutathione *S*-transferases," *Methods in Enzymology*, vol. 77, pp. 398–405, 1981.

[32] O. Erel, "A novel automated direct measurement method for total antioxidant capacity using a new generation, more stable ABTS radical cation," *Clinical Biochemistry*, vol. 37, no. 4, pp. 277–285, 2004.

[33] A. Buico, C. Cassino, M. Ravera, P. G. Betta, and D. Osella, "Oxidative stress and total antioxidant capacity in human plasma," *Redox Report*, vol. 14, no. 3, pp. 125–131, 2009.

[34] B. Halliwell, "Antioxidant defence mechanisms: from the beginning to the end (of the beginning)," *Free Radical Research*, vol. 31, no. 4, pp. 261–272, 1999.

[35] A. Stanek, G. Cieślar, E. Romuk et al., "Decrease in antioxidant status in patients with ankylosing spondylitis," *Clinical Biochemistry*, vol. 43, no. 6, pp. 565–570, 2010.

[36] A. Stanek, A. Cholewka, T. Wielkoszyński, E. Romuk, K. Sieroń, and A. Sieroń, "Increased levels of oxidative stress markers, soluble CD40 ligand, and carotid intima-media thickness reflect acceleration of atherosclerosis in male patients with ankylosing spondylitis in active phase and without the classical cardiovascular risk factors," *Oxidative Medicine and Cellular Longevity*, vol. 2017, Article ID 9712536, 8 pages, 2017.

[37] B. Halliwell, "Oxidative stress and neurodegeneration: where are we now?," *Journal of Neurochemistry*, vol. 97, no. 6, pp. 1634–1658, 2006.

[38] B. Halliwell, "Role of free radicals in the neurodegenerative diseases: therapeutic implications for antioxidant treatment," *Drugs and Aging*, vol. 18, no. 9, pp. 685–716, 2001.

[39] A. Jelenković, B. Janać, V. Pešić, D. M. Jovanović, I. Vasiljević, and Z. Prolić, "Effects of extremely low-frequency magnetic field in the brain of rats," *Brain Research Bulletin*, vol. 68, no. 5, pp. 355–360, 2006.

[40] M. Z. Akdag, S. Dasdag, E. Ulukaya, A. K. Uzunlar, M. A. Kurt, and A. Taşkın, "Effects of extremely low-frequency magnetic field on caspase activities and oxidative stress values in rat brain," *Biological Trace Element Research*, vol. 138, no. 1–3, pp. 238–249, 2010.

[41] B. C. Lee, H. M. Johng, J. K. Lim et al., "Effects of extremely low frequency magnetic field on the antioxidant defense system in mouse brain: a chemiluminescence study," *Journal of Photochemistry and Photobiology B: Biology*, vol. 73, no. 1-2, pp. 43–48, 2004.

[42] S. Falone, A. Mirabilio, M. C. Carbone et al., "Chronic exposure to 50 Hz magnetic fields causes a significant weakening of antioxidant defence systems in aged rat brain," *The International Journal of Biochemistry & Cell Biology*, vol. 40, no. 12, pp. 2762–2770, 2008.

[43] M. M. Rageh, R. H. el-Gebaly, and N. S. el-Bialy, "Assessment of genotoxic and cytotoxic hazards in brain and bone marrow cells of newborn rats exposed to extremely low-frequency magnetic field," *Journal of Biomedicine and Biotechnology*, vol. 2012, Article ID 716023, 7 pages, 2012.

[44] E. Ciejka, P. Kleniewska, B. Skibska, and A. Goraca, "Effects of extremely low frequency magnetic field on oxidative balance in brain of rats," *Journal of Physiology and Pharmacology*, vol. 62, no. 6, pp. 657–661, 2011.